Activation and inhibition mechanisms of the cGMP-dependent protein kinase studied by mass spectrometry

Activation and inhibition mechanisms of the cGMP-dependent protein kinase studied by mass spectrometry

Activerings en remmings mechanismen van het cGMP-afhankelijk eiwit kinase bestudeerd met behulp van massa spectrometrie

(met een samenvatting in het Nederlands)

Proefschrift

ter verkrijging van de graad van doctor aan de Universiteit Utrecht op gezag van de Rector Magnificus, Prof. dr. W. H. Gispen ingevolge het besluit van het College voor Promoties in het openbaar te verdedigen op woensdag 19 januari 2005 des middags te 12.45 uur.

door

Martinus Wijnandus Hendrikus Pinkse

Geboren op 12 augustus 1977, te Alkmaar

Promotor:

Prof. dr. A. J. R. Heck

Verbonden aan de Faculteit Farmacie der Universiteit Utrecht

Financial support for the printing of this thesis was kindly provided by the J. E. Jurriaanse Stichting.

ISBN: 90-393-3893-0

Cover: Non-realistic ribbon diagram model of PKG based on PKA X-ray structure 1BKX and 1RL3. Combined ESI-mass spectra of unfolded PKG and W64$^{Phe(Tmd)}$ crosslinked PKG.

Printing: Ponsen & Looijen B.V., Wageningen

The work described in the thesis was financially supported by Pfizer Global Research and Development, Sandwich, United Kingdom.

Aan Astrid

Table of contents

General Introduction

1

I Reversible protein phosphorylation

- *Functional proteomics in the post-genomic era*
- *Protein phosphorylation*
- *Protein kinases*

II Structure and function of the cGMP-dependent protein kinase

- *Background*
- *The amino terminal domain*
- *Regulatory cGMP-binding pockets*
- *Catalytic core*
- *PKG regulation*
- *Physiological role of PKG*

III Mass spectrometric approaches for protein analysis

- *Biomolecular mass spectrometry*
- *Liquid chromatography and mass spectrometry*
- *Protein phosphorylation and mass spectrometry*
- *Structural analysis of proteins*

IV Aim and outline of this thesis

I Reversible protein phosphorylation

Functional proteomics in the post-genomic era.

The completion of the sequencing of the human genome and ongoing sequencing of the genomes of many other organisms has undoubtedly changed the outlook of biological research to the point that biochemists define the present one as "the post-genomic era", marking the need to approach the study of living organisms from a different perspective. In the post-genomic era research interest is turning more and more to unraveling the nature and function of all proteins within the cell, since they are the effectors of all the reactions and interactions that characterize living organisms [1-4]. It has been estimated that the 30.000-40.000 human genes [5, 6] may lead to a number of proteins that is at least 10 times higher, all of them having specific functions in our body. Hence, understanding the role of each individual protein is an enormous task that leans largely onto the shoulders of the rapidly emerging field of proteomics. Proteomics, the study of the protein complement expressed by a genome, includes besides the identification and quantification of large numbers of proteins, also the characterization of their localization, modifications, interactions, activities, and, ultimately, their function [7, 8]. Current functional proteomics studies emphasize the need of determining protein-protein interactions, but it also includes the study of small-molecule ligand-protein interactions, protein localization, protein activity and mapping post-translational protein modifications [9]. Especially this last feature plays an important role in understanding protein activity. In a cell a large amount of different proteins with ranging tasks and functions can coexist and in order to control this large and diverse group of proteins, nature cleverly developed several strategies for protein-activity regulating. One of these strategies involves the chemical modification of a protein after it has been synthesized. These post-translational modifications extend the range of possible functions a protein can have and for simplicity it can be regarded as molecular switches that define protein activity. In cellular signaling pathways cascades of protein modifying reactions can occur and in each step a protein will activate-deactivate another protein so that eventually a signal in conducted through the cell. In this sense these post-translational modifications can be regarded as of one the many languages proteins use to distribute messages in reaction to certain stimuli.

Protein phosphorylation.

The reversible phosphorylation of proteins, first discovered in 1955 [10], ranks amongst the most important post-translational modifications that occur in the cell. This reversible reaction involves the covalent attachment of a phosphate group to one of the side-chains of the protein. Phosphorylation is a highly effective means of controlling the activity of proteins from a structural, thermodynamic, and kinetic point of view [11]: *(i)* Upon phosphorylation two negative charges are added to the protein. These can disrupt electrostatic interactions in the unmodified protein and they can form new electrostatic interactions, thereby changing protein structure. Changes in protein structure can lead to alterations in ligand binding or catalytic activity. *(ii)* A phosphoryl group can form three hydrogen bonds. The tetrahedral geometry makes these interactions highly directional. *(iii)* The free energy of phosphorylation is large. Of the –12 kcal/mol provided by ATP, about half is consumed in making phosphorylation irreversible; the other half is conserved in the phosphorylated protein. *(iv)* Phosphorylation and dephosphorylation can occur in less than a second or over a span of hours. The kinetics can be adjusted to meet the time needed for physiologic processes. *(v)* Phosphorylation often evokes highly amplified effects. A single activated protein can phosphorylate hundreds of target proteins in a short interval.

In this respect, phosphorylation can be considered as a highly effective molecular switch by which proteins can be either turned off or on. It is now generally accepted that a plethora of biological processes, such as cell cycle, cell-growth, cell differentiation and metabolism are orchestered and tightly controlled by this reversible modification. Today, it is believed that one third of the proteins present in a typical mammalian cell are phosphorylated. This large number of phosphoproteins highlights the important role of phosphorylation in controlling cellular activities. The phosphorylation state of a protein can determine its biological activity, or aid in moving proteins between subcellular compartments, allow interactions between proteins to occur as well as labeling proteins for degradation. The variety is immense and now many human diseases such as cancer and Alzheimer have been recognized to be caused by, or result in, the abnormal phosphorylation of cellular proteins [12-14].

Protein kinases.

Key players in the protein phosphorylation events are protein kinases, the catalyst of phosphorylation reaction and phosphatases, the proteins responsible for dephosphorylation reaction (Figure 1). Protein kinases cascades are the predominant component of signal transduction pathways. Almost every known signaling pathway eventually impinges on a protein kinase, or in some instances, a protein phosphatase. Signaling is terminated and components of the pathway are returned to ground state largely by dephosphorylation. Therefore protein kinases and phosphatases can be considered as the *'yin'* and *'yang'* of protein phosphorylation and signaling [15].

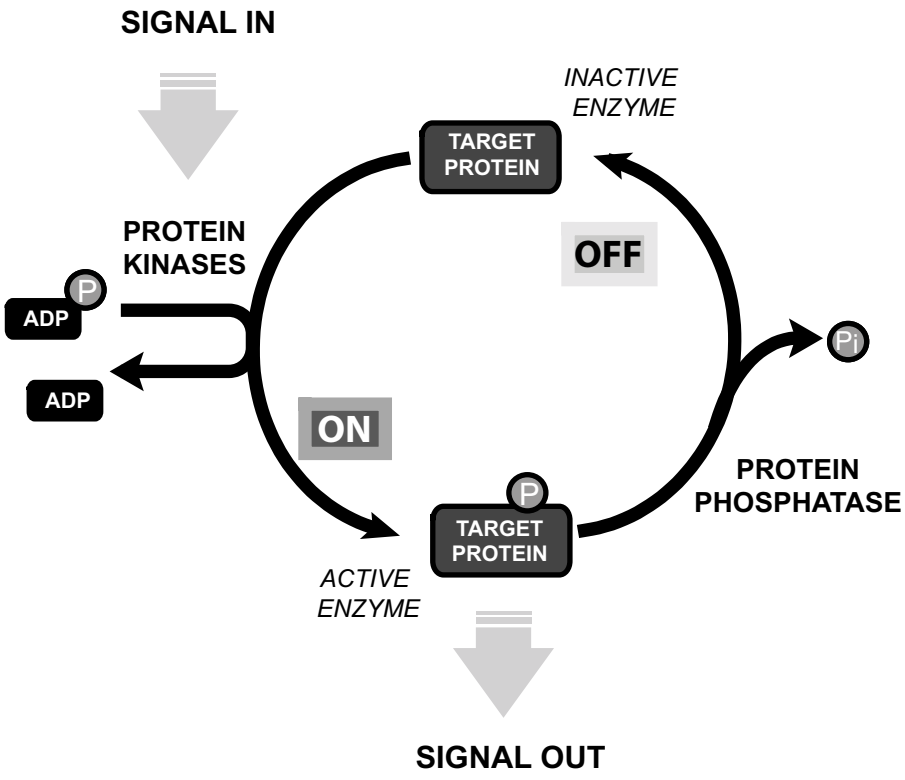

Figure 1: Simplified model of the mode of action of protein kinases and protein phosphatases in cellular signaling pathways

Initially estimates have placed the potential number of protein kinases encoded by the mammalian genome at greater than 1000 [16, 17]. With the completion of deciphering the human genome sequence it is possible to identify almost all human kinases and the actual number of protein kinases that is catalogued up till now is about half that predicted several

years ago. Comprehensive analysis of the human and mouse genome placed the number at 518 human and 540 mouse kinases [18, 19]. Consequently, elucidation of the role of each protein kinase is a challenging task given the size of the enzyme family and the numerous pathways in which these phosphoryl transfer catalysts serve as participants. This task is even more rendered by the general nature of the reaction catalyzed by these enzymes and by their nearly universal utilization of the common substrate, ATP. The basis of this precision is build up from several parameters, such as (*i*) the primary sequence that harbors the phosphate accepting residue [20-22], (*ii*) secondary or tertiary structure elements around the site of phosphorylation on the target protein substrate [23], (*iii*) microenvironment to which the enzyme is confined within the cell [24, 25].

The work described in this thesis focuses on a single protein kinase, namely the cGMP-dependent protein kinase Type Iα (PKG Iα). This kinase catalyses the cGMP-stimulated phosphorylation of serine and threonine residues in various proteins and peptides and has been implicated in the signal transduction of many drugs and hormones. A definitive function of PKG has not been established yet, however this kinase has been implicated in the regulation of smooth muscle relaxation [26-28], platelet function [29, 30], cell division and gene expression [31]. Although there is significant progress in understanding the specific functional role of PKG in smooth muscle and other cellular systems, relatively little is known about the overall structure of PKG, the significance of the autophosphorylation process, the nature of conformational changes induced by the binding of cyclic nucleotides, substrate peptides or proteins and peptide inhibitors, the dimerization of the enzyme or the nature of the interaction of the autoinhibitory site with the active site. The aim of the work described in this thesis is to develop and apply mass spectrometry based approaches, which will yield new information on the molecular determinants that are crucial for regulation, cyclic nucleotide binding and kinase activity of PKG.

II Structure and function of the cGMP-dependent protein kinase

Background

The cGMP-dependent protein kinase (PKG) and the cAMP-dependent protein kinase (PKA) serve as major receptors for respectively intracellular cGMP and cAMP and they play central roles in cyclic-nucleotide signaling pathways. Both kinases are allosterically regulated proteins and much of our current understanding of protein kinases regarding their structure, function and regulation are based on studies on PKG and even more so PKA. PKG was discovered in 1970 [32]. At the time it showed a high homology PKA, which was first described in 1963. Since their discovery the many years of research have resulted in a complex understanding of both kinases. In particular for PKA detailed pictures of all the processes from regulation to enzymatic turnover exist. Studies on the function, structure and regulation of PKA and PKG continue to provide insight into the enzymology of the diverse family of protein kinases and into the roles of these particular kinases in cellular processes. Below follows a brief overview on the structural and functional features of PKG type I, and throughout the text its differences and its similarities with the PKA system are highlighted.

PKGs: cGMP-dependent protein kinases have been identified in several different organisms, ranging from simple organisms to mammals. Comparison of PKG sequences indicated that the PKG coding gene evolved as the result of a fusion between the genes of a nucleotide binding protein and a protein with catalytic properties. This fusion occurred early in evolution, since the cGMP-kinases from simple organisms and mammals have cyclic nucleotide binding sites and catalytic activities on the same polypeptide chain. The mammalian genome encodes a Type I [33, 34] and a Type II PKG [35]. The mammalian Type I PKGs are homodimeric cytosolic proteins containing two identical polypeptides of ~76 kDa. Alternative mRNA splicing produces a Type Iα and a Type Iβ PKG, which are identical proteins apart from their first ~100 amino terminal residues [36, 37]. PKGs purified from *tetrahymena cilia* [38], *paramecium* [39] and *dictyostelum discoideum* [40] are apparently monomeric enzymes. Type II PKG, with a native molecular monomeric mass of 86 kDa was shown to differ from Type I PKGs in that it behaves as a membrane or cytoskeleton associated protein [41].

Overall structure: The cGMP-dependent protein kinase harbors several functional domains on a single polypeptide chain. In order to understand the complexity of this enzyme, the primary sequence of the subunits have been divided into three separate segments; an amino-terminal, a regulatory and a catalytic segment [42]. The amino-terminal segment contains a dimerization site, an autoinhibitory motif and several autophosphorylation sites. A hinge region connects the amino-terminal site with the two in-tandem cGMP binding pockets. The C-terminal part of the protein harbors the catalytic domain, which consists of a MgATP binding pocket and a peptide binding site (Figure 2). In contrast, in the PKA system the regulatory components and the catalytic domain are present on two separate subunits.

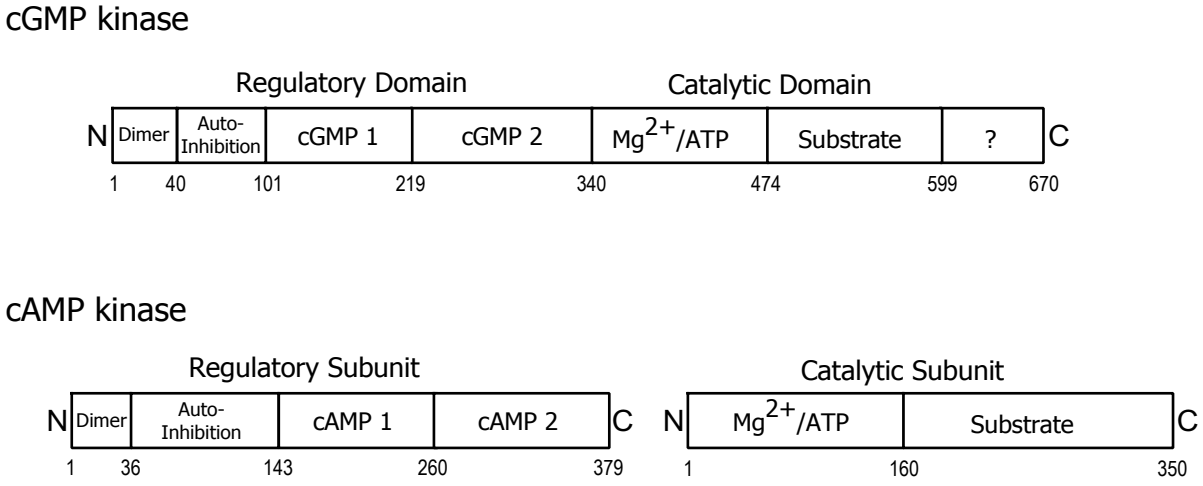

Figure 2: Linear arrangement of the functional domains of the Type I cGMP-dependent protein kinase and the regulatory and catalytic subunits of the cAMP-dependent protein kinase.

The amino terminal domain.

The amino terminus of cGMP kinase regulates four important functions: (*i*) dimerization of homologous subunits, (*ii*) autoinhibition of the catalytic domain in the absence of bound cGMP, (*iii*) the affinity and cooperative behavior of the cGMP-binding sites A and B, and (*iv*) the intracellular localization of the enzymes. Additionally the amino terminus harbors multiple autophosphorylation sites.

Dimerization: The amino terminal domain of PKG Iα and Iβ contains a leucine/isoleucine zipper motif (6 repeats in Type Iα and 7-8 repeats in Type Iβ [43]), which is a well-known dimerization motif in transcriptional activators [44]. A typical leucine zipper contains a leucine at every seventh position in a stretch of ~35 residues and forms an α-helical coiled coil [45]. Synthetic peptide models with a strong helical motif of this dimerization domain were shown to dimerize in solution with hydrophobic interaction along a leucine/isoleucine interface [46]. The Type Iα monomers are probably also linked to each other via a disulfide bridge at Cys-42, where Type Iβ lacks a cysteine in this region. Partial proteolysis with trypsin or chymotrypsin results in the removal of the amino terminal dimerization domain of Type Iα and Iβ and monomerizes the enzymes [47]. In the absence of cAMP, PKA forms a tetramer of the two regulatory and two catalytic subunits (R_2C_2), and this conformational state offers probably the closest resemblance to PKG. Binding of cAMP causes a dissociation of the inactive R_2C_2 into two active C subunits and one R_2 dimer. This in contrast to PKG, where as mentioned the regulatory domain and catalytic domain are present on one single polypeptide chain. Binding of cGMP to the kinase does not dissociate the dimeric enzyme into R and C subunits but induces an apparent conformational change that leads to kinase activation.

Autoinhibition: Autoinhibition is a key biochemical regulatory mechanism by which catalytic activities or other protein functions are controlled. The release of autoinhibition is often initiated by allosteric ligand binding, association/dissociation with other proteins, or a covalent modification such as phosphorylation. PKA and PKG are autoinhibited through multiple interactions between their regulatory and catalytic domains. A large contribution to autoinhibition is presented by the interaction between residues within the catalytic domain and those within a pseudosubstrate region in the regulatory domain. This interaction effectively inhibits catalysis by preventing binding of substrate. Alignment of the pseudosubstrate sequence of PKGs, the regulatory subunits of PKA and of the PKA specific protein kinase inhibitor PKI reveals that they all harbor a common kinase autoinhibitory motif; RRX-A/G-Ψ (Figure 3) that closely resembles a typical PKA and/or PKG consensus sequence. The underlined residues represent the designated phosphorylation-site (P0) usually occupied by a glycine or an alanine. The nature of residue X at the P-1 position has little or no role in the interaction, whereas Ψ at the P+1 position is in general a hydrophobic residue.

One exception is the regulatory RII subunit of PKA which contains a substrate like sequence that can be phosphorylated by the catalytic subunit of PKA [48]

hPKG Iα (56-67)	- R T T R A Q G I S A E P -
hPKG Iβ (71-82)	- P R T K R Q A I S A E P -
hPKG II (118-129)	- R R G A K A G V S A E P -
hPKA Iα (92-113)	- G R R R R G A I S A E V -
hPKA Iβ (92-113)	- A R R R R G G V S A E V -
hPKA II (91-112)	- R F N R R V S V C A E T -
hPKI Iα (15-26)	- R T G R R N A I H D I L -
hPKI Iβ (22-33)	- R A G R R N A L P D I Q -
hPKI Iγ (15-26)	- R T G R R N A V P D I Q -

Figure 3: Primary sequence alignment of pseudosubstrate sequence containing regions of PKG Iα, Iβ, II, the regulatory subunits Iα and Iβ of PKA and three isoforms of the cAMP-dependent protein kinase inhibitor

PCR-driven random mutagenesis studies revealed that the hydrophobic residue at the P+1 position in the pseudosubstrate sequence plays an important role in the interaction with the substrate-binding site. Replacement of isoleucine-63 in PKG Type Iβ by a threonine enhanced both autophosphorylation and basal kinase activity [49]. Besides these conserved residues within the pseudosubstrate sequences there are also more distal residues needed for high affinity binding of these autoinhibitory domains to the catalytic site, since the corresponding pseudosubstrate-peptides of Iβ isozyme are poor inhibitors of PKG [50-53]

Regulation of cGMP-binding: Another important function of the amino terminus lies in controlling the affinity of both cGMP-binding pockets for cyclic nucleotides. This became clear from studying the kinetics of cGMP-binding of both Type Iα and Type Iβ, which only differ from each other in the first ~100 amino acids. Type Iα and Iβ have association constants for cGMP of 0.1 μM and 1.3 μM respectively. This dramatic shift of K_A is caused by a 10 fold decrease in kinetics of the high affinity site in Type Iα [54]. Since both proteins are identical in both cGMP-binding pockets as well as the catalytic components, this large difference must be ascribed to the N-terminal residues. However, the exact mechanism of how the N-terminus causes the difference in cGMP affinity is not known.

Targeting: One of the mechanisms thought to contribute to substrate specificity by protein kinases is compartmentalization. In general compartmentalization of signaling molecules through association with anchoring proteins ensures specificity in signal transduction by placing enzymes close to their appropriate effectors and substrates. Intracellular localization of PKA is mediated by interaction with A-Kinase Anchoring Proteins (AKAPs) [55] that recruit PKA close to its substrates and to sites where it can respond optimally to local changes in intracellular cAMP concentration, thereby directing and amplifying the effects of cAMP [56-58]. By binding to additional signaling molecules, AKAPs might function to coordinate multiple components of signal-transduction pathways. For PKA the AKAP-binding site is located at the amino-terminal site of the dimerization domain in the regulatory subunit [59-61]. Given the structural and functional similarity between PKA and PKG, it is not unlikely that also PKGs are targeted to certain cellular compartments by anchoring proteins. Vo *et al.* reported on the existence of several proteins, called G-kinase anchoring proteins (GKAPs), that appeared to be specific for PKG Type II, and which differed from known AKAPs [62]. Furthermore, yeast two-hybrid screening that used PKG Iα as a bait, isolated a novel male germ cell-specific 42-kDa cGMP-dependent protein kinase anchoring protein (GKAP42) [63]. Additionally Type I PKGs are able to interact with other proteins through their amino-terminus. Recently it was found that Type Iα PKG binds directly to the myosin-binding subunit of myosin phosphatase via the leucine/isoleucine zipper motif of PKG [64]. Type Iβ PKG, the IP3-receptor and an IP3R-associated cGMP kinase substrate (IRAG) form an essential NO/cGMP-dependent regulator of IP3-induced calcium release [65]. It was found that IRAG binds specifically to the amino-terminal region of PKG Iβ, but not to that of PKA Iα or PKG II [66].

Autophosphorylation: A particular protein kinase not only phosphorylates one or more cellular proteins (heterophosphorylation), but it commonly phosphorylates itself as well, a process termed autophosphorylation [67]. Protein kinase autophosphorylation is functionally important, since it frequently alters kinase function, e.g. by increasing the catalytic activity, increasing the affinity for allosteric ligand binding, or increasing the kinase binding to cellular proteins such as those containing SH2 domains [68, 69]. Many protein kinases are activated by either allosteric ligand binding or by autophosphorylation. PKGs autophosphorylate multiple sites in their amino-terminal ~100 amino acids [70]. Residues that are autophosphorylated were identified by labeling with ^{32}P-ATP and isolation and

characterization of ^{32}P labeled peptides with the Edman sequencing and/or amino acid analysis. The sites that are autophosphorylated in the presence of cAMP and Mg-ATP have been identified as Ser-1, Ser-50, Thr-58, Ser-64, Ser-72 and Thr-84 for Type Iα [71] and Ser-63 and Ser-79 for Type Iβ [72]. For Type Iα the degree of autophosphorylation been determined to be higher in the presence of cAMP (4 mol phosphate / mol subunit) than in the presence of cGMP (1 mol phosphate / mol subunit) [73]. Although several autophosphorylation sites on PKG are identified, their exact individual role in protein kinase regulation is not fully understood. Overall autophosphorylation induces a significant functional change in several properties of PKG *in-vitro*. For instance, *in-vitro* autophosphorylation lowers the concentration of cAMP that is needed to activate the enzyme [73], however it is uncertain whether autophosphorylation has any significance *in-vivo*. For Type Iβ PKG effects of autophosphorylation on the conformation of the protein were compared with the effects induced by cGMP-binding. In order to assess possible conformational changes produced by cyclic nucleotide binding, cyclic nucleotide free and cyclic nucleotide bound PKG was examined by (*i*) ion exchange chromatography, (*ii*) gel chromatography (*iii*) and native gel electrophoresis. Binding of cGMP caused a large electronegative charge shift on ion exchange chromatography, an increase in the Stokes radius (>3Å) and a decreased mobility on native gel electrophoresis [74]. Comparison of non- and highly- autophosphorylated protein was done in a similar fashion. Apparently binding of cyclic nucleotides to or autophosphorylation of the PKG produces a similar conformational change in the enzyme [75]. The mechanism of partial activation of PKG by autophosphorylation may be similar to the activation mechanism upon cGMP binding, since negatively charged phosphates are added in each case. The increased negativity could repel elements within the catalytic domain such as those interact with the positively charged amino acids of the autoinhibitory domain. This latter possibility was more or less demonstrated by the work of Busch *et al.* [76]. They found that autophosphorylation of Serine-64 of Type Iα PKG *in-vitro* activates the kinase in the absence of cGMP. This serine is conserved in Type Iβ and is just outside the autoinhibition site. In fact, the autoinhibition sequences ^{59}RAQGISAEP^{67} in Type Iα and ^{74}KRQAISAEP^{82} in Type Iβ, are immediately surrounded by the autophosphorylation sites Thr-58 and Ser-64 for Iα and Ser-79 for Iβ. If autophosphorylation of this residue also occurs *in-vivo,* this could provide a mechanism to maintain PKG activity after elevated cGMP levels have been restored to ground levels by phosphodiesterases.

Regulatory cGMP-binding pockets.

The two homologous cyclic nucleotide binding sites of PKG I (~110 amino acids each) are arranged in tandem in the amino-terminal half of PKG. Like those in PKA, the binding sites in PKG are related evolutionary to the catabolite gene activator protein (CAP) family of cyclic nucleotide-binding protein [42, 77]. PKG and PKA are distinct in this family since they both contain two in-tandem cyclic nucleotide-binding domains. The cyclic nucleotide binding sites of PKG preferentially bind cGMP over cAMP with a >100 fold selectivity, whereas the cyclic nucleotide binding sites of PKA bind preferentially cAMP over cGMP with a >50 fold selectivity. Although both cyclic nucleotide binding sites of PKG are homologues in sequence, they both have different analog specificities and have different dissociation rates for cGMP [78, 79]. In type Iβ the N-terminal site is commonly assigned as the slow site, due to its high cGMP affinity that causes a slow exchange rate, and the C-terminal site as the fast site, due its lower cGMP affinity that causes a faster exchange rate. This order of arrangement is surprisingly the opposite of what is found with the two in-tandem cAMP binding site in the regulatory subunit of PKA, where the more amino terminal cAMP binding sites is supposedly the fast site [80-82].

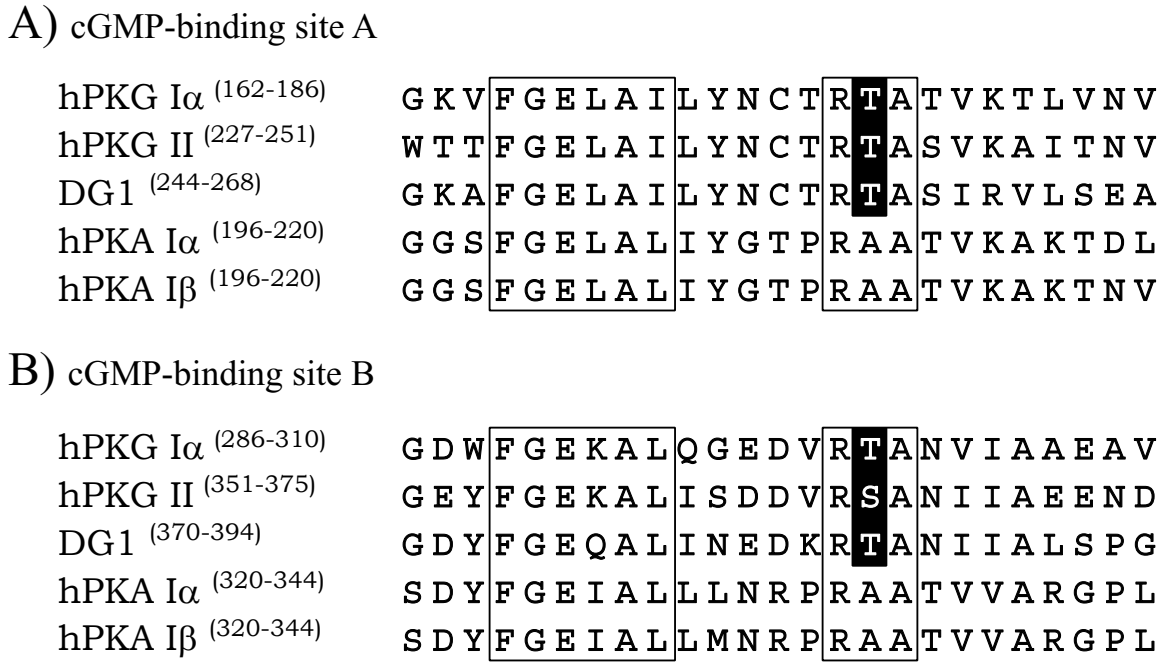

Figure 4: Sequence comparison of the cyclic nucleotide binding sites A and B of PKG. The following sequences were aligned, human PKG Iα (hPKG Iα), human PKG II (hPKG II), Drosophila cGMP-kinase (DG1) and the regulatory subunits Iα and Iβ of human PKA. Boxed residues show conserved regions; Black boxed threonine and serine display invariant residues.

The cyclic nucleotide-specificity of PKG for cGMP is largely determined by the presence of an invariant threonine, rather than an alanine that is present in cyclic AMP-binding site of cAMP dependent protein kinase (Figure 4). cGMP-binding sites of PKG, as well as those of cGMP-gated ion channels, phosphodiesterases, all contain this invariant threonine residue. Substitution of a threonine for the alanine in the cAMP-binding sites of type Iα R subunit of PKA significantly improves the affinity of the R subunit for cGMP with little effect on the affinity for cAMP [83, 84]. In a similar fashion, mutation of the threonine into an alanine in cGMP-gated ion channels and PKG Iβ results in the loss of cGMP/cAMP selectivity by decreasing the affinity cGMP while no change in cAMP affinity was observed [85-88]

For PKA insight into the dynamics associated with ligand binding was obtained from the cAMP-free [89] and cAMP bound [90] crystal structures of the regulatory subunit (Figure 5). The crystal structure of the regulatory subunit with cGMP bound to site A and an unoccupied site B varies from the crystal structure with cAMP bound to both A and B sites, primarily in the C-terminal tail. With an unoccupied B-site, the phosphate-binding cassette (PBC) of the B-site is highly dynamic and the carboxyl terminus is extended away from the binding pocket reflecting an opening of the B-site. When cAMP is bound, the PBC-motif and cAMP form a compact core maintained by numerous contacts and the C-terminal tail locks cAMP in place by contacts with the PBC and cAMP. This latter movement will position the C-terminal tail so that it seals the cAMP into the B-site, which accounts for the higher affinity and the slower dissociation rate of this site. In addition, conformational changes upon cAMP binding were probed in a $RI\alpha^{(94\text{-}244)}$ deletion mutant via hydrogen/deuterium exchange and mass spectrometry [91, 92]. It was found that the overall changes in H/D exchange were relatively small in the presence and absence of cAMP. The major difference, in the absence of cAMP, is the increased dynamics of the PBC domains of both Site A and Site B and the carboxy-terminus as measured by a significant increase in backbone amide exchange [93-95]. The conformational movement of the C-terminal helix is also sensed by Site A, since the N-terminal region of the C-terminal helix is linked to a helix, which is in the proximity of Site A. This provides an explanation for the obligatory ordered binding of cAMP first to Site B and then to Site A and gives insight into the communication between both sites. However, the structure of the fully cyclic-nucleotide free and of the holoenzyme (R_2C_2) are still needed to fully understand the allosteric communication between all different domains

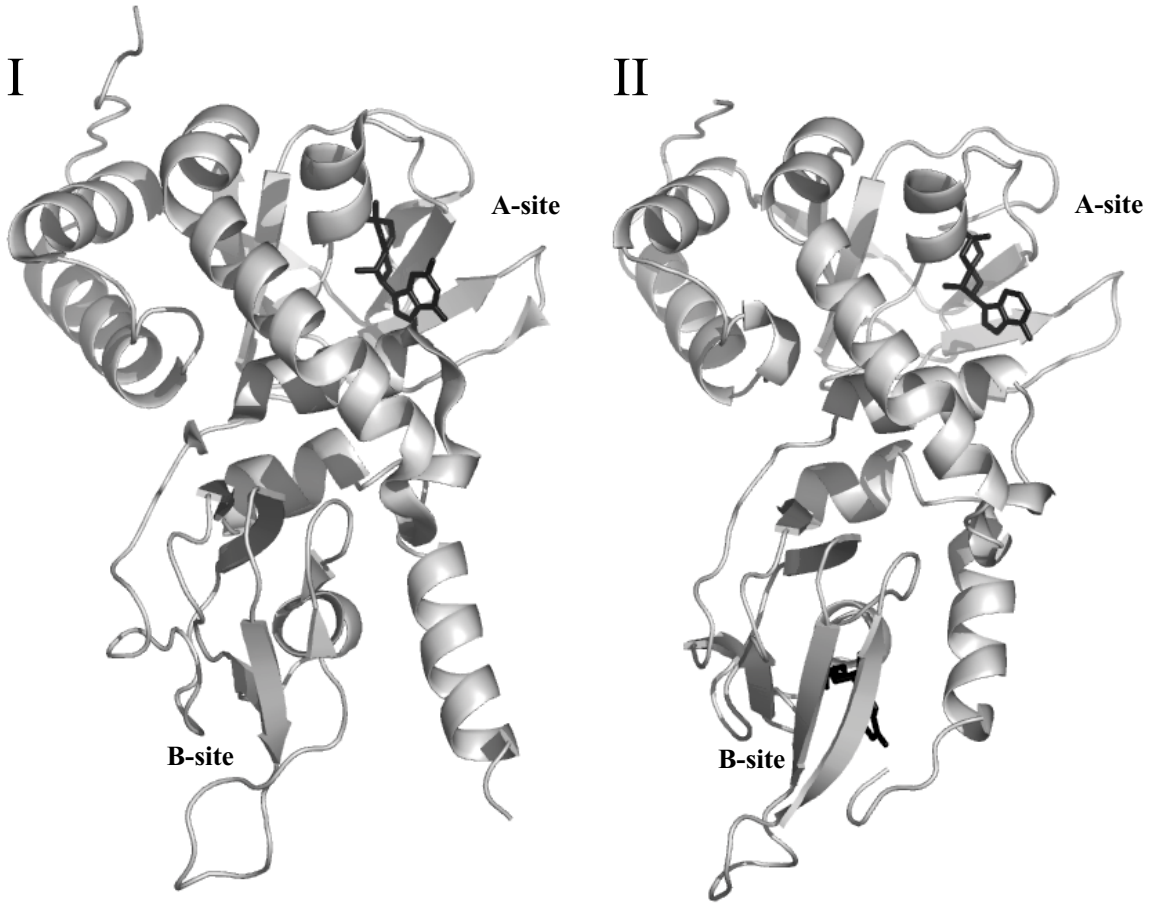

Figure 5: Ribbon representation diagram of the regulatory subunit of PKA. **(I)** The structure of the regulatory subunit where site A is occupied by cGMP and site B is unoccupied (1RL3). **(II)** The structure of the regulatory subunit where site A and B are occupied by cAMP (PDB 1RGS).

Catalytic core.

The catalytic domain of protein kinases functions in the transfer of the γ-phosphate of ATP onto a serine, threonine or tyrosine of the target peptide or protein. Much of what we currently know about the structure of this core and the mechanism behind the reaction was obtained by looking at the crystal structure of the catalytic subunit of cAMP kinase, which was first elucidated in 1991 [96-99]. Currently, several crystal structures of the catalytic subunit of PKA in the presence of nucleotide, substrate and inhibitors [100, 101], as well as the apo-enzyme [102] are available. These structures probably provide the best examples of how a kinase recognizes its substrates, as well as inhibitors, and also how the enzyme moves through catalysis. To complement crystallographic structures, fluorescence anisotropy [103,

104], NMR [105] and hydrogen/deuterium (H/D) exchange coupled with mass spectrometry [91, 92] have been used to probe the dynamical behavior of PKA. Based upon the X-ray coordinates of the cAMP kinase catalytic subunit, the structure of the catalytic domains of PKG and Myosin Light Chain Kinase (MLCK) have been modeled [106-108], upon what is now recognized as the conserved core of essentially all mammalian protein kinases [109, 110].

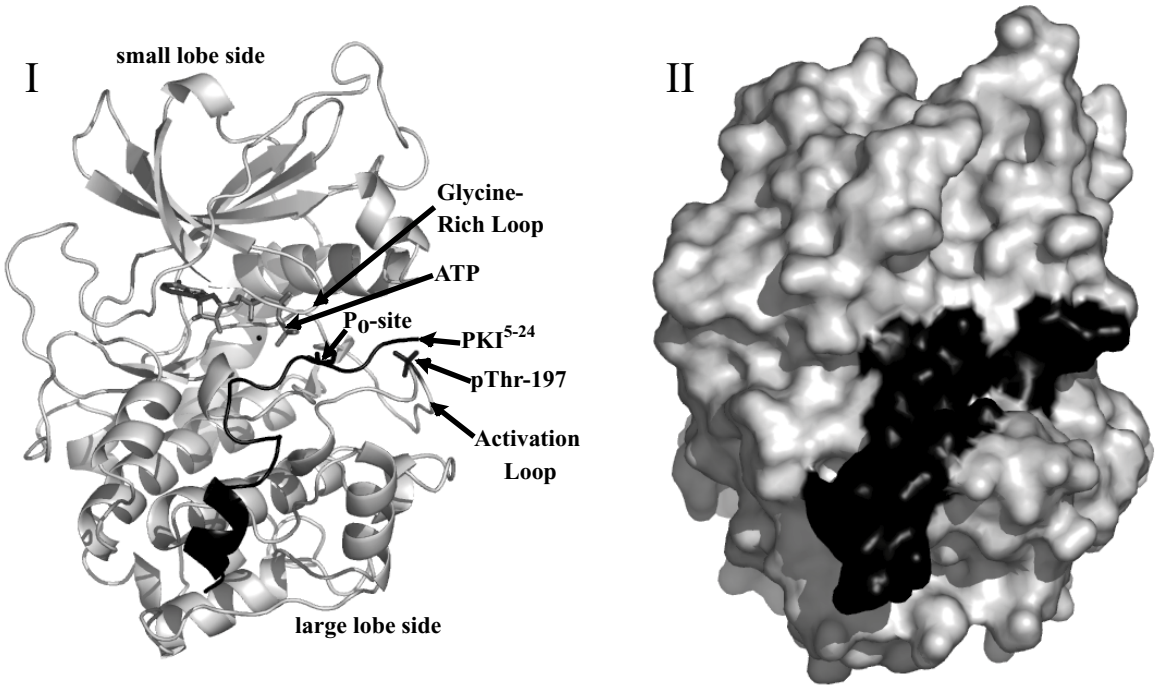

Figure 6: Ribbon **(I)** and surface **(II)** representation of the crystal structure of the catalytic subunit of PKA, co-crystallized with MnATP and PKI (PDB 1ATP). The catalytic subunit is shown in light grey and ATP (stick) PKI (ribbon) are shown in dark black.

Structure: The crystal structure of the catalytic subunit of PKA, shown in Figure 6, displays a bilobal layout. The smaller amino terminal lobe is associated primarily with binding of ATP [100, 111, 112], whereas the larger lobe, associated with recognition and binding of peptide substrates, contains most of the residues that contribute directly to the phosphoryl transfer [96]. While β strands dominate the small lobe, the large lobe is mostly helical. Together the two domains form a small cleft in which the ATP is buried. The surface of the large lobe at the outer edge of the cleft provides a stable surface on which peptides dock. As mentioned this core is conserved amongst all protein kinases, although the outer segments that flank this core, the N-terminal and C-terminal residues are not [113]. Within the catalytic core of PKA and PKG an essential threonine is phosphorylated. This phosphothreonine is part of a loop

segment known as the activation loop and phosphorylation of the threonine is a crucial on/off step for the activation of many kinases. The activation loop of protein kinases is a conserved and essential motif in the protein kinase family. Although the exact function of the activation loop is unclear, in phosphorylated form it appears to facilitate the phosphoryl transfer step through stabilizing effects [114].

Me^{2+}/ATP binding: To transfer the γ-phosphate from ATP to a protein substrate, all protein kinases require a metal ion. The serine/threonine protein kinases require a Mg-ATP complex while MnATP is the specific substrate of tyrosine-specific protein kinases [115, 116]. The role of the metal ion in catalysis has been studied the most for phosphorylase kinase and PKA using various methods [117-123]. From the crystal structure of PKA, co-crystallized with ATP and metal ions it became apparent that two metal ion binding sites are present. One metal binding site is required for catalysis and one is associated with inhibition. The activating metal ion bridges the β- and γ- phosphates and ultimately forms an enzyme-ATP-metal bridge. The second inhibitory metal binding site was predicted to be an enzyme-metal-ATP bridge between the α- and γ-phosphate of ATP. The activating metal binding site has a K_d of ~10 μM for MgATP and the affinity for the second magnesium is 1.4 mM [117].

Peptide substrate recognition: The structurally conserved bilobal core possesses most of the determinants necessary for substrate binding in the larger amino terminal lobe. It is assumed that subtle difference in the larger lobe determines to a large degree the substrate specificity of each protein kinases. Substrate recognition plays an eminent role in the determination of protein kinase specificity. In general, kinases recognize target sequence regions on basis of the residues immediately flanking the site of phosphorylation. These local residues define a consensus sequence for recognition by a particular kinase. The primary sequence requirement of the catalytic site of cGMP kinase follows the rules established for cAMP kinase. Peptide substrates with a primary amino acid sequence motif RRX-S/T-X are in general recognized by both PKA and PKG. In this consensus sequence the phosphate excepting serine or threonine is preceded by two or three positively charged amino acids. Detailed insight into high affinity substrate recognition of PKA was obtained from the crystal structure of the ternary complex of the catalytic subunit of PKA and a 20 amino-acid peptide inhibitor $PKI^{(5-24)}$ [124, 125]. Kinetic studies with substrate analogues of $PKI^{(5-25)}$ have shown that besides the basic residues adjacent of the phosphate accepting serine, the amino terminal residues of

$PKI^{(5-24)}$ are essential for high affinity recognition by PKA. This part of PKI adapts an amphipathic α helix of which the hydrophobic site binds to a hydrophobic pocket on PKA (see Figure 6). PKG recognizes the basic domain of $PKI^{(5-24)}$, but does not recognize the amino-terminal parts [126]. Screening of synthetic peptide libraries elucidated the optimal substrate recognition motifs KRAERKASIY and TQAKRKKSNA for PKA and PKG, respectively [127]. The catalytic core of PKG shows a high degree of homology with the catalytic core of PKA; 40% of the residues in the small lobe and 47% of the residues in the large lobe are conserved [42]. However due to difference in their target substrates it is likely that the peptide binding site of cGMP kinase differs from that of the cAMP kinase, since kinase specificity for peptide substrates is primarily determined by the peptide binding domain.

Catalysis: Due to the availability of crystal structures and a large set of experimental data on the kinetics a detailed picture for catalysis exists for PKA. Many of the relevant conformational states associated with catalysis of catalytic subunit of PKA have been captures in crystal lattices (For reviews see Taylor *et al*. [128], Smith *et al.* [129], Johnson *et al.* [130] and Taylor *et al.* [131]).

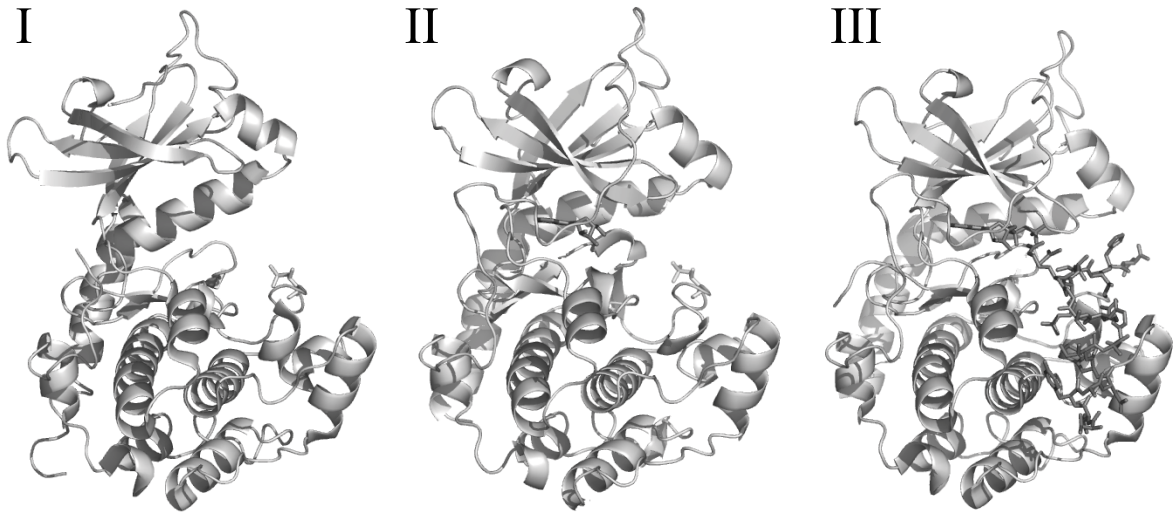

Figure 7: Opening and closing of the catalytic cleft as seen in crystal structures of the catalytic subunit of PKA. Shown are **(I)** the apoenzyme (PDB 1J3H), **(II)** the adenosine binary complex (PDB 1BKX) and **(III)** a transition state complex with aluminum fluoride:ADP, and a substrate peptide, TTYADFIASGRTGRRASIHD (PDB (1L3R). The apoenzyme represents the most open conformation, the binary complex represents an intermediate state and the aluminum:ADP, peptide complex represents the fully closed conformation.

Together with kinetic data this provided a basis for a structural framework that serves as a model for all protein kinases. Three different crystal structures of the catalytic subunit of PKA revealed that opening and closing of the catalytic cleft, and in particular the glycine rich loop is essential for catalysis. Figure 7 displays three crystal structures of PKA; *(I)* the apo-enzyme of the catalytic subunit (1J3H), *(II)* a binary complex of the catalytic subunit of cAMP-dependent protein kinase and adenosine (1BKX) and *(III)* a quaternary complex of the catalytic subunit, ADP, the peptide inhibitor PKI and aluminum fluoride (1L3R).
In the apo-enzyme the smaller N-terminal lobe is positioned further away from the larger C-terminal lobe. Upon binding of ATP the N-terminal lobe moves closer to the C-terminal lobe. Finally when substrate peptide and ATP are bound simultaneously both lobes are oriented even closer to each other (See Figure 7). In more detail, the ATP is bound to a high affinity site in the anti-conformation, and two Mg^{2+} ions neutralize the negative charge of the ATP phosphates. Following formation of the enzyme-Mg^{2+}/ATP-peptide substrate quaternary complex, the γ-phosphate of ATP is rapidly transferred to the substrate. A general base catalyst at the active site may mediate phosphotransfer, but direct nucleophilic attack by the acceptor serine of the substrate peptide has also been suggested. Following transfer of the phosphate to peptide substrate, the phosphopeptide quickly dissociates from the catalytic site, followed by the rate limiting dissociation of Mg^{2+}/ADP [132]. Phosphoryl transfer for the catalytic subunit of PKA is extremely fast, greater then 500 s^{-1}. The actual rate turnover rate (k_{cat}) is only 20^{-1}. The rate limiting step is the release of ADP or more realistic the conformational change that allows the release of ADP.

PKG regulation.

Most serine/threonine- or tyrosine-specific protein kinases are activated by allosteric ligand binding (e.g. cAMP, cGMP, calcium, insulin, EGF), but the molecular mechanism involved in activation of the protein by ligands is in most cases not fully understood. In the case of PKA, binding of cAMP to the inactive R_2C_2 heterotetramer induces dissociation, which liberates the catalytic subunits from regulatory subunits. In contrast, in PKG the catalytic and regulatory domain reside on a single polypeptide chain and a similar dissociation cannot occur. In the absence of cGMP, PKG is maintained in a catalytically basal or inactive state of phosphorylation of exogenous substrates (heterophosphorylation) by autoinhibition. When intracellular cyclic nucleotide levels increase, heterophosphorylation is activated, but the mechanism by which cGMP stimulated this activity is largely unknown. It is suggested that

activation of PKG either by cyclic nucleotide association with the two allosteric cyclic nucleotide-binding sites or by autophosphorylation is associated with a conformational change that removes the influence of the autoinhibitory domain on the catalytic site, thus reducing the efficiency of pseudosubstrate site competition for substrate binding [53, 75]. Activation of PKG by cGMP is associated with a dramatic elongation of the protein as shown by small angle light scattering. Fourier transform infrared spectroscopy data suggest that the conformational change induced by cGMP binding is primarily due to a topographical movement of the structural domains of PKG rather than secondary structural changes within one or more of the individual domains [133]. Studying cGMP induced changes by combination of ion exchange chromatography, gel filtration chromatography, native polyacrylamide gel electrophoresis and partial proteolysis showed that the apparent elongation of the protein is associated with an increase in the net negative surface charge [74]. The conformational change induced by cGMP is believed to induce the release of the autoinhibitory domain from the active site, thereby activating the kinase. This is indicated by a remarkable increase in the proteolytic sensitivity of the autoinhibitory domain in the presence of cGMP, indicating that a conformational change has occurred that increases the solvent exposure of this region [74]. Small angle x-ray scattering studies on a monomeric deletion mutant of PKG ($\Delta^{1\text{-}52}$PKG Iβ) suggested that the elongation occurs upon binding of cGMP to both sites simultaneously [134]. Cyclic nucleotide binding also stimulates the intermolecular autophosphorylation of Type I PKG, resulting in altered functional characteristics of the enzyme. cGMP binding to the high affinity site primarily stimulates autophosphorylation. cGMP binding to the low affinity site in combination with occupation of cGMP at the high affinity site is stimulatory for heterophosphorylation [67, 72]. Therefore, if cellular levels of cGMP increase, it would be predicted that initially the rate of autophosphorylation would accelerate because of cGMP binding to the high affinity site. However further elevation in cGMP would lead to cGMP-binding to the low affinity site as well and thereby increase heterophosphorylation and decrease the rate of autophosphorylation even though the rate of this latter process is still faster than that with no cGMP. A maximally active kinase is obtained when all four binding sites of the dimeric cGMP kinase are occupied. Activation by cGMP binding does not show cooperative behavior, although the binding sites A and B show positive cooperativity. The binding of the two substrates and MgATP to the enzyme, a process that decreases the affinity for the high affinity site B and increases that for the low-affinity site A, causes this apparent difference.

Physiological role of PKG

Although a great number of PKGs are known, the physiological function of these proteins has only been established in some cases. The highest concentrations of Type I PKG are found in the lung, cerebellum, smooth muscle and smooth muscle related tissue, platelets and intestinal mucosa [135-138]. Type II is less common and expressed only in intestinal epithelial cells [139], kidney, and brain [140]. Due to the structural similarity between PKA and PKG it is extremely difficult to study PKG pathways independent of those mediated by PKA, which is nearly ubiquitous. Furthermore, *in-vitro* studies initially led to the hypothesis of a cross-talk mechanism between the cGMP and cAMP signaling pathways (i.e. cross-activation of PKG by cAMP, or vice versa) [141-144]. This hypothesis was supported by the observation that cAMP stimulates autophosphorylation of PKG stronger than cGMP itself. In addition autophosphorylation lowers the cAMP concentration needed to activate PKG [67, 72, 145]. More recently mice lacking the PKG I coding gene demonstrated that the PKG isozymes regulate distinct cellular functions separate from those mediated by PKA [146, 147].

NO/cGMP signaling cascade: The cGMP dependent protein kinases have been shown to play an important role in the regulation of smooth muscle tone and blood pressure [148]. PKG is the major downstream target of the nitric oxide (NO) / cGMP signaling cascade (Figure 8). Interest in NO has exploded in recent years, due to the recognition that the gas plays an important role in many physiological processes, and that manipulating the NO pathway can have medicinal benefits. Nitric oxide activates soluble guanylyl cyclase (sGC), which catalyzes the conversion of GTP to the signaling molecule cyclic GMP (cGMP). Cyclic GMP is also synthesized by particulate gyanlyly cyclases (pGC's) that are activated by hormonal peptides. cGMP is an important second messenger that is capable of modulating a plethora of cellular functions. In contrast to the cAMP system, where activation of a specific protein kinase is responsible for most, if not all, off the biological effects, cGMP regulates a variety of enzymes and proteins including cGMP-gated ion channels, cGMP-regulated phosphodiesterases, and cGMP-dependent protein kinases. The vast majority of the biological actions of cGMP can be attributed to the activation of a specific cGMP-dependent protein kinase. Identifying the specific functions that are mediated by PKGs is the key to our understanding of the biological role of the nitric oxide/cGMP-signaling cascade. Recent advances have clearly identified specific intracellular targets of PKG. These include various

ion-channels [149], calcium-ATPase [150] and more recently, the PKG-IRAG-IP3R complex and the myosin binding subunit (MBS) and MLCK [151].

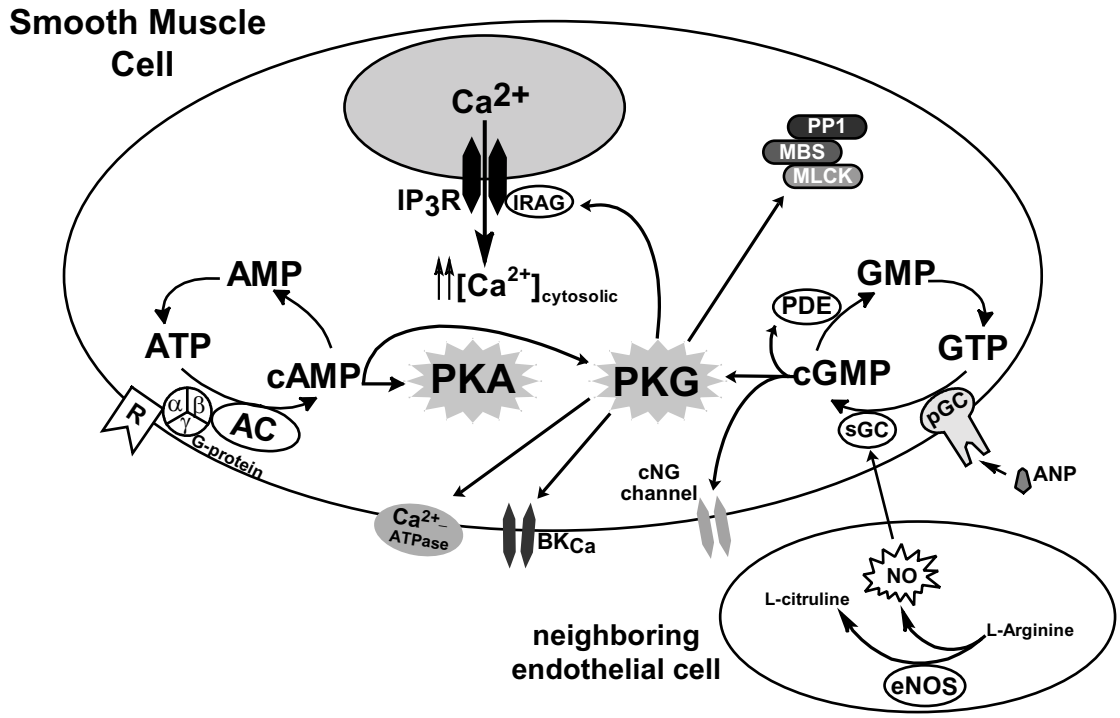

Figure 8: Simplified model for the role of PKG in the NO-cGMP signaling pathway in smooth muscle cells NO/cGMP signaling cascade. Neuronal and endothelial NO synthases are regulated by the intracellular calcium concentration, a rise of the calcium concentration leads to their activation and subsequently the formation of nitric oxide (NO). NO can diffuse into neighboring smooth muscle cells and where it stimulates soluble guanylyl cyclases, the enzymes that catalyze the conversion of GTP to cGMP. Cyclic GMP alters the activity of the cGMP receptor molecules (cGMP-dependent protein kinases, cGMP-regulated phosphodiesterases, cGMP-regulated ion channels) finally leading to changes in cellular function. Several target of PKG are known and their phosphorylation ultimately leads to relaxation of the smooth muscle cell

Negative feedback control of cellular cGMP levels is provided by the action of the cGMP-regulated phosphodiesterases. These enzymes are modulated by both allosteric regulation and protein phosphorylation [152, 153]. A particular phosphodiesterase PDE5 that is probable best known, is the site of action of the male impotence drug Sildenafil (Viagra), which causes penile erection [154].

III Mass spectrometric approached for protein analysis.

Biomolecular mass spectrometry

Characterization of post-translational protein modifications, such as phosphorylation, is one of the many tasks to be accomplished in the post-genomic era. From a technical standpoint a major requirement is the development of assays that allow temporal analysis of phosphorylation events, eventually at high spatial resolution in cells. In addition, rapid detection of phosphorylation sites, identification of protein kinase and protein phosphatase targets and in particular the understanding of protein kinase regulation and dynamics play eminent roles in unraveling phosphorylation mediated cellular signaling. The primary goal of the work described in this thesis is the use of mass spectrometry to study structural and functional aspects of the cGMP-dependent protein kinase. This protein kinase has been extensively studied for several decades using a plethora of biochemical and biophysical techniques, however many aspects about PKG are not fully understood. Understanding the cGMP-dependent protein kinase involves determining its structure and dynamics, the transient interaction with cyclic nucleotides, substrates and inhibitors as well as identifying and characterizing target substrates. Mass spectrometry (MS) has developed in the last decades to a powerful technique to study biomolecules such as proteins and peptides. In proteomics mass spectrometry is an indispensable tool in determining primary sequence information of proteins, including post-translational modifications. Additionally mass spectrometry can provide insight into secondary and tertiary structures of proteins as well as their interactions with ligands, inhibitors and/or substrates. The relative 'soft' nature of electrospray ionization allows the survival of non-covalent interactions during the ionization process and subsequently the determination of the mass of such a non-covalent complex. In this section several aspects relevant for the mass spectrometric analysis of proteins as used to conduct the work described in this thesis will be discussed below.

Ionization techniques: The mass of biomolecules or molecules in general is determined by accurately measuring its mass/charge (*m/z*) ratio. This ratio is determined in a high vacuum, which means the analyte has to be transferred from solid or solution into the gas phase and the analyte must also be charged. Biomolecules such as peptides and proteins are practically involatile and until the late seventies it was not possible to convert these large biomolecules into intact charged molecules in the gas phase. At that time mass spectrometry was primarily

used for the analysis of low molecular weight molecules in organic chemistry. Over the last decades several important developments have led to ionization methods that will allow the analysis of for instance peptides, proteins and oligonucleotides. Although initially fast atom bombardment (FAB) and plasma desorption (PD) already allowed successful analysis and characterization of peptides and small proteins by mass spectrometry, a real breakthrough came at the end of the 1980's with the development of electrospray ionization (ESI) and matrix-assisted laser desorption ionization (MALDI). With these two techniques the upper mass limit of mass spectrometers was tremendously raised to over 100 kDa. Both techniques are fast, simple and reproducible and allow picomole to femtomole amounts of material. ESI was originally described by Dole *et al.* in studies on the intact ions of synthetic and natural polymers of molecular mass around 100.000 Da [155, 156]. The utility of ESI for the analysis for biomolecules and as an interface for the coupling of liquid chromatography to mass spectrometry was later developed by Fenn *et al.* [157, 158]. Electrospray ionization allows the ionization of involatile compounds directly from a spray solution, which makes them amendable for mass spectrometric analysis. In electrospray, a spray solution is passed through a nozzle or a capillary. A plume of droplets is generated by electrically charging the liquid using a very high voltage (~1-3 kV). The charged liquid in the electrospray tip becomes unstable as it is forced to hold more and more charge. The liquid reaches a critical point, at which it can hold no more electrical charge and at the tip it blows apart into a cloud of tiny, highly charged droplets. The highly charged droplets shrink as neutral solvent evaporates. At some point the charge repulsion overcomes the cohesive droplet forces leading to a 'Coulombic fission' of the droplet in two or more smaller droplets. Repeated evaporation and fission leads to very small charged droplets, which are the precursors of the gas phase ions. These ions generally arise by attachment of protons, alkali cations, or ammonium ions for positive ion formation or, by reversing the electrospray polarity, by proton abstraction for negative ion formation. The actual mechanism by which molecular ions are ultimately formed is not completely understood. Currently two models exist that describe the formation of molecular ions by electrospray ionization, (*i*) the ion-evaporation model and (*ii*) the charge residue model. In the ion-evaporation model, relative small and volatile molecules are able to escape from a highly charge droplet as charged species [159, 160]. In the charge residue model [161, 162], which appears to holds for the larger biomolecules, the analyte resides within the center of the droplets, unable to escape from the droplet. Eventually the size of the droplet will reach the size of the biomolecules and the charged compounds still present within

the final stages of the droplet will charge functional groups within the biomolecules. In the last stages the residual solvent components are removed from the biomolecule and what remains are charged biomolecules. Electrospray ionization is in general conducted under atmospheric pressure. A big instrumental challenge is the transfer of ions generated in the ion source into the high vacuum of the mass spectrometer. Mass spectrometer manufactures have overcome this by usage of a pinhole aperture around 100-500 μm in diameter. In this design, the created ions are drifted (with the help of an electric field) towards the aperture. Once the ions have passed through the aperture, they can be refocused and analyzed.

The other ionization technique that, together with electrospray ionization, has conquered the field of biomolecular mass spectrometry is MALDI [163]. In this method of ionization, the analyte is mixed with a saturated solution of matrix. The resulting mixture is deposited on a target and allowed to dry. Following, the target is transferred into the vacuum of the mass spectrometer. The matrix is a non-volatile solid organic compound (typical matrices are 2,5 dihydroxybenzoic acid, α-cyano-4-hydroxycinnamic acid or sinapinic acid) that serves to absorb the energy from the laser (typically a nitrogen laser of 337 nm), which causes the material to vaporize. The matrix is believed to facilitate the ionization process when sample and matrix are in the gas phase via processes not entirely understood. The charged matrix and analyte molecules are abstracted from the ion source and directed to the mass analyzer. MALDI is relatively tolerant for heterogeneous samples and for the presence of salt. A major advantage is that MALDI consumes small quantities of sample and hence acquisitions time is longer compared to ESI. Where ESI is capable of forming multiply charged molecules, MALDI forms (in general) singly charged molecules. This latter is advantageous when analyzing complex mixtures, such as protein digests.

Mass spectrometers: At the basis of most modern mass spectrometers are three essential parts; *(i)* an ion source, *(ii)* a mass analyzer and *(iii)* an ion detector. The ions that are generated from the analyte in the ion source are accelerated into the mass analyzer due to a voltage potential between ion source and mass analyzer. The mass analyzer separates the ions on basis of their mass-to-charge *(m/z)* ratios. The detector registers the m/z values of all ions and a mass spectrum is generated, in which the ion intensity vs. m/z is plotted. In addition to measuring masses of molecules, structural information may be obtained in a tandem mass spectrometer, for instance by collision induced dissociation (CID) experiments

***Mass analyzers*:** Mass analyzers separate ions by making use of appropriate electric fields, sometimes in combination with magnetic fields. Nowadays the most widely used mass analyzers include the quadrupole mass analyzers and the time-of flight (TOF) mass analyzer, which will be briefly discussed below. A quadrupole mass analyzer is composed of four parallel rods, positioned in a radial array (for a review see [164]). The rods are electrically connected to each other in opposite pairs. A constant (DC) voltage and an alternating (AC) voltage are applied to the two pairs of electrodes. The alternating electric field makes the ions go off into spirals as they pass down the quadrupole. Each ion will have a stable trajectory through the quadrupole at certain alternating frequency and/or DC potentials. Varying these two voltages during a single scan will provide transmission of all ions within a certain *m/z* range. CID spectra can be recorded on a triple quadrupole instrument. The first quadrupole serves as the mass filter for isolation of the parent ion, the second quadruple is then used as a collision cell and the third quadrupole analyzes the fragment ions. An alternative to linear quadrupoles is the quadrupole ion trap (for a review see [165]). In this instrument the ions are trapped in a cavity between a circular electrode and two hyperbolically shaped end-caps. The simplest kind of mass analyzer is probably the time of flight (ToF) analyzer (for reviews see [166, 167]). In a ToF mass analyzer ions are accelerated into a field-free flight tube, with a known length *d*. All ions will travel through the tube within a certain time *t*, which is related to the *m/z* ratio of the ion. The time *t* and length *d* can be used to deduce the velocity of the ion. All ions were given the same kinetic energy U_{kin}. Since $U_{kin} = ½mv^2$, knowing the initial kinetic energy and the velocity allows the determination of their *m/z* ratio. A main drawback of linear ToF analyzer is the limited resolving power, which is mainly due to a spread in the initial kinetic energies of the ions or a spread in the initial spatial positions of the ions. Resolution can be increased by making use of a reflectron, which improves resolution, but this at the cost of sensitivity and the upper mass limit. The reflectron consists of an electrostatic ion mirror that refocuses and reflects the ion towards the detector surface. The use of a reflectron results in extending the drift length and in providing nearly constant flight time for ions with equal *m/z* by correction for the initial kinetic energy spread. Higher energy ions pass the flight tube faster, but spend more time in the reflectron, while less energetic ions passing more slowly spend less time in the reflectron. With optimal settings ions of the same *m/z*, but with an initial kinetic energy spread will arrive at the detector together.

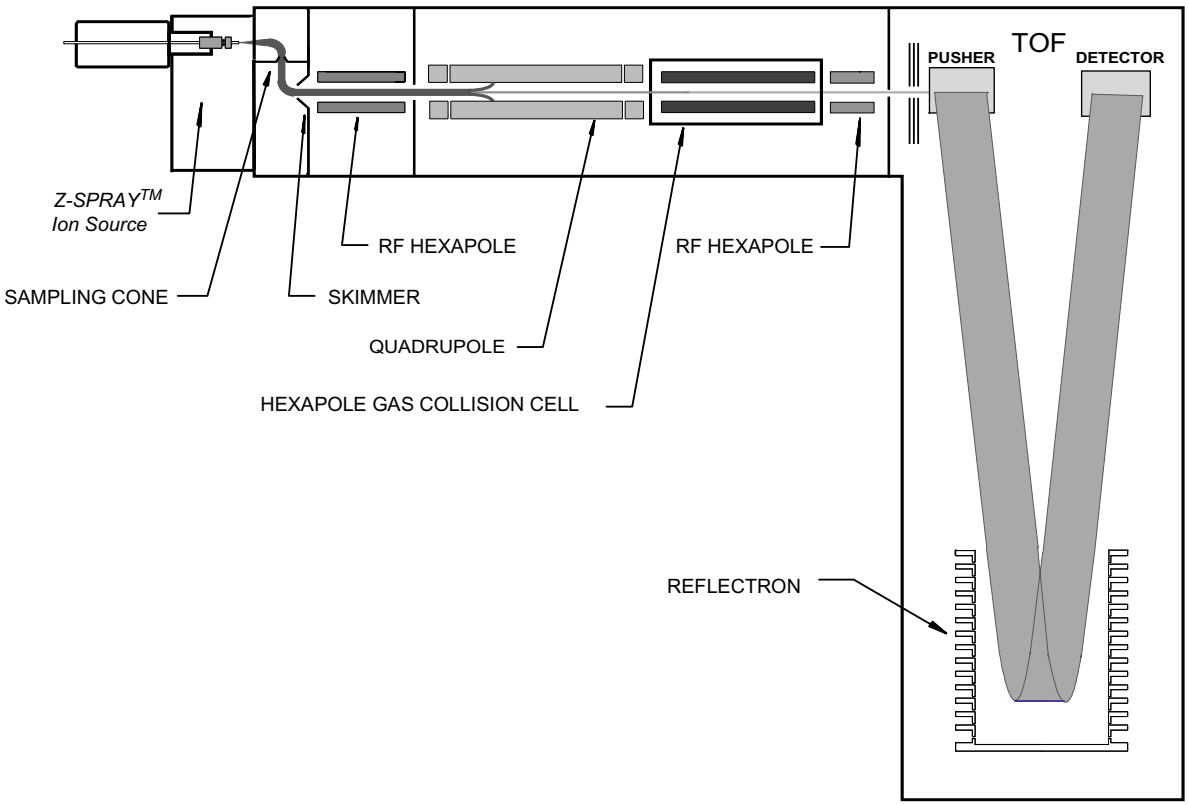

Figure 9: Schematic representation of a hybrid quadrupole orthogonal time-of-flight instrument.

By combining a quadrupole and ToF mass analyzer a hybrid Q-ToF mass spectrometer is generated, which is schematically shown in Figure 9 (for a review see [168]). In this instrumental setup the ToF mass analyzer is positioned orthogonally to the quadrupole. In general orthogonal configuration of the ToF has the advantage that it is compatible with continuous ionization methods such as ESI [169]. The quadrupole, when operating in the RF-only mode, acts as a wideband-pass mass filter transmitting ions across a broad *m/z* range and those ions are analyzed by the ToF (ms-mode). In the tandem ms/ms mode, the quadrupole acts as *m/z* filter for selection of the precursor ion, which is activated by collisions with an inert gas in the collision cell. Again the ToF analyzer separates all the fragment ions.

Fourier transform ion cyclotron resonance mass spectrometry (FTICR-MS) is playing an increasing role in the characterization of cellular systems owing to its capabilities for providing higher confidence of identification, increased dynamic range and sensitivity unmatched by other MS platforms. The basis behind FTICR (for a review see [170]) is that a small cloud of ions is trapped inside a strong magnetic field. The magnetic field forces the ions to make a circular, so-called cyclotron, motion. The angular frequency of that motion is

dependent on the field strength and the *m/z* ratio of the ions. Ions are exposed to an oscillating electric field that produces a net outward electric force on the ions for a limited period of time. This oscillating electric field is created by applying a RF potential on the two excitation electrodes and is referred to as the excitation pulse. The ions will only experience a net continuous outward force if the frequency of the oscillating electric field is resonant with the cyclotron frequency of the ions. To excite all ions a RF-pulse is generated, which consists of multiple frequencies. After excitation the radius of the ion clouds is increased and all ions with the same *m*/*z* move coherently in a circular orbit. The ions are detected by measuring the oscillating image current they create when passing the detector electrodes. CID experiments are conducted by exciting the trajectories of all ions of no interest to radii outside the boundaries of the cell. The selected ion can be excited by collisions with an inert gas, often invoked by sustained off resonance irradiation (SORI). Particularly in proteomics, where global and quantitative approaches are essential, FTICR-MS is expected to make expanding contributions. Recent advances in the fields that have particular importance for proteomic applications include the use of high-performance micro-capillary column separation techniques coupled to FTICR, as well as methods that improve protein identification, sensitivity, dynamic range and throughput [171-173]

Detectors: In all mass spectrometers other than FTICR-MS instruments, the ions are detected after they are separated by converting detector-surface collision energy of the ions into emitted ions, electrons, or photons that are then sensed with various light or charge detectors. As already discussed above, in FT-ICR mass spectrometers ions are detected by the oscillating signal they induce on the detecting plates when orbiting in the FTICR cell. In most of the time-of-flight mass spectrometers, ions are amplified using a multiplier. Most common multipliers are electron multiplier, photomultipliers or multi channel plates (MCP). Electron multipliers are made up from series of dynodes, which are made from electron emitting material. Ions that hit the first dynode, liberate electrons from the dynode, which are attracted to the next dynode and will liberate again electrons which will travel to the next dynode and so on. In a photomultiplier, electrons liberated from a first dynode strike on a phosphorus screen, which will release photons that are detected by a photomultiplier. Multi channel plates are flat glass plates with numerous small channels. These channels are not perpendicular to the surface but have a bias angle of several degrees. Therefore ions entering the channel will always hits the wall of the channel and this sets secondary electrons free.

These electrons are accelerated by the electric potential applied to the plates. On their way through the channels the electrons themselves hit the wall several times and in that way eventually a small current is generated, which is used to register the ion event These multipliers have the disadvantage that the higher the mass of the ion, the lower the gain (detection efficiency) for constant energy ions. Important to note here is that besides ionization efficiency, these detectors thereby also discriminate against the higher *m/z* range.

Primary sequence information: In proteomic research the determination of the primary sequence of proteins and peptides is highly important. Primary sequence information on peptides and proteins can be obtained by low energy CID experiments on protonated peptides, of which the resulting fragmentation spectra are relatively easily interpreted. Fragmentation of peptides under low energy CID mainly occurs on the peptide backbone**.**

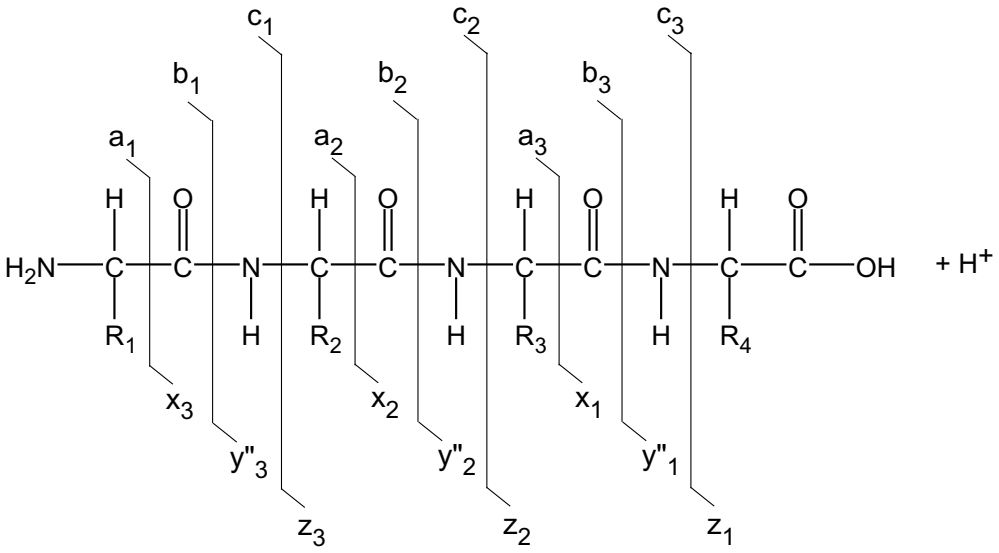

Figure 10: Roepstorff and Fohlman nomenclature for peptide fragmentation [174]. Fragmentation is predominantly observed at the amide bond. N-terminal fragment are named a_n, b_n and c_n type ions and C-terminal fragments x_n, y_n and z_n type ions.

There are three different types of bonds that can fragment along the amino acid backbone: the NH-CH, CH-CO, and CO-NH bonds. Each bond breakage gives rise to two species, one neutral and the other one charged, and only the charged species are monitored by the mass spectrometer. The charge can stay on either one of the two fragments depending on the chemistry and relative proton affinity of the two species. Hence there are six possible fragment ions for each amino acid residue and these are generally labelled as the a, b, and c"

ions having the charge retained on the N-terminal fragment, and the x, y", and z ions having the charge retained on the C-terminal fragment (see Figure 10). This accepted nomenclature for peptide fragment ions was first proposed by Roepstorff and Fohlman [174], and subsequently modified by Johnson *et. al.* [175]. In practise the most common cleavage sites are at the CO-NH bonds which give rise to the b and/or the y" ions. Hence, primary sequence information can be deduced from these peptide fragmentation spectra by determining the mass difference between two adjacent b or y" ions, as this mass difference match the residual mass of the amino acid at that position of cleavage. General drawback of this sequencing approach is that neither leucine and isoleucine, nor lysine and glutamine can be differentiated because they have (almost) the same residual mass.

Liquid Chromatography-Mass Spectrometry

Proteomics represents a significant challenge to separation scientists because of the diversity and complexity of proteins and peptides present in biological systems. To reduce sample complexity prior to mass spectrometry, proteins or peptides can chromatographically separated using liquid chromatography techniques. Liquid chromatography is recognized as an indispensable tool in proteomics research since it provides high-speed, high-resolution and high-sensitivity separations. Most of protein and peptide separations in proteomics are done in the reversed-phase liquid chromatography mode, mainly due to its direct coupling compatibility with electrospray ionization. Although relatively complex samples can be well separated by RPLC, the continuously increasing complexity of proteomics samples demands the development of separation techniques that have higher separation and identification capabilities. Nowadays, commercially available column materials (typically 3.5-5 μm in diameter) are extensively used in conventional and capillary LC systems. Theory predicts an increase in efficiency with decreasing particle size due to reduced eddy diffusion and resistance to mass-transfer contributions to band broadening [176]. The use of smaller stationary-phase spherical supports (1-3 μm in diameter) is gaining popularity in capillary chromatography. In combination with ultra high pressure liquid chromatography this offers an alternative method to increase separation speed and thus decrease analysis time [177, 178]. One of the disadvantages of this approach is that it requires special high pressure pumping equipment and that its peak capacity is still too low to adequately resolve complex mixtures often encountered in proteomics. Monolithic stationary phases have been developed as an alternative to granular packed columns. They consist of a polymeric monolithic stationary

phase which has the advantage that there is no intra-particular void volume. These columns have attracted interest due to their ease if preparation, reliable performance, good permeability and versatile surface chemistry [179]. Finally, an alternative method to improve resolution, two-dimensional liquid chromatography is routinely used. In most cases ion-exchange chromatography is used as the first dimension and RPLC as the second dimension.

Protein phosphorylation and mass spectrometry

Mass spectrometry is ideally suited for mapping protein modifications such as phosphorylation since changes in primary structure are directly observed as alterations in protein or peptide mass. Historically the analysis of protein phosphorylation sites was restricted to studies at the single-protein level. More recently, attempts have been made to study protein-phosphorylation on a larger scale by elucidating the phosphorylation status of all proteins present in a cell [180, 181]. Detailed characterization of protein phosphorylation is often hampered by the low amount of material available for analysis and by the fact that the stoichiometry of protein phosphorylation is in many cases very low (i. e. the phosphopeptides exist as minor fraction in a large background of unphosphorylated peptides). In addition mass spectrometric responses of phosphopeptides may be potentially suppressed by unphosphorylated peptides. The analysis of phosphopeptides could be significantly enhanced when the number of non-phosphorylated peptides is reduced. Several strategies have been developed to enrich samples for phosphorylated peptides or phosphoproteins before analysis. Although of eminent importance, there is at present no unique or complete method for analyzing phosphoproteins by mass spectrometry. Instead, many alternative approaches exist, all with their own advantages and disadvantages, that, when used in combination, can yield detailed information on the phosphorylation status of a protein. Enrichment and subsequent identification of phosphorylation sites can be performed with the phosphopeptide-fishing techniques such as immobilized metal-ion affinity chromatography (IMAC) [182] or chemical approaches [183, 184]. IMAC is probably the most widely used method for the selective enrichment of phosphopeptides. In this technique, metal ions (usually Fe^{3+} or Ga^{3+}) are immobilized on a chelating support. Phosphopeptides will selectively bind to this support because they have affinity for the metal ions. Phosphopeptides can be released by increasing the pH or by using a phosphate buffer. Chemical derivatization involves the replacement of the phosphate group with for example ethanedithiol, via β-elimination, followed by a Michael addition. In this latter step several functional groups (e.g.

biotin) could be introduced, which would allow further specific isolation steps. It should be noted that other O-linked modified serine and threonine residues (e.g., modified by glycosylation), would also undergo β-elimination and subsequent derivatization to form the same end product. Hence, this approach for the detection of phosphoserine and phosphothreonine containing peptides may overestimate their levels in cases where O-linked glycosylation is involved. Differentiating between O-linked phosphorylation and glycosylation has become an important issue since the discovery of the O-GlcNac modification to Ser/Thr [185]. Immunoaffinity chromatography is another powerful tool for the isolation and purification of phosphorylated peptides or proteins [186-188]. In this technique, the antibody, directed against phosphoserine, phosphothreonine or phosphotyrosine is immobilized on a resin. Peptide digests of a phosphoprotein or a pool of protein containing phosphoproteins is loaded onto the column followed by washing and selective elution of the antigenic peptides or proteins. This approach has the advantage that it has the powerful selectivity of an antigen-antibody system [189]. Detection methods for the identification of phosphopeptides in complex mixtures without any enrichment steps have also been reported. In CID experiments phosphorylated serine and threonine containing peptides readily undergo a gas-phase β-elimination of the phosphate moiety. This reaction can be monitored in a neutral loss scanning experiments. Peptides displaying this characteristic neutral loss can be easily sequenced in a MS3 experiment, where formerly phosphorylated serine or threonine will be identified as dehydroalanine of dehydroamino-2-butyric acid, respectively [190-192]. Another approach takes advantage of the formation of phosphospecific marker ions that are produced in CID conditions in the negative ion mode. Using relatively high collision energies, phosphoserine, phosphothreonine and phosphotyrosine containing peptide-fragmentation yields ions at *m/z* 63 and *m/z* 79, corresponding to PO_2^- and PO_3^-. Scanning for these diagnostic ions during negative ion LC-ESI-MS analysis offers a sensitive and selective approach to detect phosphopeptides in complex mixtures [193-195]. Drawback of this approach is that sequencing of the phosphopeptides requires switching back the mass spectrometer to the positive ion mode.

Structural analysis of proteins

Besides the determination of accurate masses, obtaining primary sequence information and characterizing posttranslational modifications, mass spectrometry can also be used to study the secondary, tertiary and even quaternary structures of proteins. Since the advent of

electrospray ionization it has become possible to ionize biomolecular complexes of increasing complexity and masses exceeding 1 megaDalton [196-198]. Of particular importance in this research area is the development of nanoflow electrospray [199]. Nanoflow electrospray mass spectrometry is a simple modification of electrospray mass spectrometry [157], in which the diameter of the nanospray capillary is reduced to a few micrometers. Nanoflow ESI allows sample introduction from aqueous solutions containing appropriate buffer conditions to maintain proteins in native conformations. A variety of innovative approaches emerged in recent years that allow deducing more information from a mass spectrum then solely the mass of biomolecules (for reviews on this topic see [200-202]. These include the detection of non-covalent interactions [200, 203, 204], detection of conformational changes [205, 206], measurement of relative dissociation constants [207, 208] and determination of cooperativity in the binding of ligands to multisubunit enzymes [209].

Protein mass spectra: A typical *m/z* spectrum of a protein ionized by electrospray displays a bell shape distribution of ion signals, each referring to the protein mass in a range of different charge states (the so called charge state envelope). For the positive ion ESI spectra of proteins the determinations of the protein mass M_r is straightforward given two assumptions. (*i*) Adjacent peaks of a series differ only by one charge and (*ii*) and charging is solely due to one and the same cation attachment (preferentially a proton). With this it follows that the measured *m/z* ratios for each peak in the charge state envelope are related by a series of simple linear equations where M_r and charge n are unknown (see Figure 11 for an example). Calculation of M_r for each of the observed *m/z* values provides enhanced precision. For the data presented in Figure 11 a standard deviation of ± 0.24 Da is observed for 16 *m/z* values from one spectrum (Theoretical mass 14264.18, measured mass 14264.36). The error in the determination $[(M_r^{theoretical} - M_r^{measured})/ M_r^{theoretical}) \times 100\%]$ is 0.001%.

Charge state distributions: Information about the folding a protein can be extrapolated from its charge state distribution. Under denaturing conditions all solvent exposed chargeable residues can be charged, hence unfolded protein mass spectra display a charge state envelop in the low *m/z* region. If the protein is kept un-denatured or folded conditions, for example by spraying it from a buffered aqueous solution at neutral pH, a protein may remain folded and the only chargeable residues reside on the outer surface of the protein. The amount of chargeable residues is thereby lower then when the protein is unfolded. This is reflected in the obtained mass spectra with the appearance of ion signal in the higher *m/z* region [206].

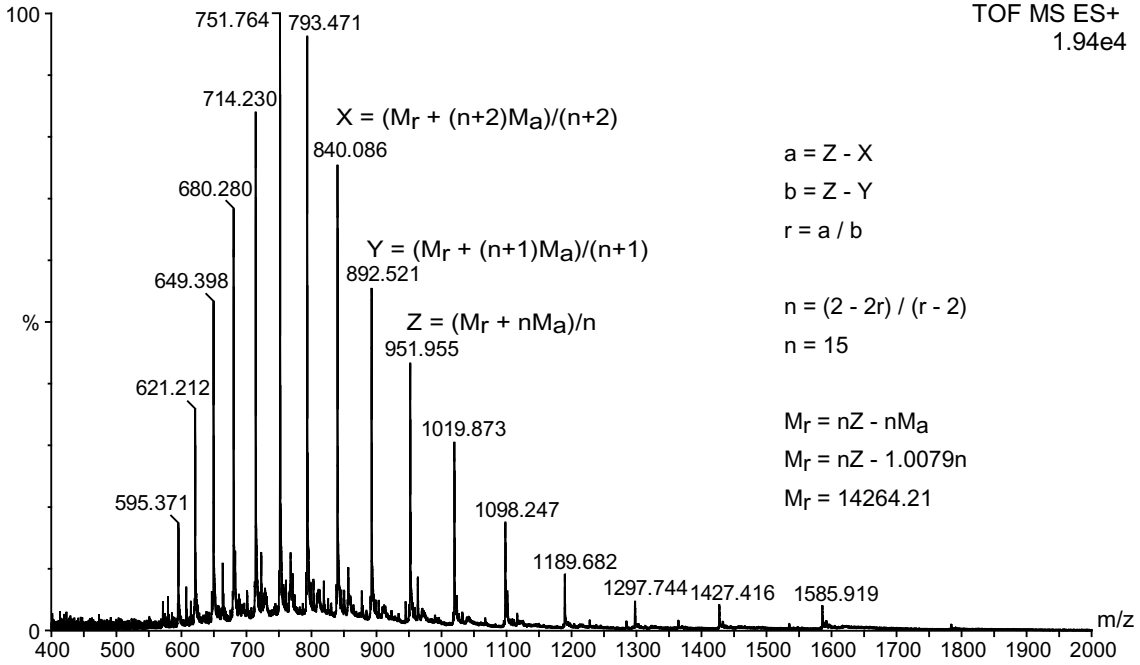

Figure 11: ESI-TOF-MS spectrum of human activated RNA polymerase II transcriptional coactivator p15 (M_r 14264.178 Da) electrosprayed from a solution containing ~10 µM p15 in 50% acetonitrile and 0.1% formic acid. Peaks *m/z* 595.371 through *m/z* 1585.919 are centroid values for these multiply (24+ through 11+) ions. The simultaneous mathematical relations between three adjacent peaks X at *m/z* 840.086, Y at *m/z* 892.521 and Z at *m/z* 951.955 are listed, including the determination of the charge *n* and molecular mass M_r.

Hydrogen/Deuterium Exchange: Additional information about the unfolded and folded state of proteins may be obtained via hydrogen/deuterium exchange mass spectrometry [210]. H/D-exchange mass spectrometry involves the measurement of the time course of the replacement of surface-exposed backbone amide hydrogens for deuteriums. Unfolded proteins are more susceptible to deuterium exchange then folded proteins. Although deuterium exchange procedures are experimentally simple, they suffer from the principal disadvantage of the ease of re-exchange, which can occur readily due to absorbed water on glassware or mass spectrometer surface, or in solvents or air [211]. Over the past several years H/D exchange coupled with mass spectrometry has evolved as a powerful tool to study protein:protein interaction sites as well as ligand induced or protein induces conformational changes [212, 213] and has for example been used to study the interface of the catalytic and regulatory subunits of PKA [91, 92].

Non-covalent interactions: Besides information about protein conformation, interaction between proteins may also be detectable with ESI-MS. In solution intermolecular non-covalent interactions are responsible for aggregation of folded polypeptide chains into multimers, which determine a protein system's quaternary structure. Electrospray ionization is a gentle ionization method, yielding no molecular fragmentation (unless induced in the ESI atmosphere-vacuum interface) and allowing weakly bound complexes to remain intact in the gas phase. For example Figure 12 shows the mass spectrum of p15, in this case acquired by electrospraying it from a 500 mM aqueous ammonium acetate solution pH 6.7. The spectrum is completely different from the one acquired in 50% acetonitrile and formic acid (Figure 11). The most abundant ion signals in this spectrum match a mass of 28528, which corresponds to the mass of two p15 polypeptides, illustrating it is possible to detect its dimerization (p15 is a dimeric transcriptional regulator) [214].

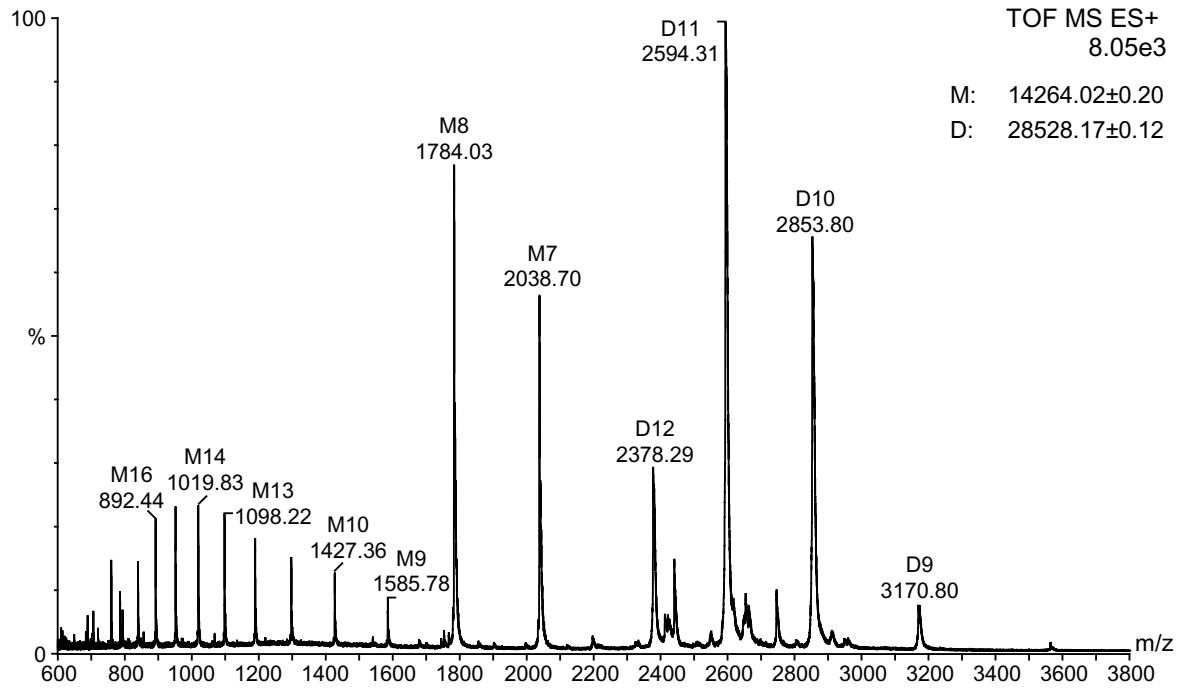

Figure 12: ESI-TOF-MS spectrum of human activated RNA polymerase II transcriptional coactivator p15 electrosprayed from a solution containing ~10 µM p15 in 500 mM ammonium acetate pH 6.7.

Of particular interest is often the detection of small molecule such as ligands or metal ions on the biomolecules. In one the first examples of this approach is the study of the non-covalent binding of various peptide ligands to SH2-domain containing proteins. ESI-MS of a solution of the SH2-protein with a mixture of phosphopeptides showed the expected protein-

phosphopeptide complex as the dominant species in the mass spectrum, demonstrating the method's potential for screening mixtures from peptide libraries [215]. Mass spectra of non-covalent systems are relatively simple to interpret. Determination of the ligand stoichiometry is straightforward since the mass increases should be well-defined intervals. In addition screening of peptide/ligand libraries with mass-spectrometry has the advantage that in a rather fast way high affinity binding peptide/ligand can be identified from mixtures of peptides or ligands. Unfortunately, the typical solvent conditions used in ESI-MS to achieve maximum sensitivity are not always optimal for maintaining an intact biomolecular complex. Careful control of all experimental parameters is necessary for studying non-covalent protein-protein or protein-ligand interaction with mass spectrometry. Besides the direct measurement of non-covalent protein-protein or protein-ligand interaction, indirect methods exist, that also allow the determination of complex stoichiometry etc. Amongst these approaches are numerous chemical strategies that allow one to probe protein secondary, tertiary and quaternary structure as well as locate binding interfaces and binding pockets of ligands.

Chemical strategies: Amongst other methods devoted to the determination of tertiary or quaternary structure of proteins are chemical derivatization [203] and chemical crosslinking methods [216]. Chemical derivatization approaches have the potential to map interactions sites between proteins or protein ligands. [217, 218]. Whereas in the latter approach, two or more biomolecular targets are covalently linked by a crosslinking reagent. When combined with mass spectrometry, cross-linking can yield valuable information. Besides identification of the cross-linked products, information can be obtained about the quaternary structure of for example heterogeneous protein complexes, which could be used to construct a rough topological model. Detailed analysis of cross-links at the level of the amino-acid residues provides further insight into distances between two proteins. This could aid in the modeling the supramolecular architecture of complexes of which the structure of individual interacting partners have been solved.

Photoaffinity labeling: One of the major events occurring at biological interfaces is the specific recognition of bioactive ligands by the receptor protein. The elucidation of interacting partners plays in important role in the field of drug discovery. The method of photoaffinity labeling enables the direct probing of target protein through a covalent bond, which is photochemically introduced between a ligand and its specific receptor [219]. This provides us with 'snap-shots' of even transient interaction between biological molecules. The

principle behind a photoaffinity labeling experiment (schematically depicted in Figure 13A) lies within the UV-light activation a small photolabile group that is contained within one of the interacting molecules is converted into a highly reactive species. This reactive species attacks adjacent residues to form a stable chemical bridge between the interacting partners. The product formed reflects the structural and dynamic organization of the system as well as the chemical characteristics of the reaction molecules. Typical photoactivatable functionalities (Figure 13B) are diazirine and its linear isomer diazo, which both yield a carbene as the reactive intermediate. An excited carbonyl has a relatively long lifetime compared to carbene or nitrene, however it preferentially abstracts hydrogen from carbon atoms than from oxygen atoms, which has the advantage that site-reactions with watermolecules hardly occur.

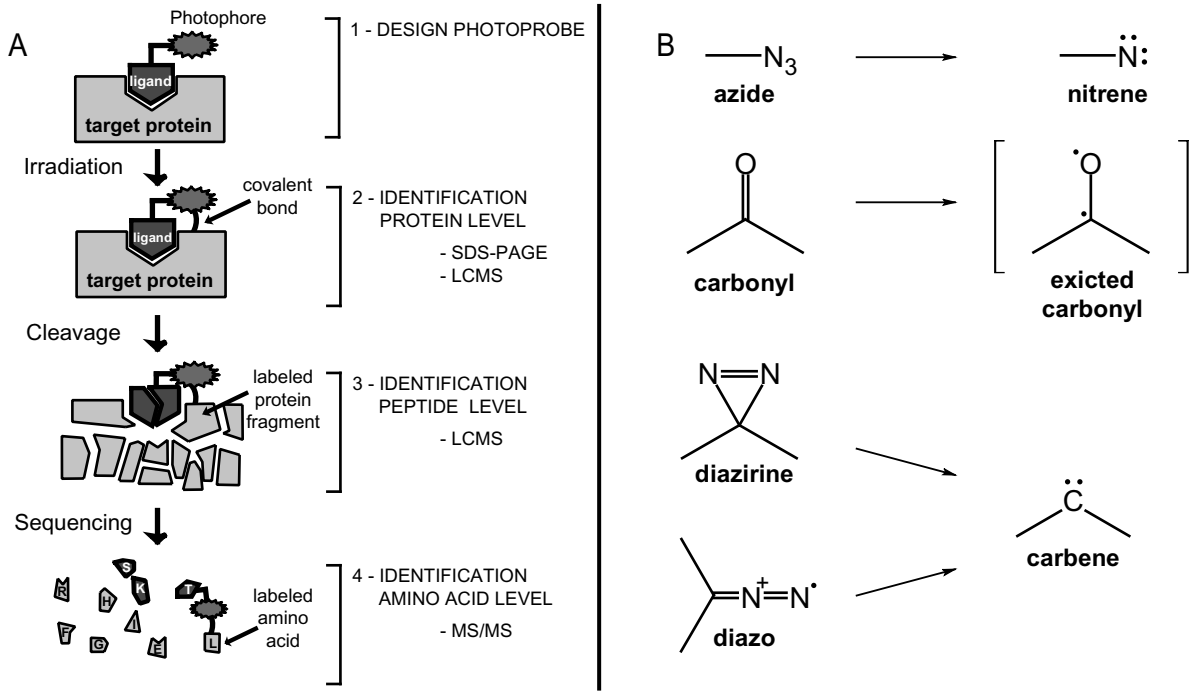

Figure 13: (A) schematic flow chart of a photoaffinity labeling experiment. **(B)** Four major photoreactive groups and their photochemically generated reactive intermediates.

Due to the recent developments of recombinant DNA techniques and mass spectrometry the investigation of biofunctional machinery at their interaction level by photoaffinity labeling is taking an interesting direction. Chin *et al.* constructed an aminoacyl-tRNA synthetase/tRNA pair that made it possible to incorporate *in-vivo p*-benzoyl-L-phenylalanine into proteins in Escherichia coli [220]. This methodology could ultimately lead to a new elegant way to discover and to delineate transient protein-protein interaction networks within the cell, by providing actual 'snap-shots' under different stimulating conditions.

IV Aim and outline of this thesis

The primary goal of the work described in this thesis is to investigate structure-function relationships of cGMP-dependent protein kinase Iα. For this purpose mass spectrometric-based approaches are applied or developed in order to study the mechanistic aspects of this protein. The development of gentle ionization techniques, in particular electrospray ionization (ESI) has led to the emergence of mass spectrometry as powerful tool in the field of non-covalent protein-protein, and protein-ligand interaction studies. The strength of mass spectrometry is that measured differences in mass directly mirror changes in the composition of the protein-protein and protein-ligand complexes. Mass spectrometry therefore allows the direct mass determination of protein-protein and protein-ligand, from which stoichiometry and binding order can be deduced.

Chapter 2 describes a detailed analysis on binding order and stoichiometry of non-covalent complexes of PKG, its natural activator cGMP and one of its substrates, ATP. Using this system it will be illustrated that nanoflow electrospray ionization time-of-flight mass spectrometry is a powerful tool to deduce both binding order and stoichiometry of this multi-component system. In addition, by using limited proteolysis and electrospray ionization mass spectrometry insight is obtained into the overall phosphorylation state of PKG under different autophosphorylation conditions

In chapter 3 an innovative and sensitive method for the enrichment of phosphopeptides is presented and applied to PKG to study its autophosphorylation reaction in more dept. The method is based on a novel base material for liquid chromatography, called Titansphere. This material consists of porous particles of titanium oxide, and it will be shown that this material is capable to very selectively trap phosphorylated peptides. An on-line two-dimensional column switching setup is presented that allows the isolation of phosphopeptides from complex mixtures. The autophosphorylation reaction of PKG will be re-examined using this newly developed method.

Chapter 4 will focus on the other process after protein kinase activation, namely heterophosphorylation. The peptide substrate binding properties of PKG Iα will be investigated using a combination of photoaffinity labeling and mass spectrometry. The

method of photoaffinity labeling allows the direct probing of target proteins through a covalent bond introduced between a ligand and a specific receptor. Using a photoreactive amino acid incorporated into a highly selective peptide substrate of PKG, the active site of PKG is examined. Using a stable isotope labeled photoreactive substrate, a new method for the fast retrieval of cross-linked products out of a complex pool of peptides is presented

Chapter 5 describes initial experiments to unravel the inhibitory mechanism behind the highly potent and selective PKG inhibitor DT2. This inhibitor has an unprecedented inhibition constant as well as specificity and is shown to be very useful to study cGMP/PKG-pathways *in-vivo*, However the mechanism behind DT-2 inhibition is unknown. Nanoflow electrospray ionization time of flight mass spectrometry will demonstrates that cGMP activation is necessary for observation of a tight complex between PKG and DT2. Surprisingly is the observation that DT2 binds in an apparent dimer:inhibitor ratio of 1:1. In chapter 6, the results presented in this thesis are summarized.

References

1. Abbott, A. *A post-genomic challenge: learning to read patterns of protein synthesis.* Nature **1999**, 402, 715-720.
2. Eisenberg, D., Marcotte, E.M., Xenarios, I. and Yeates, T.O. *Protein function in the post-genomic era.* Nature **2000**, 405, 823-826.
3. Brower, V. *Proteomics: biology in the post-genomic era. Companies all over the world rush to lead the way in the new post-genomics race.* EMBO Rep **2001**, 2, 558-560.
4. Fields, S. *Proteomics. Proteomics in genomeland.* Science **2001**, 291, 1221-1224.
5. Lander, E.S., Linton, L.M., Birren, B., Nusbaum, C., Zody, M.C.*, et al. Initial sequencing and analysis of the human genome.* Nature **2001**, 409, 860-921.
6. Venter, J.C., Adams, M.D., Myers, E.W., Li, P.W., Mural, R.J.*, et al. The sequence of the human genome.* Science **2001**, 291, 1304-1351.
7. Neet, K.E. and Lee, J.C. *Biophysical characterization of proteins in the post-genomic era of proteomics.* Mol Cell Proteomics **2002**, 1, 415-420.
8. Auerbach, D., Thaminy, S., Hottiger, M.O. and Stagljar, I. *The post-genomic era of interactive proteomics: facts and perspectives.* Proteomics **2002**, 2, 611-623.
9. Godovac-Zimmermann, J. and Brown, L.R. *Perspectives for mass spectrometry and functional proteomics.* Mass Spectrom Rev **2001**, 20, 1-57.
10. Fischer, E.H. and Krebs, E.G. *Conversion of phosphorylase b to phosphorylase a in muscle extracts.* J Biol Chem **1955**, 216, 121-132.
11. Stryer, L., *Biochemistry*. 4th ed. 1995, New York, N.Y.: Freeman. XXXIV, 1064.
12. Hunter, T. *Signaling--2000 and beyond.* Cell **2000**, 100, 113-127.
13. Blume-Jensen, P. and Hunter, T. *Oncogenic kinase signalling.* Nature **2001**, 411, 355-365.
14. Cohen, P. *Protein kinases--the major drug targets of the twenty-first century?* Nat Rev Drug Discov **2002**, 1, 309-315.
15. Hunter, T. *Protein kinases and phosphatases: the yin and yang of protein phosphorylation and signaling.* Cell **1995**, 80, 225-236.
16. Hunter, T. *A thousand and one protein kinases.* Cell **1987**, 50, 823-829.
17. Hunter, T. *1001 protein kinases redux--towards 2000.* Semin Cell Biol **1994**, 5, 367-376.
18. Caenepeel, S., Charydczak, G., Sudarsanam, S., Hunter, T. and Manning, G. *The mouse kinome: Discovery and comparative genomics of all mouse protein kinases.* Proc Natl Acad Sci U S A **2004**, 101, 11707-11712.
19. Manning, G., Whyte, D.B., Martinez, R., Hunter, T. and Sudarsanam, S. *The protein kinase complement of the human genome.* Science **2002**, 298, 1912-1934.
20. Kennelly, P.J. and Krebs, E.G. *Consensus sequences as substrate specificity determinants for protein kinases and protein phosphatases.* J Biol Chem **1991**, 266, 15555-15558.
21. Pinna, L.A. and Ruzzene, M. *How do protein kinases recognize their substrates?* Biochim Biophys Acta **1996**, 1314, 191-225.
22. Holland, P.M. and Cooper, J.A. *Protein modification: docking sites for kinases.* Curr Biol **1999**, 9, R329-331.
23. Biondi, R.M. and Nebreda, A.R. *Signalling specificity of Ser/Thr protein kinases through docking-site-mediated interactions.* Biochem J **2003**, 372, 1-13.
24. Mochly-Rosen, D. *Localization of protein kinases by anchoring proteins: a theme in signal transduction.* Science **1995**, 268, 247-251.

25. Hubbard, M.J. and Cohen, P. *On target with a new mechanism for the regulation of protein phosphorylation.* Trends Biochem Sci **1993**, 18, 172-177.
26. Murad, F. *Regulation of cytosolic guanylyl cyclase by nitric oxide: the NO-cyclic GMP signal transduction system.* Adv Pharmacol **1994**, 26, 19-33.
27. Lincoln, T.M., Dey, N.B., Boerth, N.J., Cornwell, T.L. and Soff, G.A. *Nitric oxide--cyclic GMP pathway regulates vascular smooth muscle cell phenotypic modulation: implications in vascular diseases.* Acta Physiol Scand **1998**, 164, 507-515.
28. Boerth, N.J., Dey, N.B., Cornwell, T.L. and Lincoln, T.M. *Cyclic GMP-dependent protein kinase regulates vascular smooth muscle cell phenotype.* J Vasc Res **1997**, 34, 245-259.
29. Geiger, J., Nolte, C., Butt, E., Sage, S.O. and Walter, U. *Role of cGMP and cGMP-dependent protein kinase in nitrovasodilator inhibition of agonist-evoked calcium elevation in human platelets.* Proc Natl Acad Sci U S A **1992**, 89, 1031-1035.
30. Gambaryan, S., Geiger, J., Schwarz, U.R., Butt, E., Begonja, A., Obergfell, A. and Walter, U. *Potent inhibition of human platelets by cGMP analogs independent of cGMP-dependent protein kinase.* Blood **2004**, 103, 2593-2600.
31. Lincoln, T.M., Dey, N. and Sellak, H. *Invited review: cGMP-dependent protein kinase signaling mechanisms in smooth muscle: from the regulation of tone to gene expression.* J Appl Physiol **2001**, 91, 1421-1430.
32. Kuo, J.F. and Greengard, P. *Cyclic nucleotide-dependent protein kinases. VI. Isolation and partial purification of a protein kinase activated by guanosine 3',5'-monophosphate.* J Biol Chem **1970**, 245, 2493-2498.
33. Sandberg, M., Natarajan, V., Ronander, I., Kalderon, D., Walter, U., Lohmann, S.M. and Jahnsen, T. *Molecular cloning and predicted full-length amino acid sequence of the type I beta isozyme of cGMP-dependent protein kinase from human placenta. Tissue distribution and developmental changes in rat.* FEBS Lett **1989**, 255, 321-329.
34. Wernet, W., Flockerzi, V. and Hofmann, F. *The cDNA of the two isoforms of bovine cGMP-dependent protein kinase.* FEBS Lett **1989**, 251, 191-196.
35. Uhler, M.D. *Cloning and expression of a novel cyclic GMP-dependent protein kinase from mouse brain.* J Biol Chem **1993**, 268, 13586-13591.
36. Francis, S.H., Woodford, T.A., Wolfe, L. and Corbin, J.D. *Types I alpha and I beta isozymes of cGMP-dependent protein kinase: alternative mRNA splicing may produce different inhibitory domains.* Second Messengers Phosphoproteins **1988**, 12, 301-310.
37. Wolfe, L., Corbin, J.D. and Francis, S.H. *Characterization of a novel isozyme of cGMP-dependent protein kinase from bovine aorta.* J Biol Chem **1989**, 264, 7734-7741.
38. Murofushi, H. *Protein kinases in Tetrahymena cilia. II. Partial purification and characterization of adenosine 3',5'-monophosphate-dependent and guanosine 3',5'-monophosphate-dependent protein kinases.* Biochim Biophys Acta **1974**, 370, 130-139.
39. Miglietta, L.A. and Nelson, D.L. *A novel cGMP-dependent protein kinase from Paramecium.* J Biol Chem **1988**, 263, 16096-16105.
40. Wanner, R. and Wurster, B. *Cyclic GMP-activated protein kinase from Dictyostelium discoideum.* Biochim Biophys Acta **1990**, 1053, 179-184.
41. de Jonge, H.R. *Cyclic GMP-dependent protein kinase in intestinal brushborders.* Adv Cyclic Nucleotide Res **1981**, 14, 315-333.

42. Takio, K., Wade, R.D., Smith, S.B., Krebs, E.G., Walsh, K.A. and Titani, K. *Guanosine cyclic 3',5'-phosphate dependent protein kinase, a chimeric protein homologous with two separate protein families.* Biochemistry **1984**, 23, 4207-4218.
43. Richie-Jannetta, R., Francis, S.H. and Corbin, J.D. *Dimerization of cGMP-dependent protein kinase Ibeta is mediated by an extensive amino-terminal leucine zipper motif, and dimerization modulates enzyme function.* J Biol Chem **2003**, 278, 50070-50079.
44. McKnight, S.L. *Molecular zippers in gene regulation.* Sci Am **1991**, 264, 54-64.
45. Alber, T. *Structure of the leucine zipper.* Curr Opin Genet Dev **1992**, 2, 205-210.
46. Atkinson, R.A., Saudek, V., Huggins, J.P. and Pelton, J.T. *1H NMR and circular dichroism studies of the N-terminal domain of cyclic GMP dependent protein kinase: a leucine/isoleucine zipper.* Biochemistry **1991**, 30, 9387-9395.
47. Monken, C.E. and Gill, G.N. *Structural analysis of cGMP-dependent protein kinase using limited proteolysis.* J Biol Chem **1980**, 255, 7067-7070.
48. Erlichman, J., Rosenfeld, R. and Rosen, O.M. *Phosphorylation of a cyclic adenosine 3':5'-monophosphate-dependent protein kinase from bovine cardiac muscle.* J Biol Chem **1974**, 249, 5000-5003.
49. Yuasa, K., Michibata, H., Omori, K. and Yanaka, N. *Identification of a conserved residue responsible for the autoinhibition of cGMP-dependent protein kinase Ialpha and beta.* FEBS Lett **2000**, 466, 175-178.
50. Poteet-Smith, C.E., Corbin, J.D. and Francis, S.H. *The pseudosubstrate sequences alone are not sufficient for potent autoinhibition of cAMP- and cGMP-dependent protein kinases as determined by synthetic peptide analysis.* Adv Second Messenger Phosphoprotein Res **1997**, 31, 219-235.
51. Poteet-Smith, C.E., Shabb, J.B., Francis, S.H. and Corbin, J.D. *Identification of critical determinants for autoinhibition in the pseudosubstrate region of type I alpha cAMP-dependent protein kinase.* J Biol Chem **1997**, 272, 379-388.
52. Francis, S.H., Smith, J.A., Colbran, J.L., Grimes, K., Walsh, K.A., Kumar, S. and Corbin, J.D. *Arginine 75 in the pseudosubstrate sequence of type Ibeta cGMP-dependent protein kinase is critical for autoinhibition, although autophosphorylated serine 63 is outside this sequence.* J Biol Chem **1996**, 271, 20748-20755.
53. Francis, S.H., Poteet-Smith, C., Busch, J.L., Richie-Jannetta, R. and Corbin, J.D. *Mechanisms of autoinhibition in cyclic nucleotide-dependent protein kinases.* Front Biosci **2002**, 7, d580-592.
54. Ruth, P., Landgraf, W., Keilbach, A., May, B., Egleme, C. and Hofmann, F. *The activation of expressed cGMP-dependent protein kinase isozymes I alpha and I beta is determined by the different amino-termini.* Eur J Biochem **1991**, 202, 1339-1344.
55. Colledge, M. and Scott, J.D. *AKAPs: from structure to function.* Trends Cell Biol **1999**, 9, 216-221.
56. Barradeau, S., Imaizumi-Scherrer, T., Weiss, M.C. and Faust, D.M. *Intracellular targeting of the type-I alpha regulatory subunit of cAMP-dependent protein kinase.* Trends Cardiovasc Med **2002**, 12, 235-241.
57. Coghlan, V.M., Bergeson, S.E., Langeberg, L., Nilaver, G. and Scott, J.D. *A-kinase anchoring proteins: a key to selective activation of cAMP-responsive events?* Mol Cell Biochem **1993**, 127-128, 309-319.
58. Pawson, T. and Scott, J.D. *Signaling through scaffold, anchoring, and adaptor proteins.* Science **1997**, 278, 2075-2080.

59. Hausken, Z.E., Dell'Acqua, M.L., Coghlan, V.M. and Scott, J.D. *Mutational analysis of the A-kinase anchoring protein (AKAP)-binding site on RII. Classification Of side chain determinants for anchoring and isoform selective association with AKAPs.* J Biol Chem **1996**, 271, 29016-29022.
60. Hausken, Z.E., Coghlan, V.M., Hastings, C.A., Reimann, E.M. and Scott, J.D. *Type II regulatory subunit (RII) of the cAMP-dependent protein kinase interaction with A-kinase anchor proteins requires isoleucines 3 and 5.* J Biol Chem **1994**, 269, 24245-24251.
61. Newlon, M.G., Roy, M., Morikis, D., Hausken, Z.E., Coghlan, V., Scott, J.D. and Jennings, P.A. *The molecular basis for protein kinase A anchoring revealed by solution NMR.* Nat Struct Biol **1999**, 6, 222-227.
62. Vo, N.K., Gettemy, J.M. and Coghlan, V.M. *Identification of cGMP-dependent protein kinase anchoring proteins (GKAPs).* Biochem Biophys Res Commun **1998**, 246, 831-835.
63. Yuasa, K., Omori, K. and Yanaka, N. *Binding and phosphorylation of a novel male germ cell-specific cGMP-dependent protein kinase-anchoring protein by cGMP-dependent protein kinase Ialpha.* J Biol Chem **2000**, 275, 4897-4905.
64. Surks, H.K. and Mendelsohn, M.E. *Dimerization of cGMP-dependent protein kinase 1alpha and the myosin-binding subunit of myosin phosphatase: role of leucine zipper domains.* Cell Signal **2003**, 15, 937-944.
65. Schlossmann, J., Ammendola, A., Ashman, K., Zong, X., Huber, A.*, et al. Regulation of intracellular calcium by a signalling complex of IRAG, IP3 receptor and cGMP kinase Ibeta.* Nature **2000**, 404, 197-201.
66. Ammendola, A., Geiselhoringer, A., Hofmann, F. and Schlossmann, J. *Molecular determinants of the interaction between the inositol 1,4,5-trisphosphate receptor-associated cGMP kinase substrate (IRAG) and cGMP kinase Ibeta.* J Biol Chem **2001**, 276, 24153-24159.
67. Smith, J.A., Francis, S.H. and Corbin, J.D. *Autophosphorylation - a Salient Feature of Protein-Kinases.* Molecular and Cellular Biochemistry **1993**, 128, 51-70.
68. Pawson, T., Olivier, P., Rozakis-Adcock, M., McGlade, J. and Henkemeyer, M. *Proteins with SH2 and SH3 domains couple receptor tyrosine kinases to intracellular signalling pathways.* Philos Trans R Soc Lond B Biol Sci **1993**, 340, 279-285.
69. Yaffe, M.B. and Cantley, L.C. *Signal transduction. Grabbing phosphoproteins.* Nature **1999**, 402, 30-31.
70. de Jonge, H.R. and Rosen, O.M. *Self-phosphorylation of cyclic guanosine 3':5'-monophosphate-dependent protein kinase from bovine lung. Effect of cyclic adenosine 3':5'-monophosphate, cyclic guanosine 3':5'-monophosphate and histone.* J Biol Chem **1977**, 252, 2780-2783.
71. Aitken, A., Hemmings, B.A. and Hofmann, F. *Identification of the residues on cyclic GMP-dependent protein kinase that are autophosphorylated in the presence of cyclic AMP and cyclic GMP.* Biochim Biophys Acta **1984**, 790, 219-225.
72. Smith, J.A., Francis, S.H., Walsh, K.A., Kumar, S. and Corbin, J.D. *Autophosphorylation of type Ibeta cGMP-dependent protein kinase increases basal catalytic activity and enhances allosteric activation by cGMP or cAMP.* J Biol Chem **1996**, 271, 20756-20762.
73. Hofmann, F. and Flockerzi, V. *Characterization of phosphorylated and native cGMP-dependent protein kinase.* Eur J Biochem **1983**, 130, 599-603.
74. Chu, D.M., Corbin, J.D., Grimes, K.A. and Francis, S.H. *Activation by cyclic GMP binding causes an apparent conformational change in cGMP-dependent protein kinase.* J Biol Chem **1997**, 272, 31922-31928.

75. Chu, D.M., Francis, S.H., Thomas, J.W., Maksymovitch, E.A., Fosler, M. and Corbin, J.D. *Activation by autophosphorylation or cGMP binding produces a similar apparent conformational change in cGMP-dependent protein kinase.* J Biol Chem **1998**, 273, 14649-14656.
76. Busch, J.L., Bessay, E.P., Francis, S.H. and Corbin, J.D. *A conserved serine juxtaposed to the pseudosubstrate site of type I cGMP-dependent protein kinase contributes strongly to autoinhibition and lower cGMP affinity.* J Biol Chem **2002**, 277, 34048-34054.
77. Weber, I.T., Takio, K., Titani, K. and Steitz, T.A. *The cAMP-binding domains of the regulatory subunit of cAMP-dependent protein kinase and the catabolite gene activator protein are homologous.* Proc Natl Acad Sci U S A **1982**, 79, 7679-7683.
78. Doskeland, S.O., Vintermyr, O.K., Corbin, J.D. and Ogreid, D. *Studies on the interactions between the cyclic nucleotide-binding sites of cGMP-dependent protein kinase.* J Biol Chem **1987**, 262, 3534-3540.
79. Corbin, J.D., Ogreid, D., Miller, J.P., Suva, R.H., Jastorff, B. and Doskeland, S.O. *Studies of cGMP analog specificity and function of the two intrasubunit binding sites of cGMP-dependent protein kinase.* J Biol Chem **1986**, 261, 1208-1214.
80. Corbin, J.D. and Rannels, S.R. *Perturbation and structural organization of the two intrachain cAMP binding sites of cAMP-dependent protein kinase II.* J Biol Chem **1981**, 256, 11671-11676.
81. Rannels, S.R. and Corbin, J.D. *Studies on the function of the two intrachain cAMP binding sites of protein kinase.* J Biol Chem **1981**, 256, 7871-7876.
82. Bubis, J. and Taylor, S.S. *Correlation of photolabeling with occupancy of cAMP binding sites in the regulatory subunit of cAMP-dependent protein kinase I.* Biochemistry **1987**, 26, 3478-3486.
83. Shabb, J.B., Ng, L. and Corbin, J.D. *One amino acid change produces a high affinity cGMP-binding site in cAMP-dependent protein kinase.* J Biol Chem **1990**, 265, 16031-16034.
84. Shabb, J.B., Buzzeo, B.D., Ng, L. and Corbin, J.D. *Mutating protein kinase cAMP-binding sites into cGMP-binding sites. Mechanism of cGMP selectivity.* J Biol Chem **1991**, 266, 24320-24326.
85. Altenhofen, W., Ludwig, J., Eismann, E., Kraus, W., Bonigk, W. and Kaupp, U.B. *Control of ligand specificity in cyclic nucleotide-gated channels from rod photoreceptors and olfactory epithelium.* Proc Natl Acad Sci U S A **1991**, 88, 9868-9872.
86. Reed, R.B., Sandberg, M., Jahnsen, T., Lohmann, S.M., Francis, S.H. and Corbin, J.D. *Fast and slow cyclic nucleotide-dissociation sites in cAMP-dependent protein kinase are transposed in type Ibeta cGMP-dependent protein kinase.* J Biol Chem **1996**, 271, 17570-17575.
87. Reed, R.B., Sandberg, M., Jahnsen, T., Lohmann, S.M., Francis, S.H. and Corbin, J.D. *Structural order of the slow and fast intrasubunit cGMP-binding sites of type I alpha cGMP-dependent protein kinase.* Adv Second Messenger Phosphoprotein Res **1997**, 31, 205-217.
88. Smith, J.A., Reed, R.B., Francis, S.H., Grimes, K. and Corbin, J.D. *Distinguishing the roles of the two different cGMP-binding sites for modulating phosphorylation of exogenous substrate (heterophosphorylation) and autophosphorylation of cGMP-dependent protein kinase.* J Biol Chem **2000**, 275, 154-158.
89. Wu, J., Brown, S., Xuong, N.H. and Taylor, S.S. *RIalpha subunit of PKA: a cAMP-free structure reveals a hydrophobic capping mechanism for docking cAMP into site B.* Structure (Camb) **2004**, 12, 1057-1065.
90. Su, Y., Dostmann, W.R., Herberg, F.W., Durick, K., Xuong, N.H., Ten Eyck, L., Taylor, S.S. and Varughese, K.I. *Regulatory subunit of protein kinase A: structure of deletion mutant with cAMP binding domains.* Science **1995**, 269, 807-813.

91. Anand, G.S., Hughes, C.A., Jones, J.M., Taylor, S.S. and Komives, E.A. *Amide H/2H exchange reveals communication between the cAMP and catalytic subunit-binding sites in the R(I)alpha subunit of protein kinase A.* J Mol Biol **2002**, 323, 377-386.
92. Anand, G.S., Law, D., Mandell, J.G., Snead, A.N., Tsigelny, I., Taylor, S.S., Ten Eyck, L.F. and Komives, E.A. *Identification of the protein kinase A regulatory RIalpha-catalytic subunit interface by amide H/2H exchange and protein docking.* Proc Natl Acad Sci U S A **2003**, 100, 13264-13269.
93. Hamuro, Y., Anand, G.S., Kim, J.S., Juliano, C., Stranz, D.D., Taylor, S.S. and Woods, V.L., Jr. *Mapping intersubunit interactions of the regulatory subunit (RIalpha) in the type I holoenzyme of protein kinase A by amide hydrogen/deuterium exchange mass spectrometry (DXMS).* J Mol Biol **2004**, 340, 1185-1196.
94. Zawadzki, K.M., Hamuro, Y., Kim, J.S., Garrod, S., Stranz, D.D., Taylor, S.S. and Woods, V.L., Jr. *Dissecting interdomain communication within cAPK regulatory subunit type IIbeta using enhanced amide hydrogen/deuterium exchange mass spectrometry (DXMS).* Protein Sci **2003**, 12, 1980-1990.
95. Hamuro, Y., Zawadzki, K.M., Kim, J.S., Stranz, D.D., Taylor, S.S. and Woods, V.L., Jr. *Dynamics of cAPK type IIbeta activation revealed by enhanced amide H/2H exchange mass spectrometry (DXMS).* J Mol Biol **2003**, 327, 1065-1076.
96. Knighton, D.R., Zheng, J.H., Ten Eyck, L.F., Xuong, N.H., Taylor, S.S. and Sowadski, J.M. *Structure of a peptide inhibitor bound to the catalytic subunit of cyclic adenosine monophosphate-dependent protein kinase.* Science **1991**, 253, 414-420.
97. Knighton, D.R., Zheng, J.H., Ten Eyck, L.F., Ashford, V.A., Xuong, N.H., Taylor, S.S. and Sowadski, J.M. *Crystal structure of the catalytic subunit of cyclic adenosine monophosphate-dependent protein kinase.* Science **1991**, 253, 407-414.
98. Knighton, D.R., Xuong, N.H., Taylor, S.S. and Sowadski, J.M. *Crystallization studies of cAMP-dependent protein kinase. Cocrystals of the catalytic subunit with a 20 amino acid residue peptide inhibitor and MgATP diffract to 3.0 A resolution.* J Mol Biol **1991**, 220, 217-220.
99. Zheng, J.H., Knighton, D.R., Parello, J., Taylor, S.S. and Sowadski, J.M. *Crystallization of catalytic subunit of adenosine cyclic monophosphate-dependent protein kinase.* Methods Enzymol **1991**, 200, 508-521.
100. Zheng, J., Knighton, D.R., ten Eyck, L.F., Karlsson, R., Xuong, N., Taylor, S.S. and Sowadski, J.M. *Crystal structure of the catalytic subunit of cAMP-dependent protein kinase complexed with MgATP and peptide inhibitor.* Biochemistry **1993**, 32, 2154-2161.
101. Madhusudan, Akamine, P., Xuong, N.H. and Taylor, S.S. *Crystal structure of a transition state mimic of the catalytic subunit of cAMP-dependent protein kinase.* Nat Struct Biol **2002**, 9, 273-277.
102. Akamine, P., Madhusudan, Wu, J., Xuong, N.H., Ten Eyck, L.F. and Taylor, S.S. *Dynamic features of cAMP-dependent protein kinase revealed by apoenzyme crystal structure.* J Mol Biol **2003**, 327, 159-171.
103. Li, F., Gangal, M., Jones, J.M., Deich, J., Lovett, K.E., Taylor, S.S. and Johnson, D.A. *Consequences of cAMP and catalytic-subunit binding on the flexibility of the A-kinase regulatory subunit.* Biochemistry **2000**, 39, 15626-15632.
104. Li, F., Gangal, M., Juliano, C., Gorfain, E., Taylor, S.S. and Johnson, D.A. *Evidence for an internal entropy contribution to phosphoryl transfer: a study of domain closure, backbone flexibility, and the catalytic cycle of cAMP-dependent protein kinase.* J Mol Biol **2002**, 315, 459-469.
105. Banky, P., Roy, M., Newlon, M.G., Morikis, D., Haste, N.M., Taylor, S.S. and Jennings, P.A. *Related protein-protein interaction modules present drastically different surface topographies despite a conserved helical platform.* J Mol Biol **2003**, 330, 1117-1129.

106. Hofmann, F., Dostmann, W., Keilbach, A., Landgraf, W. and Ruth, P. *Structure and physiological role of cGMP-dependent protein kinase.* Biochim Biophys Acta **1992**, 1135, 51-60.
107. Dostmann, W.R., Nickl, C., Thiel, S., Tsigelny, I., Frank, R. and Tegge, W.J. *Delineation of selective cyclic GMP-dependent protein kinase Ialpha substrate and inhibitor peptides based on combinatorial peptide libraries on paper.* Pharmacol Ther **1999**, 82, 373-387.
108. Knighton, D.R., Pearson, R.B., Sowadski, J.M., Means, A.R., Ten Eyck, L.F., Taylor, S.S. and Kemp, B.E. *Structural basis of the intrasteric regulation of myosin light chain kinases.* Science **1992**, 258, 130-135.
109. Hanks, S.K. and Hunter, T. *The eukaryotic protein kinase superfamily: kinase (catalytic) domain structure and classification.* Faseb J **1995**, 9, 576-596.
110. Hanks, S.K., Quinn, A.M. and Hunter, T. *The protein kinase family: conserved features and deduced phylogeny of the catalytic domains.* Science **1988**, 241, 42-52.
111. Zheng, J.H., Trafny, E.A., Knighton, D.R., Xuong, N.H., Taylor, S.S., Teneyck, L.F. and Sowadski, J.M. *2.2-Angstrom Refined Crystal-Structure of the Catalytic Subunit of Camp-Dependent Protein-Kinase Complexed with Mnatp and a Peptide Inhibitor.* Acta Crystallographica Section D-Biological Crystallography **1993**, 49, 362-365.
112. Bossemeyer, D., Engh, R.A., Kinzel, V., Ponstingl, H. and Huber, R. *Phosphotransferase and substrate binding mechanism of the cAMP-dependent protein kinase catalytic subunit from porcine heart as deduced from the 2.0 A structure of the complex with Mn2+ adenylyl imidodiphosphate and inhibitor peptide PKI(5-24).* Embo J **1993**, 12, 849-859.
113. Taylor, S.S. and Radzio-Andzelm, E. *Three protein kinase structures define a common motif.* Structure **1994**, 2, 345-355.
114. Adams, J.A. *Kinetic and catalytic mechanisms of protein kinases.* Chem. Rev. **2001**, 101, 2271-2290.
115. Sugden, P.H., Holladay, L.A., Reimann, E.M. and Corbin, J.D. *Purification and characterization of the catalytic subunit of adenosine 3':5'-cyclic monophosphate-dependent protein kinase from bovine liver.* Biochem J **1976**, 159, 409-422.
116. Swarup, G., Dasgupta, J.D. and Garbers, D.L. *Tyrosine-specific protein kinases of normal tissues.* Adv Enzyme Regul **1984**, 22, 267-288.
117. Herberg, F.W., Doyle, M.L., Cox, S. and Taylor, S.S. *Dissection of the nucleotide and metal-phosphate binding sites in cAMP-dependent protein kinase.* Biochemistry **1999**, 38, 6352-6360.
118. Yuan, C.J., Huang, C.Y. and Graves, D.J. *Phosphorylase kinase, a metal ion-dependent dual specificity kinase.* J Biol Chem **1993**, 268, 17683-17686.
119. Adams, J.A. and Taylor, S.S. *Divalent metal ions influence catalysis and active-site accessibility in the cAMP-dependent protein kinase.* Protein Sci **1993**, 2, 2177-2186.
120. Bhatnagar, D., Roskoski, R., Jr., Rosendahl, M.S. and Leonard, N.J. *Adenosine cyclic 3',5'-monophosphate dependent protein kinase: a new fluorescence displacement titration technique for characterizing the nucleotide binding site on the catalytic subunit.* Biochemistry **1983**, 22, 6310-6317.
121. Granot, J., Gibson, K.J., Switzer, R.L. and Mildvan, A.S. *NMR studies of the nucleotide conformation and the arrangement of substrates and activators on phosphoribosylpyrophosphate synthetase.* J Biol Chem **1980**, 255, 10931-10937.
122. Granot, J., Mildvan, A.S., Hiyama, K., Kondo, H. and Kaiser, E.T. *Magnetic resonance studies of the effect of the regulatory subunit on metal and substrate binding to the catalytic subunit of bovine heart protein kinase.* J Biol Chem **1980**, 255, 4569-4573.

123. Armstrong, R.N., Kondo, H., Granot, J., Kaiser, E.T. and Mildvan, A.S. *Magnetic resonance and kinetic studies of the manganese(II) ion and substrate complexes of the catalytic subunit of adenosine 3',5'-monophosphate dependent protein kinase from bovine heart.* Biochemistry **1979**, 18, 1230-1238.

124. Scott, J.D., Fischer, E.H., Takio, K., Demaille, J.G. and Krebs, E.G. *Amino acid sequence of the heat-stable inhibitor of the cAMP-dependent protein kinase from rabbit skeletal muscle.* Proc Natl Acad Sci U S A **1985**, 82, 5732-5736.

125. Scott, J.D., Fischer, E.H., Demaille, J.G. and Krebs, E.G. *Identification of an inhibitory region of the heat-stable protein inhibitor of the cAMP-dependent protein kinase.* Proc Natl Acad Sci U S A **1985**, 82, 4379-4383.

126. Mitchell, R.D., Glass, D.B., Wong, C.W., Angelos, K.L. and Walsh, D.A. *Heat-stable inhibitor protein derived peptide substrate analogs: phosphorylation by cAMP-dependent and cGMP-dependent protein kinases.* Biochemistry **1995**, 34, 528-534.

127. Tegge, W., Frank, R., Hofmann, F. and Dostmann, W.R. *Determination of cyclic nucleotide-dependent protein kinase substrate specificity by the use of peptide libraries on cellulose paper.* Biochemistry **1995**, 34, 10569-10577.

128. Taylor, S.S., Radzio-Andzelm, E., Madhusudan, Cheng, X., Ten Eyck, L. and Narayana, N. *Catalytic subunit of cyclic AMP-dependent protein kinase: structure and dynamics of the active site cleft.* Pharmacol Ther **1999**, 82, 133-141.

129. Smith, C.M., Radzio-Andzelm, E., Madhusudan, Akamine, P. and Taylor, S.S. *The catalytic subunit of cAMP-dependent protein kinase: prototype for an extended network of communication.* Prog Biophys Mol Biol **1999**, 71, 313-341.

130. Johnson, D.A., Akamine, P., Radzio-Andzelm, E., Madhusudan, M. and Taylor, S.S. *Dynamics of cAMP-dependent protein kinase.* Chem Rev **2001**, 101, 2243-2270.

131. Taylor, S.S., Yang, J., Wu, J., Haste, N.M., Radzio-Andzelm, E. and Anand, G. *PKA: a portrait of protein kinase dynamics.* Biochim Biophys Acta **2004**, 1697, 259-269.

132. Lew, J., Taylor, S.S. and Adams, J.A. *Identification of a partially rate-determining step in the catalytic mechanism of cAMP-dependent protein kinase: a transient kinetic study using stopped-flow fluorescence spectroscopy.* Biochemistry **1997**, 36, 6717-6724.

133. Zhao, J., Trewhella, J., Corbin, J., Francis, S., Mitchell, R., Brushia, R. and Walsh, D. *Progressive cyclic nucleotide-induced conformational changes in the cGMP-dependent protein kinase studied by small angle X-ray scattering in solution.* J Biol Chem **1997**, 272, 31929-31936.

134. Wall, M.E., Francis, S.H., Corbin, J.D., Grimes, K., Richie-Jannetta, R., Kotera, J., Macdonald, B.A., Gibson, R.R. and Trewhella, J. *Mechanisms associated with cGMP binding and activation of cGMP-dependent protein kinase.* Proc Natl Acad Sci U S A **2003**, 100, 2380-2385.

135. Walter, U. *Distribution of cyclic-GMP-dependent protein kinase in various rat tissues and cell lines determined by a sensitive and specific radioimmunoassay.* Eur J Biochem **1981**, 118, 339-346.

136. Lohmann, S.M., Walter, U., Miller, P.E., Greengard, P. and De Camilli, P. *Immunohistochemical localization of cyclic GMP-dependent protein kinase in mammalian brain.* Proc Natl Acad Sci U S A **1981**, 78, 653-657.

137. Lohmann, S.M., Vaandrager, A.B., Smolenski, A., Walter, U. and De Jonge, H.R. *Distinct and specific functions of cGMP-dependent protein kinases.* Trends Biochem Sci **1997**, 22, 307-312.

138. Joyce, N.C., DeCamilli, P., Lohmann, S.M. and Walter, U. *cGMP-dependent protein kinase is present in high concentrations in contractile cells of the kidney vasculature.* J Cyclic Nucleotide Protein Phosphor Res **1986**, 11, 191-198.

139. Lincoln, T.M. and Cornwell, T.L. *Intracellular cyclic GMP receptor proteins.* Faseb J **1993**, 7, 328-338.
140. Vaandrager, A.B. and de Jonge, H.R. *Signalling by cGMP-dependent protein kinases.* Mol Cell Biochem **1996**, 157, 23-30.
141. Lincoln, T.M., Cornwell, T.L. and Taylor, A.E. *cGMP-dependent protein kinase mediates the reduction of Ca2+ by cAMP in vascular smooth muscle cells.* Am J Physiol **1990**, 258, C399-407.
142. Jiang, H., Shabb, J.B. and Corbin, J.D. *Cross-activation: overriding cAMP/cGMP selectivities of protein kinases in tissues.* Biochem Cell Biol **1992**, 70, 1283-1289.
143. Jiang, H., Colbran, J.L., Francis, S.H. and Corbin, J.D. *Direct evidence for cross-activation of cGMP-dependent protein kinase by cAMP in pig coronary arteries.* J Biol Chem **1992**, 267, 1015-1019.
144. Chao, A.C., de Sauvage, F.J., Dong, Y.J., Wagner, J.A., Goeddel, D.V. and Gardner, P. *Activation of intestinal CFTR Cl- channel by heat-stable enterotoxin and guanylin via cAMP-dependent protein kinase.* Embo J **1994**, 13, 1065-1072.
145. Landgraf, W., Hullin, R., Gobel, C. and Hofmann, F. *Phosphorylation of cGMP-dependent protein kinase increases the affinity for cyclic AMP.* Eur J Biochem **1986**, 154, 113-117.
146. Pfeifer, A., Aszodi, A., Seidler, U., Ruth, P., Hofmann, F. and Fassler, R. *Intestinal secretory defects and dwarfism in mice lacking cGMP-dependent protein kinase II.* Science **1996**, 274, 2082-2086.
147. Pfeifer, A., Klatt, P., Massberg, S., Ny, L., Sausbier, M.*, et al. Defective smooth muscle regulation in cGMP kinase I-deficient mice.* Embo J **1998**, 17, 3045-3051.
148. Carvajal, J.A., Germain, A.M., Huidobro-Toro, J.P. and Weiner, C.P. *Molecular mechanism of cGMP-mediated smooth muscle relaxation.* J Cell Physiol **2000**, 184, 409-420.
149. White, R.E. *Cyclic GMP and ion channel regulation.* Adv Second Messenger Phosphoprotein Res **1999**, 33, 251-277.
150. Cornwell, T.L. and Lincoln, T.M. *Regulation of intracellular Ca2+ levels in cultured vascular smooth muscle cells. Reduction of Ca2+ by atriopeptin and 8-bromo-cyclic GMP is mediated by cyclic GMP-dependent protein kinase.* J Biol Chem **1989**, 264, 1146-1155.
151. Surks, H.K., Mochizuki, N., Kasai, Y., Georgescu, S.P., Tang, K.M., Ito, M., Lincoln, T.M. and Mendelsohn, M.E. *Regulation of myosin phosphatase by a specific interaction with cGMP- dependent protein kinase Ialpha.* Science **1999**, 286, 1583-1587.
152. Gopal, V.K., Francis, S.H. and Corbin, J.D. *Allosteric sites of phosphodiesterase-5 (PDE5). A potential role in negative feedback regulation of cGMP signaling in corpus cavernosum.* Eur J Biochem **2001**, 268, 3304-3312.
153. Mullershausen, F., Russwurm, M., Koesling, D. and Friebe, A. *In Vivo Reconstitution of the Negative Feedback in Nitric Oxide/cGMP Signaling: Role of Phosphodiesterase Type 5 Phosphorylation.* Mol Biol Cell **2004**, 15, 4023-4030.
154. Corbin, J.D. and Francis, S.H. *Cyclic GMP phosphodiesterase-5: target of sildenafil.* J Biol Chem **1999**, 274, 13729-13732.
155. Dole, M., Mack, L.L., Hines, R.L., Mobley, R.C., Ferguson, L.D. and Alice, M.B. *Molecular Beams of Macroions.* The Journal of Chemical Physics **1968**, 49, 2240-2249.
156. Mack, L.L., Kralik, P., Rheude, A. and Dole, M. *Molecular Beams of Macroions. II.* The Journal of Chemical Physics **1970**, 52, 4977-4986.
157. Fenn, J.B., Mann, M., Meng, C.K., Wong, S.F. and Whitehouse, C.M. *Electrospray ionization for mass spectrometry of large biomolecules.* Science **1989**, 246, 64-71.
158. Whitehouse, C.M., Dreyer, R.N., Yamashita, M. and Fenn, J.B. *Electrospray interface for liquid chromatographs and mass spectrometers.* Anal Chem **1985**, 57, 675-679.

159. Gamero-Castano, M. and Mora, J.F. *Kinetics of small ion evaporation from the charge and mass distribution of multiply charged clusters in electrosprays.* J Mass Spectrom **2000**, 35, 790-803.
160. Kebarle, P. and Peschke, M. *On the mechanisms by which the charged droplets produced by electrospray lead to gas phase ions.* Analytica Chimica Acta **2000**, 406, 11-35.
161. de la Mora, J.F. *Electrospray ionization of large multiply charged species proceeds via Dole's charged residue mechanism.* Analytica Chimica Acta **2000**, 406, 93-104.
162. Felitsyn, N., Peschke, M. and Kebarle, P. *Origin and number of charges observed on multiply-protonated native proteins produced by ESI.* International Journal of Mass Spectrometry **2002**, 219, 39-62.
163. Karas, M. and Hillenkamp, F. *Laser desorption ionization of proteins with molecular masses exceeding 10,000 daltons.* Anal Chem **1988**, 60, 2299-2301.
164. Douglas, D.J., Frank, A.J. and Mao, D. *Linear ion traps in mass spectrometry.* Mass Spectrom Rev **2004**.
165. March, R.E. *An introduction to quadrupole ion trap mass spectrometry.* Journal of Mass Spectrometry **1997**, 32, 351-369.
166. Mamyrin, B.A. *Time-of-flight mass spectrometry (concepts, achievements, and prospects).* International Journal of Mass Spectrometry **2001**, 206, 251-266.
167. Cotter, R.J. *Time-of-flight mass spectrometry: an increasing role in the life sciences.* Biomed Environ Mass Spectrom **1989**, 18, 513-532.
168. Chernushevich, I.V., Loboda, A.V. and Thomson, B.A. *An introduction to quadrupole-time-of-flight mass spectrometry.* J Mass Spectrom **2001**, 36, 849-865.
169. Guilhaus, M., Selby, D. and Mlynski, V. *Orthogonal acceleration time-of-flight mass spectrometry.* Mass Spectrom Rev **2000**, 19, 65-107.
170. Heeren, R.M., Kleinnijenhuis, A.J., McDonnell, L.A. and Mize, T.H. *A mini-review of mass spectrometry using high-performance FTICR-MS methods.* Anal Bioanal Chem **2004**, 378, 1048-1058.
171. Belov, M.E., Anderson, G.A., Angell, N.H., Shen, Y., Tolic, N., Udseth, H.R. and Smith, R.D. *Dynamic range expansion applied to mass spectrometry based on data-dependent selective ion ejection in capillary liquid chromatography fourier transform ion cyclotron resonance for enhanced proteome characterization.* Anal Chem **2001**, 73, 5052-5060.
172. Smith, R.D., Anderson, G.A., Lipton, M.S., Masselon, C., Pasa-Tolic, L., Udseth, H., Belov, M., Shen, Y. and Veenstra, T.D. *High-performance separations and mass spectrometric methods for high-throughput proteomics using accurate mass tags.* Adv Protein Chem **2003**, 65, 85-131.
173. Belov, M.E., Anderson, G.A., Wingerd, M.A., Udseth, H.R., Tang, K.*, et al. An automated high performance capillary liquid chromatography-Fourier transform ion cyclotron resonance mass spectrometer for high-throughput proteomics.* J Am Soc Mass Spectrom **2004**, 15, 212-232.
174. Roepstorff, P. and Fohlman, J. *Proposal for a common nomenclature for sequence ions in mass spectra of peptides.* Biomed Mass Spectrom **1984**, 11, 601.
175. Johnson, R.S., Martin, S.A., Biemann, K., Stults, J.T. and Watson, J.T. *Novel fragmentation process of peptides by collision-induced decomposition in a tandem mass spectrometer: differentiation of leucine and isoleucine.* Anal Chem **1987**, 59, 2621-2625.
176. Snyder, L.R. and Kirkland, J.J. *Introduction to Modern Liquid Chromatography.* John Wiley & Sons **1979**, 2nd edition, New York.
177. MacNair, J.E., Lewis, K.C. and Jorgenson, J.W. *Ultrahigh-pressure reversed-phase liquid chromatography in packed capillary columns.* Anal Chem **1997**, 69, 983-989.

178. Wu, N., Lippert, J.A. and Lee, M.L. *Practical aspects of ultrahigh pressure capillary liquid chromatography.* J Chromatogr A **2001**, 911, 1-12.
179. Gusev, I., Huang, X. and Horvath, C. *Capillary columns with in situ formed porous monolithic packing for micro high-performance liquid chromatography and capillary electrochromatography.* J Chromatogr A **1999**, 855, 273-290.
180. Ficarro, S.B., McCleland, M.L., Stukenberg, P.T., Burke, D.J., Ross, M.M., Shabanowitz, J., Hunt, D.F. and White, F.M. *Phosphoproteome analysis by mass spectrometry and its application to Saccharomyces cerevisiae.* Nat Biotechnol **2002**, 20, 301-305.
181. Nuhse, T.S., Stensballe, A., Jensen, O.N. and Peck, S.C. *Large-scale Analysis of in Vivo Phosphorylated Membrane Proteins by Immobilized Metal Ion Affinity Chromatography and Mass Spectrometry.* Mol Cell Proteomics **2003**, 2, 1234-1243.
182. Posewitz, M.C. and Tempst, P. *Immobilized gallium(III) affinity chromatography of phosphopeptides.* Anal Chem **1999**, 71, 2883-2892.
183. Zhou, H., Watts, J.D. and Aebersold, R. *A systematic approach to the analysis of protein phosphorylation.* Nat Biotechnol **2001**, 19, 375-378.
184. Oda, Y., Nagasu, T. and Chait, B.T. *Enrichment analysis of phosphorylated proteins as a tool for probing the phosphoproteome.* Nat Biotechnol **2001**, 19, 379-382.
185. Hart, G.W., Greis, K.D., Dong, L.Y., Blomberg, M.A., Chou, T.Y.*, et al. O-linked N-acetylglucosamine: the "yin-yang" of Ser/Thr phosphorylation? Nuclear and cytoplasmic glycosylation.* Adv Exp Med Biol **1995**, 376, 115-123.
186. Pandey, A., Podtelejnikov, A.V., Blagoev, B., Bustelo, X.R., Mann, M. and Lodish, H.F. *Analysis of receptor signaling pathways by mass spectrometry: identification of vav-2 as a substrate of the epidermal and platelet-derived growth factor receptors.* Proc Natl Acad Sci U S A **2000**, 97, 179-184.
187. Ficarro, S., Chertihin, O., Westbrook, V.A., White, F., Jayes, F.*, et al. Phosphoproteome analysis of capacitated human sperm. Evidence of tyrosine phosphorylation of a kinase-anchoring protein 3 and valosin-containing protein/p97 during capacitation.* J Biol Chem **2003**, 278, 11579-11589.
188. Brill, L.M., Salomon, A.R., Ficarro, S.B., Mukherji, M., Stettler-Gill, M. and Peters, E.C. *Robust phosphoproteomic profiling of tyrosine phosphorylation sites from human T cells using immobilized metal affinity chromatography and tandem mass spectrometry.* Anal Chem **2004**, 76, 2763-2772.
189. Burgess, R.R. and Thompson, N.E. *Advances in gentle immunoaffinity chromatography.* Curr Opin Biotechnol **2002**, 13, 304-308.
190. Schroeder, M.J., Shabanowitz, J., Schwartz, J.C., Hunt, D.F. and Coon, J.J. *A neutral loss activation method for improved phosphopeptide sequence analysis by quadrupole ion trap mass spectrometry.* Anal Chem **2004**, 76, 3590-3598.
191. Bateman, R.H., Carruthers, R., Hoyes, J.B., Jones, C., Langridge, J.I., Millar, A. and Vissers, J.P. *A novel precursor ion discovery method on a hybrid quadrupole orthogonal acceleration time-of-flight (Q-TOF) mass spectrometer for studying protein phosphorylation.* J Am Soc Mass Spectrom **2002**, 13, 792-803.
192. Chang, E.J., Archambault, V., McLachlin, D.T., Krutchinsky, A.N. and Chait, B.T. *Analysis of protein phosphorylation by hypothesis-driven multiple-stage mass spectrometry.* Anal Chem **2004**, 76, 4472-4483.
193. Carr, S.A., Huddleston, M.J. and Annan, R.S. *Selective detection and sequencing of phosphopeptides at the femtomole level by mass spectrometry.* Anal Biochem **1996**, 239, 180-192.
194. Annan, R.S., Huddleston, M.J., Verma, R., Deshaies, R.J. and Carr, S.A. *A multidimensional electrospray MS-based approach to phosphopeptide mapping.* Anal Chem **2001**, 73, 393-404.

195. Zappacosta, F., Huddleston, M.J., Karcher, R.L., Gelfand, V.I., Carr, S.A. and Annan, R.S. *Improved sensitivity for phosphopeptide mapping using capillary column HPLC and microionspray mass spectrometry: comparative phosphorylation site mapping from gel-derived proteins.* Anal Chem **2002**, 74, 3221-3231.
196. van Berkel, W.J., van den Heuvel, R.H., Versluis, C. and Heck, A.J. *Detection of intact megaDalton protein assemblies of vanillyl-alcohol oxidase by mass spectrometry.* Protein Sci **2000**, 9, 435-439.
197. Pinkse, M.W., Maier, C.S., Kim, J.I., Oh, B.H. and Heck, A.J. *Macromolecular assembly of Helicobacter pylori urease investigated by mass spectrometry.* J Mass Spectrom **2003**, 38, 315-320.
198. Sanglier, S., Leize, E., Van Dorsselaer, A. and Zal, F. *Comparative ESI-MS study of approximately 2.2 MDa native hemocyanins from deep-sea and shore crabs: from protein oligomeric state to biotope.* J Am Soc Mass Spectrom **2003**, 14, 419-429.
199. Wilm, M. and Mann, M. *Analytical properties of the nanoelectrospray ion source.* Anal Chem **1996**, 68, 1-8.
200. Loo, J.A. *Studying noncovalent protein complexes by electrospray ionization mass spectrometry.* Mass Spectrometry Reviews **1997**, 16, 1-23.
201. Hernandez, H. and Robinson, C.V. *Dynamic protein complexes: insights from mass spectrometry.* J Biol Chem **2001**, 276, 46685-46688.
202. Heck, A.J. and Van Den Heuvel, R.H. *Investigation of intact protein complexes by mass spectrometry.* Mass Spectrom Rev **2004**, 23, 368-389.
203. Przybylski, M. and Glocker, M.O. *Electrospray mass spectrometry of biomacromolecular complexes with noncovalent interactions - New analytical perspectives for supramolecular chemistry and molecular recognition processes.* Angewandte Chemie-International Edition in English **1996**, 35, 807-826.
204. Pramanik, B.N., Bartner, P.L., Mirza, U.A., Liu, Y.H. and Ganguly, A.K. *Electrospray ionization mass spectrometry for the study of non-covalent complexes: an emerging technology.* J Mass Spectrom **1998**, 33, 911-920.
205. Veenstra, T.D., Johnson, K.L., Tomlinson, A.J., Craig, T.A., Kumar, R. and Naylor, S. *Zinc-induced conformational changes in the DNA-binding domain of the vitamin D receptor determined by electrospray ionization mass spectrometry.* J Am Soc Mass Spectrom **1998**, 9, 8-14.
206. McCammon, M.G. and Robinson, C.V. *Structural change in response to ligand binding.* Curr Opin Chem Biol **2004**, 8, 60-65.
207. Tjernberg, A., Carno, S., Oliv, F., Benkestock, K., Edlund, P.O., Griffiths, W.J. and Hallen, D. *Determination of dissociation constants for protein-ligand complexes by electrospray ionization mass spectrometry.* Anal Chem **2004**, 76, 4325-4331.
208. Bligh, S.W., Haley, T. and Lowe, P.N. *Measurement of dissociation constants of inhibitors binding to Src SH2 domain protein by non-covalent electrospray ionization mass spectrometry.* J Mol Recognit **2003**, 16, 139-148.
209. Rogniaux, H., Sanglier, S., Strupat, K., Azza, S., Roitel, O., Ball, V., Tritsch, D., Branlant, G. and Van Dorsselaer, A. *Mass spectrometry as a novel approach to probe cooperativity in multimeric enzymatic systems.* Anal Biochem **2001**, 291, 48-61.
210. Smith, D.L., Deng, Y. and Zhang, Z. *Probing the non-covalent structure of proteins by amide hydrogen exchange and mass spectrometry.* J Mass Spectrom **1997**, 32, 135-146.
211. Demmers, J.A., Rijkers, D.T., Haverkamp, J., Killian, J.A. and Heck, A.J. *Factors affecting gas-phase deuterium scrambling in peptide ions and their implications for protein structure determination.* J Am Chem Soc **2002**, 124, 11191-11198.

212. Katta, V. and Chait, B.T. *Conformational changes in proteins probed by hydrogen-exchange electrospray-ionization mass spectrometry.* Rapid Commun Mass Spectrom **1991**, 5, 214-217.
213. Mandell, J.G., Falick, A.M. and Komives, E.A. *Identification of protein-protein interfaces by decreased amide proton solvent accessibility.* Proc Natl Acad Sci U S A **1998**, 95, 14705-14710.
214. Brandsen, J., Werten, S., van der Vliet, P.C., Meisterernst, M., Kroon, J. and Gros, P. *C-terminal domain of transcription cofactor PC4 reveals dimeric ssDNA binding site.* Nat Struct Biol **1997**, 4, 900-903.
215. Loo, J.A., Peifeng, H., McConnell, P., Mueller, W.T., Sawyer, T.K. and Thanabal, V. *A Study of Src SH2 Domain Protein-Phosphopeptide Binding Interactions by Electrospray Ionization Mass Spectrometry.* Journal of the American Society for Mass Spectrometry **1997**, 8, 234-243.
216. Back, J.W., de Jong, L., Muijsers, A.O. and de Koster, C.G. *Chemical cross-linking and mass spectrometry for protein structural modeling.* J Mol Biol **2003**, 331, 303-313.
217. Glocker, M.O., Borchers, C., Fiedler, W., Suckau, D. and Przybylski, M. *Molecular characterization of surface topology in protein tertiary structures by amino-acylation and mass spectrometric peptide mapping.* Bioconjug Chem **1994**, 5, 583-590.
218. Suckau, D., Mak, M. and Przybylski, M. *Protein surface topology-probing by selective chemical modification and mass spectrometric peptide mapping.* Proc Natl Acad Sci U S A **1992**, 89, 5630-5634.
219. Brunner, J. *Use of photocrosslinkers in cell biology.* Trends Cell Biol **1996**, 6, 154-157.
220. Chin, J.W., Santoro, S.W., Martin, A.B., King, D.S., Wang, L. and Schultz, P.G. *Addition of p-azido-L-phenylalanine to the genetic code of Escherichia coli.* J Am Chem Soc **2002**, 124, 9026-9027.

Probing non-covalent protein-ligand interactions of cGMP-dependent protein kinase by nanoflow ESI orthogonal time of flight MS.

2

Martijn W. H. Pinkse[1], Klaus Rumpel[2], Frank Pullen[2] and Albert J. R. Heck[1]

[1] Department of Biomolecular Mass Spectrometry, Bijvoet Center for Biomolecular Research and Utrecht Institute for Pharmaceutical Sciences, Utrecht University, Sorbonnelaan 16, 3584 CA Utrecht, The Netherlands.

[2] Pfizer Global Research and Development, Ramsgate Road, Sandwich CT13 9NJ, UK.

Based on: *J. Am. Soc. Mass Spectrom.*, ***15***, *1392-1399 (2004)*

Abstract

Nanoflow electrospray ionization time of flight mass spectrometry (ESI-TOF-MS) was used to study activation properties of the cGMP-dependent protein kinase (PKG). Our nanoflow ESI-TOF-MS analysis confirms that PKG mainly occurs as a 153 kDa homodimer and is able to bind four cGMP molecules, which is in agreement with the known stoichiometry. Binding order and stoichiometry of cGMP, the non-hydrolysable ATP analog β, γ-methyleneadenosine 5'-triphosphate (AMPPNP) and Mn^{2+} for PKG were characterized as model for the active PKG-cGMP-ATP/Mg^{2+} complex. Already in the absence of cGMP, a non-covalent complex between PKG and two molecules of AMP-PNP could be observed. This complex was only detectable in the presence of Mn^{2+}, reflecting the specific nature of this non-covalent interaction. This finding could imply that within the inactive conformation of PKG, the autoinhibition-domain, when in contact with the substrate-docking domain, does not block the entrance to the ATP-binding site. In the presence of cGMP, less of the fully saturated PKG-$(cGMP)_4$(AMP-PNP/Mn^{2+})$_2$ complex was observed, suggesting that the PKG-ATP interaction is weakened in the active conformation of PKG. Additionally, limited proteolysis in combination with native-ESI MS showed to be a useful tool to study the contact regions on the PKG-dimer and also allowed the rapid determination of the overall autophosphorylation status of the protein. These measurements indicated that autophosphorylation mainly occurs within the first 80 aminoterminal residues and involves in total 3-4 phosphates per subunit.

Introduction

Protein kinases are members of a huge family of enzymes that share together with protein phosphatases the responsibility of regulating virtually every kind of cellular function. Activation of protein kinases is one of the major mechanisms by which cellular events are controlled. Hence, intense effort is presently directed towards understanding the molecular basis and mechanisms of protein kinases. Protein kinases serve as molecular switches and are thus by definition highly dynamic proteins that can toggle between different conformational states. Most protein kinases are also phosphoproteins, and those phosphates are an integral

determinant for both structure and function. Crystal structures of several kinases revealed that the active forms of these enzymes show similar conformations in key regions, but their inactive conformations exhibit surprisingly large structural variations [1]. Within the large and diverse family of protein kinases, the cAMP dependent protein kinase (PKA) is one of the simplest and best understood members and often serves as a prototype for the entire family [2-4]. PKA is a heterotetramer composed of a regulatory dimer and two catalytic subunits. The catalytic subunits are active when cAMP binds to the regulatory dimer and induces dissociation of the tetramer. The catalytic subunit of PKA is comprised of a bilobal core that is shared by all members of the protein kinase family. The two lobes, which are connected via a small linker region, generate a binding pocket for ATP and a docking site for protein/peptide substrates. The ATP is nestled deep between the two domains, while substrate peptides/proteins dock onto the more exposed region of the larger C-terminal lobe. Protein kinases poorly phosphorylate free amino acids and rely partly on local residues within the substrate for high affinity. Subtle differences within the peptide-docking domain in the large lobe of the catalytic core of each kinase play an important role in substrate specificity. In order to understand the role of these kinases in signaling pathways it is important to gain deeper insight into how specificity and different mechanisms of control within the common protein kinase fold are regulated. In general, regulation of protein kinases is achieved through phosphorylation/dephosphorylation, binding of second messengers, interaction with regulatory domains or subunits and/or assembly with accessory proteins. In the present study we have used mass spectrometry to study structural and biochemical aspects of the cGMP-dependent protein kinase (PKG) Iα. PKG is involved in the nitric oxide/cGMP-signaling pathway, serves as a major receptor protein for intracellular cGMP and controls a variety of cellular responses, including smooth muscle relaxation [5, 6]. PKG is the closest homologue of PKA and in particular the catalytic domains of the two enzymes show a remarkable high sequence homology [7].

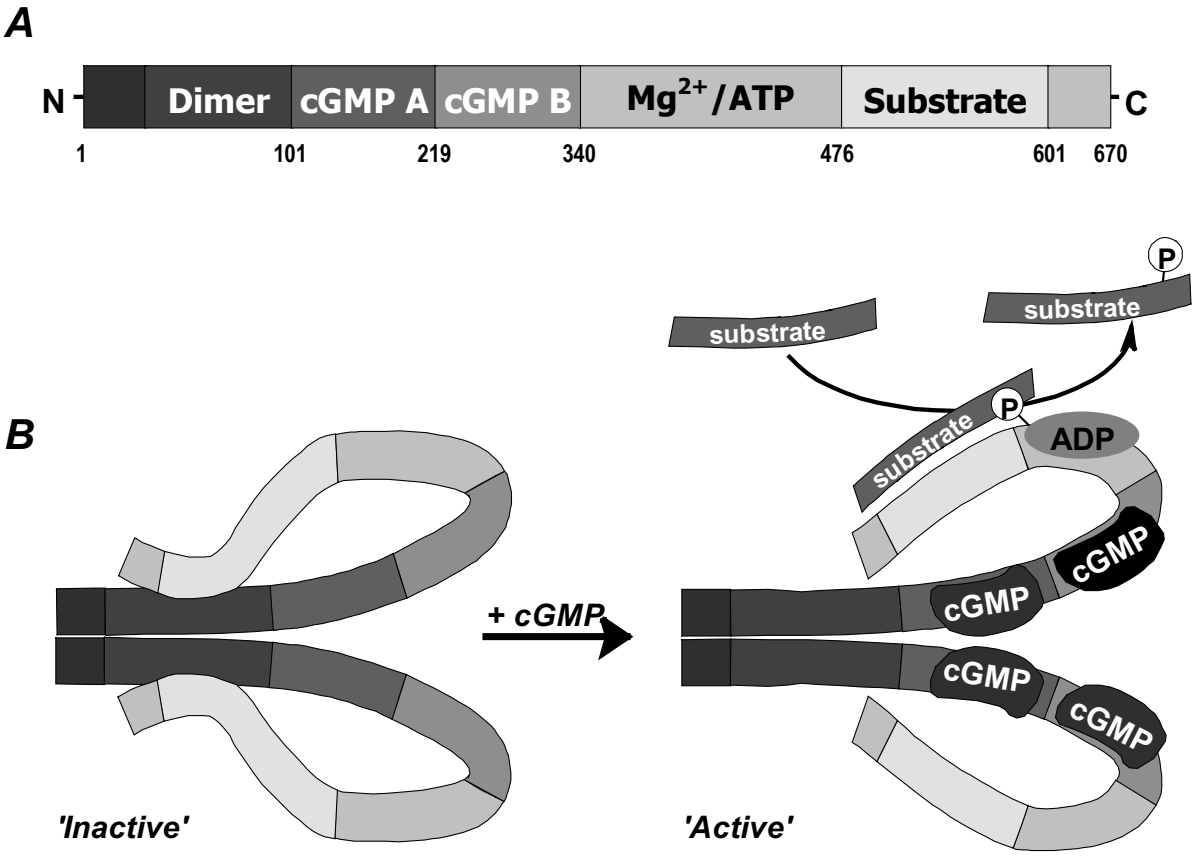

Figure 1: Schematic representation of the structure and the activation process of PKG. **(A)** Linear rearrangement of the functional domains of PKG. The N-terminal regulatory domain contains a leucine/isoleucine dimerization domain, an autoinhibitory domain, including autophosphorylation sites and a hinge region, which connects the aminoterminus with the two in-tandem cGMP binding pockets (site A, high affinity, slow dissociation; and site B, low affinity, rapid dissociation) cGMP binding sites). The catalytic domain contains the MgATP binding pocket and the peptide/protein-substrate docking site. **(B)** Schematic representation of the current working model of cGMP-induced activation of PKG. Dimerization occurs via the N-terminal leucine/isoleucine zipper motif. Autoinhibition of enzymatic activity involves interaction between the catalytic domain and the N-terminal autoinhibition domain. cGMP-binding induces a conformational change which releases PKG from its inactive conformation.

No detailed structural information for PKG is yet available, but on basis of biochemical data and by comparing the functional domains of PKG (Figure 1A) with PKA a simplified structure of PKG has evolved which is schematically depicted in Figure 1B. PKG Iα exists as a dimer of two identical subunits (Mr ~76 kDa). Each subunit possesses two functional moieties, a regulatory and a catalytic. The N-terminal regulatory domain contains a

leucine/isoleucine dimerization domain, an autoinhibitory domain, including autophosphorylation sites and a hinge region, which connects the aminoterminus with the two in-tandem cGMP binding pockets. The catalytic domain contains the MgATP binding pocket and the peptide/protein-substrate docking site. In the inactive state of the protein, components of the inhibitory domain in the N-terminal part of the protein interact with the substrate-docking domain. Binding of cGMP induces a conformational change in PKG that modulates this interaction and this leads to activation of the enzyme [8]. Once activated by cGMP, PKG phosphorylates target substrates and it autophosphorylates residues within the inhibitory domain [4, 9, 10]. Extensive autophosphorylation of PKG in the presence of either cGMP or cAMP increases basal kinase activity. Furthermore, it has been shown that both cGMP-binding and autophosphorylation apparently alter the protein in a similar manner [10]. In the present study we have examined cGMP and ATP binding processes of PKG Iα by mass spectrometry based techniques. Recent examples have shown that electrospray ionization under non-denaturing conditions can provide detailed information about protein-ligand complexes, including binding order and stoichiometry of binding partners, binding affinity and cooperativity [11-13]. In this study nanoflow ESI-TOF-MS allowed the detection of non-covalent interactions between PKG, the high affinity ligand cGMP and the ATP substrate-analogue AMP-PNP. Our nanoflow ESI-TOF-MS analysis revealed that dimeric PKG binds four cGMP molecules, thus confirming the known PKG/cGMP stoichiometry of two cGMP's per monomer [14]. Non-covalent complex between PKG and 2 AMP-PNP molecules could be observed already in the absence of cGMP and only in the presence of the divalent metal Mn^{2+}. Additionally, we examined the phosphorylation state of the protein after incubation with Mg^{2+} and ATP at a global level. PKG Iα is labile to specific proteolysis [15]. Limited proteolysis of the kinase with chymotrypsin yields two large fragments and an additional small peptide. Monitoring for 80 Da mass-increments of these fragments along the autophosphorylation process by nano-ESI-TOF-MS allowed further insight into the overall amount of phosphate incorporation into the different parts of the kinase.

Experimental

Material and reagents. Bovine lung PKG type Iα was purified to homogeneity essentially as described by Francis *et al.* [16]. Recombinant PKG Iα was expressed and purified from SF9-insect cells according to Dostmann *et al.* [17]. Guanosine 3',5'-cyclic monophosphate,

Adenosine 5'-triphosphate sodium salt, β,γ-imidoadenosine 5'-triphosphate tetralithium salt, magnesium acetate tetrahydrate and manganese(II) chloride were purchased from Sigma (St. Louis, MO, USA). Sequencing grade chymotrypsin was purchased from Boehringer (Boehringer, Mannheim, Germany).

Sample preparation. Prior to mass spectrometric measurements PKG was buffer exchanged to 200 mM ammonium acetate, pH 6.7 using Ultrafree-0.5 Centrifugal Filter Units (5000 NMWL) (Millipore, Bedford MA). cGMP, AMP-PNP and magnesium acetate or manganese chloride were dissolved in 200 mM ammonium acetate, pH 6.7, and added to a recombinant PKG solution (~5 μM). For the preparation of differentially phosphorylated protein, PKG isolated from bovine lung was incubated with ATP and magnesium. Non-phosphorylated protein was not incubated with $MgCl_2$ and ATP. In order to obtain partially- and highly-autophosphorylated protein, PKG was incubated with 5 mM $MgCl_2$ and 100 μM ATP at 30°C for 10 minutes and 3 hours respectively. Limited proteolysis of autophosphorylated PKG with chymotrypsin was performed as essentially described by Monken *et al.* [15]. The chymotrypsin/protein ratio used was 1:200 by weight.

Electrospray Ionization Mass Spectrometry. Electrospray ionization mass spectrometry analyses of the intact protein were carried out on a Micromass LC-T time-of-flight instrument (Micromass UK Ltd., Wythenshawe, Manchester, United Kingdom) equipped with a 'Z-Spray' nanoflow electrospray source using in-house pulled and gold coated borosilicate glass needles. Typical ESI-TOF-MS operating parameters were as follows: capillary voltage, 1.0-1.5 kV; sample cone voltage, 100-200 V; extraction cone voltage, 50-100 V; source block temperature, 70°C; source pressure 9.0 mbar (standard 2.0 mbar), TOF analyzer pressure 1.3 x 10^{-6} mbar (standard 6.2 x 10^{-7} mbar). Spectra were recorded in the positive ion mode and the standard *m/z* of 200-10000 was monitored. The mass spectrometer was calibrated on the singly charged $Cs_{n+1}I_n$ clusters obtained after electrospraying an aqueous cesium iodide solution (1 mg/ml). Molecular masses of protein and protein-ligand complexes were calculated using a maximum entropy (MaxEnt1) based approach [18, 19] incorporated as part of the MassLynx software (MassLynx v3.5) supplied with the mass spectrometer.

Results and Discussion

Non-covalent cGMP binding: Figure 2 shows the mass spectrum of native PKG sprayed from an aqueous 200 mM ammonium acetate solution at an estimated PKG dimer concentration of ~1-2 µM. The mass spectrum displays abundant ion signals around *m/z* 5500-7000 originating from dimeric PKG Iα. The molecular weight derived from this charge state envelope is 152,883 Da. The theoretical average mass of the dimeric protein, calculated

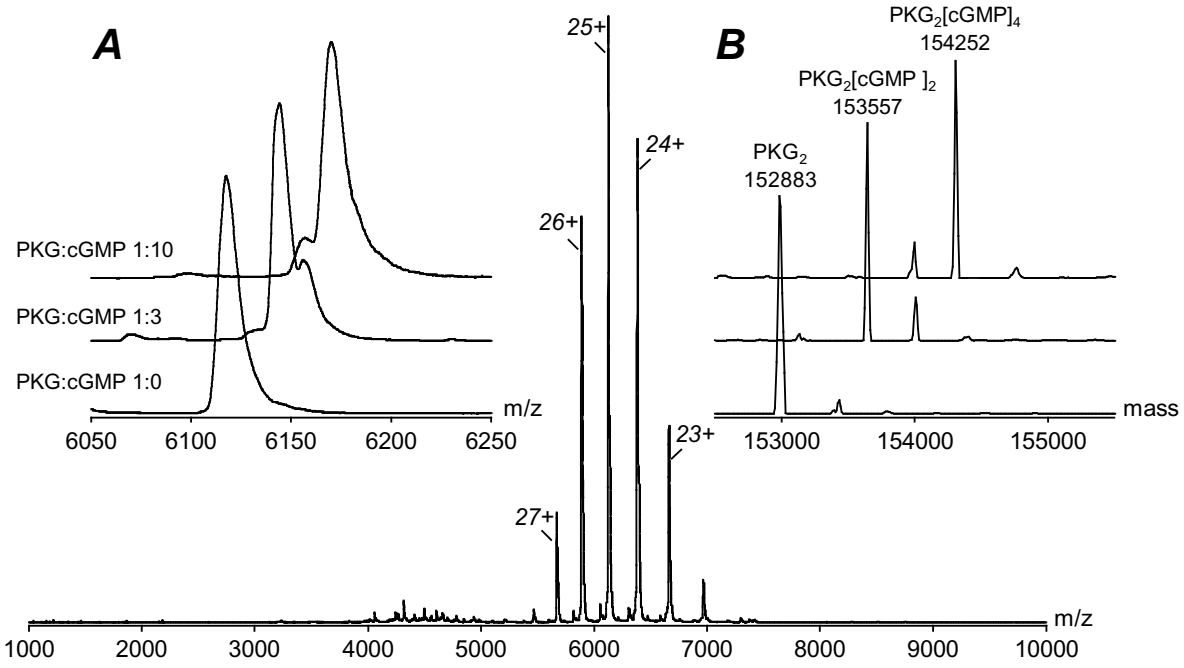

Figure 2: Electrospray ionization mass spectrum of native PKG electrosprayed from an aqueous 200 mM Ammonium acetate solution, pH 6.7, at an estimated dimer concentration of ~1-2 µM. Inset **(A)** shows the effect on the $[M+25H]^{25+}$ signal of dimeric PKG upon addition of cGMP. Inset **(B)** shows the corresponding deconvoluted (MaxEnt1) mass spectra of PKG acquired in absence or presence of cGMP.

from the sequence with acetylated N-termini and without any additional cyclic nucleotides or phosphorylated residues is 152,657 Da. A common feature amongst protein kinase involves activation by phosphorylation of a threonine in the activation loop, which when unphosphorylated may inhibit primarily by blocking the access to the ATP binding site, or by preventing catalytically competent structuring of the active site [1]. Proteolytic digests of PKG analyzed by nanoflow-ESI-TOF-MS/MS revealed that Thr516 within the activation

loop is indeed phosphorylated (data not shown). In fact, pure preparations of PKG are known to contain 1,0-1,5 mol phosphate / mol subunit [20]. By taking into account the phosphorylation of this residue, the theoretical mass of dimeric PKG increases to 152,817 Da, which is in more agreement with the measured mass. Each subunit of PKG contains two cyclic nucleotide binding sites with slow and fast dissociation behavior. The amino-terminal binding pocket binds cGMP with an apparent K_d of 10 nM while the C-terminal binding pocket binds cGMP with an apparent K_d of 100-150 nM [21-23]. Addition of free cGMP to the electrospray solution at an estimated cGMP concentration of 3 μM results in a direct mass shift of the ion signals of PKG as illustrated for $[M+25H]^{25+}$ ion signal shown in inset A of Figure 2. Deconvolution [18, 19] (MaxEnt1) of the charge state envelope indicates that the mass of PKG has increased by ~700 Da (Inset B), which would correspond to the binding of two cGMP molecules (M_r cGMP = 345.2). Increasing the amount of cGMP added to 10 μM results in a further shift of the ion-signals to higher *m/z* ratios. Deconvolution indicates that under these conditions up to four cGMP molecules bind to the dimeric protein, which is in agreement with previous performed biochemical determinations [14].

Ternary PKG-cGMP-AMP-PNP/Mn^{2+} complex. In order to investigate the binding order and stoichiometry of ATP-binding to PKG and at the same time prevent possible autophosphorylation during the measurement, the non-hydrolyzable ATP analogue β, γ-iminoadenosine triphosphate (AMP-PNP) was used. Figure 3A shows the mass spectrum of PKG in the presence of 25 μM AMP-PNP. Deconvolution of the mass spectrum displays binding of 1 AMP-PNP molecule, however the most abundant species is still dimeric PKG without any additional ligands. Addition of 50 μM $MnCl_2$ to the spray solution results in a shift of the ion signals to higher *m/z*. After deconvolution it appears that the mass of PKG has increased by 1225 Da, which corresponds to binding of two times AMP-PNP/$2Mn^{2+}$ (Figure 3B). The mass spectrum of PKG in presence of cGMP (10 μM) and AMP-PNP (50 μM) (Figure 3C) shows solely binding of 4 cGMP molecules. When PKG was electrosprayed with cGMP (10 μM), AMP-PNP (50 μM) and $MnCl_2$ (100 μM), binding of 2 AMP-PNP/$2Mn^{2+}$ is visible, however binding of 1 AMP-PNP/$2Mn^{2+}$ is the most abundant species and PKG with only 4 cGMP molecules is also visible (Figure 3D). In another set of experiments, magnesium instead of manganese was added to the spray solution. Although Mg^{2+} is the physiological cation activator of PKG, complete saturation of PKG with AMP-PNP by magnesium could not be observed in the mass spectrum.

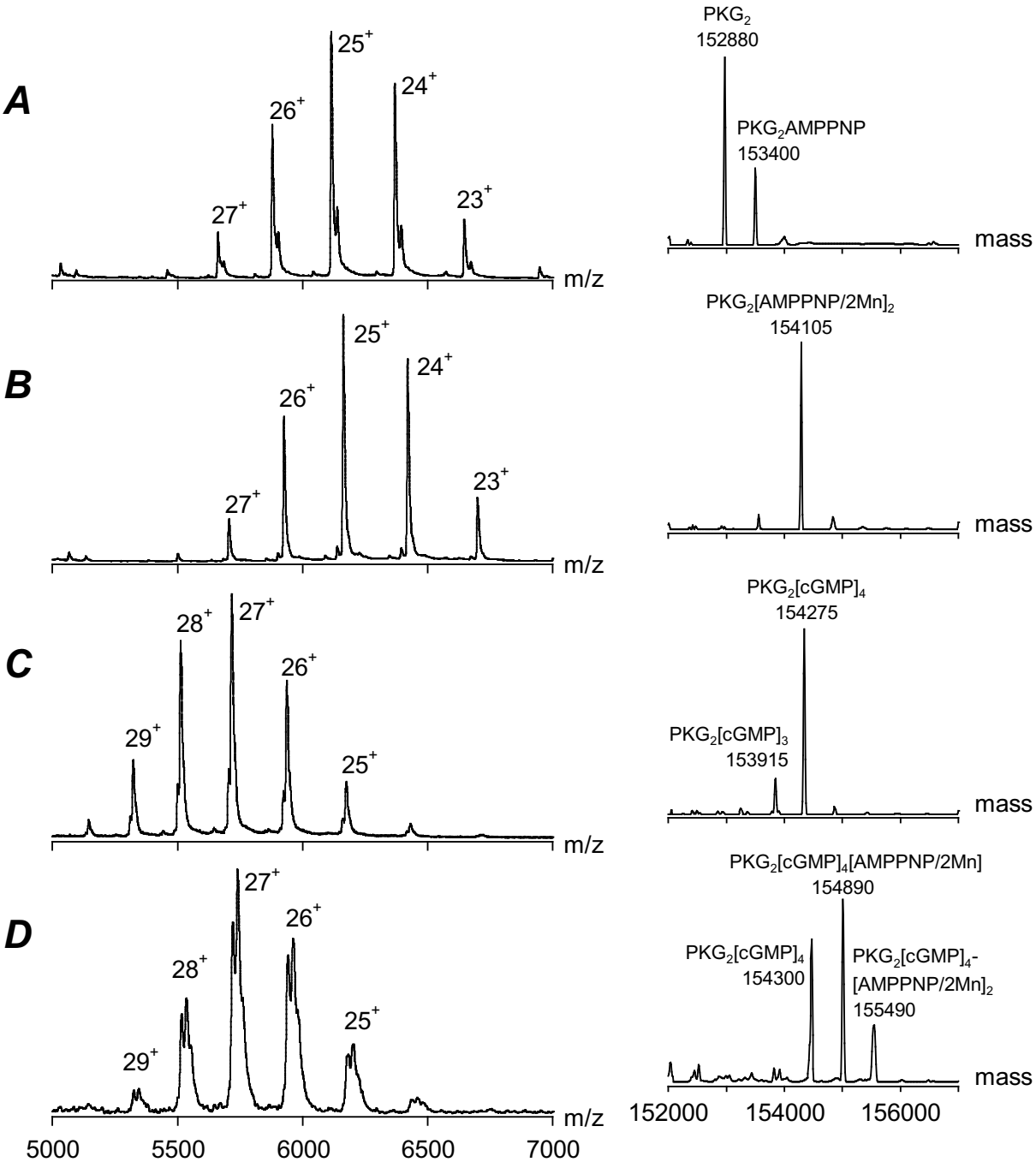

Figure 3: Electrospray ionization mass spectra of PKG at an estimated dimer concentration of ~1-2 µM (A) in the presence of 25 µM AMP-PNP, (B) PKG in the presence of 25 µM AMP-PNP and 50 µM $MnCl_2$, (C) PKG in the presence of 10 µM cGMP and 50 µM AMP-PNP and (D) PKG in the presence of 10 µM cGMP, 50 µM AMP-PNP and 100 µM $MnCl_2$.

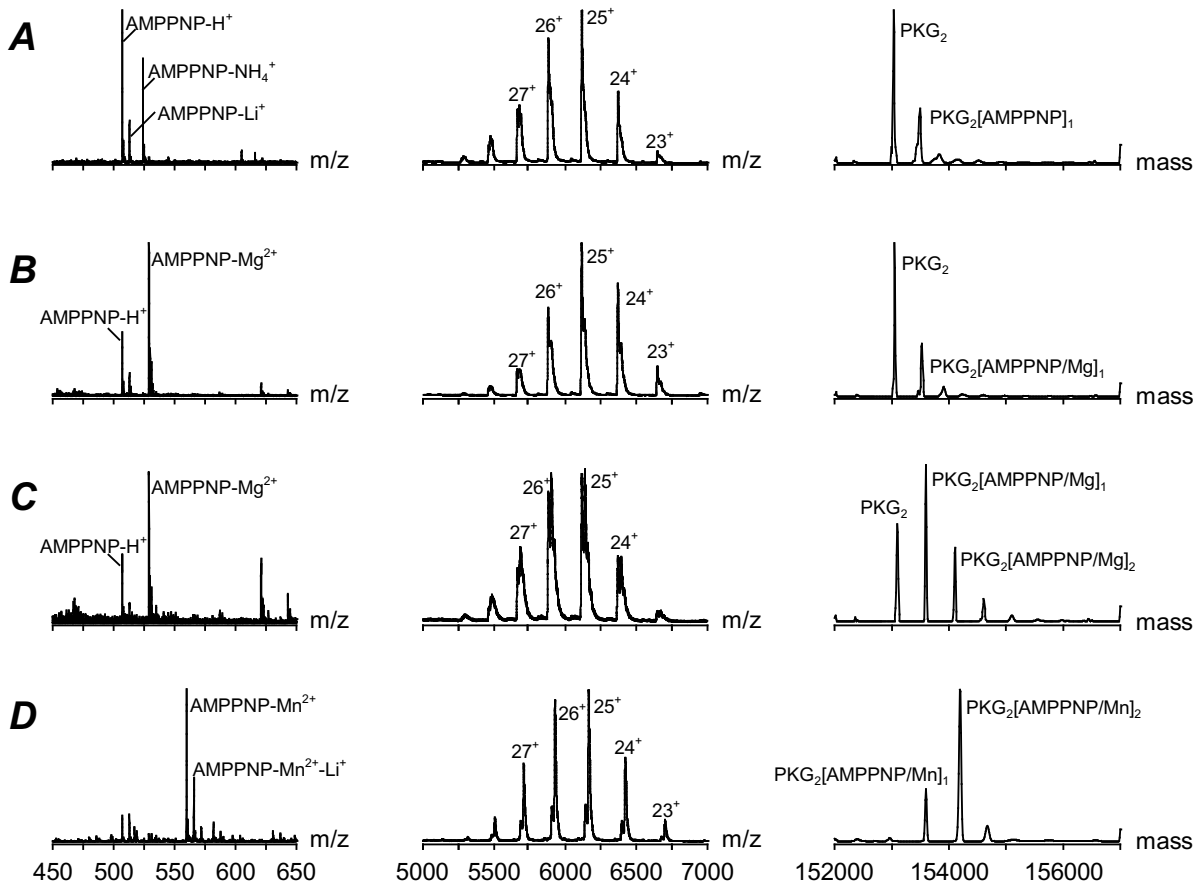

Figure 4: Electrospray ionization mass spectra of PKG at an estimated dimer concentration of ~1-2 µM **(A)** in the presence of 25 µM AMP-PNP, **(B)** in the presence of 25 µM AMP-PNP and 1.2 mM Mg^{2+}-acetate, **(C)** in the presence of 125 µM AMP-PNP and 1.2 mM Mg^{2+}-acetate and **(D)** in the presence of 25 µM AMP-PNP and 100 µM Mn^{2+}-chloride. Mass spectra on the left display the low *m/z* region from 450-650, displaying the free AMP-PNP molecular ion. Mass spectra in the middle display the charge state envelope of dimeric PKG and mass spectra on the right display the corresponding deconvoluted mass spectra.

Figure 4 shows electrospray ionization mass spectra of PKG in the presence of AMP-PNP, AMP-PNP-Mn^{2+} and AMP-PNP-Mg^{2+}. In the low *m/z* region coordination of Mg^{2+} and Mn^{2+} to AMP-PNP is clearly visible, however with an increased AMP-PNP (125 µM) concentration and relatively high magnesium concentration used (1.2 µM) AMP-PNP/Mg^{2+} complexation to PKG is observed (Figure 4B-C), but it is still much less pronounced than with Mn^{2+}.

Limited proteolysis: Type I PKGs homo-dimerize through interactions at the N-terminus of each monomer [24]. This sections has been designated the dimerization domain on the basis

of a leucine/isoleucine zipper motif and for type Iα also on the presence of a cysteine residue within. Removal of the N-terminal inhibition and dimerization domain by limited proteolysis completely monomerizes the protein, which will still bind 2 mol of cGMP/subunit with an unchanged enzymatic activity [15, 25].

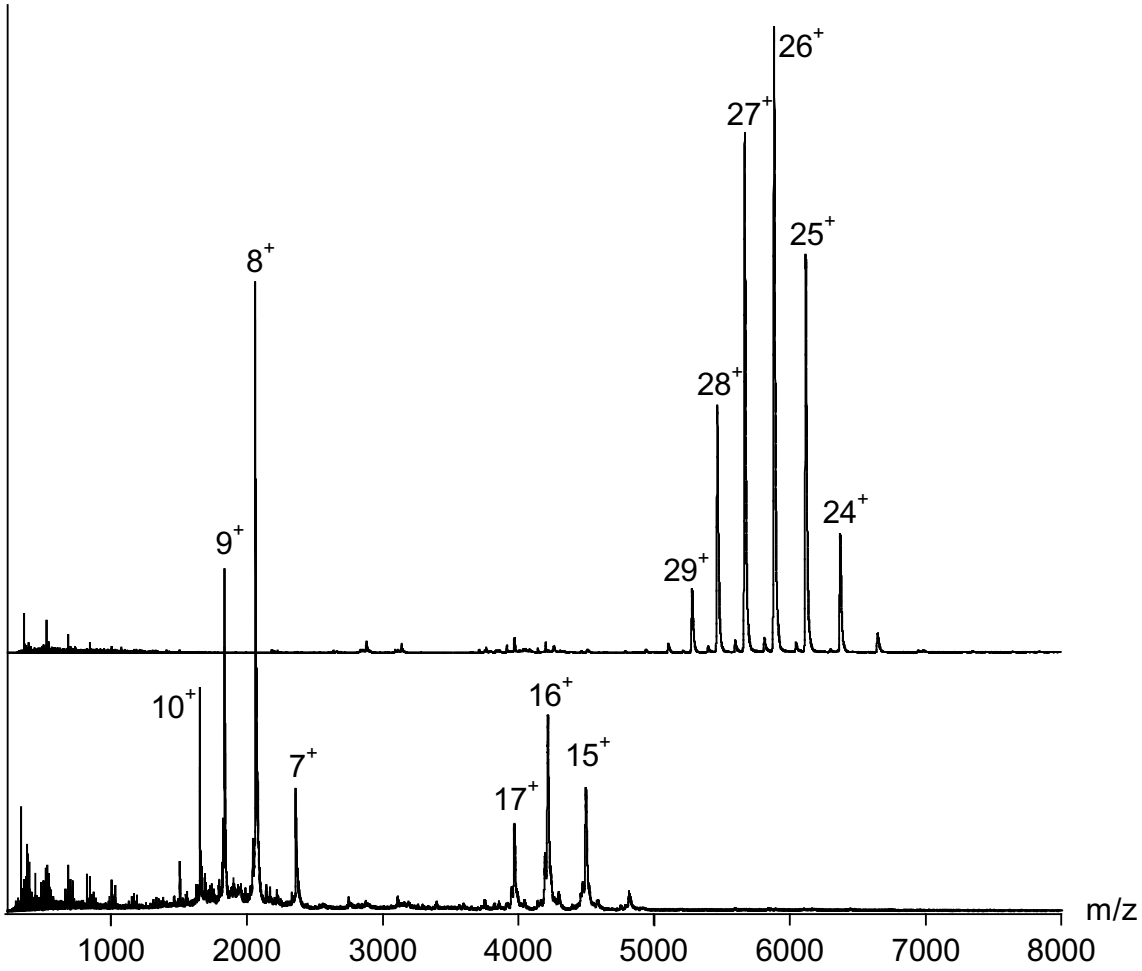

Figure 5: Electrospray ionization mass spectra of native PKG at an estimated dimer concentration of ~1-2 µM before (top) and after (bottom) limited proteolysis with chymotrypsin. Around *m/z* = 2000 ion signals corresponding to the dimer of residues 1-70 are visible, around *m/z* = 4000 ion signals for residues 81-670 are visible. Occasionally the double charged peptide of residues 71-80 was detectable in the low *m/z* range.

Figure 5 shows the mass spectrum of PKG Iα before (5A) and after (5B) limited proteolysis with chymotrypsin. As mentioned the mass spectrum of non-proteolyzed protein shows abundant ion peaks around *m/z* 5500-7000. Figure 5B shows the electrospray ionization mass spectrum of PKG after limited chymotryptic hydrolysis. Two charge state envelopes are clearly visible around *m/z* 2000 and *m/z* 4500. These two envelopes correspond to the dimeric

species of the first 70 N-terminal residues of PKG, and to the large monomer comprising of residues 81-670. Occasionally, the doubly charged peptide of residues 71-80 could be observed in the low *m/z* region. Limited proteolysis of differentially autophosphorylated protein was performed to gain further insight into the overall amount of phosphate incorporation during the autophosphorylation reaction.

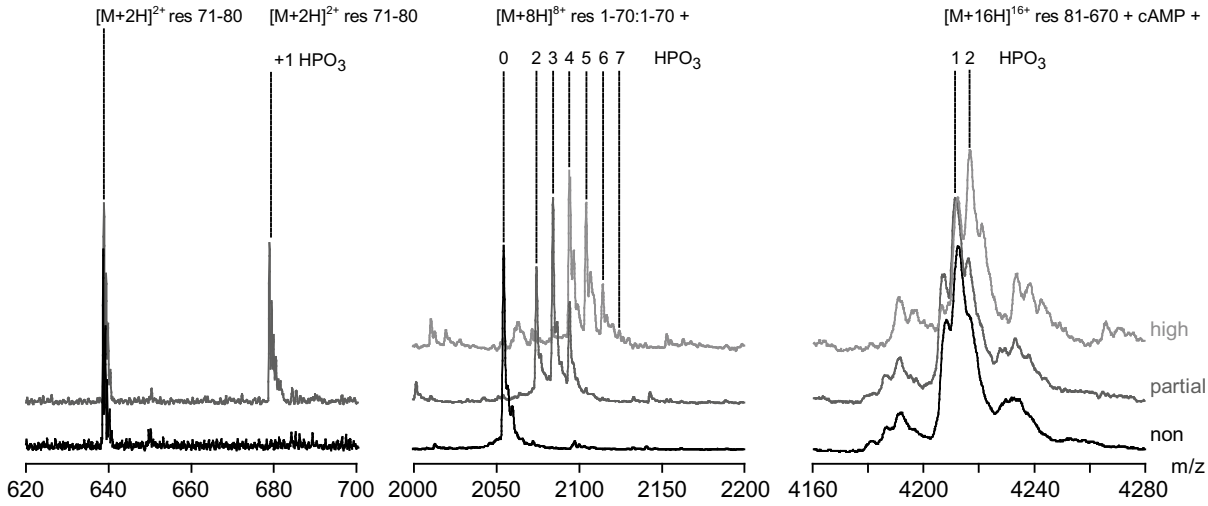

Figure 6: Enlarged parts of the nanoflow ESI mass spectrum of partially proteolyzed PKG Iα, which was autophosphorylated to different levels. Enlarged parts of the mass spectra are displayed for partially proteolyzed PKG, which was (from top to bottom) non-, partially- and highly- autophosphorylated. Mass spectra on the left display the low *m/z* region from *m/z* 620-700, displaying the double charge molecular ion of residues 71-80. Mass spectra in the middle display the $[M+8H]^{8+}$ of the dimeric N-terminus (residues 1-70). Mass spectra on the right display the $[M+16H]^{16+}$ of the C-terminal residues 81-670. The number of phosphate groups present on each of the three proteolytic fragments is listed above each ion signal.

Figure 6 shows enlarged parts of the electrospray ionization mass spectrum of partially proteolyzed PKG, which was non-, partially- and highly- autophosphorylated. In the low mass range (*m/z* 620-700) the doubly charged peptide of residues 71-80 displayed a single mass increase of 80 Da in the partially phosphorylated state. Unfortunately, this peptide could not be observed in the highly autophosphorylated sample. The charge state envelope around *m/z* 2000, corresponding to the dimeric species of the first 70 residues of PKG, shows multiple increases in mass of 80 Da. The $[M+8H]^{8+}$ ion signal of the dimer of residues 1-70 shows no sign of phosphorylation in the non-phosphorylated protein sample. Partially phosphorylated protein contains on average 2 phosphate moieties within the dimer of the first

70 residues, while highly autophosphorylated protein contains on average 4 phosphate moieties within the first 70 residues and shows a maximum of 7-8 phosphorylation sites within this part of PKG. As previously mentioned PKG is already phosphorylated on threonine 516 in non-autophosphorylated protein samples. Additionally the large monomeric subunit (residues 81-670) shows in the highly autophosphorylated protein sample an additional single mass increase of 80 Da, indication that one autophosphorylation site lies within the residues 81-670.

Conclusions

Activity modulation via phosphorylation is the predominant mechanism of signal transduction in cellular pathways. Phosphorylation and dephosphorylation events are catalyzed by protein kinases and protein phosphatases, respectively. In particular protein kinases are themselves tightly regulated by phosphorylation or allosteric activation. In this study we have examined the activation properties of PKG using a mass spectrometry based approach. Our nanoflow ESI-TOF-MS analysis under non-denaturing conditions confirms that PKG mainly occurs as a 153 kDa homodimer and is able to bind four cGMP molecules, which is in agreement with the known stoichiometry. Additionally, nanoflow ESI-TOF-MS data of PKG in complex with AMP-PNP/Mn^{2+} clearly demonstrates that PKG is able to bind two AMP-PNP-molecules in an inactive conformation of the protein (i.e. in the absence of cGMP). Moreover, this interaction was only observed in the presence of the divalent metal Mn^{2+}, indicative for a specific interaction. In the inactive conformation the autoinhibitory domain within the N-terminal regulatory domain interacts with the substrate-docking domain on larger lobe of the catalytic core. Our finding could imply that within this inactive conformation the ATP binding pocket is not blocked and AMP-PNP or ATP are still able to enter this part of the catalytic domain. In the active conformation (i.e. when cGMP is bound) AMP-PNP binding is still observed in the mass spectrum, however at a higher concentration of AMP-PNP and less of the fully saturated product is observed. In the crystal structure of PKA ATP is bound inside the cleft between the smaller and larger lobe of the catalytic domain. Opening and closing of this active site cleft serves to position the ATP for catalysis. When PKG is inactive, the interaction between the N-terminal domain and the substrate-docking domain might have a stabilizing effect on the flexibility in opening and closing of the active cleft. Hence the obtained complex between AMP-PNP/Mn^{2+} and PKG might be

more stable. In the presence of cGMP, the interaction between the N-terminal domain and the substrate binding site is released. Hence it might be well possible that the two lobes of the catalytic domain receive more degrees of freedom, as a result ATP-binding is less strong and this is somehow reflected in the mass spectrum of PKG in presence of cGMP and AMP-PNP/Mn^{2+}. For PKA, nucleotide binding and the influence of divalent metals has been studied extensively [26-28]. Magnetic resonance studies of the interaction between the catalytic subunit of PKA, nucleotides and Mn^{2+} revealed the binding of two Mn^{2+} ions per molecule PKA. Affinities of the Mn^{2+} for the two binding sites in a binary PKA-AMP-PCP complex were 6-10 μM and 50-60 μM respectively. Kinetic analysis revealed that the high affinity Mn^{2+} binding has activation properties, while the lower affinity has an inhibitory effect [26]. In the same study, two binding sites of Mg^{2+} were detected with apparent much lower binding affinity of 1.6 mM for both sites. The effect of the physiological activator Mg^{2+} was analogous to those found with Mn^{2+}, however the inhibition by Mg^{2+} was less pronounced than that observed with Mn^{2+}. Additionally, thermal stability measurements on PKA have shown that MnATP enhances stability stronger than MgATP [29]. These observations made with PKA might explain why in our study no homogenous PKG-[AMP-PNP/Mg^{2+}]$_2$ complex was observed. Although magnesium seems to bind to AMP-PNP as illustrated in Figure 4B-C, complete saturation of PKG with AMP-PNP/Mg^{2+} was not achieved. Due to the high homology in the catalytic cores of PKG and PKA, it is not unlikely that the affinities for ATP and divalent metal ions are similar for both protein kinases. This would explain why the complex between PKG and AMP-PNP in the presence of magnesium as divalent metal ion is more difficult to saturate than that in the presence of manganese.

Upon cGMP-activation PKG phosphorylates in an autocatalytic manner. In this study limited proteolysis in combination with nanoflow ESI-TOF-MS allowed accurate mass measurement of the N-terminal domain. This introduces a higher level of resolution in the part in which almost all known autophosphorylation events occur [30]. This resolution might not have been present for the intact protein. Partially phosphorylated protein showed a single phosphorylation within residues 71-80, and 2 phosphorylations within the dimer of residues 1-70. Highly autophosphorylated protein shows phosphorylation within residues 81-670, and further a higher phosphorylation degree in the N-terminal 1-70 residues. In conclusions, limited chymotryptic proteolysis of PKG in combination with ESI-TOF-MS allows a fast and accurate determination of the overall phosphorylation status.

Acknowledgements

We kindfully thank Jennifer L. Busch, Jackie D. Corbin and Sharron H. Francis from the Vanderbilt University, School of Medicine for the preparation of autophosphorylated PKG. We kindfully thank Arjen Scholten and Wolfgang R. G. Dostmann of the University of Vermont for the recombinant PKG samples.

References

1. Adams, J.A. *Kinetic and catalytic mechanisms of protein kinases.* Chem. Rev. **2001**, *101*, 2271-2290.
2. Taylor, S.S.; Buechler, J.A.; Yonemoto, W. *cAMP-dependent protein kinase: framework for a diverse family of regulatory enzymes.* Annu. Rev. Biochem. **1990**, *59*, 971-1005.
3. Johnson, D.A.; Akamine, P.; Radzio-Andzelm, E.; Madhusudan, M.; Taylor, S.S. *Dynamics of cAMP-dependent protein kinase.* Chem. Rev. **2001**, *101*, 2243-2270.
4. Francis, S.H.; Poteet-Smith, C.; Busch, J.L.; Richie-Jannetta, R.; Corbin, J.D. *Mechanisms of autoinhibition in cyclic nucleotide-dependent protein kinases.* Frontiers in Bioscience **2002**, *7*, D580-D592.
5. Carvajal, J.A.; Germain, A.M.; Huidobro-Toro, J.P.; Weiner, C.P. *Molecular mechanism of cGMP-mediated smooth muscle relaxation.* J. Cell. Physiol. **2000**, *184*, 409-420.
6. Hofmann, F.; Ammendola, A.; Schlossmann, J. *Rising behind NO: cGMP-dependent protein kinases.* J. Cell. Sci. **2000**, *113 (Pt 10)*, 1671-1676.
7. Takio, K.; Wade, R.D.; Smith, S.B.; Krebs, E.G.; Walsh, K.A.; Titani, K. *Guanosine cyclic 3',5'-phosphate dependent protein kinase, a chimeric protein homologous with two separate protein families.* Biochemistry **1984**, *23*, 4207-4218.
8. Francis, S.H.; Poteet-Smith, C.; Busch, J.L.; Richie-Jannetta, R.; Corbin, J.D. *Mechanisms of autoinhibition in cyclic nucleotide-dependent protein kinases.* Front. Biosci. **2002**, *7*, d580-592.
9. Pfeifer, A.; Ruth, P.; Dostmann, W.; Sausbier, M.; Klatt, P.; Hofmann, F. *Structure and function of cGMP-dependent protein kinases.* Rev. Physiol. Biochem. Pharmacol. **1999**, *135*, 105-149.
10. Chu, D.M.; Francis, S.H.; Thomas, J.W.; Maksymovitch, E.A.; Fosler, M.; Corbin, J.D. *Activation by autophosphorylation or cGMP binding produces a similar apparent conformational change in cGMP-dependent protein kinase.* J. Biol. Chem. **1998**, *273*, 14649-14656.
11. Robinson, C.V.; Chung, E.W.; Kragelund, B.B.; Knudsen, J.; Aplin, R.T.; Poulsen, F.M.; Dobson, C.M. *Probing the nature of noncovalent interactions by mass spectrometry. A study of protein-CoA ligand binding and assembly.* Journal of the American Chemical Society **1996**, *118*, 8646-8653.
12. McCammon, M.G.; Scott, D.J.; Keetch, C.A.; Greene, L.H.; Purkey, H.E.; Petrassi, H.M.; Kelly, J.W.; Robinson, C.V. *Screening transthyretin amyloid fibril inhibitors: characterization of novel multiprotein, multiligand complexes by mass spectrometry.* Structure (Camb) **2002**, *10*, 851-863.
13. Loo, J.A. *Studying noncovalent protein complexes by electrospray ionization mass spectrometry.* Mass Spectrometry Reviews **1997**, *16*, 1-23.
14. Corbin, J.D.; Doskeland, S.O. *Studies of two different intrachain cGMP-binding sites of cGMP-dependent protein kinase.* J. Biol. Chem. **1983**, *258*, 11391-11397.
15. Monken, C.E.; Gill, G.N. *Structural analysis of cGMP-dependent protein kinase using limited proteolysis.* J. Biol. Chem. **1980**, *255*, 7067-7070.

16. Francis, S.H.; Wolfe, L.; Corbin, J.D. *Purification of type I alpha and type I beta isozymes and proteolyzed type I beta monomeric enzyme of cGMP-dependent protein kinase from bovine aorta.* Methods Enzymol. **1991**, *200*, 332-341.
17. Dostmann, W.R.; Taylor, M.S.; Nickl, C.K.; Brayden, J.E.; Frank, R.; Tegge, W.J. *Highly specific, membrane-permeant peptide blockers of cGMP-dependent protein kinase Ialpha inhibit NO-induced cerebral dilation.* Proc. Natl. Acad. Sci. U.S.A. **2000**, *97*, 14772-14777.
18. Ferrige, A.G.; Seddon, M.J.; Jarvis, S. *Maximum-Entropy Deconvolution in Electrospray Mass-Spectrometry.* Rapid Com. Mass Spectrom. **1991**, *5*, 374-377.
19. Ferrige, A.G.; Seddon, M.J.; Green, B.N.; Jarvis, S.A.; Skilling, J. *Disentangling Electrospray Spectra With Maximum-Entropy.* Rapid Comm. Mass Spectrom. **1992**, *6*, 707-711.
20. Hofmann, F.; Flockerzi, V. *Characterization of phosphorylated and native cGMP-dependent protein kinase.* Eur. J. Biochem. **1983**, *130*, 599-603.
21. Hofmann, F.; Gensheimer, H.P.; Gobel, C. *cGMP-dependent protein kinase. Autophosphorylation changes the characteristics of binding site 1.* Eur. J. Biochem. **1985**, *147*, 361-365.
22. Reed, R.B.; Sandberg, M.; Jahnsen, T.; Lohmann, S.M.; Francis, S.H.; Corbin, J.D. *Fast and slow cyclic nucleotide-dissociation sites in cAMP-dependent protein kinase are transposed in type Ibeta cGMP-dependent protein kinase.* J. Biol. Chem. **1996**, *271*, 17570-17575.
23. Reed, R.B.; Sandberg, M.; Jahnsen, T.; Lohmann, S.M.; Francis, S.H.; Corbin, J.D. *Structural order of the slow and fast intrasubunit cGMP-binding sites of type I alpha cGMP-dependent protein kinase.* Adv. Second Messenger Phosphoprotein Res. **1997**, *31*, 205-217.
24. Richie-Jannetta, R.; Francis, S.H.; Corbin, J.D. *Dimerization of cGMP-dependent protein kinase Ibeta is mediated by an extensive amino-terminal leucine zipper motif, and dimerization modulates enzyme function.* J. Biol. Chem. **2003**, *278*, 50070-50079.
25. Wolfe, L.; Francis, S.H.; Corbin, J.D. *Properties of a cGMP-dependent monomeric protein kinase from bovine aorta.* J. Biol. Chem. **1989**, *264*, 4157-4162.
26. Armstrong, R.N.; Kondo, H.; Granot, J.; Kaiser, E.T.; Mildvan, A.S. *Magnetic resonance and kinetic studies of the manganese(II) ion and substrate complexes of the catalytic subunit of adenosine 3',5'-monophosphate dependent protein kinase from bovine heart.* Biochemistry **1979**, *18*, 1230-1238.
27. Adams, J.A.; Taylor, S.S. *Divalent metal ions influence catalysis and active-site accessibility in the cAMP-dependent protein kinase.* Protein Sci. **1993**, *2*, 2177-2186.
28. Bhatnagar, D.; Roskoski, R., Jr.; Rosendahl, M.S.; Leonard, N.J. *Adenosine cyclic 3',5'-monophosphate dependent protein kinase: a new fluorescence displacement titration technique for characterizing the nucleotide binding site on the catalytic subunit.* Biochemistry **1983**, *22*, 6310-6317.
29. Herberg, F.W.; Doyle, M.L.; Cox, S.; Taylor, S.S. *Dissection of the nucleotide and metal-phosphate binding sites in cAMP-dependent protein kinase.* Biochemistry **1999**, *38*, 6352-6360.
30. Aitken, A.; Hemmings, B.A.; Hofmann, F. *Identification of the residues on cyclic GMP-dependent protein kinase that are autophosphorylated in the presence of cyclic AMP and cyclic GMP.* Biochim. Biophys. Acta **1984**, *790*, 219-225.

Selective enrichment of phosphopeptides from proteolytic digest using 2D-LC-ESI-MS and titanium oxide pre-columns.

3

Martijn W. H. Pinkse[1], Pauliina M. Uitto[1], Martijn J. Hilhorst[2], Bert Ooms[2] and Albert J. R. Heck[1]

[1] Department of Biomolecular Mass Spectrometry, Bijvoet Center for Biomolecular Research and Utrecht Institute for Pharmaceutical Sciences, Utrecht University, Sorbonnelaan 16, 3584 CA Utrecht, The Netherlands.

[2] Spark Holland BV, P. de Keyserstraat 8, 7800 AJ Emmen, The Netherlands.

Based on: *Anal. Chem.* ***76*** *(14), 3935-3943 (2004)*

Abstract

Selective detection of phosphopeptides from proteolytic digests is a challenging and highly relevant task in many proteomics applications. Often phosphopeptides are present in small amounts and need selective isolation and/or enrichment before identification. Here we report a novel automated method for the enrichment of phosphopeptides from complex mixtures. The method employs a two-dimensional column setup, with titanium oxide (TiO_2) based solid phase material (Titansphere) as the first dimension and reversed phase material as the second dimension. Phosphopeptides are separated from non-phosphorylated peptides by trapping them under acidic conditions on a titanium oxide pre-column. Non-phosphorylated peptides break through and are trapped on a reversed phase pre-column after which they are analyzed by nanoflow LC-ESI-MS/MS. Subsequently, phosphopeptides are desorbed from the titanium oxide column under alkaline conditions, re-concentrated onto the reversed phase pre-column and analyzed by nanoflow LC-ESI-MS/MS. The selectivity and practicality of using TiO_2 pre-columns for trapping phosphopeptides are demonstrated via the analysis of a model peptide RKISASEF, in a 1:1 mixture of a non- and a mono-phosphorylated form. A sample of 125 femtomole of the phosphorylated peptide could easily be isolated from the non-phosphorylated peptide with a recovery above 90%. In addition, proteolytic digests of three different autophosphorylation forms of the 153 kDa homo-dimeric cGMP-dependent protein kinase are analyzed. From proteolytic digests of the fully autophosphorylated protein at least 8 phosphorylation sites are identified, including two previously uncharacterized sites, namely Ser-26 and Ser-44. Ser-26 was characterized as a minor phosphorylation site in purified PKG samples, while Ser-44 was identified as a novel *in-vitro* autophosphorylation target. These results clearly show that TiO_2 has strong affinity for phosphorylated peptides and thus we conclude that this material has a high potential in the field of phosphoproteomics.

Introduction

Dynamic post-translational modification is a general mechanism for fine-tuning protein structure and function. In particular protein phosphorylation plays a key role in the regulation of virtually all cellular events. Many crucial biological processes such as cell cycle, cell growth, cell-differentiation and metabolism are orchestered and tightly controlled by reversible protein phosphorylation, modulating protein activity, stability, interaction and localization [1, 2]. To gain further insight into the regulation of these processes by reversible phosphorylation it is often necessary to characterize the phosphorylation state of specific proteins under certain conditions. Several analytical techniques exist for the analysis of protein phosphorylation, such as (i) ^{32}P-labeling, (ii) Edman sequencing and (iii) mass spectrometric methods, of which most are based either upon the mass increment of 80 amu of a single phosphorylation event or upon specific fragmentation patterns of the incorporated phosphate moiety in for instance neutral loss scans [3-5]. Mass spectrometric methods for identifying and characterizing phosphoproteins are inherently faster than Edman sequencing or radiolabeling. Nevertheless the identification and detailed investigation of phosphoproteins including the localization of phosphorylation sites by mass spectrometry remains challenging. Often specific isolation of phosphoproteins or phosphopeptides is a prerequisite for mass spectrometric analysis. Commonly used enrichment techniques are immobilized metal affinity chromatography (IMAC) [6], immunoprecipitation using phosphoprotein specific antibodies [7] or specific chemical modification strategies, targeted for phosphorylated amino acids [8, 9]. Immobilized metal affinity chromatography combined with electrospray ionization mass spectrometry has been successfully used in off-line [10] and on-line [11-13] applications and probably offers so far the highest potency in sample recovery and sample throughput. However, enrichment and recovery strongly depends on the type of metal ion, column material and loading/eluting procedures that are used [6, 14, 15]. Furthermore, IMAC requires additional metal-ion loading and washing steps, increasing total sample analysis time and tedious to configure in on-line applications. Here we report a novel automated method for the selective enrichment of phosphopeptides from complex mixtures using a two-dimensional column switching setup, with titanium oxide based solid phase material (Titansphere). This relatively new base material for HPLC columns consists of porous titania microspheres with a smooth and alkaline surface and unique amphotheric ion-exchange properties [16-20]. The property of titanium oxide to selectively absorb water-soluble organic

phosphates has been previously demonstrated [21-26]. The objective of this study is to critically evaluate the potential applicability of TiO_2 as chromatographic medium capable to selectively isolate and enrich phosphorylated peptides from complex mixtures in a fast and automated manner. For this purpose an automated on-line two-dimensional liquid chromatography system was developed, which allows isolation and mass spectrometric identification of phosphorylated peptides from proteolytic digests. Selectivity and sensitivity of the developed method are demonstrated first using model peptides. At least 125 femtomole of the synthetic phosphopeptide RKIpSASEF was selectively isolated and detected from its non-phosphorylated form. Furthermore, using this method the autophosphorylation status of the cGMP-dependent protein (PKG) was characterized. PKG is a 153 kDa homodimeric protein that acts directly downstream in the nitric oxide (NO)/cGMP-mediated signaling pathway in control of a variety of cellular responses, including smooth muscle relaxation [27]. *In-vitro*, PKG autophosphorylates in the presence of Mg^{2+}-ATP and cAMP or cGMP [28]. The major sites of autophosphorylation have been previously identified as Ser-50, Thr-58, Ser-72 and Thr-84. Minor phosphorylation was observed on Ser-1 and Ser-64 [29]. Using this model protein and the developed phosphopeptide enrichment method we were able to retrieve several phosphopeptides from highly autophosphorylated PKG, including di- and tri-valent phosphopeptides, covering almost all known autophosphorylated residues. Additionally, we were able to identify a known *in-vivo* phosphorylation site and to postulate two novel target residues, one for *in-vivo* phosphorylation and one for *in-vitro* autophosphorylation.

Experimental

Material and reagents. Synthetic peptides RKISASEF and RKIpSASEF were obtained from respectively Promega (Madison, WI, USA) and Neosystem Laboratoire (Strasbourgh, France). Human [Glu^1]-Fibrinopeptide B was obtained from Sigma (St. Louis, MO, USA). Bovine lung PKG type Iα was purified to homogeneity essentially as described by Francis *et al.* [30]. Aqua™ C_{18} (5 µm, 200Å) reversed phase material was purchased from Phenomenex (Torrance, CA, USA). Titanium oxide (Titansphere, 5 µm) was a gift from GL-Sciences (GL-Sciences Inc., Japan). Sequencing grade trypsin, chymotrypsin and Glu-C were purchased from Boehringer (Boehringer, Mannheim, Germany).

Preparation of frits and columns. Porous ceramic frits were prepared in 50-100 µm ID undeactivated, fused silica capillaries as essentially as described by Meiring *et al.* [31]. In short, fused silica capillaries of 10-15 cm length were shortly immersed in a fresh solution of 75% potassium silicate and 25% formamide. Following, the capillaries filled with 1-2 cm silicate/formamide solution were heated overnight at 100ºC. Columns were packed using a 50 bar pressure vessel essentially as described by van der Heeft *et al.* [32]. In short, 50 µm ID analytical reversed phase columns were prepared by back flushing a 100 µm ID pre-packed fused silica capillary, filled with ~5-6 cm of a Aqua™ C_{18} stationary phase, directly into a 50 µm fritted fused silica capillary, thereby avoiding long packing time. Titanium oxide and C_{18} pre-columns were made by directly packing 100 µm ID fritted fused silica capillaries to column lengths of 10-15 mm of either Titansphere or Aqua™ C_{18} stationary phase.

2D-nanoLC-MS/MS. The two-dimensional nanoflow LC system consisted of a LC-Packings Ultimate quaternary solvent delivery system, a FAMOS autosampler and a Switchos 6-port valve switching module (LC-Packings, Amsterdam, The Netherlands) operating in a nanoflow HPLC setup as described by Meiring *et al.* [31]. Double stage pre-columns consisted of a 100 µm ID x 10 mm L Titanium oxide pre-column butt-connected to a 100 µm ID x 10 mm L Aqua™ C_{18} pre-column by means of a True ZDV MicroTight union (Upchurch Scientific, Oak Harbor, WA, USA). A schematic representation of the nano-HPLC-MS setup is given in Figure 1.

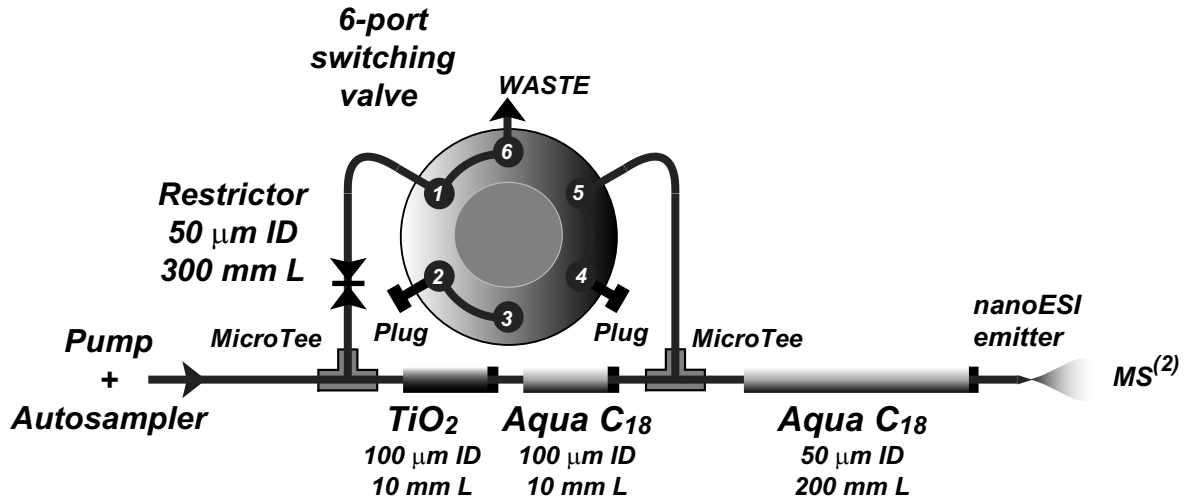

Figure 1: Schematic representation of the two-dimensional LC-MS setup. This setup comprises of a 6-port switching valve, a dual TiO_2/C_{18} pre-column and a C_{18} analytical column.

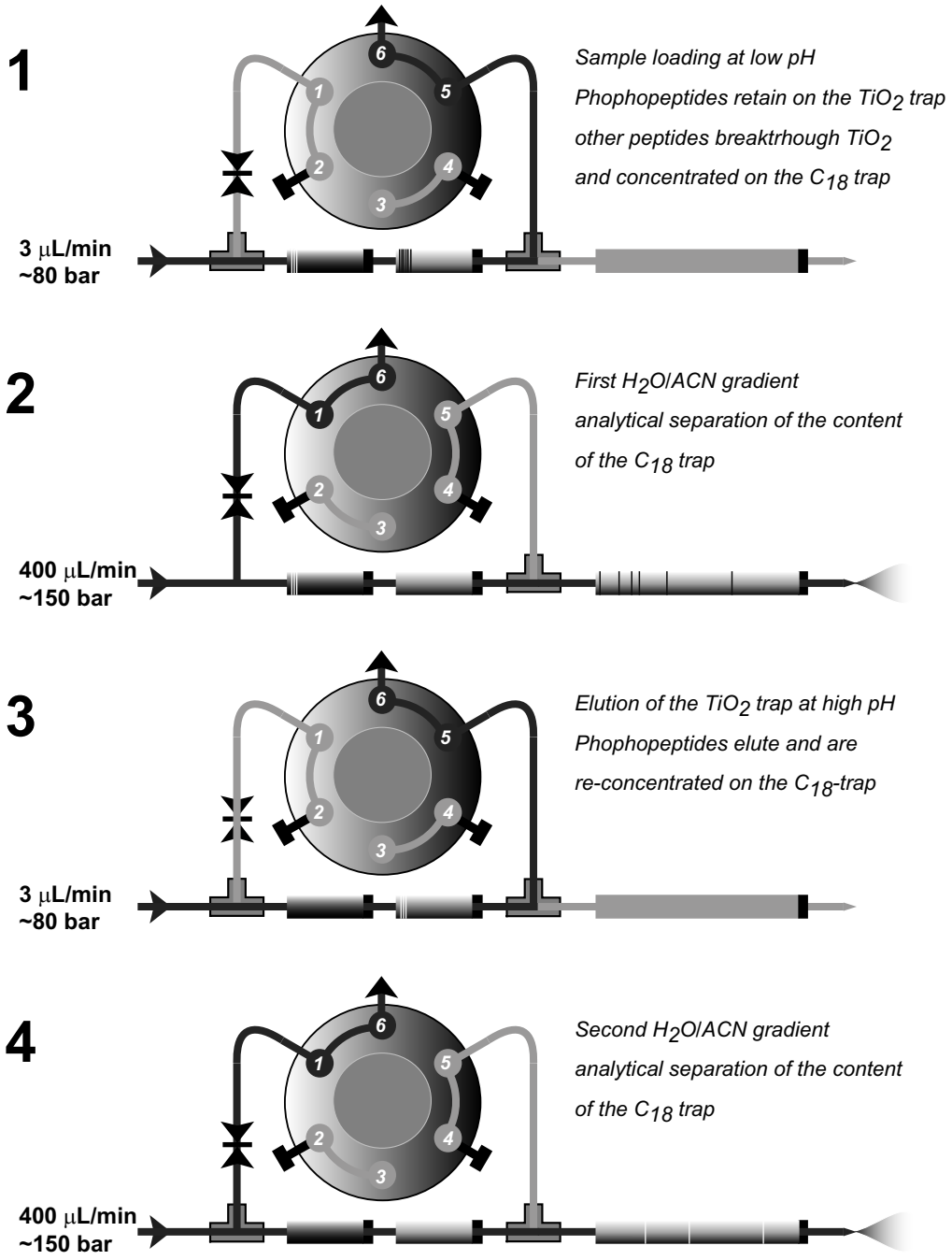

Figure 2: During sample loading from the injection loop of the autosampler the flow is 3 µl min^{-1} and the restrictor is closed. In this situation the content of the sample loop is transported directly over the double pre-column, where phosphopeptides are trapped on the TiO_2 particles and non-phosphopeptides are trapped on the C_{18} particles. After sample loading the six-port valve switches the restrictor to the waste line and at the same time the flow is increased to 400 µl min^{-1}. This results in a pressure increase to ~150 bar and a column flow over the analytical column of ~100 nl min^{-1} is obtained. The gradient pump delivers a linear H_2O/acetonitrile gradient, which analytically separates the content of the C_{18} pre-column. After this first analysis the content of the TiO_2 pre-column is loaded onto the C_{18} pre-column using a strong base. A second H_2O/acetonitrile gradient is used to analytically separate the trapped phosphopeptides.

Two-dimensional separation of phosphopeptides from non-phosphopeptides is achieved by loading the analytes onto the double pre-column in 100% solvent A (i.e. water and 0.1 M acetic acid) using an unsplit flow of 3 µl/min during 20 minutes (resulting pre-column pressure ~80-100 bar). Phosphopeptides are retained on the titanium oxide, while non-phosphorylated peptide flow through the titanium oxide pre-column and are concentrated on the C_{18} pre-column. After sample loading the 6-port valve is switched and the flow is increased to 400 µl/min. The restrictor (50 µm ID x 30 cm L fused silica) provides a column backpressure of ~130-150 bar and a resulting column flow of ~100-150 nl/min is obtained. A linear gradient to 100% solvent B (i.e. 80% acetonitrile and 0.1 M acetic acid) is used to analytically separate the content of the C_{18} pre-column. After this first reversed phase gradient, trapped phosphopeptides are eluted and reconcentrated on the C_{18} pre-column by injecting 30 µl 250 mM ammonium bicarbonate, pH 9.0. A second H_2O/acetonitrile gradient is used to analytically separate the content of the C_{18} pre-column.

The flow of the analytical column was directly infused into a Micromass Q-Tof 1 mass spectrometer (Micromass UK Ltd., Manchester, United Kingdom) using home-made nano-ESI spray tips (~7 µm ID), prepared as described by Meiring *et al.* [31]. Proteolytic digests of PKG were analyzed in both continuous mode and data-dependent mode. Scans were acquired in positive ion continuous mode from *m/z* 300-1200 sec^{-1}. During data-dependent analysis 3 precursors/scan were allowed at a threshold of 50 counts. TOF-MS/MS spectra were acquired for 2 seconds, using an interscan time of 0.1 seconds. Data were analyzed using the MassLynx 3.5 software (Micromass) and using the MASCOT software (www.matrixscience.com). MASCOT searches were performed in the SWISSPROT database and a mammalian taxonomy restriction was used. The mass tolerance of both precursor ion and fragment ions was set to ± 0.3 Da. Carbamidomethyl cysteine was set as a fixed modification, while serine, threonine or tyrosine phosphorylation was set as variable modification. All phosphopeptides identified during MASCOT searches were confirmed by manual interpretation of the spectra.

Sample preparation. Autophosphorylated PKG Iα was prepared by incubating PKG with 5 mM $MgCl_2$ and 100 µM ATP. For partial and high levels of phosphate incorporation, the protein was incubated at 30 ºC for 10 min and 3 hours respectively. Non-autophosphorylated enzyme was not incubated with $MgCl_2$ and ATP. The autophosphorylation reactions were

stopped with the addition of a molar excess of EDTA. After treatment with dithiothreitol and iodoacetamide, protein samples were buffer exchanged to 25 mM ammonium hydrogen carbonate, pH 8.0 using Ultrafree-0.5 Centrifugal Filter Units (5000 NMWL) (Millipore, Bedford MA, USA). Protein samples were digested with trypsin, chymotrypsin or GluC at a concentration of 1 pmol/µl in 25 mM ammonium hydrogen carbonate and 10% acetonitrile at 37 ºC for 16 hours. The trypsin/protein ratio used was 1:50 by weight, while chymotrypsin/protein and GluC/protein ratios were 1:20 by weight. Prior to injection the sample was diluted 40 times in MilliQ water containing 0.6 % acetic acid.

Results and discussion

2D-LC-MS setup. To explore the general applicability of Titansphere for phosphopeptide trapping a nanoflow-LC setup (Figure 1), comprising of a 6-port switching valve, a 100 µm ID pre-column and a 50 µm ID analytical column was employed. A test sample, consisting of 125 femtomole of a stoichiometric mixture of the monophosphorylated peptide, RKIpSASEF and its non-phosphorylated counterpart, RKISASEF, was used. A normal reversed phase analysis was obtained by loading the two peptides onto the C_{18} pre-column in 100% solvent A. A linear H_2O/acetonitrile gradient was used to analytically separate the content of the C_{18} pre-column at a flow rate of 100-150 nl/min. In Figure 2A are shown from top to bottom the base peak intensity (BPI) chromatogram and the selected ion chromatogram (SIC) of respectively the $[M+2H]^{2+}$ of RKISASEF (at *m/z* 469.2) and the $[M+2H]^{2+}$ of RKIpSASEF (at *m/z* 509.2). Around 28 minutes both RKISASEF and RKIpSASEF eluted with similar mass spectrometric responses. To demonstrate the capability of TiO_2 to selectively retain phosphorylated peptides the same peptide mixture was loaded onto a double pre-column consisting of a TiO_2 pre-column placed in front of the C_{18} pre-column. After sample loading a linear H_2O/acetonitrile gradient was started. Figure 2B shows the acquired BPI and selected ion chromatograms for both peptides of this first reversed phase run. The peak that elutes around 29 minutes is the non-phosphorylated peptide, indicated by the selected ion chromatogram of the non-phosphorylated peptide (SIC of *m/z* 469.2). A small amount of the doubly protonated species of the phosphorylated peptide was also observed, however compared to Figure 2A the intensity is approximately 100 times lower. This initial result directly indicates that TiO_2 is capable of trapping specifically the phosphorylated peptide

under acidic conditions. The basis for this affinity must be ascribed to the phosphate moiety, since the non-phosphorylated peptide was not retained. In order to elute the phosphorylated

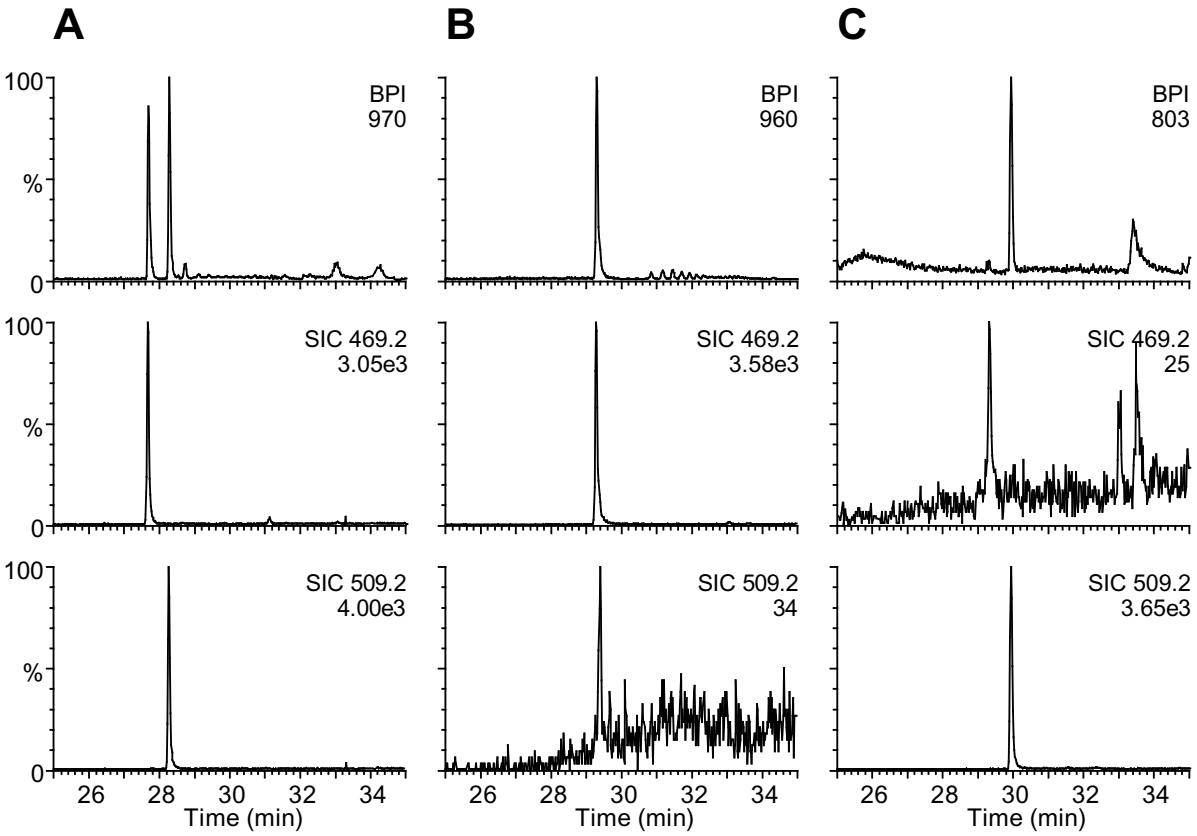

Figure 2: Selective isolation of 125 femtomole of the synthetic phosphopeptide RKIpSASEF from its non-phosphorylated form. Panel **A** shows from top to bottom; BPI chromatogram, the selected ion chromatogram for the doubly charged molecular ions of RKISASEF and of RKIpSASEF, respectively, of a normal reversed phase analysis (i.e. without using a TiO_2 pre-column). Panel **B** shows from top to bottom; BPI chromatogram, the selected ion chromatograms for the doubly charged molecular ions of RKISASEF and of RKIpSASEF, respectively, from the analysis of the first gradient which contains the breakthrough of the TiO_2 pre-column. Panel **C** shows from top to bottom; BPI chromatogram, the selected ion chromatograms for the doubly charged molecular ions of RKISASEF and of RKIpSASEF, respectively, from the analysis of the second gradient which contains the eluate of the TiO_2 pre-column. Values given for the base peak intensity and for the selected ion counts, listed in the upper right corner of each chromatogram, are in arbitrary units.

peptide from the TiO_2 column 30 µl of 250 mM ammonium bicarbonate, pH 9.0, was directed over the double TiO_2/C_{18} pre-column at a flow rate of 3 µl/min. After 20 minutes a second linear H_2O/acetonitrile gradient was used to analytically separate the content of the C_{18} pre-column. Figure 2C shows the acquired BPI and selected ion chromatograms for both peptides

of this second reversed phase run. Figure 2C clearly demonstrates that under these conditions the phosphorylated peptide was recovered from the TiO_2 pre-column. Furthermore, it shows that the phosphopeptide was retained on the TiO_2 pre-column even under hydrophobic conditions, since the first H_2O/acetonitrile gradient was directed over the TiO_2 column.

PKG autophosphorylation. To further explore the general applicability of TiO_2 for the selective enrichment of phosphopeptides from more complex mixtures, the homo-dimeric 153 kDa cGMP-dependent protein kinase (PKG) was analyzed. PKG is a serine/threonine specific kinase that is allosterically regulated by the second messenger molecule cGMP. Upon activation PKG undergoes autophosphorylation and this process affects the kinetic properties of PKG [33]. Proteolytic digests of differentially autophosphorylated PKG (see experimental) were subjected to analysis using the developed 2D-LC setup in order to determine residues involved in the autophosphorylation reaction and to determine the basal phosphorylation state of purified PKG. For this purpose proteolytic digests of differentially autophosphorylated PKG were analyzed in two separate experiments. In the first analysis mass spectrometric data were acquired in the data-dependent acquisition mode in order to obtain primary sequence information of the proteolytic fragments. A second analysis was repeated and this time only LC-ESI-MS spectra were acquired. From this latter analysis extracted ion chromatograms were generated for each phosphopeptide that was identified from the MS/MS spectra obtained in the first data-dependent analysis. This allowed semi-quantitative comparison of each individual phosphopeptide between the non-, partially- and highly- autophosphorylated state of PKG.

Table 1: Identified tryptic phosphopeptides from PKG.

No	Residues	Sequence [a]	Mass [b]		peptide observed in [c]		
			$M_{r\ found}$	$M_{r\ calc}$	Non	Partial	High
1	24-37	(K)-RL**pS**EKEEEIQELKR-(K)	1865.91	1865.92	+	+	+
2	42-56	(K)-C*QSVLPVP**pS**THIGPR-(T)	1726.87	1726.82	-	++	++
3	42-56	(K)-C*Q**pS**VLPVP**pS**THIGPR-(T)	1806.86	1806.78	-	+	++
4	72-77	(R)-**pS**FHDLR-(Q)	853.33	853.35	-	+	++
5	60-77	(R)-AQGISASEPQTYR**pS**FHDLR-(Q)	2155.08	2154.99	-	+	-
6	57-71	(R)-T**pT**RAQGISAEPQTYR-(S)	1757.84	1757.81	-	++	+
7	57-71	(R)-T**pT**RAQGI**pS**AEPQTYR-(S)	1837.82	1837.78	-	+	+
8	57-77	(R)-T**pT**RAQGISAEPQTYR**pS**FHDLR-(Q)	2593.18	2593.15	-	+	++
9	57-77	(R)-T**pT**RAQGI**pS**AEPQTYR**pS**FHDLR(-Q)	2673.21	2673.11	-	+	++
10	514-532	(K)-TW**pT**FC*GTPEYVAPEIILNK-(G)	2318.21	2318.07	+	+	+
11	513-532	(K)-KTW**pT**FC*GTPEYVAPEIILNK-(G)	2446.31	2446.16	+	+	+

[a] Amino acid sequence of phosphorylated peptides identified from tryptic digests on basis of their low-energy CID spectrum; C* denotes carbamido-methyl cysteine, pS denotes phosphoserine, pT denotes phosphothreonine. [b] All mass values are listed as monoisotopic mass. [c] Semi-quantitative information about the presence of the identified phosphopeptide derived from its elution profiles (extracted ion chromatogram), (-) not present; (+) low abundant (++) highly abundant.

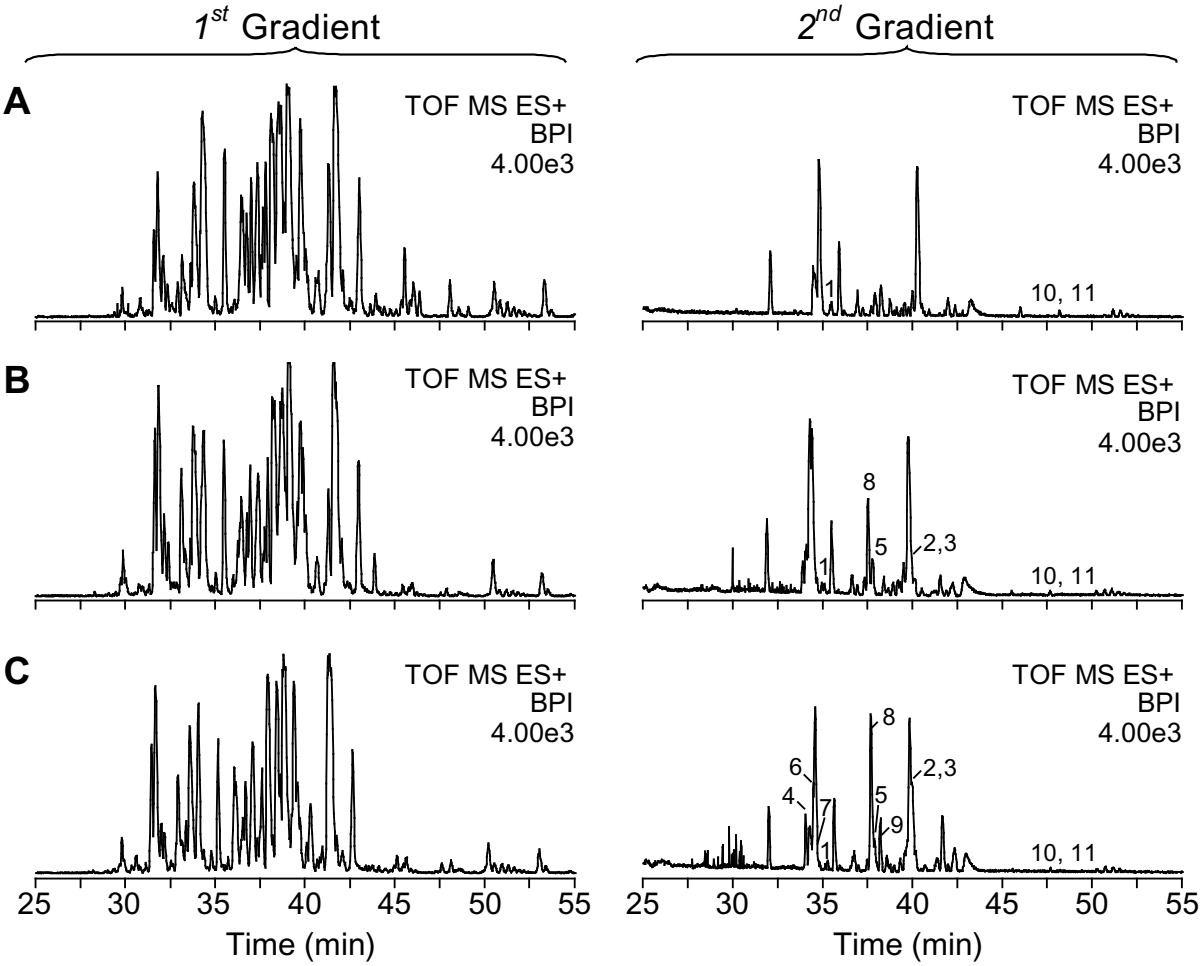

Figure 3: nano 2D-LC-MS analysis of 250 fmol tryptic PKG, phosphorylated to different degrees. Shown are the BPI elution profiles of **(A)** the first and second gradient of native (non-autophosphorylated) PKG, **(B)** the first and second gradient of partially autophosphorylated PKG and **(C)** the first and second gradient of highly autophosphorylated PKG. The phosphopeptides, which were identified from low-energy CID spectra in a separate 2D-LC-MS/MS analysis, are labeled and listed in table 1. Values given for the base peak intensity, listed in the upper right corner of each chromatogram, are in arbitrary units.

Figure 3A-C show on the left the BPI chromatograms of the first and second analytical gradient of approximately 250 fmol of the tryptic digests of non-, partially- and highly-autophosphorylated PKG. Approximately 80 peptides were recovered in these first gradients amongst which no phosphopeptides were identified. The chromatograms on the right in Figure 3A-C show the BPI chromatograms obtained after elution of the TiO_2 pre-column at high pH for non-, partially- and highly- autophosphorylated PKG, respectively. All phosphopeptides that were identified in these analyses are listed in Table 1 and labeled in Figure 3. The tryptic digest of non-autophosphorylated PKG contained three

phosphopeptides, which were identified as residues 24-37, 514-532 and 513-532, carrying a single phosphate moiety. The deconvoluted low-energy CID spectrum of residues 24-37 + 1P is given in Figure 4A. The phosphorylation site was unambiguously assigned to Ser-26, which is a previously uncharacterized phosphorylation site of PKG. In a similar fashion phosphopeptides 514-532 and 513-532 were found to be both phosphorylated on Thr-516. Non-phosphorylated PKG is not stimulated to autophosphorylate *in-vitro* and all phosphorylations in this state of the protein are likely due to *in-vivo* autophosphorylation or due to *in-vivo* activity of other protein kinases. Purified fractions of PKG are known to contain 1.1-1.4 mol phosphate/mol subunit [29]. The peptide containing pThr-516 originates from the activation loop within the catalytic core of the protein kinase. Previously mutation studies showed that this phosphothreonine is essential for protein kinase activity [34]. However this is the first direct evidence that this residue is phosphorylated in PKG isolated from bovine lung tissue. Additionally, the non-phosphorylated form of this peptide was not observed and therefore it is postulated that this site is almost completely phosphorylated in PKG isolated from bovine lung tissue. The tryptic digest of partially autophosphorylated PKG contained besides the three phosphopeptides, which were also identified in the non-autophosphorylated PKG sample, a series of phosphopeptides that originate from the N-terminal part of the protein. PKG is known to autophosphorylate within minutes on residues Ser-50, Thr-58, Ser-72 and Thr-84 [28, 29]. The most abundant peak in the second gradient of partial autophosphorylated PKG (Peak 6 in Figure 3C) originates from the monophosphorylated peptide 57-71. The low-energy CID spectrum of this phosphopeptide confirmed that Thr-58 is the phosphorylated residue. It appears that phosphorylation of Thr-58 is nearly complete after 10 minutes of incubation, since only low-abundant non-phosphorylated peptides containing Thr-58 were detected in the first gradient (data not shown). Apparently partial phosphorylation of Ser-64 also occurred already after 10 minutes as indicated by the presence of the doubly phosphorylated peptide 57-71, of which the MS/MS spectra confirmed phosphorylation of both Thr-58 and Ser-64. Simultaneously, partial phosphorylation of Ser-72 occurred as indicated by the presence of phosphopeptides 72-77 and 60-77 and the doubly phosphorylated peptide 57-77. The doubly phosphorylated peptide 57-77 is amongst the most abundant peaks in the chromatogram of highly autophosphorylated PKG. The triply phosphorylated peptide of residues 57-77 is also observed and its deconvoluted low-energy CID spectrum confirming phosphorylation of Thr-58, Ser-64 and Ser-72 is given in Figure 4D.

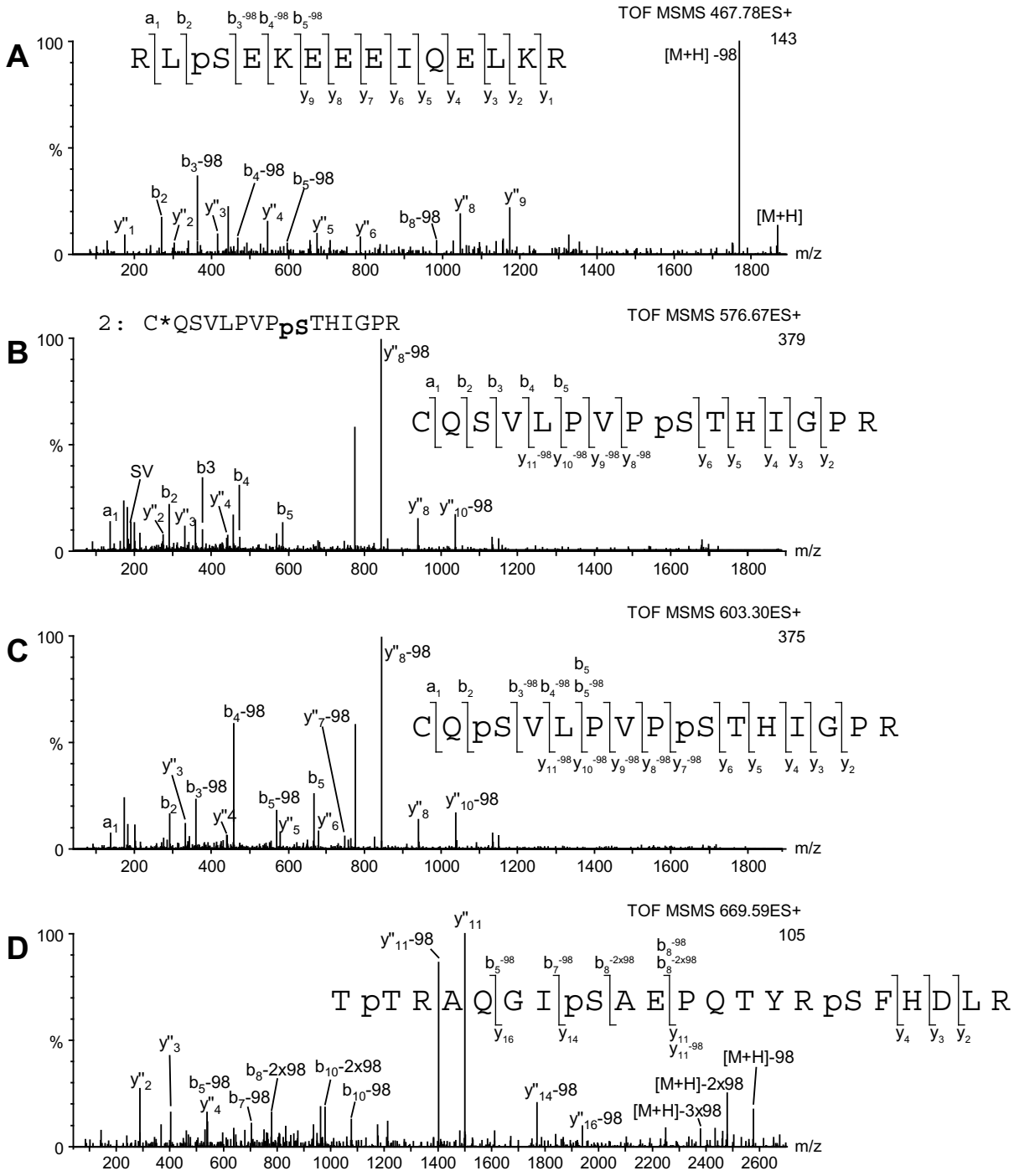

Figure 4: Singly-charged or deconvoluted (MaxEnt3) low-energy CID spectra of **(A)** the $[M+4H]^{4+}$ of residues 24-37 carrying 1 phosphate situated at Ser-26, **(B)** the $[M+3H]^{3+}$ of residues 42-56 carrying 1 phosphate at Ser-50, **(C)** the $[M+3H]^{3+}$ of residues 42-56 carrying 2 phosphates at Ser-44 and Ser-50 and **(D)** the $[M+4H]^{4+}$ of residues 57-77 carrying 3 phosphate moieties at Thr-58, Ser-64 and Ser-72. The a, b and y ions are labeled in each spectrum, as well as b or y ions corresponding to the neutral loss of phosphoric acid (-98). Additionally, an internal acyl ion (annotated by SV) is highlighted in figure 4B. This internal acyl ion is absent in the low-energy CID spectrum of the doubly phosphorylated peptide of residues 42-56 (figure 4C), suggesting it is this serine that is phosphorylated in this doubly phosphorylated peptide.

Phosphorylation of Ser-50 also occurred within the first 10 minutes of autophosphorylation. The deconvoluted low-energy CID spectrum of the monophosphorylated peptide 42-56 is given in Figure 4B. Interestingly a doubly phosphorylated peptide of residues 42-56 was also identified in both partially and highly autophosphorylated PKG. The deconvoluted low-energy CID spectrum of this peptide (Figure 4C) confirmed phosphorylation of both Ser-50 and Ser-44. This latter serine is a previously uncharacterized phosphorylation site of PKG. Chymotryptic and GluC digests were prepared and analyzed in the same way as the tryptic digests. All phosphopeptides that were identified in these analyses are listed in Table 2. The overall amount of phosphopeptides identified from these two digests is lower compared to the tryptic digests. However, it turned out that both proteases are complementary to trypsin. Both chymotrypsin and GluC digests of highly autophosphorylated PKG contained peptides phosphorylated on Thr-84. This phosphorylation site could not be identified from the tryptic digests. Thr-84 is located in a region with a relative high amount of arginine and lysine residues. For now it is assumed that proteolytic digestion with trypsin generates too small fragments, containing threonine-84 (phosphorylated or non-phosphorylated) to be detected by the current method.

Table 2: Identified GluC and chymotryptic phosphopeptides from PKG.

No	Residues	Sequence [a]	Mass [b]		peptide observed in[c]		
			$M_{r\ found}$	$M_{r\ calc}$	Non	Partial	High
12	71-80	(Y)-R**pS**FHDLRQAF-(R)	1355.64	1355.61	-	+	++
13	69-76	(Q)-TYR**pS**FHDL-(R)	1117.53	1117.45	-	+	++
14	53-70	(H)-IGPRT**pT**RAQGISAEPQTY-(R)	2025.09	2024.97	-	+	+
15	81-92	(F)-RKF**pT**KSERSKDL-(I)	1573.88	1573.79	-	-	+
16	516-530	(W)-**pT**FC*GTPEYVAPEIIL-(N)	1788.88	1788.80	+	+	+
17	76-87	(D)-LRQAFRKF**pT**KSE-(R)	1589.94	1589.81	-	-	+
18	502-522	(D)-FGFAKKIGFGKKTW**pT**FC*GTPE-(Y)	2486.30	2486.19	+	+	+

[a] Amino acid sequence of phosphorylated peptides identified from GluC or chymotryptic digests on basis of their low-energy CID spectrum; C* denotes carbamido methyl cysteine, pS denotes phosphoserine, pT denotes phosphothreonine. [b] All mass values are listed as monoisotopic mass. [c] Semi-quantitative information about the presence of the identified phosphopeptide derived from its elution profiles (extracted ion chromatogram), (-) not present; (+) low abundant (++) highly abundant.

Semi-quantitation of PKG phosphorylation. After several phosphopeptides were identified from the proteolytic digests, selected ion-chromatograms were generated for the parent mass of each phosphopeptide from the ion chromatograms of the separate LC-MS runs. From these selected ion-chromatograms (see Figure 5) it is possible to obtain a semi-quantitative indication about the kinetics of each phosphorylation site along the autophosphorylation reaction. For instance, by comparing extracted ion chromatograms of the $[M+4H]^{4+}$ at *m/z* 467.53 corresponding to residues 24-37 + 1P (Figure 5A) it appears that the amount of this phosphopeptide is not influenced by the autophosphorylation process. Furthermore by comparing the mass spectrometric response of this phosphopeptide with the non-phosphory-

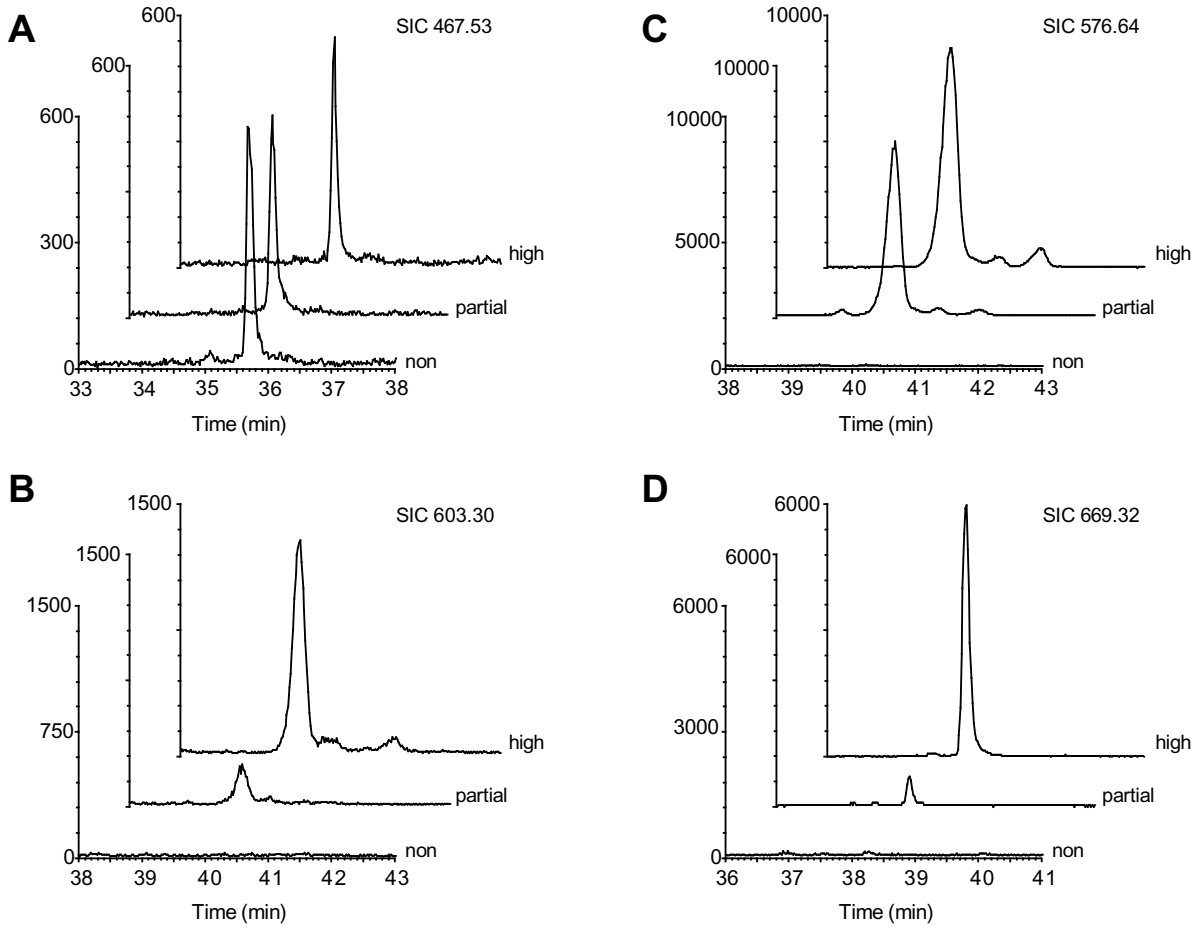

Figure 5: Selected ion chromatograms generated for the parent mass of several identified phosphopeptides from non-, partially- and highly- autophosphorylated PKG. Panel **A** shows that the amount of the phosphopeptide of residues 24-37 does not change during autophosphorylation. Panel **B** and **C** show that the mono and di- phosphorylated peptides of residues 42-56 increase upon autophosphorylation. Panel **D** shows that the tri-phosphorylated peptide of residues 57-77 increases during autophosphorylation. Values given for the selected ion counts are in arbitrary units.

lated form it appears that the phosphorylation level of Ser-26 is rather low (data not shown). This could indicate that Ser-26 is not an *in-vitro* autophosphorylation site of PKG and its phosphorylation is probably due to the action of an other protein kinase *in-vivo*. The intensity of the extracted mass chromatograms for residues 42-56 with one and two phosphate moieties are given in Figure 5B and 5C, respectively. From these extracted mass chromatograms it seems that both these sites are in fact autophosphorylation sites of PKG *in-vitro*, since both peaks show an increase along the incubation time of the autophosphorylation reaction. The extracted mass chromatograms of the triply phosphorylated peptide of residues 57-77 (Figure 5D) show that after 10 minutes of autophosphorylation already a small amount of PKG is phosphorylated on Ser-64, while this increases further with longer incubation. Autophosphorylation of Ser-64 was previously associated with activation of type Iα PKG in the absence of cyclic nucleotides [35]. Our results suggest that after 10 minutes a substantial amount of PKG is phosphorylated on Ser-64. In summary, using this strategy we confirmed complete phosphorylation of Thr-516 and minor phosphorylation of Ser-26 and both are most likely phosphorylated *in-vivo*. *In-vitro* stimulated autophosphorylation results in rapid phosphorylation of Ser-50, Thr-58, Ser-72 and Thr-84 and slower phosphorylation of Ser-44 and Ser-64.

Non-specific absorption. The LC-MS/MS data of the second gradients of non-, partially- and highly- autophosphorylated PKG contained besides the previously mentioned phosphopeptides several non-phosphorylated peptides that had generally in common that they were relatively acidic (i.e. the peptides contained several aspartic and glutamic acids) (sequence information not shown). Apparently they also have some affinity for the alkaline surface of TiO_2, although it should be noted that most of these peptides were also present (often in much higher abundance) in the first linear gradient, suggesting they are not that well retained on the TiO_2. Although phosphopeptides are easily discriminated from non-phosphorylated peptides on basis of the parent mass and fragment ion spectra, the occurrence of these non-phosphorylated peptides in the second gradient could be considered as a negative side effect. Non-specific absorption of non-phosphorylated peptides with an acidic nature is something which is also commonly observed in IMAC experiments.[10, 15] Ficarro *et al.*[10] showed that the conversion of carboxylic acids into their methyl-ester derivatives decreased the non-specific binding of acidic peptides in IMAC. In order to determine whether esterification of carboxyl groups could also reduce the absorption of acidic peptides on TiO_2,

the relative acidic peptide [Glu[1]]-Fibrinopeptide B (EGVNDNEEGFFSAR) was used. This peptide showed to have a relative high affinity for TiO_2. Methylated [Glu[1]]-Fibrinopeptide was obtained with acetyl-chloride and methanol, essentially as described by Ficarro *et al.*[10] A mixture of 100 femtomole [Glu[1]]-Fibrinopeptide and methylated-[Glu[1]]-Fibrinopeptide was loaded onto the double TiO_2/C_{18} pre-column. Figure 6 shows the BPI chromatogram and selected ion chromatograms for both peptides of the first (6A) and second gradient (6B) of this analysis. Figure 6A shows that methylated-[Glu[1]]-Fibrinopeptide has no affinity for TiO_2, while Figure 6B shows that [Glu[1]]-Fibrinopeptide has affinity for TiO_2, and could be recovered in the same way the phosphopeptides were recovered (i.e. desorbtion from TiO_2 under alkaline conditions). This illustrates that the absorption of acidic non-phosphorylated peptides by TiO_2 can be decreased by methylation of the carboxylic acids.

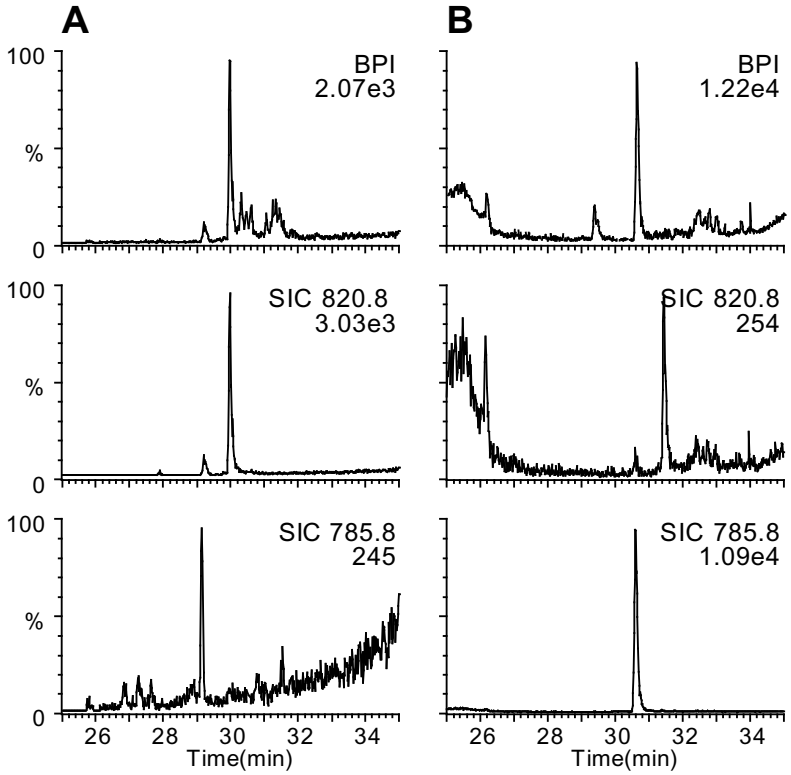

Figure 6: Selective isolation of 100 femtomole of [Glu[1]]-Fibrinopeptide from fully methylated [Glu[1]]-Fibrinopeptide. Panel **A** shows from top to bottom; BPI chromatogram, the selected ion chromatograms for the doubly charged molecular ion of methylated-[Glu[1]]-Fibrinopeptide (at *m/z* 820.8) and of [Glu[1]]-Fibrinopeptide (at *m/z* 785.8), respectively, from the analysis of the first gradient. Panel **B** shows from top to bottom; BPI chromatogram, the selected ion chromatograms for the doubly charged molecular ion of methylated-[Glu[1]]-Fibrinopeptide (at *m/z* 820.8) and of [Glu[1]]-Fibrinopeptide (at *m/z* 785.8), respectively, from the analysis of the second gradient which contains the eluate of the TiO_2 pre-column. Values given for the BPI and the SIC, listed in the upper right corner of each chromatogram are in arbitrary units.

Conclusions

Due to the biological importance of reversible protein phosphorylation a continuing development of techniques for the identification and localization of phosphorylation sites in proteins is highly desirable. In particular the availability of robust enrichment techniques seems to be especially promising for attempting global analysis of protein phosphorylation events in the future [10, 36, 37]. Here we report a novel analytical procedure for phosphopeptide enrichment prior to mass spectrometric analysis. The procedure relies on unique ion-exchange properties of Titansphere, a new type of column material that consists of spherical particles of titanium oxide. Titania has attracted interest as an alternative support to silica for column packing material in high performance liquid chromatography because it exhibits high mechanical, chemical and thermal stability. Additionally, Titansphere possesses unique surface chemistry which displays amphoteric ion-exchange properties [16, 20]. Previously it was shown that titanium oxide can effectively retain organic phosphates [21-23]. In this work the objective was to use TiO_2 as chromatographic medium for the selective isolation and enrichment of phosphorylated peptides from complex mixtures in a fast, robust and automated manner. The developed nanoflow 2D-LC-MS/MS setup allows mass spectrometric characterization of both non-phosphorylated and phosphorylated peptides in two separate measurements. The prepared TiO_2 pre-columns could be used for over 200 runs without showing signs of reduced performance (data not shown). Configuration of an autosampler that injects both the sample and the buffer for the elution of the TiO_2 pre-column allows simple automation and abolishes the need for an additional third pump. In comparison with IMAC, this chromatographic approach has the advantage that lesser column handling steps are required, and therefore it seems to be a more robust enrichment strategy for the selective enrichment and characterization of phosphopeptides from complex mixtures. Using the developed setup the phosphorylated peptide RKIpSASEF could be easily separated from its non-phosphorylated counterpart at the low femtomole level with a yield above 90%. In addition the analysis of highly autophosphorylated PKG showed that even di- and tri-phosphorylated peptides could be retained and recovered. Comparison of the elution profiles of identified phosphopeptides between the three different autophosphorylated PKG samples allowed the discrimination between *in-vitro* autophosphorylation and *in-vivo* phosphorylation events. In the case of the previously uncharacterized phosphorylation of Ser-26, elution profiles revealed that this phosphopeptide does not increase in abundance during incubation

with cAMP and Mg^{2+}/ATP, indicating it is not an autophosphorylation site *in-vitro*. In fact, purified PKG from bovine lung already contained this phosphorylated residue. These observations strongly support the idea that this residue is in fact phosphorylated in PKG isolated from bovine tissue and its phosphorylation is most likely due to the action of another protein kinase. In contrast, the level of phosphorylation of another previously uncharacterized phosphorylation site, Ser-44, increased during autophosphorylation. This strongly suggests that this residue is in fact a newly characterized autophosphorylation site of PKG.

The nature of the tight interaction between phosphor-amino acids and the Titansphere is not fully understood. Relative acidic peptides appear to have some affinity for Titansphere as well, although it is less pronounced than the affinity of phosphopeptides. This is a negative side effect and could lead to false positives in the search for phosphorylation sites of unknown samples. Ficarro *et al.*[10] have overcome this problem in IMAC by treatment of all peptides with a methyl esterification reaction that actually reduced non-specific binding of acidic peptides. Using the relative acidic [Glu^1]-Fibrinopeptide B, which showed to have affinity for TiO_2 and the esterification protocol described by Ficarro *et al.* [10] we show that the absorption of acidic peptides to TiO_2 can be minimized. In conclusion, these results clearly show that TiO_2 has a high potential in the field of phosphoproteomics.

Acknowledgements

We acknowledge GL Sciences Inc. in Tokyo, Japan for initiating this application and making the TiO_2 Titansphere material available to us. We kindfully thank Jennifer L. Busch, Jackie D. Corbin and Sharron H. Francis from the Vanderbilt University School of Medicine, Nashville, Tennessee for the preparation of autophosphorylated PKG. We thank Klaus Rumpel and Frank Pullen of Pfizer Research UK for financial support. This work was supported by the Netherlands Proteomics Centre.

References

1. Graves, J.D.; Krebs, E.G. *Protein phosphorylation and signal transduction.* Pharmacol. Ther. **1999**, *82*, 111-121.
2. Hunter, T. *Signaling--2000 and beyond.* Cell **2000**, *100*, 113-127.
3. Huddleston, M.J.; Annan, R.S.; Bean, M.F.; Carr, S.A. *Selective detection of phosphopeptides in complex mixtures by electrospray liquid chromatography/mass spectrometry.* J. Am. Soc. Mass Spectrom. **1993**, *4*, 710-717.
4. Carr, S.A.; Huddleston, M.J.; Annan, R.S. *Selective detection and sequencing of phosphopeptides at the femtomole level by mass spectrometry.* Anal. Biochem. **1996**, *239*, 180-192.
5. Zappacosta, F.; Huddleston, M.J.; Karcher, R.L.; Gelfand, V.I.; Carr, S.A.; Annan, R.S. *Improved sensitivity for phosphopeptide mapping using capillary column HPLC and microionspray mass spectrometry: comparative phosphorylation site mapping from gel-derived proteins.* Anal. Chem. **2002**, *74*, 3221-3231.
6. Posewitz, M.C.; Tempst, P. *Immobilized gallium(III) affinity chromatography of phosphopeptides.* Anal. Chem. **1999**, *71*, 2883-2892.
7. Pandey, A.; Podtelejnikov, A.V.; Blagoev, B.; Bustelo, X.R.; Mann, M.; Lodish, H.F. *Analysis of receptor signaling pathways by mass spectrometry: identification of vav-2 as a substrate of the epidermal and platelet-derived growth factor receptors.* Proc. Natl. Acad. Sci. U.S.A. **2000**, *97*, 179-184.
8. Oda, Y.; Nagasu, T.; Chait, B.T. *Enrichment analysis of phosphorylated proteins as a tool for probing the phosphoproteome.* Nat. Biotechnol. **2001**, *19*, 379-382.
9. Zhou, H.; Watts, J.D.; Aebersold, R. *A systematic approach to the analysis of protein phosphorylation.* Nat. Biotechnol. **2001**, *19*, 375-378.
10. Ficarro, S.B.; McCleland, M.L.; Stukenberg, P.T.; Burke, D.J.; Ross, M.M.; Shabanowitz, J.; Hunt, D.F.; White, F.M. *Phosphoproteome analysis by mass spectrometry and its application to Saccharomyces cerevisiae.* Nat. Biotechnol. **2002**, *20*, 301-305.
11. Cao, P.; Stults, J.T. *Mapping the phosphorylation sites of proteins using on-line immobilized metal affinity chromatography/capillary electrophoresis/electrospray ionization multiple stage tandem mass spectrometry.* Rapid Commun. Mass Spectrom. **2000**, *14*, 1600-1606.
12. Cao, P.; Stults, J.T. *Phosphopeptide analysis by on-line immobilized metal-ion affinity chromatography-capillary electrophoresis-electrospray ionization mass spectrometry.* J. Chromatogr., A **1999**, *853*, 225-235.
13. Nuwaysir, L.M.; Stults, J.T. *Electrospray-Ionization Mass-Spectrometry of Phosphopeptides Isolated by Online Immobilized Metal-Ion Affinity- Chromatography.* J. Am. Soc. Mass Spectrom. **1993**, *4*, 662-669.
14. Haydon, C.E.; Eyers, P.A.; Aveline-Wolf, L.D.; Resing, K.A.; Maller, J.L.; Ahn, N.G. *Identification of Novel Phosphorylation Sites on Xenopus laevis Aurora A and Analysis of Phosphopeptide Enrichment by Immobilized Metal-affinity Chromatography.* Mol. Cell Proteomics **2003**, *2*, 1055-1067.
15. Nuhse, T.S.; Stensballe, A.; Jensen, O.N.; Peck, S.C. *Large-scale Analysis of in Vivo Phosphorylated Membrane Proteins by Immobilized Metal Ion Affinity Chromatography and Mass Spectrometry.* Mol. Cell Proteomics. **2003**, *2*, 1234-1243.
16. Kawahara, M.; Nakamura, H.; Nakajima, T. *Titania and Zirconia - Possible New Ceramic Microparticulates for High-Performance Liquid-Chromatography.* J. Chromatography., A **1990**, *515*, 149-158.

17. Tani, K.; Suzuki, Y. *Investigation of the ion-exchange behaviour of titania: Application as a packing material for ion chromatography.* Chromatographia **1997**, *46*, 623-627.
18. Tani, K.; Suzuki, Y. *Syntheses of Spherical Silica and Titania from Alkoxides on a Laboratory-Scale.* Chromatographia **1994**, *38*, 291-294.
19. Tani, K.; Sumizawa, T.; Watanabe, M.; Tachibana, M.; Koizumi, H.; Kiba, T. *Evaluation of titania as an ion-exchanger and as a ligand-exchanger in HPLC.* Chromatographia **2002**, *55*, 33-37.
20. Jiang, Z.T.; Zuo, Y.M. *Synthesis of porous titania microspheres for HPLC packings by polymerization-induced colloid aggregation (PICA).* Anal. Chem. **2001**, *73*, 686-688.
21. Matsuda, H.; Nakamura, H.; Nakajima, T. *New Ceramic Titania - Selective Adsorbent for Organic-Phosphates.* Anal. Sci. **1990**, *6*, 911-912.
22. Ikeguchi, Y.; Nakamura, H. *Selective enrichment of phospholipids by titania.* Anal. Sci. **2000**, *16*, 541-543.
23. Ikeguchi, Y.; Nakamura, H. *Determination of organic phosphates by column-switching high performance anion-exchange chromatography using on-line preconcentration on titania.* Anal. Sci. **1997**, *13*, 479-483.
24. Kawahara, M.; Nakamura, H.; Nakajima, T. *Group Separation of Ribonucleosides and Deoxyribonucleosides on a New Ceramic Titania Column.* Anal. Sci. **1989**, *5*, 763-764.
25. Sano, A.; Nakamura, H. *Titania as a chemo-affinity support for the column-switching HPLC analysis of phosphopeptides: application to the characterization of phosphorylation sites in proteins by combination with protease digestion and electrospray ionization mass spectrometry.* Anal. Sci. **2004**, *20*, 861-864.
26. Sano, A.; Nakamura, H. *Chemo-affinity of titania for the column-switching HPLC analysis of phosphopeptides.* Anal. Sci. **2004**, *20*, 565-566.
27. Hofmann, F.; Dostmann, W.; Keilbach, A.; Landgraf, W.; Ruth, P. *Structure and physiological role of cGMP-dependent protein kinase.* Biochim. Biophys. Acta **1992**, *1135*, 51-60.
28. Hofmann, F.; Flockerzi, V. *Characterization of phosphorylated and native cGMP-dependent protein kinase.* Eur. J. Biochem. **1983**, *130*, 599-603.
29. Aitken, A.; Hemmings, B.A.; Hofmann, F. *Identification of the residues on cyclic GMP-dependent protein kinase that are autophosphorylated in the presence of cyclic AMP and cyclic GMP.* Biochim. Biophys. Acta **1984**, *790*, 219-225.
30. Francis, S.H.; Wolfe, L.; Corbin, J.D. *Purification of type I alpha and type I beta isozymes and proteolyzed type I beta monomeric enzyme of cGMP-dependent protein kinase from bovine aorta.* Methods Enzymol. **1991**, *200*, 332-341.
31. Meiring, H.D.; van der Heeft, E.; ten Hove, G.J.; de Jong, A.P.J.M. *Nanoscale LC-MS$^{(n)}$; technical design and applications to peptide and protein analysis.* J. Sep. Sci. **2002**, *25*, 557-568.
32. van der Heeft, E.; ten Hove, G.J.; Herberts, C.A.; Meiring, H.D.; van Els, C.A.; de Jong, A.P. *A microcapillary column switching HPLC-electrospray ionization MS system for the direct identification of peptides presented by major histocompatibility complex class I molecules.* Anal. Chem. **1998**, *70*, 3742-3751.
33. Chu, D.M.; Francis, S.H.; Thomas, J.W.; Maksymovitch, E.A.; Fosler, M.; Corbin, J.D. *Activation by autophosphorylation or cGMP binding produces a similar apparent conformational change in cGMP-dependent protein kinase.* J. Biol. Chem. **1998**, *273*, 14649-14656.
34. Feil, R.; Kellermann, J.; Hofmann, F. *Functional cGMP-dependent protein kinase is phosphorylated in its catalytic domain at threonine-516.* Biochemistry **1995**, *34*, 13152-13158.

35. Busch, J.L.; Bessay, E.P.; Francis, S.H.; Corbin, J.D. *A conserved serine juxtaposed to the pseudosubstrate site of type I cGMP-dependent protein kinase contributes strongly to autoinhibition and lower cGMP affinity.* J. Biol. Chem. **2002**, *277*, 34048-34054.
36. Resing, K.A.; Ahn, N.G. *Protein phosphorylation analysis by electrospray ionization-mass spectrometry.* Methods Enzymol. **1997**, *283*, 29-44.
37. McLachlin, D.T.; Chait, B.T. *Analysis of phosphorylated proteins and peptides by mass spectrometry.* Curr. Opin. Chem. Biol. **2001**, *5*, 591-602.

Peptide substrate resides near the glycine-rich loop of the cGMP-dependent protein kinase.

4

Martijn W. H. Pinkse[1], Dirk T.S. Rijkers[2], Wolfgang R. G. Dostmann[3] and Albert J. R. Heck[1]

[1] Department of Biomolecular Mass Spectrometry, Utrecht University, Utrecht, The Netherlands

[2] Department of Medicinal Chemistry, Utrecht University, Utrecht, The Netherlands

[3] Department of Pharmacology, University of Vermont, Burlington, Vermont, USA.

Abstract

The substrate binding site of cGMP-dependent protein kinase Iα was investigated with a synthetic substrate peptide containing the photoreactive amino acid 4'-[(trifluoromethyl)diazirinyl-*L*-phenylalanine incorporated at the P+4 position, TQAKRKKSLAMF$^{(Tmd)}$LR. Covalent substrate linkage was primarily observed when photolysis was performed in the presence of cGMP, which is in support of the current working model of PKG activation. It was found that up to two substrate molecules could be cross-linked to dimeric PKG. To identify residues that were cross-linked, the protein was cleaved with trypsin. The resulting peptide fragments were separated by nanoflow-HPLC and analyzed by ESI-TOF-MS/MS. In order to facilitate the retrieval of cross-linked products, the photoreactive substrate was labeled by incorporating for 50% $C^{13}N^{15}$-leucine at the P+1 position during peptide synthesis, providing a unique mass tag for the cross-linked proteolytic peptides. Covalent linkage could be localized to occur in the catalytic core on residues 356-372, also known as the glycine-rich loop essential for ATP binding. The coincident covalent modification of the glycine rich loop suggests that the substrate binds PKG near the catalytic center. Low energy CID spectra of the cross-linked product located Ile361 as the residue of coupling. Incubation of the cross-linked protein with ATP and Mg^{2+}, followed by proteolysis and HPLC tandem MS demonstrated that the substrate when coupled near the glycine rich loop is still properly oriented to act as phosphoacceptor.

Introduction

It is now well known that reversible protein phosphorylation is an important regulatory mechanism involved in many different cellular functions [1]. Intense efforts are presently directed to elucidating the molecular basis and mechanisms of protein kinases, the enzymes that catalyze the protein phosphorylation reaction. Comprehensive analysis of the human genome placed the number of encoded kinases on 518 [2] and all these protein kinases share a conserved catalytic core [3]. Despite structural homology of protein kinases and their common utilization of ATP, all protein kinases operate in distinct cellular pathways and have different target substrates. Hence protein kinases must have a tremendous selectivity. Central to our understanding of protein phosphorylation is the question how protein kinases achieve this specificity. In general, kinases phosphorylate substrates on basis of residues immediately

flanking phosphate accepting residues and these local residues define a consensus sequence for substrate phosphorylation [4]. Besides these primary sequence requirements protein kinase specificity may be obtained via processes such as allosteric regulation and subcellular localization. It should also be anticipated that phosphorylation site recognition could also be determined by secondary and/or tertiary structure elements outside the primary sequence of the phosphorylation site.

Among the superfamily of protein kinases the two cyclic nucleotide regulated protein kinases, cAMP-dependent protein kinase and cGMP-dependent protein kinase, form a closely related subfamily of serine/threonine kinases. Both proteins share several structural elements, such as the N-terminal dimerization domain, an autoinhibition site, two in-tandem cyclic nucleotide binding sites and a highly conserved catalytic core. Despite these similarities, these two enzymes display distinct differences, which account for their unique properties. Whereas PKA is nearly ubiquitous, PKG is primarily found in the lung, cerebellum and smooth muscles. From a structural point of view these cyclic-nucleotide-dependent protein kinases differ as well. The holoenzyme of PKA is a tetramer composed of two regulatory and two catalytic subunits. The catalytic subunits are non-covalently attached to the regulatory subunit dimer. Upon interaction with cAMP, the catalytic subunits dissociate from the holoenzyme and are free to catalyze heterophosphorylation. In contrast, PKG is a dimeric species of which each subunit is composed of a regulatory and a catalytic domain on a single polypeptide chain. Consequently, when cGMP activates PKG, the catalytic and regulatory components remain physically attached. Within the catalytic domain PKA and PKG share a strong primary sequence homology [5]. Not surprisingly, these enzymes also exhibit overlapping substrate specificities, a feature that often interferes with efforts to elucidate their distinct biological pathways. Peptide substrates with a primary amino acid sequence motif RRX-S/T-Ψ (where X is generally a hydrophobic residues) are in general recognized by both PKA and PKG [6]. Besides this strong overlapping substrate specificity, several studies report on subtle differences in determinants that discriminate for PKA and PKG substrate specificity [7-13]. Kinetic constants for both PKA and PKG of several substrate peptides analyzed in these studies are listed in table 1. The bifunctional enzyme 6-phosphofructo-2-kinase/fructose-2,6-biphosphatase (6PF-2-K/Fru-2,6-P2ASE) is kinetically a good substrate for PKA. PKG is unable to phosphorylate the intact protein, but is able to phosphorylate the synthetic peptide VLQRRRGSSIPQ, which is modeled after the sequence in the native 6PF-2-K/Fru-2,6-P2ASE protein [14], suggesting structures other than the primary sequence

define substrate specificity differences between PKA and PKG. In addition, both proteins phosphorylate the analogous peptide VLQRRRGTSIPQ with similar K_m values, but where PKA specifically phosphorylates the threonine, PKG equally distributes the phosphate between the threonine and serine [7]. For PKA detailed insight into substrate recognition was obtained from the crystal structure of the ternary complex of the catalytic subunit of PKA, ADP and a 20 amino-acid peptide inhibitor $PKI^{(5-24)}$ [15]. Kinetic studies with substrate analogues of $PKI^{(5-25)}$ have shown that besides the basic residues adjacent of the phosphate accepting serine, the amino terminal residues of $PKI^{(5-24)}$ are essential for high affinity recognition by PKA. $PKI^{(5-24)}$ adapts an amphipathic α helix of which the hydrophobic site binds to a hydrophobic pocket on PKA. The cGMP dependent protein recognizes the basic domain of $PKI^{(5-24)}$, but does not recognize the amino-terminal parts [16] (see table 1). Evidence that PKG requires a C-terminal extension to obtain high substrate specificity emerged from two independent lines of research. In one particular study, the sequence surrounding the phosphorylation site of bovine lung cGMP-binding cGMP specific phosphodiesterase, a potent and relative specific substrate for PKG, was used to identify determinants for substrate recognition of PKG in comparison to PKA. Peptide analogs derived from the phosphorylation site in this substrate were screened to determine residues that contribute to differences in PKG and PKA specificity. Both proteins phosphorylate RKISASE with comparable kinetics, but by addition of a phenylalanine at the C-terminus to yield RKISASEF, specificity for PKG is increased almost 5-fold. Hence the phenylalanine at the P+4 position appears to be a strong negative determinant for PKA [9] (see table 1). In a another study, substrate library screening of dodecameric peptide libraries elucidated a consensus sequence for both PKG and PKA in systematic manner [11, 17]. As previously mentioned basic residues lysine or arginine are required downstream the phosphate accepting serine for both proteins to achieve high enzymatic turnover. The selectivity for PKG over PKA could be substantially improved by a C-terminal extension. For example, by adding a methionine and a phenylalanine C-terminal of the decameric substrate TQAKRKKSLA-amide the K_m shifts from 1.74 µM to 0.5 µM without affecting V_{max} (see table 1). Additionally, molecular modeling of the PKG specific substrate TQAKRKKSLAMA-amide and a structural model of the catalytic domain of PKG suggested a preferred conformation of this peptide that differs substantially from conformation of the heat-stable $PKI^{(5-24)}$ in the crystal structure of the catalytic domain of PKA [11].

Table 1: K_m and k_{cat} values for the phosphorylation of synthetic peptides

Peptide	PKG			PKA			PKG / PKA (Specificity Index)
	K_m (µM)	k_{cat} (µmol/min /mg)	k_{cat} / K_m	K_m (µM)	k_{cat} (µmol/min /mg)	$k_{ca\ t}$ / K_m	
VLQRRRG**SS**IPQ [(1)]	32.9	0.9	0.027	3.8	13.6	3.6	0.008
VLQRRRG**TS**IPQ [(1)]	25.7	0.18	0.007	39.2	4.6	0.12	0.06
TYADFIASGRTGRRN**S**I [(2)]	2.4	1.0	0.42	0.12	1.0	8.33	0.05
IASGRTGRRN**S**I [(2)]	2.7	0.74	0.27	0.18	1.4	7.78	0.03
GRTGRRN**S**I [(2)]	7.0	0.79	0.11	0.32	0.56	1.75	0.63
TQAKRKK**S**LAMFLR [(3)]	0.26	11.5	44.23	1.7	3.9	2.29	19.2
TQAKRKK**S**LAMF [(3)]	0.5	11.0	22	3.3	5.7	1.72	12.9
TQAKRKK**S**LA [(3)]	1.74	11.1	6.37	2.68	7.9	5.22	2.16
RKI**S**ASEFDRPLR [(4)]	68	11	0.162	320	3.2	0.010	16.2
RKI**S**ASEF [(4)]	120	5.2	0.043	480	2.6	0.006	8.1
RKI**S**ASE [(4)]	80	5.6	0.070	93	3.7	0.040	1.8

The phosphate-accepting residue is depicted in bold.
[(1)] Glass *et al.* [7]
[(2)] Mitchell *et al.* [10]
[(3)] Dostmann *et al.* [11]
[(4)] Colbran *et al.* [9]

Since high-resolution structural data are not available for PKG, one of our goals is to elucidate binding sites for PKG specific substrates and inhibitors in more detail using a combination of photoaffinity labeling and mass spectrometry. New information on the molecular determinants that are crucial for binding of substrate and/or inhibitor peptides to PKG is of importance in the design of new molecular tools to delineate cGMP signaling networks and eventually for future therapeutics that may target PGK-mediated signaling pathways. The method of photoaffinity labeling enables the direct probing of target proteins through a covalent bond which is photochemically introduced between a ligand and its specific receptor [18]. In combination with modern mass spectrometric techniques this is a powerful approach for the characterization of peptide-protein interactions [19]. In this investigation we characterized the conditions for the covalent labeling of recombinant cGMP-dependent protein kinase with a synthetic peptide substrate containing a photoreactive amino acid, 4'-(trifluoromethyl)diazirinyl-*L*-phenylalanine, at the P+4 position. To directly identify sites of proximity between PKG and peptide substrates, we carried out photoaffinity labeling studies followed by protein digestion and nanoflow high performance liquid chromatography

and electrospray ionization time of flight mass spectrometry. Using this strategy we have successfully cross-linked a high affinity PKG specific substrate to PKG. Cross-linking primarily occurred in the presence of cGMP, which is in support of the current working model of PKG activation. The site of cross-linkage was located at Ile-361. Additionally we validated that the cross-linked PKG-substrate complex is still active as we were able to show that covalently attached substrate could be phosphorylated by PKG.

Experimental

Chemicals and reagents: ArgoGel™ Rink-NH-Fmoc resin (Argonaut Technologies, Muttenz, Switzerland) functionalized with a 4-((2',4'-dimethoxyphenyl) aminomethyl) phenoxy-acetamido moiety (Rink amide linker) [20] was used to obtain C-terminal peptide amides. The coupling reagent 2-(1H-benzotriazol-1-yl)-1,1,3,3-tetramethyluronium hexafluorophosphate (HBTU) [21] was obtained from Richelieu Biotechnologies Inc. (Montreal, Canada). The coupling reagents N-[(dimethylamino)-1H-1,2,3-triazolo[4,5-bipyridin-1-yl-methylene]-N-methylmethanaminium hexafluorophosphate/N-hydroxy-7-azabenzotriazole (HATU/HOAt) [22] were obtained from Applied Biosystems. N-hydroxybenzotriazole (HOBt), 9-fluorenylmethyloxycarbonyl hydroxysuccinimide (Fmoc-ONSu) and N^{α}-9-fluorenylmethyloxycarbonyl (Fmoc) amino acids were obtained from Advanced ChemTech (Machelen, Belgium). The side chain protecting groups were: Boc: tert-butyloxycarbonyl, for lysine; tBu: tert-butyl, for threonine, tyrosine and serine; Pbf: 2,2,4,6,7-pentamethyl-dihydrobenzofuran-5-sulfonyl, for arginine and Trt: trityl, for glutamine and histidine. Fmoc-Phe(Tmd)-OH (N-9-fluorenylmethyloxycarbonyl-4'-[3-(trifluoromethyl-3H-diazirin-3-yl)]phenylalanine) was obtained from photoprobes (Sins, Switzerland). U-^{13}C6/^{15}N-labeled leucine was obtained from Cambridge Isotope Laboratories (Andover, MA, USA). This amino acid was converted into its corresponding Fmoc-derivative according to the method of ten Kortenaar [23]. Peptide grade dichloromethane (DCM), N-methylpyrrolidone (NMP) methyl tert-butyl ether (MTBE), trifluoroacetic acid (TFA) and HPLC grade acetronitrile were purchased from Biosolve (Valkenswaard, The Netherlands). Piperidine and N,N-diisopropylethylamine (DIEA), were obtained from Acros Organics ('s-Hertogenbosch, The Netherlands). HPLC grade TFA and 1,2-ethanedithiol (EDT) were obtained from Merck (Amsterdam, The Netherlands). AMPPNP, ATP, cGMP, DTT, Iodoacetamide and Magnesium chloride were obtained from Sigma (St. Louis, MO, USA).

Sequencing grade trypsin was purchased from Roche Diagnostics GmbH (Mannheim, Germany). PKG was expressed in SF9 insect cells essentially as described by Dostmann *et al.* [11].

Peptide synthesis: Peptide synthesis was performed automatically on an Applied Biosystems 433A Peptide Synthesizer (Foster City, CA, USA). Analytical and preparative HPLC runs were performed on a Gilson HPLC workstation (Middleton, Wisconsin, USA). The Peptide Ac-Thr-Gln-Ala-Lys-Arg-Lys-Lys-Ser-Leu($^{12}C/^{14}N,^{13}C/^{15}N$)-Ala-Met-Phe(Tmd)-Leu-Arg-NH_2 ($W64^{Phe(Tmd)}$) was synthesized using the FastMoc protocol on a 0.25 mmol scale [24]. Each synthetic cycle consisted of N^{α}-Fmoc removal by a 10 min treatment with 20% piperidine in NMP, a 6 min NMP wash, a 45 min coupling step with 1.0 mmol of preactivated Fmoc amino acid in the presence of 2 equivalents DIPEA, and a 6 min NMP wash. N^{α}-Fmoc amino acids were activated in situ with 1.0 mmol HBTU/HOBt (0.36 M in NMP) in the presence of DIPEA (2.0 mmol). After the final Fmoc removal the free amine was acetylated with an excess of acetic acid anhydride/DIPEA/HOBt in NMP. Fmoc-Phe(Tmd)-OH was coupled with HATU/HOAt in an excess of only 2 equiv (with respect to the loading of the resin) for 90 min. Fmoc-Leu($^{13}C/^{15}N$)-OH was coupled in the presence of one equimolar equivalent Fmoc-Leu($^{12}C/^{14}N$)-OH with HATU/HOAt in an excess of only 2 equiv for 90 min. After these coupling steps any remaining free amine functionalities were acetylated with acetic acid anhydride/DIPEA/HOBt. The peptides were cleaved from the resin and deprotected by treatment with TFA/H_2O/EDT 95:2.5:2.5 v/v/v at room temperature for 3 h. The peptides were precipitated with MTBE/hexane 1:1 v/v at –20°C. The precipitates were decanted and subsequently washed with cold MTBE/hexane 1:1 v/v (3 ×) and finally lyophilized from tert-BuOH/H_2O 1:1 v/v.

Peptide purification: The crude lyophilized peptides were dissolved in a minimum amount of 0.1% TFA in CH_3CN/H_2O 5:95 v/v and loaded onto the HPLC column (Phenomenex Luna C8, 100Å pore size, 10 µm particle size, 2.2 × 25 cm). The peptides were eluted with a flow rate of 10.0 mL/min using a linear gradient of buffer B (100% in 96 min) from 100% buffer A (buffer A: 0.1% TFA in CH_3CN/H_2O 5:95 v/v, buffer B: 0.1% TFA in CH_3CN/H_2O 60:40 v/v).

***Peptide characterization*:** In order to determine purity, the synthesized peptide was subjected to liquid chromatography electrospray ionization mass spectrometry using a Shimadzu LCMS-QP8000 (Duisburg, Germany) single quadrupole bench-top mass spectrometer operating in a positive ionization mode. The purified peptide was loaded onto a Phenomenex Luna C8 column (100Å pore size, 5 μm particle size, 0.46 × 25 cm) at a flow rate of 1 mL/min using a linear gradient of buffer B (100% in 48 min) from 100% buffer A (buffer A: 0.1% TFA in CH_3CN/H_2O 5:95 v/v; buffer B: 0.1% TFA in CH_3CN/H_2O 60:40 v/v). The mass of purified peptides was finally confirmed by electrospray ionization mass spectrometry.

Photoaffinity labeling and Proteolysis: Upon irradiation with UV-light (~350 nm), Tmd(Phe) irreversibly generates a highly reactive singlet carbene by a photodissociative process. This intermediates can enforce hydrogen abstraction on appropriately oriented target C-H bonds within a distance ~3 Å or less [25, 26]. Since the electrophilic nature of the carbene intermediate renders solvent O-H bonds appropriate H- donors, the radius of the photochemical insertion reaction is limited. Specific labeling by Tmd(Phe) would therefore suggest a closer proximity between target protein and the photoprobe [26]. The protein at a concentration of 0.2 mg/mL in a 25 mM potassium phosphate buffer (pH 7.4), containing 50 mM NaCl, 1.2 mM EDTA, 4 mM Magnesium acetate and 200 μM AMPPNP, was incubated with 200 μM photoaffinity label at 30 ºC for 10 min. The protein-photolabel was illuminated at 366 nm for 15 minutes in 96 well-plate on ice using SYLVANIA light source (F8T5/BTB). For intact protein mass measurements the sample was dialyzed overnight against 200 mM ammonium acetate and finally concentrated using an Ultrafree-0.5 centrifugal filter (Millipore, Bedford, MA). Protein masses were determined by nanoflow ESI-TOF-MS on a Micromass LC-T time-of-flight instrument using home made borosilicate nano electrospray needles. For optimal detection of the intact PKG source interface pressures were optimized as previously described [27]. For the HPLC tandem MS analysis the PKG protein was proteolyzed. Prior to digestion all cysteines were reduced with dithiotreitol and alkylated using iodoacetamide. The protein sample was subsequently diluted 10 times with 50 mM ammonium bicarbonate, pH 8.0 and spun in an Ultrafree-0.5 centrifugal filter. This step was repeated three times. Finally trypsin was added to a final protein:protease concentration of 20:1 by weight. The digestion mixture was incubated at 37 ºC for 16 hours.

LC-ESI-MS and MSMS peptide analysis: Proteolytic peptide mixtures were analyzed using an Ultimate nano-HPLC system (LC Packings, Amsterdam, The Netherlands) operating essentially as described by Meiring *et al.* [28]. Samples were loaded onto Phenomenex Aqua C_{18} pre-column (200Å pore size, 5 μm particle size) at 5 μl/min in 100% Solvent A (0.6 % acetic acid). Subsequently peptides were separated on an Aqua C_{18} nano-reversed phase column (50 μm i.d., 20 cm L) with a flow of 100-150 nl/min. Elution was performed using a gradient of 0-60% Solvent B (80% acetonitrile and 0.6% acetic acid) at 1.2% min^{-1}. The column effluent of the nano-LC was directly infused into a Micromass Qtof-1 quadrupole time-of flight instrument (Micromass Ltd., Manchester, UK) using in-house prepared nanospray emitters. Mass spectra were acquired in positive ion mode and argon was used as collision gas. During LC-MS runs, analysis time of cross-linked products was increased by performing peak parking essentially as described by Meiring *et al.* [28]. In short, prior to elution of an analyte of interest the column flow was lowered to ~20-40 nl/min by instantaneously dropping the column pressure using an extra flow-splitter. Hereby the elution time was broadened to more than two minutes and this allowed sufficient time to perform a low-energy CID analysis. For the fragmentation of labeled peptides the quadruple mass resolution parameters were set to a relatively large mass window (~5 *m/z* units) in order to mass select both light and heavy leucine labeled precursors ion.

Results and discussion

The 4'-[(trifluoromethyl)diazirinyl-*L*-phenylalanine (Phe(Tmd)) containing peptide acetyl-TQAKRKKSLAMF$^{(Tmd)}$LR-amide (W64$^{Phe(Tmd)}$) was synthesized using standard solid phase peptide synthesis. This peptide is an analogue of the PKG specific substrate peptide TQAKRKKSLAMFLR (W64), in which the serine represents the phosphate acceptor site. This peptide was derived from library screens directed to identify highly PKG-specific substrates [11, 17]. With a K_m of 260 nM and a PKG/PKA specificity index of 19.2 this peptide is the most selective and specific substrate for PKG known today. The photo-activateable amino acid was positioned at the P+4 position based on dual reasoning. The primary reason is that it replaces the phenylalanine at the P+4 position of the original substrate. In this way possible negative effects, for instance steric hindrance of the bulky side chain of (Tmd)Phe, that could lower affinity are reduced as much as possible. Secondly, this phenylalanine was previously shown to have an important role in the determination of substrate selectivity between PKA and PKG [9]. PKG was irradiated for 10 min in the

presence of 200 μM W64$^{Phe(Tmd)}$. Although the kinetic properties of PKG for this photoaffinity label were not determined, it is for now assumed that these do not differ significantly from the original peptide, which displayed a K_m of 260 nM (Table 1). Hence the concentration of W64$^{Phe(Tmd)}$ used (200 μM) should be well above the actual K_m thereby assuring complete enzyme saturation. After overnight dialysis to remove the excess non-crosslinked substrate peptides, photoadduct incorporation was measured by subjecting the photolyzed protein samples to nanoflow ESI-TOF-MS analysis. Figure 1A shows the acquired mass-spectrum of the intact protein, which was irradiated in the presence of 200 μM W64$^{Phe(Tmd)}$. The deconvoluted mass spectrum contains two peaks at 153,010 Da and 154,850 Da. This first mass corresponds to the mass of dimeric PKG (theoretical mass 152,817 Da, with an intramolecular disulfide bridge on Cys-42 and complete phosphorylation of Thr-516, see Chapter 2). This peak is also the most abundant peak suggesting that the majority of PKG is not cross-linked. The second peak at 154,850 is ~1840 Da higher which matches the incorporation of one W64^{TmdPhe}. The average mass of W64$^{Phe(Tmd)}$ is 1828 Da and upon crosslinking the net average mass increase is 1799 Da (-28 Da; loss of molecular nitrogen). The mass accuracy in the current acquired data set is too low to assess whether covalent linkage has occurred or whether the observed complex is of a non-covalent nature. Hence as a control Figure 1B shows the mass spectrum of the same protein-peptide reaction mixture that was kept in the dark. By comparing Figure 1A and 1B it appears that they small amount of PKG-W64^{TmdPhe} complex in Figure 1A is indeed formed after exposure to UV-light and involves thus most likely covalent linkage. Figure 1C shows nanoflow ESI-MS-TOF spectra of PKG after irradiation in the presence of 200 μM W64$^{Phe(Tmd)}$ and 100 μM cGMP and Figure 1D shows the control sample that was kept in the dark. The aminoterminal cGMP-binding site of PKG binds cGMP with an apparent K_d of 15 nM and the C-terminal cGMP-binding site binds cGMP with an apparent K_d of 100-150 nM , hence the used cGMP concentration (100 μM) is high enough to assure complete cGMP occupation of both cGMP binding sites. The deconvoluted spectrum shows three abundant peaks of which the peak at 154,420 Da represents the cGMP-saturated PKG-$[cGMP]_4$ complex, the peak at 156,280 Da matches PKG-$[cGMP]_4$-W64$^{Phe(Tmd)}$ complex and the peak at 158,130 matches the PKG-$[cGMP]_4$-$[W64^{PheTmd}]_2$ complex. Hence, even after dialysis PKG has still 4 mol cGMP/ mol enzyme bound. More importantly, when compared to Figure 1A, Figure 1C shows that under these conditions much more substrate incorporation has occurred. Again, Figure 1D confirms that this incorporation is catalyzed by UV-light, indicative for the covalent attachment of

substrate. These spectra clearly demonstrate that covalent attachment of the W64$^{Phe(Tmd)}$ peptide is strongly enhanced in the presence of cGMP.

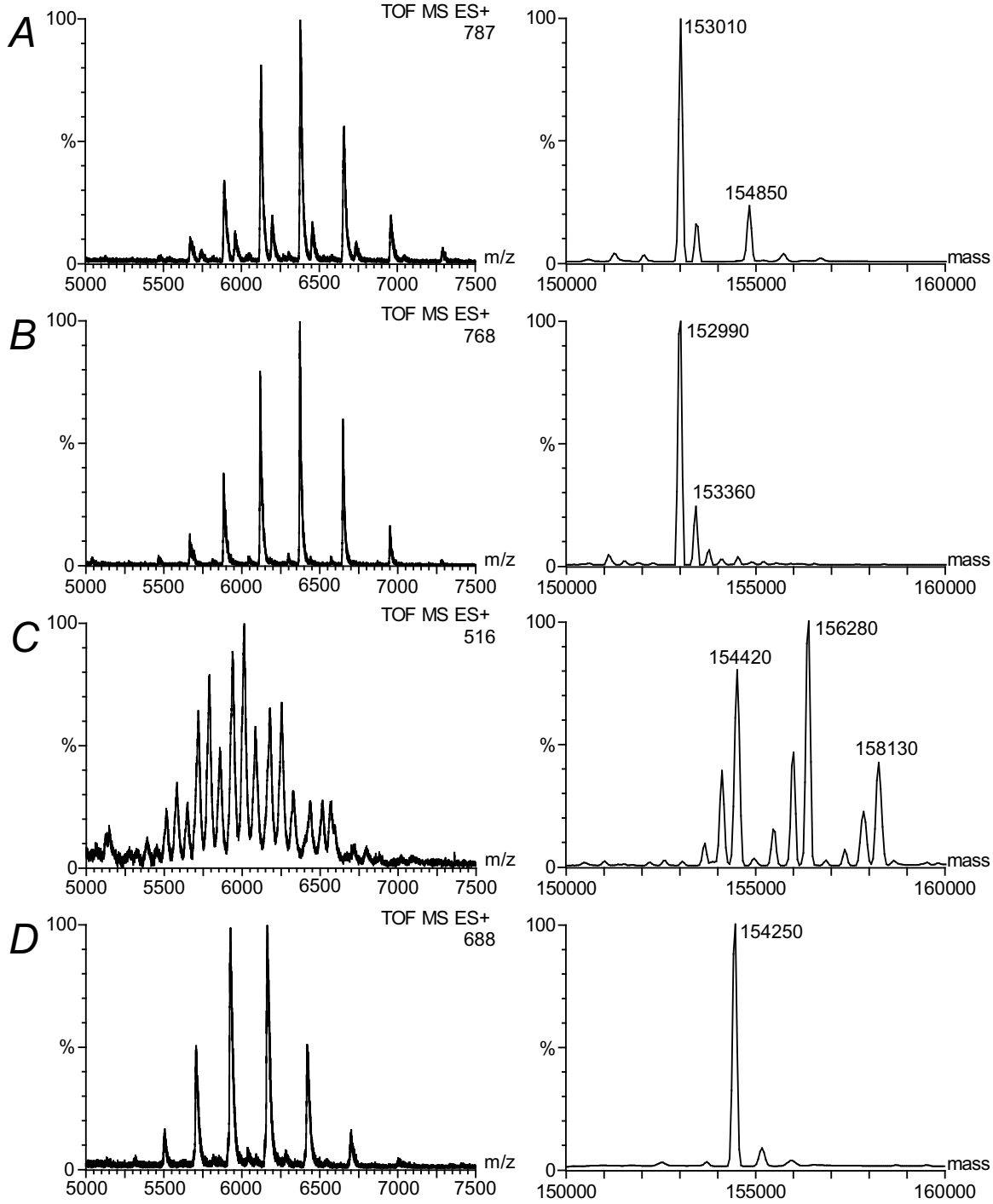

Figure 1: Nanoflow ESI TOF mass spectrometric analysis intact photoproducts. PKG in the presence of 200 µM W64$^{Phe(Tmd)}$ which was **(A)** irradiated for 10 min at 366 nm or **(B**) kept in the dark. PKG in the presence of 100 µM cGMP and 200 µM W64$^{Phe(Tmd)}$, which was **(C)** irradiated for 10 minutes at 366 nm or **(D)** kept in the dark. On the left are shown enlarged parts of the m/z spectra containing the charge state envelope of dimeric PKG. On the left are shown the corresponding deconvoluted mass spectra.

Proteolysis of W64$^{Phe(Tmd)}$ labeled PKG.

In order to identify the sites of covalent linkage W64$^{Phe(Tmd)}$-labeled cGMP-saturated-PKG was digested with trypsin and analyzed by nanoflow LC-MS. In theory the digestion of PKG with trypsin generates 93 proteolytic fragments, however in practice peptides with missed cleavage sites are often observed as well, which further increases the complexity of such a proteolytic mixture.

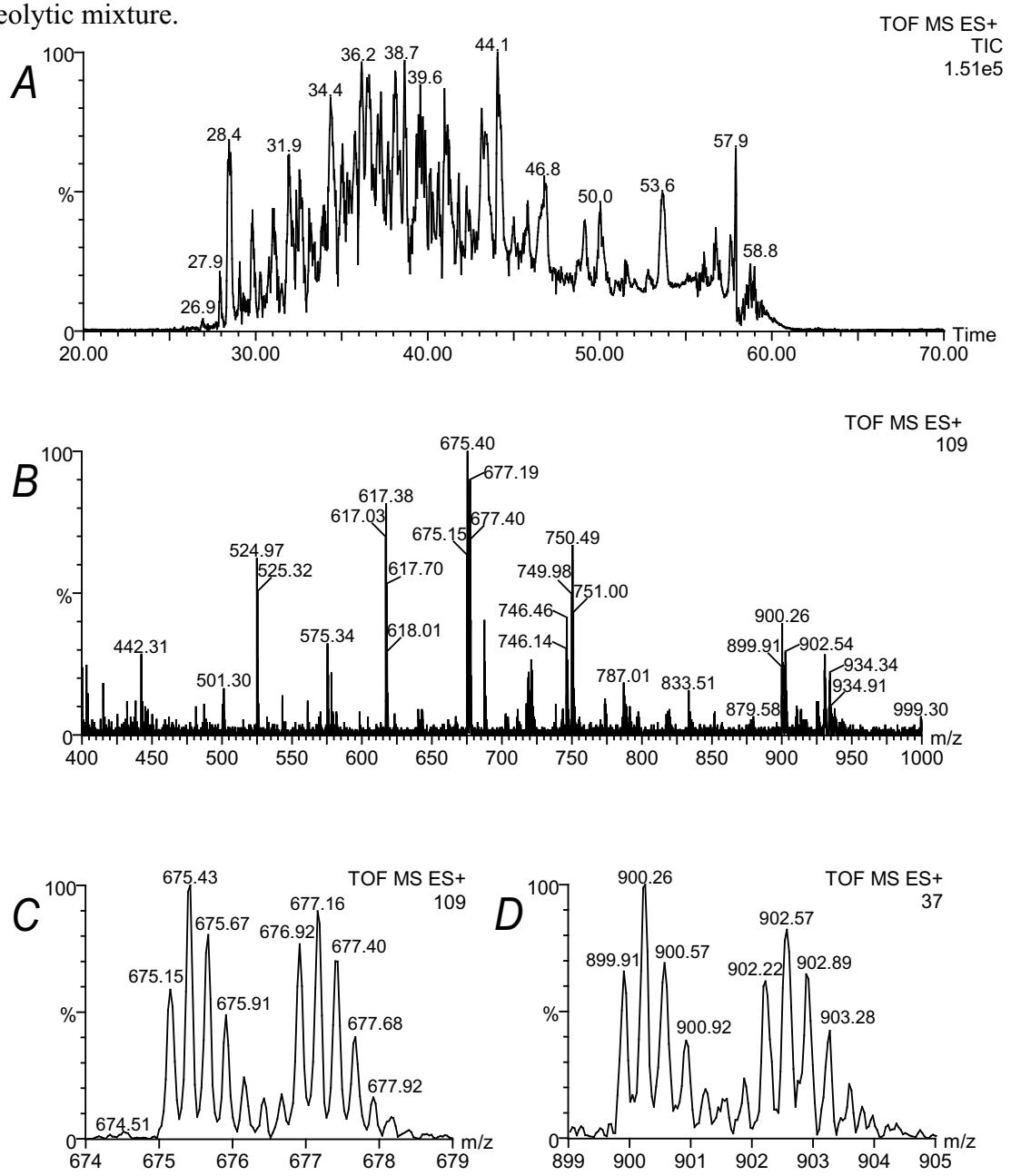

Figure 2: nanoflow LC-MS elution profile of the tryptic digest of PKG-W64$^{Phe(Tmd)}$. **(A)** total ion chromatogram (TIC) of proteolytic fragments. The mass spectrum displayed in **(B)** shows the ions that eluted around 41 min. In **(C)** and **(D)** enlarged parts of the spectrum in **B** are shown, indicating the selective isotope tag of the photo-cross linked peptides. Both isotopically labeled ion pairs correspond to the $[M+4H]^{4+}$ and $[M+3H]^{3+}$ of a peptide of 2696.4 Da.

One can easily imagine that the retrieval of cross-linked products from such a complex mixture requires the characterization of each individual proteolytic product, which was, given the amount of peptides in this particular case, be very tedious and therefore no practical. In order to facilitate the retrieval of cross-linked products from this complex mixture a stable isotope labeling strategy was employed. During peptide synthesis of the photo-affinity label the leucine adjacent to the phosphate accepting serine was for 50% incorporated as 6-C^{13},1-N^{15}-leucine (see experimental). Cross-linking the isotopically labeled substrate peptide with PKG, followed by proteolysis results in cross-link products that will display a characteristic peak-pair spaced by 7 Da. As a result cross-linked products will distinguish themselves from non-cross-linked proteolytic products by their peak-pair isotope pattern. Figure 2A shows the total ion current chromatogram of the LC-MS analysis of the tryptic digest of $W64^{Phe(Tmd)}$-labeled PKG. All spectra were analyzed manually for the presence of ion-pairs with the characteristic 7 Da mass difference. At an elution time of about 41 minutes two doublets were found at *m/z* 675 and *m/z* 900, which both matched the characteristic isotopic pattern. Figure 2B displays the mass spectrum from *m/z* 400-1000 obtained by combining ~10 scans around the LC-elution time of 41 min. Figure 2C and 2D display enlarged parts of this spectrum for both these doublets. The doublets at *m/z* 675.15 and at *m/z* 899.91 are the $[M+4H]^{4+}$ and $[M+3H]^{3+}$ of a cross-link product with an apparent mass of 2696.4 Da. Tandem MS was performed on the $[M+4H]^{4+}$ in order to identify this peptide and the results are shown in Figure 3**.** The quadrupole resolution parameters were set to a relative broad mass window in order to perform simultaneously MS/MS of both light and heavy labeled peptide (Figure 3A). The low-energy CID spectrum in Figure 3C displays a series of y”-ions that correspond to part of the sequence of PKG, namely ^{366}GVGGFGR^{372}. In the higher *m/z* region a serie of multiply charged b-ions is observed (Figure 3D) that displays the same sequence tag and more importantly, they all exhibit the photoaffinity label characteristic peak-pairs. Apparently, the photolabel is cross-linked to ^{356}LSDFNIIDTLGVGGFGR^{372}. This tryptic fragment has a monoisotopic mass of 1779.92. The remaining mass of the selected precursor ion is 916.44 Da and matches with SLAMF^{Tmd}LR, taking into account the loss of 28 Da (N_2) of the Tmd group after photoactivation and the conversion of the C-terminal amide into a carboxyl group. This part of the photolabel corresponds to tryptic cleavage after the lysine adjacent to the phosphate accepting serine. The series of y”-ions up to y“$_7$ suggest that the cross-link did not occur at one of the last seven residues of this tryptic PKG peptide. The

series of labeled b-ions was found down to Ile-361. Together with the observation of b_3 ion this suggests cross-linking occurred between Phe-359 and Ile-361.

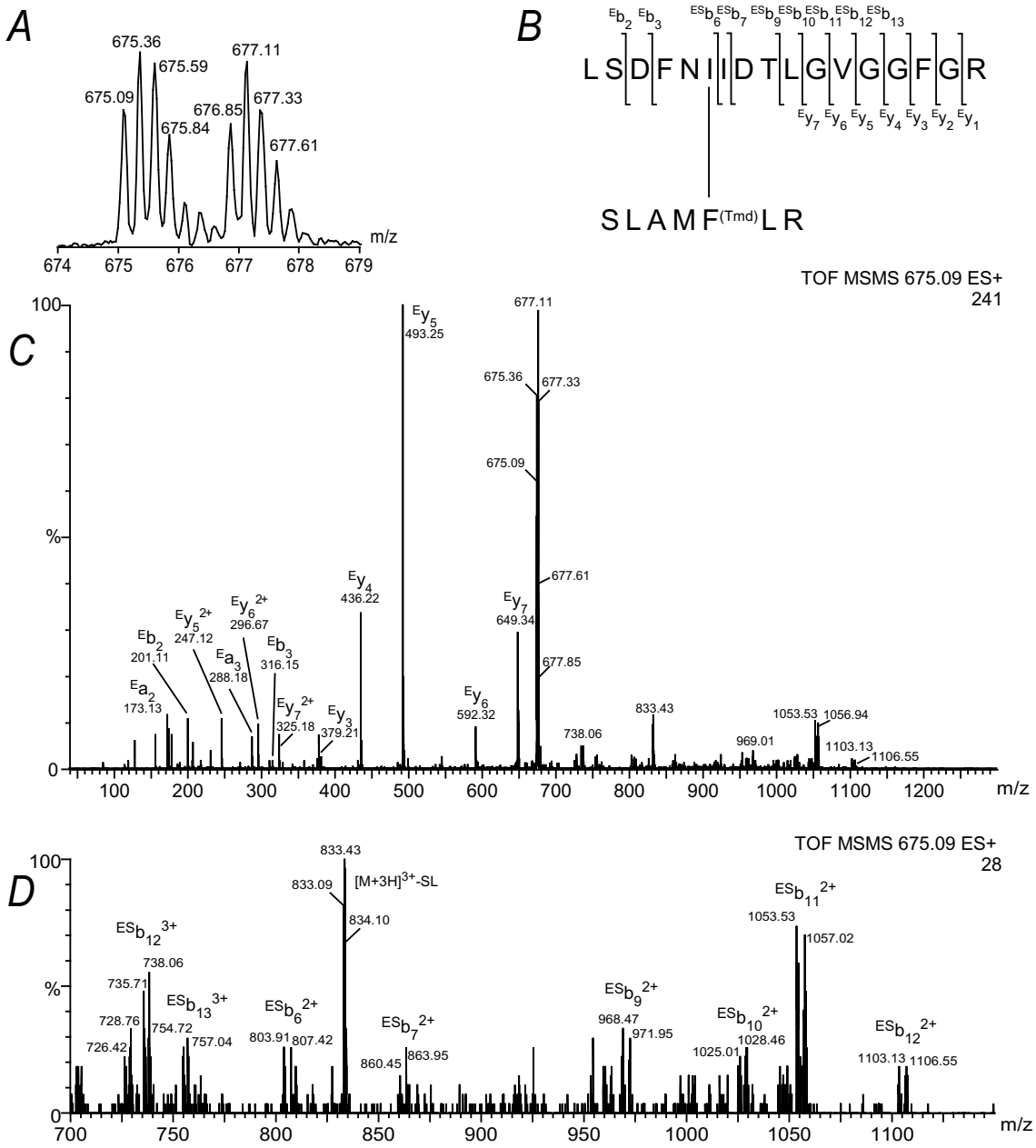

Figure 3: Tandem mass spectrometry analysis of the cross-linked tryptic peptide derived from PKG-W64$^{Phe(Tmd)}$. **(A)** The $[M+4H]^{4+}$ precursor ion that was selected by the quadrupole using a broad selection window (~5 *m/z* units) in order to allow transmission and subsequent simultaneous fragmentation of the light and heavy leucine labeled cross-linked products. **(B)** Primary sequence of the cross-linked product and identified fragment ions. The b and y" ions corresponding the primary sequence of PKG, without covalently attached substrate are annotated by $^{E}b_n$ or $^{E}y_{n,}$ whereas b or y" ions of the primary sequence of PKG that carries the covalent attached substrate are labeled $^{ES}b_n$ or $^{ES}y_n$. **(C)** MS/MS spectrum of the $[M+4H]^{4+}$ at *m/z* 675.409. **(D)** Enlarged part of the spectrum shown in **C** from *m/z* 700 to *m/z* 1150.

Phosphorylation of cross-linked PKG

To provide insight into the functionality of the cross-linked product, PKG-W64$^{Phe(Tmd)}$ was incubated with 100 µM ATP and 1 mM magnesium acetate at 30 ºC for 30 minutes. Subsequently, phosphorylated PKG-W64$^{Phe(Tmd)}$ was digested with trypsin and the proteolytic products were analyzed by LC-MS. Interpretation of the chromatogram revealed the presence of two triply charged peptides with characteristic peak pairs at *m/z* 926.38 and *m/z* 759.08. Figure 4 and 5 show the low-energy CID spectrum of both peptides, respectively. The MS/MS spectrum in Figure 4 is in fact the previously identified cross-linked product shown in Figure 3 carrying a single phosphate moiety.

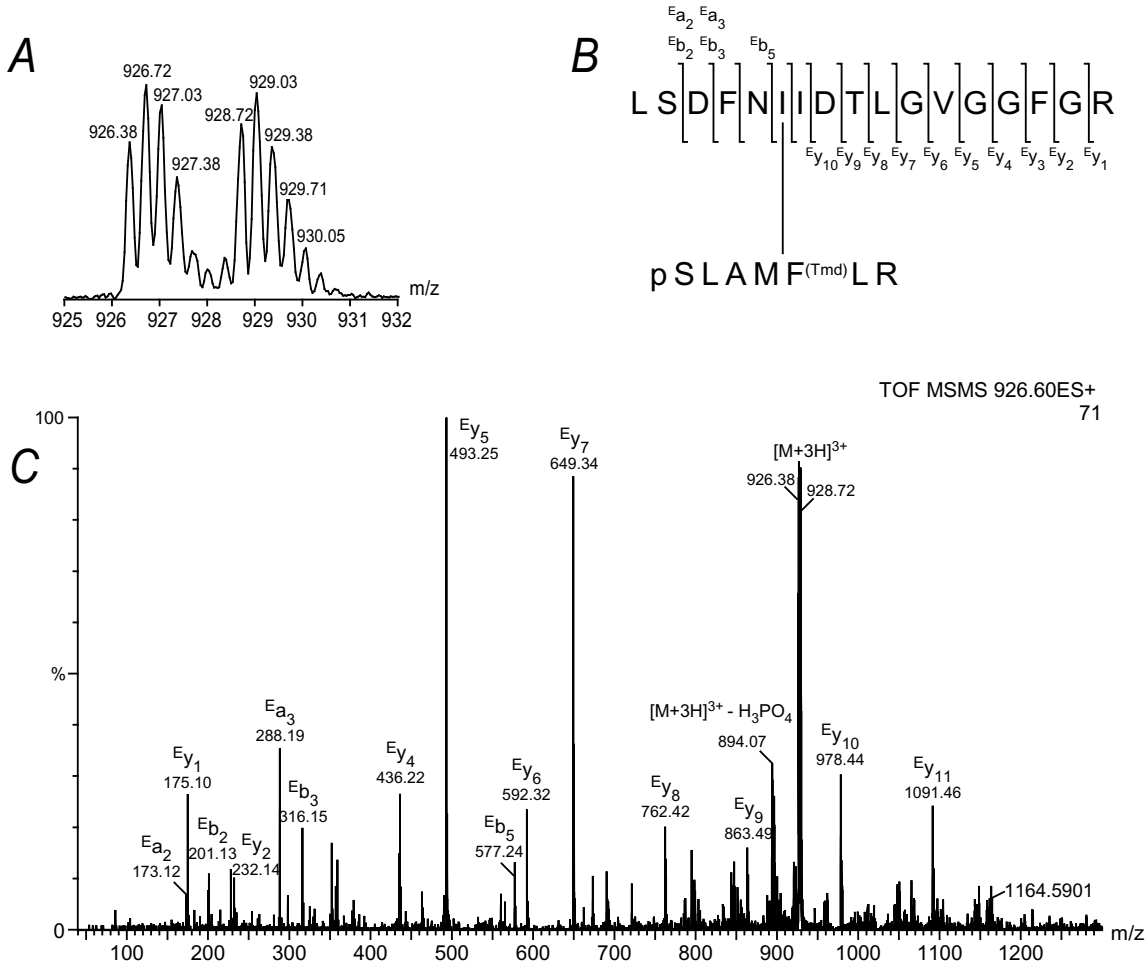

Figure 4: Tandem mass spectrometry analysis of a phosphorylated cross-linked product. **(A)** The $[M+3H]^{3+}$ precursor ion at *m/z* 926-928 that was selected by the quadrupole using a broad selection window (~5 *m/z* units) **(B)** Primary sequence of the cross-linked product and identified fragment ions. The b and y" ions corresponding the primary sequence of PKG, without covalently attached substrate are annotated by $^{E}b_n$ or $^{E}y_n$, whereas b or y" ions of the primary sequence of PKG that carries the covalent attached substrate are labeled $^{ES}b_n$ or $^{ES}y_n$. **(C)** MS/MS spectrum of the $[M+3H]^{3+}$ at *m/z* 926.38

The parent ion readily looses phosphoric acid (i.e neutral loss of 98 Da), which forms a strong indication for the presence of a phosphoserine. The b and y" fragment ions in the low energy CID spectra shown in Figure 4 and 5 clearly demonstrate that the phosphate moiety resides on the substrate part of this cross-linked peptide. This finding proofs that within the protein complex the cross-linked peptide is still properly oriented for the phosphotransfer. In contrast to the fragmentation spectrum of Figure 3, the fragmentation of the $[M+3H]^{3+}$ of this phosphorylated cross-link product displays an intense b_5 ion. This pin-points the covalent attachment of the substrate-label to Ile-361. The cross-linked product of which the MS/MS spectrum is shown in Figure 5 still carries two lysines N-terminal to the phosphorylated serine. This proteolytic fragment was not observed in the unphosphorylated digest and most likely the phosphoserine inhibited trypsin to cleave after the lysines.

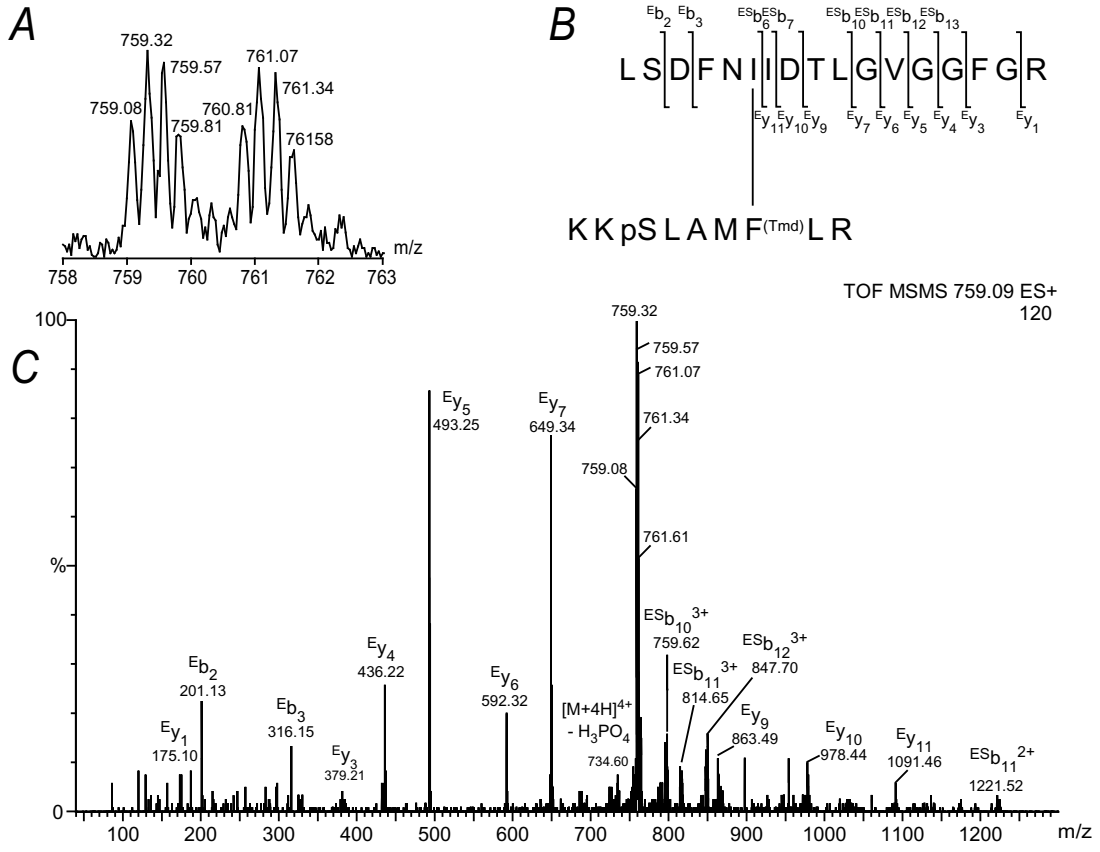

Figure 5: Tandem mass spectrometry analysis of a phosphorylated cross-linked product. **(A)** The $[M+4H]^{4+}$ precursor ion at *m/z* 759-761 that was selected by the quadrupole using a broad selection window (~5 *m/z* units) **(B)** Primary sequence of the cross-linked product and identified fragment ions. The b and y" ions corresponding the primary sequence of PKG, without covalently attached substrate are annotated by $^{E}b_n$ or $^{E}y_{n,}$ whereas b or y" ions of the primary sequence of PKG that carries the covalent attached substrate are labeled $^{ES}b_n$ or $^{ES}y_n$. **(C)** MS/MS spectrum of the $[M+4H]^{4+}$ at *m/z* 759.08.

Conclusions

When bound to protein, the synthetic peptide substrate, TQAKRKKSLAMFLR-amide, containing a photoactive amino acid analog Phe(Tmd) at the P+4 position cross-linked efficiently with nearby residues upon photoactivation. A potential problem with photoaffinity labeling experiments is the possibility of non-specific interactions on the enzyme or receptor protein surface. To address this question, PKG was photolyzed in the absence and presence of cGMP. Photolabeling of PKG with photoaffinity label occurred primarily in the presence of cGMP. In the absence of cGMP, a pseudosubstrate sequence in the N-terminal autoinhibition domain interacts with the catalytic domain, thereby blocking substrate binding [29]. The finding that substrate incorporation mainly occurs in the presence of cGMP supports the current working model of PKG of autoinhibition and cGMP activation and is indicative for a specific interaction. The photoaffinity label modified the catalytic core of PKG on residues 356-372, which bears all the conserved glycines from the glycine-rich loop, which is essential for ATP binding. This loop contains a GXGXXG motif, which is the highest conserved motif amongst protein kinases and is essential for Mg^{2+}/ATP binding. The coincident covalent modification of this peptide harboring the glycine rich loop suggests that the photoaffinity label binds PKG in the middle of the catalytic center. Location of the substrate peptide in this region rationalizes and validates our results and our approach. Tandem mass spectrometric analysis assigned Ile-361 as the residue of coupling. This isoleucine is 10 residues downstream the glycine-rich loop. In PKA this position is occupied by an arginine (Arg45), which, in the crystal structure of PKA:$PKI^{(5-24)}$ is positioned quite far from Asp-23, which mimics the P+3 position in PKI (see Figure 6). This could imply that although the catalytic cores of PKG and PKA are very similar, different regions in these two kinases play a role in peptide substrate binding and they may even utilize different peptide conformations to achieve their peptide specificity. Finally, the use of a stable-isotope label incorporated into the photoaffinity label offers a faster manner for the retrieval of cross-linked products. Without this label every peptide within the proteolytic digest has to be evaluated on composition and mass but with the mass-label peptides have only be evaluated on a typical peak-pair isotope pattern.

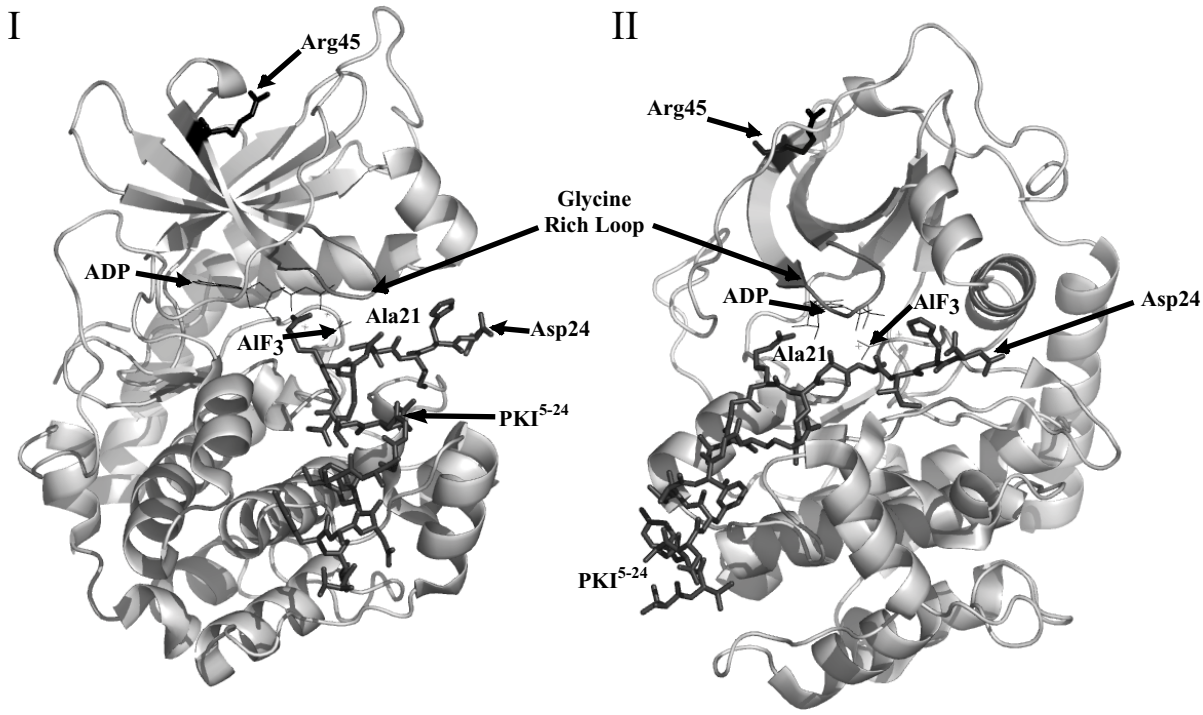

Figure 6: Ribbon diagram of the catalytic subunit of PKA cocrystallized with ADP, aluminum fluoride and the peptide inhibitor, PKI^{5-24} (TTYADFIASGRTGRRNAIHD) (shown in black). The glycine loop is thought to participate in ATP binding and/or catalysis. Highlighted are Alanine-21 of PKI, which mimics the position of phosphate accepting residue, Aspartic acid 24 at the P+3 position and Arginine-45 (shown in black) as the site of covalent attachment in PKG. The ribbon diagram on the right (II) is a 90 degrees rotation of the ribbon diagram on the left

Acknowledgements

We kindfully thank Klaus Rumpel and Frank Pullen of Pfizer Research UK for financial support.

References

1. Hunter, T. *Signaling--2000 and beyond.* Cell **2000**, *100*, 113-127.
2. Manning, G.; Whyte, D.B.; Martinez, R.; Hunter, T.; Sudarsanam, S. *The protein kinase complement of the human genome.* Science **2002**, *298*, 1912-1934.
3. Hanks, S.K.; Quinn, A.M.; Hunter, T. *The protein kinase family: conserved features and deduced phylogeny of the catalytic domains.* Science **1988**, *241*, 42-52.
4. Kennelly, P.J.; Krebs, E.G. *Consensus sequences as substrate specificity determinants for protein kinases and protein phosphatases.* J Biol Chem **1991**, *266*, 15555-15558.
5. Takio, K.; Wade, R.D.; Smith, S.B.; Krebs, E.G.; Walsh, K.A.; Titani, K. *Guanosine cyclic 3',5'-phosphate dependent protein kinase, a chimeric protein homologous with two separate protein families.* Biochemistry **1984**, *23*, 4207-4218.

6. Glass, D.B.; Krebs, E.G. *Comparison of the substrate specificity of adenosine 3':5'-monophosphate- and guanosine 3':5'-monophosphate-dependent protein kinases. Kinetic studies using synthetic peptides corresponding to phosphorylation sites in histone H2B.* J Biol Chem **1979**, *254*, 9728-9738.
7. Glass, D.B.; el-Maghrabi, M.R.; Pilkis, S.J. *Synthetic peptides corresponding to the site phosphorylated in 6-phosphofructo-2-kinase/fructose-2,6-bisphosphatase as substrates of cyclic nucleotide-dependent protein kinases.* J Biol Chem **1986**, *261*, 2987-2993.
8. Thomas, N.E.; Bramson, H.N.; Nairn, A.C.; Greengard, P.; Fry, D.C.; Mildvan, A.S.; Kaiser, E.T. *Distinguishing among protein kinases by substrate specificities.* Biochemistry **1987**, *26*, 4471-4474.
9. Colbran, J.L.; Francis, S.H.; Leach, A.B.; Thomas, M.K.; Jiang, H.; McAllister, L.M.; Corbin, J.D. *A phenylalanine in peptide substrates provides for selectivity between cGMP- and cAMP-dependent protein kinases.* J Biol Chem **1992**, *267*, 9589-9594.
10. Mitchell, R.D.; Glass, D.B.; Wong, C.W.; Angelos, K.L.; Walsh, D.A. *Heat-stable inhibitor protein derived peptide substrate analogs: phosphorylation by cAMP-dependent and cGMP-dependent protein kinases.* Biochemistry **1995**, *34*, 528-534.
11. Dostmann, W.R.; Nickl, C.; Thiel, S.; Tsigelny, I.; Frank, R.; Tegge, W.J. *Delineation of selective cyclic GMP-dependent protein kinase Ialpha substrate and inhibitor peptides based on combinatorial peptide libraries on paper.* Pharmacol Ther **1999**, *82*, 373-387.
12. Yan, X.; Corbin, J.D.; Francis, S.H.; Lawrence, D.S. *Precision targeting of protein kinases. An affinity label that inactivates the cGMP- but not the cAMP-dependent protein kinase.* J Biol Chem **1996**, *271*, 1845-1848.
13. Wood, J.S.; Yan, X.; Mendelow, M.; Corbin, J.D.; Francis, S.H.; Lawrence, D.S. *Precision substrate targeting of protein kinases. The cGMP- and cAMP-dependent protein kinases.* J Biol Chem **1996**, *271*, 174-179.
14. Murray, K.J.; El-Maghrabi, M.R.; Kountz, P.D.; Lukas, T.J.; Soderling, T.R.; Pilkis, S.J. *Amino acid sequence of the phosphorylation site of rat liver 6-phosphofructo-2-kinase/fructose-2,6-bisphosphatase.* J Biol Chem **1984**, *259*, 7673-7681.
15. Knighton, D.R.; Zheng, J.H.; Ten Eyck, L.F.; Xuong, N.H.; Taylor, S.S.; Sowadski, J.M. *Structure of a peptide inhibitor bound to the catalytic subunit of cyclic adenosine monophosphate-dependent protein kinase.* Science **1991**, *253*, 414-420.
16. Glass, D.B.; Cheng, H.C.; Kemp, B.E.; Walsh, D.A. *Differential and common recognition of the catalytic sites of the cGMP-dependent and cAMP-dependent protein kinases by inhibitory peptides derived from the heat-stable inhibitor protein.* J Biol Chem **1986**, *261*, 12166-12171.
17. Tegge, W.; Frank, R.; Hofmann, F.; Dostmann, W.R. *Determination of cyclic nucleotide-dependent protein kinase substrate specificity by the use of peptide libraries on cellulose paper.* Biochemistry **1995**, *34*, 10569-10577.
18. Brunner, J. *Use of photocrosslinkers in cell biology.* Trends Cell Biol **1996**, *6*, 154-157.
19. Jahn, O.; Eckart, K.; Tezval, H.; Spiess, J. *Characterization of peptide-protein interactions using photoaffinity labeling and LC/MS.* Anal Bioanal Chem **2004**, *378*, 1031-1036.
20. Rink, H. *Solid-phase synthesis of protected peptide fragments using a trialkoxy-diphenyl-methylester resin.* Tetrahedron Letters **1987**, *28*, 3787-3790.
21. Knorr, R.; Trzeciak, A.; Bannwarth, W.; Gillessen, D. *New coupling reagents in peptide chemistry.* Tetrahedron Letters **1989**, *30*, 1927-1930.
22. Carpino, L.A.; Elfaham, A.; Minor, C.A.; Albericio, F. *Advantageous Applications of Azabenzotriazole (Triazolopyridine)-Based Coupling Reagents to Solid-Phase Peptide-Synthesis.* Journal of the Chemical Society-Chemical Communications **1994**, 201-203.

23. Ten Kortenaar, P.B.W.; Van Dijk, B.G.; Peeters, J.M.; Raaben, B.J.; Adams, P.J.H.M.; Tesser, G.I. *Rapid and efficient method for the preparation of Fmoc-amino acids starting from 9-fluorenylmethanol.* Int. J. Peptide Protein Res. **1986**, *27*, 398-400.
24. Fields, C.G.; Lloyd, D.H.; Macdonald, R.L.; Otteson, K.M.; Noble, R.L. *HBTU activation for automated Fmoc solid-phase peptide synthesis.* Pept Res **1991**, *4*, 95-101.
25. Weber, P.J.; Beck-Sickinger, A.G. *Comparison of the photochemical behavior of four different photoactivatable probes.* J Pept Res **1997**, *49*, 375-383.
26. Ploug, M. *Identification of specific sites involved in ligand binding by photoaffinity labeling of the receptor for the urokinase-type plasminogen activator. Residues located at equivalent positions in uPAR domains I and III participate in the assembly of a composite ligand-binding site.* Biochemistry **1998**, *37*, 16494-16505.
27. Tahallah, N.; Pinkse, M.; Maier, C.S.; Heck, A.J. *The effect of the source pressure on the abundance of ions of noncovalent protein assemblies in an electrospray ionization orthogonal time-of-flight instrument.* Rapid Commun Mass Spectrom **2001**, *15*, 596-601.
28. Meiring, H.D.; van der Heeft, E.; ten Hove, G.J.; de Jong, A.P.J.M. *Nanoscale LC-MS$^{(n)}$; technical design and applications to peptide and protein analysis.* J. Sep. Sci. **2002**, *25*, 557-568.
29. Francis, S.H.; Poteet-Smith, C.; Busch, J.L.; Richie-Jannetta, R.; Corbin, J.D. *Mechanisms of autoinhibition in cyclic nucleotide-dependent protein kinases.* Front Biosci **2002**, *7*, d580-592.

Investigation of the inhibition behavior of a potent peptide inhibitor of PKG using electrospray ionization time of flight mass spectrometry.

5

Martijn W. H. Pinkse and Albert J. R. Heck

Department of Biomolecular Mass Spectrometry, Bijvoet Center for Biomolecular Research and Utrecht Institute for Pharmaceutical Sciences, Utrecht University, Sorbonnelaan 16, 3584 CA Utrecht, The Netherlands.

Abstract

The inhibitor peptide YGRKKRRQRRRPPLRKKKKKH (DT2) is the most potent and selective PKG inhibitor known today. This competitive inhibitor is a construct of a substrate competitive sequence, LRKKKKKH (W45) derived from a library screen that selected for tight PKG binding sequences, and a membrane translocation signal, YGRKKRRQRRRPP (DT6), derived from the HIV-tat protein. DT2 strongly inhibits PKG catalyzed phosphorylation (K_i = 12.5 nM) and it exhibits a high selectivity towards PKG over PKA (~1000-fold). However, the molecular nature of DT2 inhibition is not well understood. Using nanoflow electrospray ionization time-of-flight mass spectrometry (ESI-TOF-MS) we aim to gain further insight into the mechanism of DT2 inhibition. Nanoflow-ESI-TOF-MS spectra of PKG in the presence of cGMP and DT2 displayed abundant ion signals of a non-covalent $[PKG]_2$-$[cGMP]_4$-DT2 complex. Surprisingly, the spectra clearly demonstrate that only one inhibitor molecule binds to dimeric PKG. Substantial binding of DT2 to dimeric PKG, in absence of cGMP, could not be detected. Additional ESI-TOF-MS experiments revealed that DT2 binding induced a partial dissociation of cGMP from PKG, suggesting DT2 binding alters affinity of one or both of the cGMP-binding pockets. To further explore the peculiar strong binding of DT2, ESI-TOF-MS experiments were carried out with the individual DT6 and W45 peptides. DT6 binding was also enhanced by cGMP, but now up to two DT6 molecules per dimer were detected, although binding of one peptide represented the most abundant ion signals. In a similar fashion W45 showed also a cGMP dependent binding mode, although the most abundant species was in this case the $[PKG]_2$-$[cGMP]_4$ complex, suggesting W45 binds less strong than DT6 or DT2. The spectra of PKG acquired in the presence of both DT6 and W45 did not resemble the spectra acquired with PKG and DT2. Together these findings imply that: *(i)* DT2 binding to PKG is strongly enhanced by cGMP activation, *(ii)* the autoinhibitory domain of PKG could successfully compete with DT2 in absence of cGMP, *(iii)* in cGMP-activated PKG the catalytic centers of both subunits may be in close proximity to each other.

Introduction

Protein kinases are an important class of enzymes controlling virtually all cellular signaling pathways [1, 2]. Changes in the level, subcellular location and activity of protein kinases have consequences on normal cell function and many human diseases such as diabetes and especially cancer have been coupled to abnormal protein phosphorylation. Consequently, selective inhibitors of protein kinases have attracted significant interest as potential new drugs for many diseases [3, 4]. Besides, selective kinase inhibitors have the potential to elucidate roles of individual kinases in distinct cellular signaling pathways. Detailed studies of the action of selective protein kinase inhibitors could also be a source of insight into the mechanism of enzymatic functioning of that particular kinase and aid in our understanding of kinase specificity. Type I cyclic cGMP-dependent protein kinases (PKG I) mediates essential physiological functions in cGMP-signaling pathways in vascular smooth muscle cells (for reviews see [5-8]). The PKG-isoform Iα is a multidomain, homodimeric enzyme that contains an N-terminal dimerization region followed by an autoinhibitory site, two cooperative cGMP binding pockets and a catalytic domain containing an ATP- and a peptide substrate binding site [6]. In the absence of cGMP, PKG maintains a catalytically basal or inactive state of phosphorylation of exogenous substrates (heterophosphorylation). A pseudosubstrate site within the autoinhibitory domain that binds to the active site, thereby blocking the entrance for substrates, is responsible for this mode of inhibition. When intracellular cyclic nucleotide levels increase, heterophosphorylation is strongly enhanced, but the mechanism by which cyclic nucleotide binding stimulates this activity is unknown. It has been suggest that activation of PKG either by cyclic nucleotide binding of the two allosteric cyclic nucleotide-binding sites or by autophosphorylation is associated with a conformational change that removes the influence of the autoinhibitory domain on the catalytic site, thus reducing the efficiency of pseudosubstrate site competition for substrate binding [9, 10]. Recently, specific inhibitor-peptides were developed that allowed the study of PKG-controlled event in cells [11, 12]. A combinatorial library screen that selected for tight PKG binding peptides yielded the inhibitor peptide W45 (LRKKKKKH). This peptide inhibited PKG in *in-vitro* assays with a K_i of 820 nM. For internalization studies W45 was fused with a membrane translocation peptide (HIV-1 tat protein residues 47-59) yielding the inhibitor peptide DT2 (YGRKKRRQRRRPP-LRKKKKKH). Surprisingly this peptide displayed a 65 fold stronger potency to inhibit PKG *in-vitro* with an apparent K_i of 12.5 nM (see table 1) [12].

Table 1: Inhibition constants (K_i) of synthetic peptides for PKA and PKG

		PKG	PKA	Specificity Index	Ref.
Peptide	**Sequence**	K_i (µM)	K_i (µM)	PKA/PKG	
$PKI^{(5-24)}$	TTYADFIASGRTGRRNAIHD	150	0.003	0.0002	[11]
WW21	TQAKRKKALAMA	7.5	750	100	[12]
W45	LRKKKKKH	0.82 ± 0.33	559	680	[12]
DT2	YGRKKRRQRRRPPLRKKKKKH	0.0125 ± 0.003	16.5 ± 3.8	1320	[12]
DT6	YGRKKRRQRRRPP	1.1 ± 0.22	26 ± 4	23.6	[12]

DT2 is the most potent and selective PKG inhibitor known today. Previously, DT2 was shown to internalize readily into intact cerebral artery smooth muscle cells and to antagonize NO-mediated vasodilations [13]. Additionally DT2 does not only reduce cGMP-activated PKG, but also reduces basal PKG activity both *in-vitro* and *in-vivo* [14]. With this latter property, DT2 distinguishes itself from other PKG inhibitors, such as ATP or cGMP analogs. However, the molecular mechanism by which DT2 inhibits both basal and cGMP-activated PKG is not well understood. We have used nanoflow electrospray ionization time of flight mass spectrometry as a tool to study the interaction between DT2 and PKG in more detail in order to gain further insight into the inhibitory action of DT2. Electrospray ionization mass spectrometry (ESI-MS) has proven to be a useful tool to analyze the non-covalent interactions of proteins with metal ions, ligands, peptides, oligonucleotides, or other proteins [15, 16]. Important information that can be obtained by ESI-MS is the stoichiometry of the components that form the complex since ESI-MS provides an accurate molecular mass of the complex being studied. Besides ESI-MS can be a useful tool in studying conformational changes [17-19], measurement of relative dissociation constants [20, 21] and sequential binding order and cooperativity [22]. Electrospray ionization mass spectrometry confirms that PKG is primarily a homodimer and is able to bind 4 cGMP molecules. Binding of DT2 was strongly enhanced in the presence of cGMP. Surprisingly is the observation that only one DT2 molecule binds to dimeric PKG.

Experimental

Material and reagents. Recombinant PKG Iα was expressed and purified from SF9-insect cells according to Dostmann *et al.* [12]. Dr. Wolfgang Dostmann of the University of Vermont kindly provided DT2, DT6 and W45. Guanosine 3',5'-cyclic monophosphate was purchased from Sigma (St. Louis, MO, USA).

Sample preparation. Prior to mass spectrometric measurements PKG was buffer exchanged to 200 mM ammonium acetate, pH 6.7 using Ultrafree-0.5 Centrifugal Filter Units (5000 NMWL) (Millipore, Bedford, MA, USA). Stock concentrations of cGMP and peptide inhibitors were prepared in 200 mM ammonium acetate, pH 6.7, and added to a recombinant PKG solution (~5 μM). For dialysis 75 μL PKG stock solution was transferred in a 3.5K MWCO Slide-A-Lyzer mini dialysis unit (Pierce Biotechnology Inc, Rockford, IL, USA) and dialyzed against 200 mL, 200 mM ammonium acetate buffer, pH 6.7.

Electrospray Ionization Mass Spectrometry. Electrospray ionization mass spectrometry analyses of the intact protein were carried out on a Micromass LC-T time-of-flight instrument (Micromass UK Ltd., Wythenshawe, Manchester, United Kingdom) equipped with a 'Z-Spray' nanoflow electrospray source using in-house pulled and gold coated borosilicate glass needles. Typical ESI-TOF-MS operating parameters were as follows: capillary voltage, 1.0-1.5 kV; sample cone voltage, 100-200 V; extraction cone voltage, 50-100 V; source block temperature, 70°C; source pressure 9.0 mbar (standard 2.0 mbar), TOF analyzer pressure 1.1 x 10^{-6} mbar (standard 5.0 x 10^{-7} mbar). Spectra were recorded in either the positive or the negative ion mode and the standard *m/z* range of 200-10000 Th was monitored. Mass spectra were externally calibrated on either the singly charged $Cs_{n+1}I_n$ clusters for positive ion spectra or the singly charged $I_{n+1}Cs_n$ clusters for negative ion spectra, both obtained after electrospraying an aqueous cesium iodide solution (1 mg/ml). Deconvolution of mass spectra of protein and protein-ligand complexes was done using a maximum entropy (MaxEnt1, [23, 24]) based approach incorporated as part of the MassLynx software (MassLynx v3.5) supplied with the mass spectrometer. The average masses of protein species were calculated from at least four charge states. The masses measured are centroided values. All mass spectra shown are a combination of 5 – 20 scans (10-20 secs $scan^{-1}$) and were minimally smoothed (Typical settings: Savitsky Golay; 5-10 channel smooth window; number of smooths: 2)

Results

Figure 1A displays a nanoflow positive electrospray ionization mass spectrum of a solution of ~2 µM (estimated dimer concentration) PKG. Abundant ion signals between *m/z* 6000 and *m/z* 7500 originate from the dimeric protein, with an calculated mass of 152,875 DA.

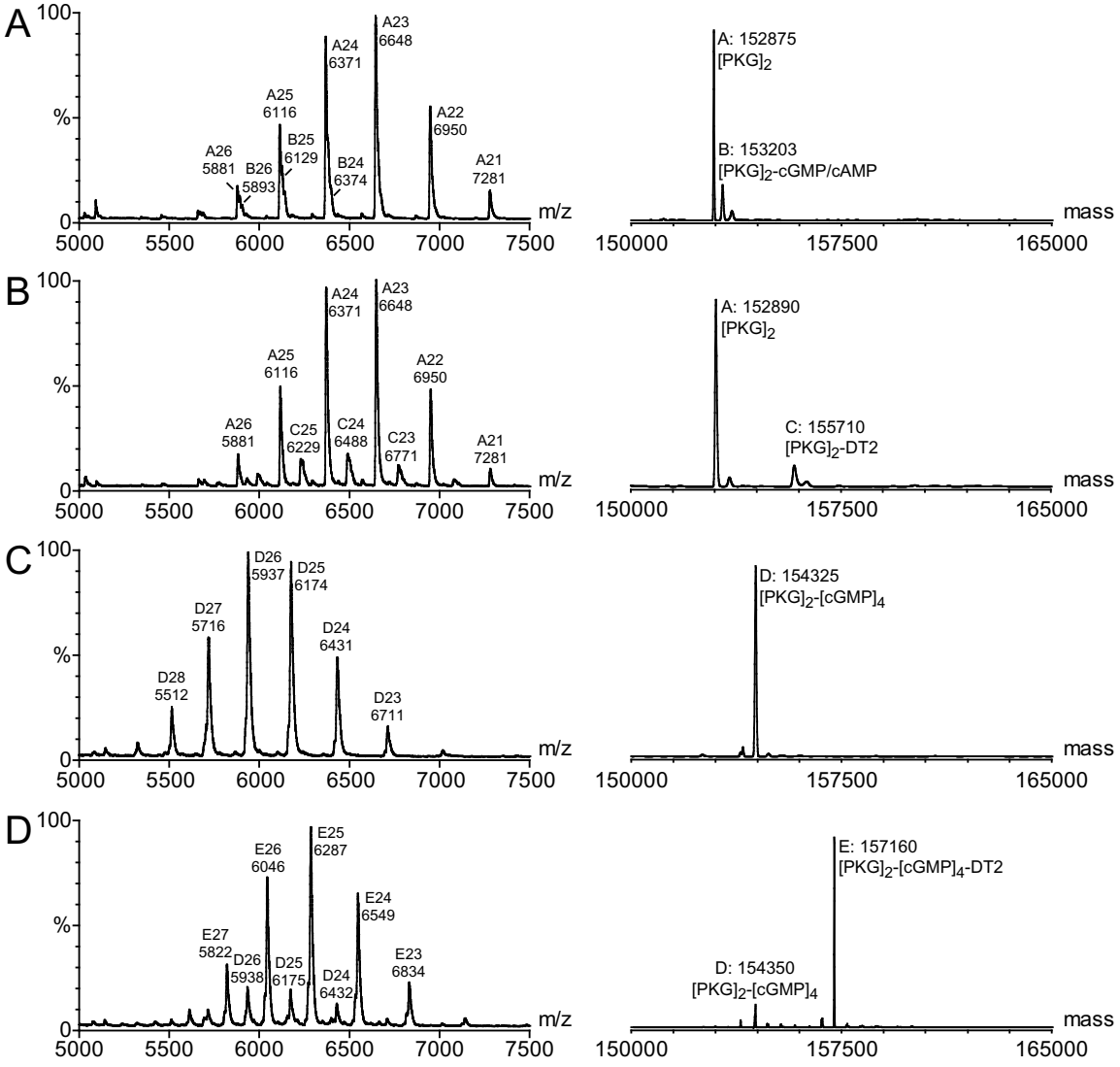

Figure 1: Nanoflow positive electrospray ionization mass spectra of **(A)** ~1-2 µM PKG, **(B)** ~1-2 µM PKG in the presence of 5 µM DT2, **(C)** ~1-2 µM PKG in the presence of 20 µM cGMP **(D)** ~1-2 µM PKG and in the presence of 5 µM DT2 and 20 µM cGMP. On the left are shown the raw *m/z* spectra and each multiply charge ion is labeled with a single letter, followed by the charge state and the centroided *m/z* value. On the right are shown the corresponding deconvoluted mass spectra. Each peak is labeled with a single letter code as in the raw spectra, followed by the measured mass and determined complex composition.

The theoretical mass of dimeric PKG is 152,819 Da and the mass difference of 56 Da between theoretical and measured mass is probably due to the presence of alkali metal ions in the spray solution or due to incomplete desolvation of the solvent molecules or buffer components. After deconvolution the spectra is Figure 1A display a small amount (~10%) of PKG binding presumably cAMP (M_r = 329) or cGMP (M_r = 345), as illustrated by the detection of a complex of 153,203 Da. Figure 1B shows the mass spectrum of PKG in the presence of 5 μM DT2. Highly abundant ion signals from the dimer remain the most abundant ion signals and non-covalent binding of DT2 (M_r = 2800) to PKG is represented by low abundant ion signals of a complex with a mass of 155,710 Da. Figure 1C shows the mass spectrum of PKG in the presence of 20 μM cGMP. From this charge state envelope a mass of 154,325 Da is obtained, which is 1450 Da higher is mass. This implies that 4 cGMP molecules (overall mass 1380 Da) are bound to the dimer. Figure 1D shows the mass spectrum of PKG in the presence of 20 μM cGMP and 5 μM DT2. The deconvoluted mass spectrum demonstrates that under these conditions 4 molecules of cGMP and 1 molecule of DT2 are bound to the dimer and this complex (with a mass of 157,160 Da) is the highest in abundance. Other complexes visible in the deconvoluted mass spectrum are PKG_2-$cGMP_4$ and PKG_2-$cGMP_3$-DT2, however these two only represent ~20 % of the total ion signal. Ion signals corresponding to the mass of a complex between 2 DT2 molecules and PKG$[cGMP]_4$ are not detected.

Effect of cGMP on DT2 binding.

Figure 1 clearly revealed that cGMP-activation is a prerequisite for strong DT2 binding. To elucidate whether either the high- or the low affinity cGMP binding sites are responsible for this phenomenon, DT2 binding was studied at low cGMP levels. Figure 2A shows again the mass spectrum of the PKG protein sample as in Figure 1A. A common observation in the mass spectra of PKG acquired in these studies is binding of residual cyclic nucleotides (cAMP or cGMP). The resolving power in the high *m/z* region of the mass spectrometer used in these studies is good enough to distinguish between PKG with no or one cyclic nucleotide bond. For example, in Figure 2A the 26+ and 25+ ion signals at *m/z* 5881 and *m/z* 6116, respectively, display some additional fine structuring. Unfortunately the mass accuracy is, mainly due to peak-overlapping, too poor to determine whether it is cAMP (molecular mass 329 Da) or cGMP (molecular mass 345 Da) that is bound. Figure 2B shows the mass spectrum of the same PKG sample used to acquire the spectrum in Figure 2A, electrosprayed

in the presence of 5 µM DT2. As previously shown in Figure 1, under these conditions only a small amount of PKG binds DT2. More importantly, the fine structuring that was observed in Figure 2A is no longer present. To further explore the cGMP-binding requirement for DT2 binding, we dialyzed a PKG sample against 50 nM cGMP in order to selectively occupy the high affinity, but not the low affinity cGMP-binding sites. Figure 2C shows the electrospray ionization mass spectrum of the PKG protein sample that was dialyzed against 50 nM cGMP.

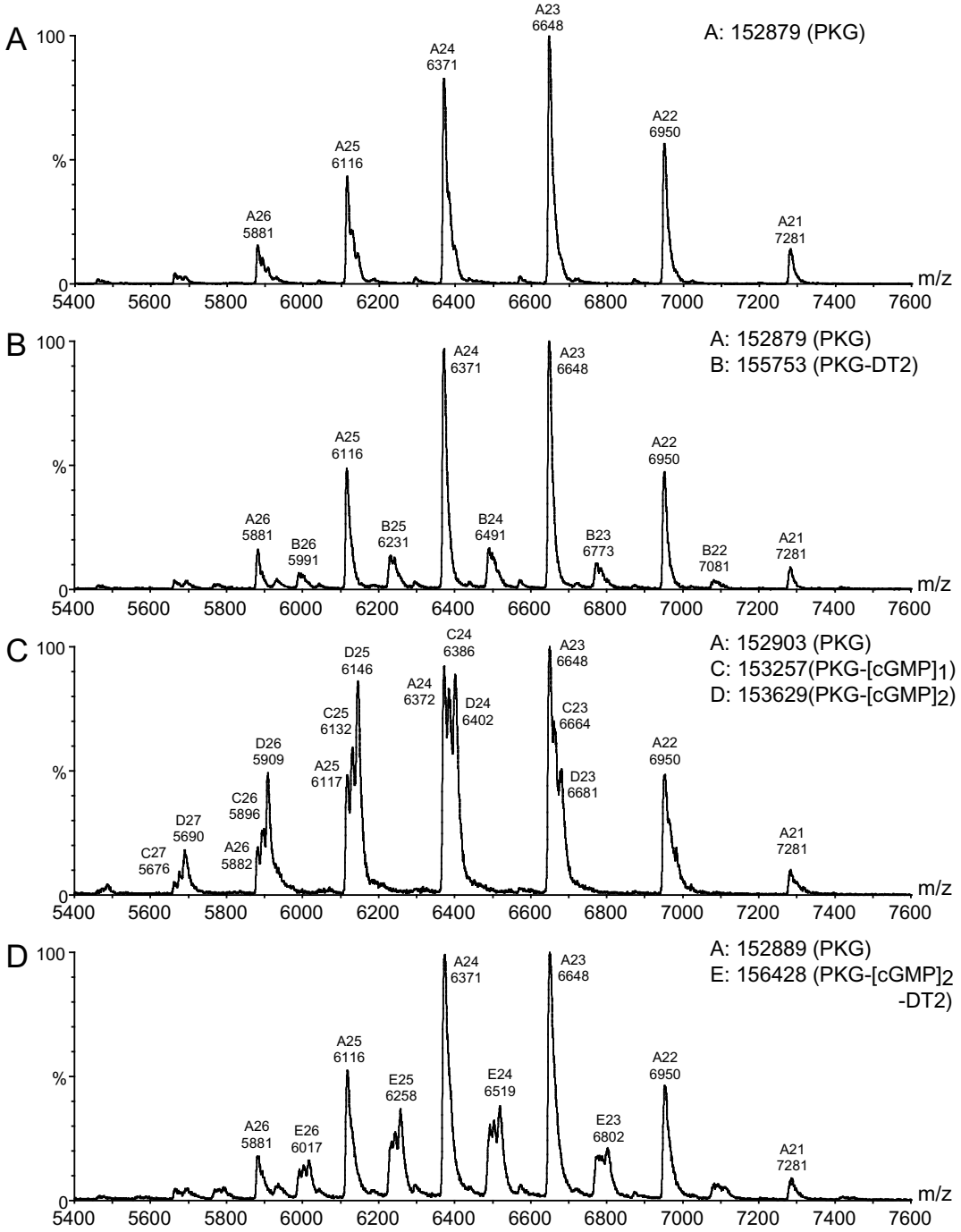

Figure 2: Electrospray ionization mass spectra of **(A)** ~1-2 µM PKG, **(B)** with 5µM DT2, **(C)** ~1-2 µM PKG, dialyzed against 50 nM cGMP and **(D)** with 5 µM DT2.

The mass spectrum shows that after these conditions, PKG has bound 1 and 2 cGMP molecules and also some free PKG is also present, hence only the high affinity sites are occupied. Addition of 5 µM DT2 to this latter protein sample results in intense ion signals for the PKG-$[cGMP]_2$-DT2 complex (Figure 2D), but ion signals for PKG-$[cGMP]_1$-DT2 and even PKG-DT2 complexes are also detected. Whether these latter complexes are formed by binding of DT2 to PKG-$[cGMP]_n$, followed by a dissociation of cGMP or whether they are formed by direct binding of DT2 to cyclic nucleotide free PKG remains unclear. Overall these measurements indicate that occupation of the high affinity sites of PKG is sufficient for enhanced DT2 binding.

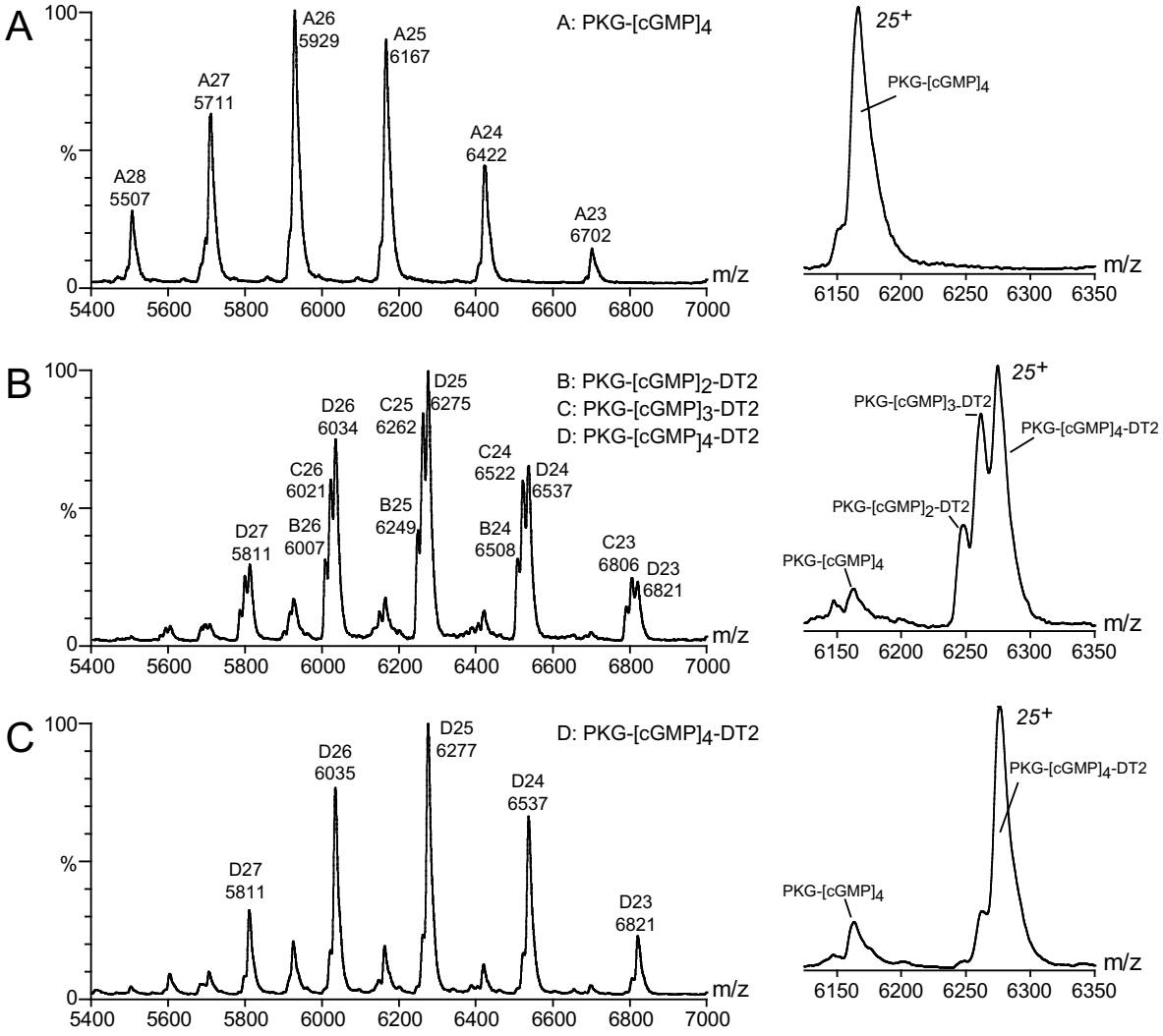

Figure 3: Effect of DT2 on cGMP saturation. **(A)** PKG in the presence of 10 µM cGMP, **(B)** PKG in the presence of 5µM DT2 and 10 µM cGMP. **(C)** PKG in the presence of 5 µM DT2 and 20 µM cGMP. Spectra on the left display the charge state envelope of dimeric PKG, enlarged parts of these spectra are displayed on the right, highlighting the fine-structure on the 25+ charge states of PKG-cGMP and PKG-cGMP-DT2 complexes.

Effect of DT2 on cGMP binding.

During the course of experiments it was found that DT2 is apparently able to influence the affinities of either the high or the low affinity cGMP binding pockets of PKG. This is illustrated in Figure 3A, which shows that by addition 10 µM cGMP to a PKG solution of approximately ~1-2 µM, all cGMP binding sites on PKG become occupied. Figure 3B illustrates that by adding 10 µM cGMP and 5 µM DT2 simultaneously to the same PKG solution, the resulting electrospray mass spectrum displays PKG-DT2 complexes with 2, 3 and 4 cGMP molecules (i.e no saturation of cGMP binding pockets). Finally, Figure 3C shows that addition of more cGMP (20 µM) complete occupation of all sites is restored. Although this difference is very subtle, binding of DT2 apparently reduces affinity of either one or two cGMP-binding pockets.

PKG-cGMP-DT2 stoichiometry

Figure 1 showed already that almost exclusively 1 DT-2 molecule binds to PKG. In order to determine the specific nature of this 2:1 stoichiometry, spectra were recorded in the negative ion mode and in the positive ion mode at difference DT2 concentrations.

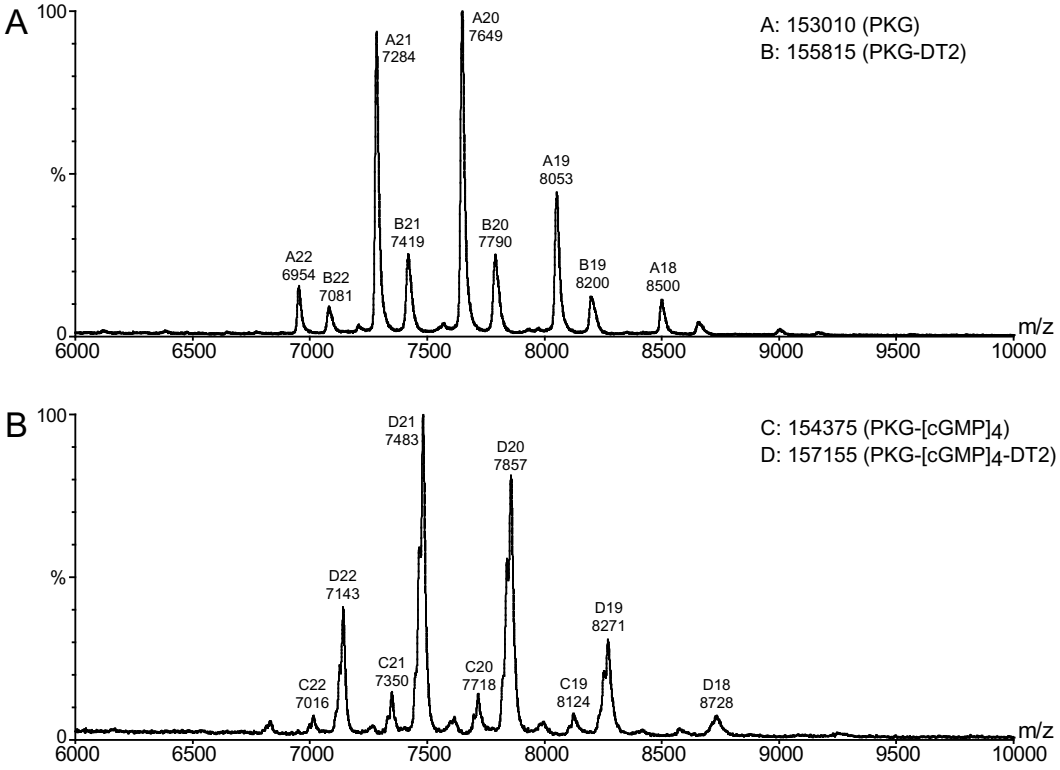

Figure 4: ESI-TOF-MS mass spectra acquired in the negative ion mode of **(A)** PKG in the presence of 5 µM DT2 and **(B)** PKG in the presence of 5 µM DT2 and 10 µM cGMP. Calculated masses and compositions of the complexes are listed in the upper right corner.

Electrospray ionization mass spectra, acquired in the negative ion mode, are shown in Figure 4. In analogy with the spectra acquired in positive ion mode DT2 binding is solely observed in the presence of cGMP with the same stoichiometry of 1 DT2 molecule per dimer. In addition, Figure 5 shows the electrospray ionization mass spectra of PKG in the presence of 20 µM cGMP and from 5A to 5D in the presence of 5 µM, 20 µM, 50 µM and 100 µM DT2, respectively. Although the protein signals are significantly suppressed by the large amount of DT2, they still display the binding of solely 1 DT2 peptide, even at fifty and hundred fold excesses of DT2

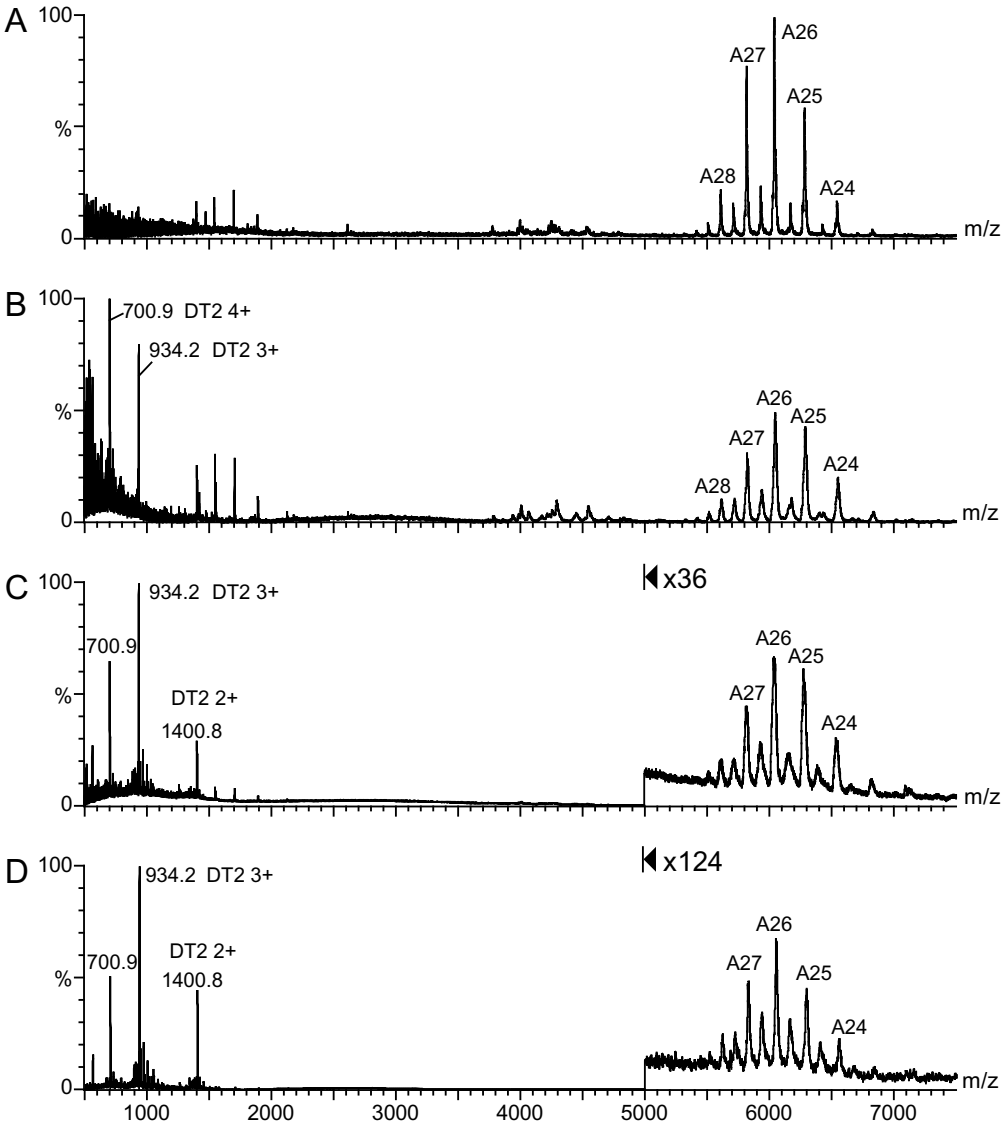

Figure 5: PKG in the presence of saturating cGMP conditions and different DT2 concentrations. **(A)** ~1-2 µM PKG in the presence of 20 µM cGMP and 5µM DT2. **(B)** ~1-2 µM PKG in the presence 20 µM cGMP and 20 µM DT2. **(C)** ~1-2 µM PKG in the presence 20 µM cGMP and 50 µM DT2. **(D)** ~1-2 µM PKG in the presence 20 µM cGMP and 100 µM DT2.

Individual role of DT6 and W45

DT2 is the fusion product of the high affinity binding W45 (LRKKKKKH) and the membrane translocating sequence from HIV-1 Tat protein (amino acid 47-59; YGRKKRRQRRRPP, DT6). In order to gain further insight into the individual contributions of each of these two peptides in the strong interaction between DT2 and PKG, as observed in our ESI-TOF-MS analysis, another set of ESI-TOF-MS measurements were performed (Figure 6). In this particular experiment the PKG solution used was not completely free of cyclic nucleotides (Figure 6A), however this did not significantly influenced the point we want to make here. As previously shown, addition of 20 μM cGMP to the spray solution results in complete saturation of all cGMP-binding pockets of PKG (Figure 6B). Figure 6C and 6D show the mass spectra of PKG in the presence of 20 μM W45 and in the absence and presence of 20 μM cGMP, respectively. In the absence of cGMP, no significant binding of W45 to PKG is observed (Figure 6C). Figure 6D clearly shows partial complexation between W45 and PKG-$[cGMP]_4$, suggesting binding of W45 is also enhanced by the addition of cGMP. Figure 6E and 6F show the mass spectra of PKG in the presence of 20 μM DT6 in the absence and presence of 20 μM cGMP, respectively. Figure 6E suggests that DT6, in analogy with DT2, binds preferentially to cyclic nucleotide activated PKG. This is further illustrated by the mass spectrum of Figure 6E, where 20 μM cGMP was added to the spray solution. Clearly this mass spectrum shows that cGMP enhances DT6 complexation and it shows that two DT6 molecules can bind PKG. Summarizing, DT6 displays a similar binding behavior towards PKG in the electrospray ionization mass spectra as previously observed for DT2. In contrast, the high affinity binding peptide W45 does not display a clear homogeneous complex with PKG. To further probe cooperative or competitive behavior of DT6 and W45, both peptides were added simultaneously to PKG. Figure 7A shows the electrospray ionization mass spectrum of PKG in the presence of 20 μM cGMP, 20 μM DT6 and 20 μM W45. Figure 7B shows the corresponding deconvoluted or singly charged mass spectrum. After deconvolution, at least 6 different heterogeneous protein complexes are detected. Amongst the most abundant are PKG-$[cGMP]_4$ and PKG-$[cGMP]_4$-DT6. Additionally PKG-$[cGMP]_4$-W45, PKG-$[cGMP]_4$-$[W45]_2$, PKG-$[cGMP]_4$-W45-DT6 and PKG-$[cGMP]_4$-$[DT6]_2$ are visible. Interestingly no protein with 3 or more peptides bound is detected. This could imply that W45 and DT6 are both targeted to similar regions on PKG.

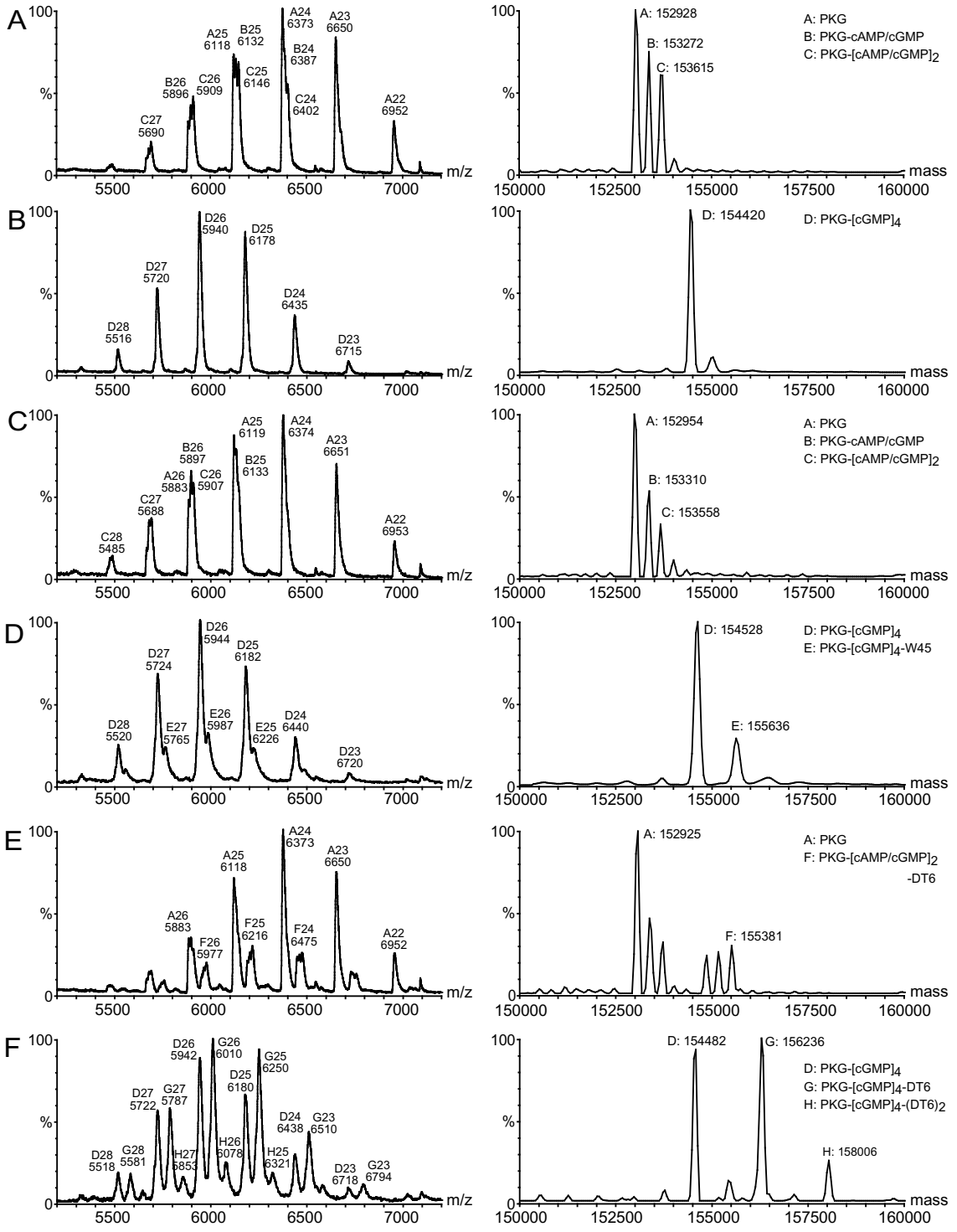

Figure 6: Nanoflow electrospray ionization mass spectra of **(A)** PKG, **(B)** PKG in the presence of 20 µM cGMP **(C)** PKG in the presence of 20 µM W45 **(D)** PKG in the presence of 20 µM cGMP and 20 µM W45, **(E)** PKG in the presence of 20 µM DT6, **(F)** PKG in the presence of 20 µM cGMP and 20 µM DT6. The estimated dimer concentration for all measurements is ~1-2 µM. On the left are shown the raw mass spectra, on the right are shown the deconvoluted (MaxEnt1) spectra. For the most abundant complexes, masses and compositions are given.

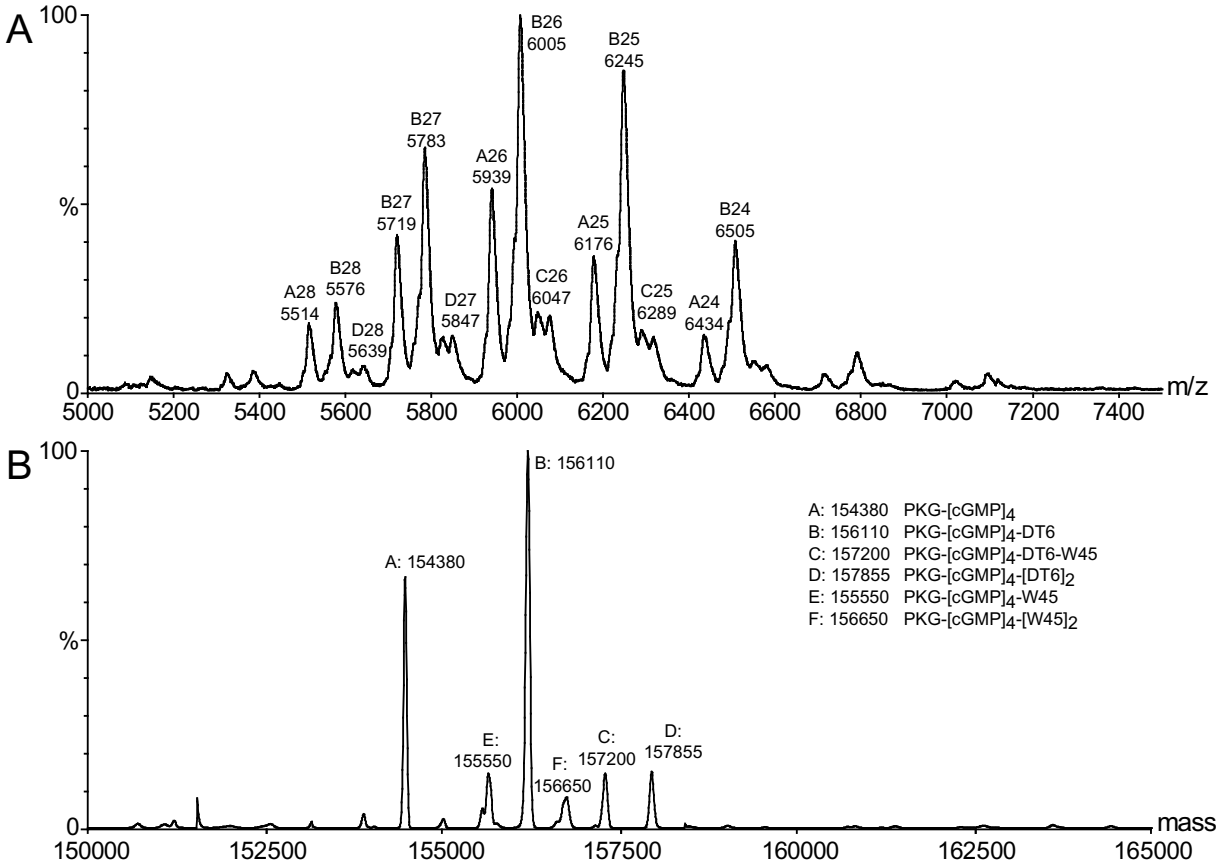

Figure 7: PKG in the presence of cGMP, W45 and DT6. **(A)** Raw spectrum of ~1-2 µM PKG, 20 µM cGMP, 20 µM W45 and 20 µM DT6. **(B)** Corresponding deconvoluted mass spectrum. For the most abundant complexes, masses and compositions are given

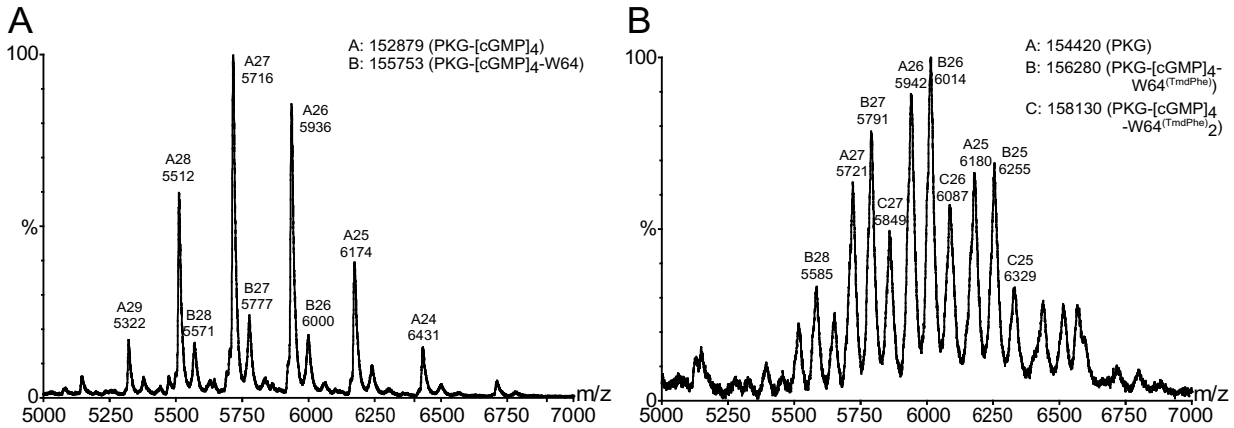

Figure 8: Electrospray ionization mass spectra of PKG and a high affinity substrate W64, (TQAKRKKSLAMFLR). **(A)** ESI mass spectra of PKG in the presence of 20 µM cGMP and 50 µM W64, **(B)** ESI mass spectrum of covalently attached $W64^{(TmdPhe)}$ (by photoaffinity labeling, see Chapter 4). Photolabeling was performed in the presence of 200 µM $W64^{(TmdPhe)}$.

Discussion

This chapter describes the preliminary results from nanoflow ESI-TOF-MS experiments conducted to gain further insight into mechanism of action of DT2, a highly potent and selective PKG peptide inhibitor. The results described in this chapter demonstrate the ability of ESI-TOF-MS to detect a non-covalent interaction between PKG and the highly potent PKG inhibitor DT2. ESI-TOF-MS measurements revealed that cGMP-binding is a prerequisite for this observation and furthermore it was found that preferentially one DT2 molecule binds per dimer. This interesting binding order and somewhat unusual stoichiometry provides further insight into the exceptionally high inhibition potency of DT2. Previously, kinetic analysis showed that W45 has a competitive inhibition pattern, indicating W45 is targeted against the substrate-binding site [12]. Fusion of W45 to a membrane translocation sequence (DT6), which is also a highly positively charged peptide, resulted in a 65-fold increase in inhibition potency. DT2 displayed a linear mixed competitive / non-competitive inhibition behavior [12]. From this it was suggested that the membrane translocation sequence DT6 binds and inhibits PKG at a different site from the catalytic cleft and fusion of DT6 and W45 accounts for the observed synergistic inhibition effect [12]. In the previous chapter we have shown by photoaffinity labeling that substrate-peptides primarily bind to the catalytic site of cGMP-activated PKG. In analogy with this, the current results indicate that cGMP-activation is a prerequisite for DT2 binding, suggesting DT2 is also targeted to or near the catalytic site. In a similar fashion, DT6 binding was also enhanced by cGMP, suggesting that the DT6 binding pocket is also only accessible after release of the autoinhibition domain. From kinetic analysis it appeared that DT2 also inhibits PKA with a K_i of 16.5 μM (see table 1). This is an order of magnitude higher than the potency of W45 to inhibit PKA (K_i(W45) = 559 μM), but is comparable with the potency of DT6 to inhibit PKA (K_i of DT6 for PKA = 26 μM) [12]. Hence fusion of the peptides does not appear to provide additional effects of PKA inhibition and this probably provides the basis for the high selectivity of DT2 for PKG over PKA. A substantial difference between PKG and PKA is that the active catalytic subunits of PKA are monomeric. In contrast the catalytic domains of PKG remain within a close distance of each other through dimerization of the N-termini. Together with the finding that preferentially one DT2 molecule binds per dimer, it is tempting to postulate that the second (DT6) binding site is the catalytic site of the other subunit of the PKG. It should be noted here that at this moment it is still uncertain whether

W45, DT6 and DT2 are targeted against the catalytic core or whether they actually bind to more distal regions from which they are able to modulate the catalytic domain. In similar manner as the experiments described in Chapter 4, photoaffinity-labeling studies will be performed to locate more precisely the binding pockets of W45, DT6 and DT2.

Although the recorded mass spectra appear to yield new insight into the nature of the inhibitor-protein complex, often the question arises how trustworthy the mass spectra are when binding of ligands in solution is the focus of interest. To answer this question the first priority is often to distinguish structurally specific non-covalent interactions present in solution from nonspecific interactions that could be formed during the electrospray ionization process [25]. Changes in solution conditions, such as cGMP and/or DT2 concentration as well as changing the polarity in the electrospray ionization process were used in an attempt to determine the specificity of the non-covalent DT2-PKG interactions and distinguish this from possible artifacts. DT2 binding was solely observed when PKG was activated by cGMP. Measuring at low cGMP levels suggest that structural changes in PKG, induced by occupation of the high-affinity cGMP binding sites, already opens up the DT2 binding pocket. This observation by itself is a strong argument for a specific interaction. Increasing the concentration of DT2 to a 50-fold excess did not results in a significant increase in the number of bound DT2 molecules. When switching the polarity of instrument neither a difference in the binding pattern, nor in the binding stoichiometry was observed. These two observations are also arguments against the occurrence of possible artifacts in electrospray ionization leading to the unusual binding behavior and stoichiometry. To further elaborate on this issue, it is well known that ESI-MS does not always provide a direct correlation between the solution phase binding studies and complexes detect in the gas phase. For example, in the present work we only observe weak binding of W45 to PKG in the mass spectra, while this peptide was identified as a tight binding peptide and has and inhibition constant of 0.82 μM. Assuming the inhibition constant is a good marker for a binding constant, one would have expected that at peptide concentrations of 20 μM or higher complete saturation of PKG would be reached. In practice, the spectra in Figure 6 suggest that only a small amount of PKG binds these peptides. For DT6, which has a slightly higher inhibition constant, binding to PKG in ESI-TOF-MS was even more pronounced than W45. The exact reason for why no complete saturation is observed with both W45 and DT6 is currently unknown, but might also be due to the buffer and salt concentration used. This latter observation strikes several

critical issues when comparing kinetic data and mass spectrometric data on ligand binding. A rational explanation for this remarkable difference between ESI-TOF-MS and kinetic analysis can be found in process of electrospray. An often underestimated but important point is the stability of formed complexes in solution and perhaps more importantly in the gas phase. One has to be aware that non-covalent interactions, as observed by electrospray ionization time of flight mass spectrometry, represent interactions that survive the transition to the gas-phase. These can differ dramatically from interactions that can exist in solution and from this point of view caution has to be reserved when interpreting electrospray ionization mass spectra of proteins and ligands [26]. In general it is anticipated that electrostatic interactions are maintained or even enhanced in the gas-phase. In contrast, hydrophobic interactions, the type of interactions that are usually enhanced in polar solvent surroundings are not favored in the gas-phase, since the driving force for these interactions (a polar environment) is no longer present in the vacuum of the mass spectrometer. In the particular case of PKG and its substrates and inhibitor peptides, interactions are likely based on strong electrostatic interactions. All substrates and inhibitor peptides contain basic lysine and arginine residues that play an important role in binding. One can easily imagine that the positively charged peptide inhibitors and substrates and negative determinant in for example the catalytic core of PKG provide a strong basis for interactions and thus, in theory, ESI-TOF-MS would be a powerful tool visualizes these complexes. It should be noted here that within the kinase consensus sequence, PKG also prefers hydrophobic residues adjacent to the phosphate-accepting site, thus hydrophobic interaction might also contribute to binding. In chapter 4 of this thesis, we have shown that a photoaffinity label based on a high affinity substrate peptide, could be covalently attached to PKG and up to two substrate peptides were incorporated into the protein. This means that during irradiation in solution two peptides substrates were in a close, bound state on PKG and thus the results could be considered as a ‘snapshot’ of the situation in solution. Initially attempts have been made to visualize the non-covalent interaction between PKG and this substrate, in a similar fashion as described for the inhibitors in this chapter. Although performed under similar concentration conditions as the photolabeling experiments (i.e. well above the K_m), little or no binding of the peptide was observed (See Figure 8), emphasizing the limited capability of ESI-TOF-MS to detect these non-covalent interactions for PKG. As mentioned, the PKG peptide inhibitors and substrate are overall positively charged and highly hydrophilic. Perhaps we have to anticipate that water molecules could accompany these hydrophilic peptides in binding to the protein. The

role of water molecules in proteins, and especially their possible involvement in the recognition and binding of substrates has been debated for many years [27, 28]. In several crystal structures of PKA six conserved water molecules were identified in the active site of the catalytic subunit. Five of these conserved water molecules coordinate MgATP to conserved residues in the core protein, whereas the sixth water molecule is locked into place by its interactions with the nucleotide, the peptide substrate/inhibitor, and the small and large lobes of the catalytic domains and Tyr330 in the C-terminal stretch of amino acids [29]. Previously Chun *et al*. have reported that under nanoflow electrospray ionization conditions, water molecules could be detected in the complex between the SH2 domain from the Src family tyrosine kinase protein, Fyn and a tyrosyl phosphopeptides, demonstrating that ESI can be used to probe interaction in which watermolecules play an important role [30, 31]. In our study the mass accuracy is too low to detect water molecules, and more importantly the possibility exist that in this particular case water molecules have been stripped from the protein during the desolvation process. If they, as the conserved water molecules in PKA crystal structures suggest, contribute in binding of W64, W45 and DT6 this could also explain why binding of these peptides is less pronounced.

Conclusions

The present results demonstrate the ability of ESI-TOF-MS to detect a non-covalent complex of one PKG dimer and 1 DT2 molecule, which was substantially enhanced by cGMP. The finding that under the conditions used in this study, preferentially one DT2 molecule binds to cGMP-activated PKG and not to inactive PKG is quite surprising. It could imply that the autoinhibition domain successfully competes with DT2 for binding the catalytic site. Assuming DT2 targets near the catalytic core of PKG, the observation of 1:1 binding stoichiometry supports the synergistic inhibition behavior found for this peptide and leads to the speculation that the catalytic binding sites are actually in the proximity of each other. Obviously further experiments are needed to unravel the exact mechanism of DT2 inhibition.

Acknowledgements

We kindfully thank Arjen Scholten and Wolfgang R. G. Dostmann of the University of Vermont for the recombinant PKG and peptide samples. We kindfully thank Klaus Rumpel and Frank Pullen of Pfizer Research UK for financial support.

References

1. Graves, J.D.; Krebs, E.G. *Protein phosphorylation and signal transduction.* Pharmacol. Ther. **1999**, *82*, 111-121.
2. Hunter, T. *Signaling--2000 and beyond.* Cell **2000**, *100*, 113-127.
3. Sridhar, R.; Hanson-Painton, O.; Cooper, D.R. *Protein kinases as therapeutic targets.* Pharm Res **2000**, *17*, 1345-1353.
4. Cohen, P. *Protein kinases--the major drug targets of the twenty-first century?* Nat Rev Drug Discov **2002**, *1*, 309-315.
5. Lincoln, T.M.; Dey, N.; Sellak, H. *cGMP-dependent protein kinase signaling mechanisms in smooth muscle: from the regulation of tone to gene expression.* J Appl Physiol **2001**, *91*, 1421-1430.
6. Pfeifer, A.; Ruth, P.; Dostmann, W.; Sausbier, M.; Klatt, P.; Hofmann, F. *Structure and function of cGMP-dependent protein kinases.* Rev. Physiol. Biochem. Pharmacol. **1999**, *135*, 105-149.
7. Schlossmann, J.; Feil, R.; Hofmann, F. *Signaling through NO and cGMP-dependent protein kinases.* Ann Med **2003**, *35*, 21-27.
8. Hofmann, F.; Ammendola, A.; Schlossmann, J. *Rising behind NO: cGMP-dependent protein kinases.* J. Cell. Sci. **2000**, *113 (Pt 10)*, 1671-1676.
9. Francis, S.H.; Poteet-Smith, C.; Busch, J.L.; Richie-Jannetta, R.; Corbin, J.D. *Mechanisms of autoinhibition in cyclic nucleotide-dependent protein kinases.* Front Biosci **2002**, *7*, d580-592.
10. Chu, D.M.; Francis, S.H.; Thomas, J.W.; Maksymovitch, E.A.; Fosler, M.; Corbin, J.D. *Activation by autophosphorylation or cGMP binding produces a similar apparent conformational change in cGMP-dependent protein kinase.* J Biol Chem **1998**, *273*, 14649-14656.
11. Dostmann, W.R.; Nickl, C.; Thiel, S.; Tsigelny, I.; Frank, R.; Tegge, W.J. *Delineation of selective cyclic GMP-dependent protein kinase Ialpha substrate and inhibitor peptides based on combinatorial peptide libraries on paper.* Pharmacol Ther **1999**, *82*, 373-387.
12. Dostmann, W.R.; Taylor, M.S.; Nickl, C.K.; Brayden, J.E.; Frank, R.; Tegge, W.J. *Highly specific, membrane-permeant peptide blockers of cGMP-dependent protein kinase Ialpha inhibit NO-induced cerebral dilation.* Proc Natl Acad Sci U S A **2000**, *97*, 14772-14777.
13. Dostmann, W.R.; Tegge, W.; Frank, R.; Nickl, C.K.; Taylor, M.S.; Brayden, J.E. *Exploring the mechanisms of vascular smooth muscle tone with highly specific, membrane-permeable inhibitors of cyclic GMP-dependent protein kinase Ialpha.* Pharmacol Ther **2002**, *93*, 203-215.
14. Taylor, M.S.; Okwuchukwuasanya, C.; Nickl, C.K.; Tegge, W.; Brayden, J.E.; Dostmann, W.R. *Inhibition of cGMP-dependent protein kinase by the cell-permeable peptide DT-2 reveals a novel mechanism of vasoregulation.* Mol Pharmacol **2004**, *65*, 1111-1119.
15. Przybylski, M.; Glocker, M.O. *Electrospray mass spectrometry of biomacromolecular complexes with noncovalent interactions - New analytical perspectives for supramolecular chemistry and molecular recognition processes.* Angewandte Chemie-International Edition in English **1996**, *35*, 807-826.
16. Loo, J.A. *Studying noncovalent protein complexes by electrospray ionization mass spectrometry.* Mass Spectrometry Reviews **1997**, *16*, 1-23.
17. Samalikova, M.; Matecko, I.; Muller, N.; Grandori, R. *Interpreting conformational effects in protein nano-ESI-MS spectra.* Anal Bioanal Chem **2004**, *378*, 1112-1123.
18. Veenstra, T.D.; Johnson, K.L.; Tomlinson, A.J.; Craig, T.A.; Kumar, R.; Naylor, S. *Zinc-induced conformational changes in the DNA-binding domain of the vitamin D receptor determined by electrospray ionization mass spectrometry.* J Am Soc Mass Spectrom **1998**, *9*, 8-14.

19. Simmons, D.A.; Konermann, L. *Characterization of transient protein folding intermediates during myoglobin reconstitution by time-resolved electrospray mass spectrometry with on-line isotopic pulse labeling.* Biochemistry **2002**, *41*, 1906-1914.
20. Bligh, S.W.; Haley, T.; Lowe, P.N. *Measurement of dissociation constants of inhibitors binding to Src SH2 domain protein by non-covalent electrospray ionization mass spectrometry.* J Mol Recognit **2003**, *16*, 139-148.
21. Tjernberg, A.; Carno, S.; Oliv, F.; Benkestock, K.; Edlund, P.O.; Griffiths, W.J.; Hallen, D. *Determination of dissociation constants for protein-ligand complexes by electrospray ionization mass spectrometry.* Anal Chem **2004**, *76*, 4325-4331.
22. Rogniaux, H.; Sanglier, S.; Strupat, K.; Azza, S.; Roitel, O.; Ball, V.; Tritsch, D.; Branlant, G.; Van Dorsselaer, A. *Mass spectrometry as a novel approach to probe cooperativity in multimeric enzymatic systems.* Anal Biochem **2001**, *291*, 48-61.
23. Ferrige, A.G.; Seddon, M.J.; Green, B.N.; Jarvis, S.A.; Skilling, J. *Disentangling Electrospray Spectra With Maximum-Entropy.* Rapid Comm. Mass Spectrom. **1992**, *6*, 707-711.
24. Ferrige, A.G.; Seddon, M.J.; Jarvis, S. *Maximum-Entropy Deconvolution in Electrospray Mass-Spectrometry.* Rapid Com. Mass Spectrom. **1991**, *5*, 374-377.
25. Prinz, H.; Lavie, A.; Scheidig, A.J.; Spangenberg, O.; Konrad, M. *Binding of nucleotides to guanylate kinase, p21(ras), and nucleoside-diphosphate kinase studied by nano-electrospray mass spectrometry.* J Biol Chem **1999**, *274*, 35337-35342.
26. Aplin, R.T.; Robinson, C.V.; Schofield, C.J.; Westwood, N.J. *Does the Observation of Noncovalent Complexes between Biomolecules by Electrospray-Ionization Mass-Spectrometry Necessarily Reflect Specific Solution Interactions.* Journal of the Chemical Society-Chemical Communications **1994**, 2415-2417.
27. Edsall, J.T.; McKenzie, H.A. *Water and proteins. II. The location and dynamics of water in protein systems and its relation to their stability and properties.* Adv Biophys **1983**, *16*, 53-183.
28. Meyer, E. *Internal water molecules and H-bonding in biological macromolecules: a review of structural features with functional implications.* Protein Sci **1992**, *1*, 1543-1562.
29. Shaltiel, S.; Cox, S.; Taylor, S.S. *Conserved water molecules contribute to the extensive network of interactions at the active site of protein kinase A.* Proc Natl Acad Sci U S A **1998**, *95*, 484-491.
30. Chung, E.W.; Henriques, D.A.; Renzoni, D.; Morton, C.J.; Mulhern, T.D.; Pitkeathly, M.C.; Ladbury, J.E.; Robinson, C.V. *Probing the nature of interactions in SH2 binding interfaces--evidence from electrospray ionization mass spectrometry.* Protein Sci **1999**, *8*, 1962-1970.
31. Chung, E.; Henriques, D.; Renzoni, D.; Zvelebil, M.; Bradshaw, J.M.; Waksman, G.; Robinson, C.V.; Ladbury, J.E. *Mass spectrometric and thermodynamic studies reveal the role of water molecules in complexes formed between SH2 domains and tyrosyl phosphopeptides.* Structure **1998**, *6*, 1141-1151.

Summary and concluding remarks

6

The most important findings of the research described in this thesis are summarized in this chapter. New insight into the activation and inhibition of the cyclic guanosine monophosphate dependent protein kinase are identified and new mass spectrometry based methods to study protein kinases and protein phosphorylation are developed.

Introduction

Post translational modification plays a vitally important role in the regulation of cellular functions *via* the modulation of the structural and functional properties of strategically selected proteins. Through the key mechanism of protein phosphorylation, proteins can be rapidly and reversibly modified, providing an 'on-off switch' for a given protein activity. Protein kinases and protein phosphatases are the key regulators in the protein phosphorylation and dephosphorylation events. Consequently, protein kinases and phosphatases are together with their corresponding target protein substrates intensely studied in an effort to elucidate signaling pathways mediated via reversible protein phosphorylation. In particular protein kinases are intriguing enzymes, since they are endowed with a tremendous precision in recognizing their targets. Among the continuing challenges in the protein kinase field is the understanding of the catalytic mechanism of the protein kinase enzymes for rational inhibitor design, identifying physiologic protein substrates for kinases as well as identifying physiological kinases that effect phosphorylation of specific substrates. It is well known now that all protein kinases share a common catalytic domain. Hence an intriguing question is how individual protein kinases recognize their own substrate targets out of the background of thousands of other proteins. The ultimate goal in protein kinase research will be defining the temporal relationships between kinase action and cellular effects, and characterizing the structural and functional effects of all site-specific phosphorylation events.

The primary goal of the work described in this thesis was aimed at gathering biochemical insight into structural and functional aspects of the cyclic guanosine monophosphate dependent protein kinase (PKG) using mass spectrometry based approaches. Chapter 1 gives a brief overview of the biochemical background of PKG and of mass spectrometric methods for the biochemical analysis of proteins in general. PKG plays a central role in the regulation of vascular smooth muscle tone and activation of PKG alters multiple cellular signaling pathways. PKG harbors multiple functional domains on a single polypeptide chain, which makes the study of each individual role of these domains rather difficult. In this thesis new methodologies were developed, tested and applied to study processes such as PKG autophosphorylation and the interactions of PKG with its various ligands and inhibitors. In this chapter, the results are summarized and critically discussed.

Summary of results

In chapter 2 we have used nanoflow electrospray ionization time-of-flight mass spectrometry to study the interaction between PKG, its allosteric ligand, cGMP, and one of its substrates ATP. Using the non-hydrolyzable ATP mimic, AMPPNP we have shown that ATP binding already occurs in the absence of cGMP. In the absence of cGMP, PKG adapts an inactive conformation in which the autoinhibition domain blocks the substrate binding site of the catalytic domain. Our observation that AMPPNP already binds to this inactive state suggests that the ATP binding pocket is readily accessible when the autoinhibition domain is bound to the active site. The interaction between PKG and AMPPNP was strongly enhanced by the addition of $MnCl_2$ to the spray solutions. This is indicative for the specific nature of the formed complex, since all protein kinases require a divalent metal ion, such as Mg^{2+} or Mn^{2+} to accompany the ATP in the ATP-binding pocket. Upon binding of cGMP or cAMP, PKG is activated and in the presence of Mg^{2+} and ATP, PKG phosphorylates itself *in-vitro* in an autocatalytic manner. Partial proteolysis by chymotrypsin of differentially autophosphorylated PKG, monitored by nanoflow-ESI-TOF-MS determined a gradual increase in phosphorylation in time. A total net amount of 4 phosphorylation sites per monomer were observed in highly autophosphorylated PKG. These results show that nanoflow-ESI-TOF-MS in combination with limited proteolysis is a fast tool to discern the overall phosphorylation state of PKG.

In chapter 3 an innovative method for phosphopeptide fishing is described. This method relies on the property of titanium oxide to absorb organic phosphorous compounds under acidic conditions and to desorb them under basic conditions. A two-dimensional column system is presented, which allows for the separation of phosphorylated peptides from non-phosphorylated peptides. A strong advantage of this approach is the automation by which this process can be performed. Additionally, from the injected sample all peptides, whether phosphorylated or non-phosphorylated are subjected to mass-spectrometric analysis, resulting in a full characterization of all peptides present in the initial injected sample. This method is comparable with the more established phosphopeptide fishing technique, IMAC. However our approach has the advantage that lesser column-handling step are required, which makes automation of the procedure less difficult. In addition, the prepared titanium oxide columns lasted more than hundred runs without showing any signs of reduced performance, hence it

appears to be a more robust procedure than IMAC and it certainly has a high potential in the field of phosphoproteomics.

The autophosphorylation reaction of PKG was examined using this newly developed strategy for phosphopeptide enrichment. For this purpose PKG was autophosphorylated *in-vitro* to different degrees and each state was subsequently digested using several proteases and analyzed using the developed method. A total of 8 phosphorylation sites were found. Two sites, Serine-26 and Threonine-516 were found to be already phosphorylated in protein samples isolated from bovine lung (which were not stimulated to autophosphorylate *in-vitro*). The first site is a previously uncharacterized site. Interesting is the idea that this residue is phosphorylated, presumably *in-vivo* by another kinase. Using NetPhos 2.0 Server [1-3], a database of experimentally verified phosphorylation sites, 4 potential kinases were found for to be responsible for the phosphorylation of this serine namely, Casein kinase II, PKA, PKC and PKG. We have shown that *in-vitro* PKG does not phosphorylate this site in an autocatalytic manner. Serine-26 resides in the middle of the N-terminal Leucine/Isoleucine zipper (LZ) motif. Mammalian PKGs form dimers through interactions of this amino terminal LZ domain. Recently, it has also been shown that Myosin Binding Subunit (MBS) and PKG interact via LZ/LZ interactions. Hence, it is tempting to speculate that a phosphorylation event within this domain has an effect on LZ interactions of the subunits of PKG and other protein such as MBS. Of course further experiments are needed to elucidate which kinase is responsible for this phosphorylation and even more important to find out the structural and functional consequence of this phosphorylation event. Another previously uncharacterized phosphorylation site is Serine-44, which is identified as a new autophosphorylation site. Serine-44 is just outside the LZ-domain, two residues upstream of Cysteine-42 of which it is hypothesized that is involved in dimerization of Type Iα PKG. Again, further experiments are needed to elucidate the biochemical consequences of this phosphorylation site on for example kinase activity, dimerization and/or the interaction with other proteins mediated through the LZ-domain.

In chapter 4 the substrate binding site of PKG was investigated using a highly specific substrate, photoaffinity labeling and mass spectrometry. For this purpose a derivative of a highly specific PKG substrate TQAKRKKSLAMFLR was synthesized with a 4'-[(trifluoromethyl)diazirinyl-*L*-phenylalanine ((Tmd)-Phe) positioned at the P+4 position, replacing the original phenylalanine. This photoaffinity label was successfully cross-linked to

PKG. Incorporation of this photoaffinity label was substantially enhanced by the activation of PKG by cGMP. This observation is in well agreement with the current working model of PKG. Namely, in absence of cGMP, PKG is maintained in a low basal/inactive state through the action of the N-terminal inhibition domain that interacts with the catalytic site in direct competition with substrate peptides. Analysis of proteolytic digests of the cross-linked protein yielded the location of cross-linkage, namely to Ile-361, which resides near the glycine rich loop. Due to the high homology between the catalytic cores of PKG and PKA and the availability of 3D-structures of PKA and substrates, it was concluded that the site of coupling was rational. In conclusion, these measurements showed that photoaffinity labeling and mass spectrometry form a powerful combination to discern peptide-binding sites on proteins. Additionally the usage of 50% stable isotope labeled photoaffinity labels elegantly facilitates the retrieval of cross-linked products.

Of more importance was the localization of the binding site of the various inhibitor peptides described in chapter 5. Chapter 5 describes preliminary results from a mass spectrometric approach to study the interaction between PKG and a highly PKG specific peptide inhibitor DT2. DT2 is the fusion product of the inhibitor peptide W45 (LRKKKKKH), which was derived from a library screen targeted for identifying high affinity PKG-binding peptides, and DT6, a membrane translocating sequence used for internalization studies of W45. Both the peptides alone have PKG inhibitory potencies with inhibition constants around 1 μM, however fusion of the two sequences yields the unprecedented DT2 peptide inhibitor of PKG with a K_i of 12.5 nM. Furthermore, DT2 is highly selective towards PKG compared to its ability to inhibit PKA. In an attempt to unravel the inhibitory action of DT2 on PKG a set of nanoflow electrospray ionization time-of-flight mass spectrometry experiments were performed with PKG, cGMP, DT2, W45 and DT6 using the same experimental procedure as described in chapter 2. Nanoflow-ESI-TOF-MS experiments indicated that DT2 binds in an apparent stoichiometry of one DT2 molecule per PKG dimer. Additionally this odd mode of binding was primarily observed when cGMP was added to the spray solution. Mass spectra obtained after electrospraying PKG in the presence of W45, DT6 and a peptide substrate W64 showed to bind to PKG, however based on the intensity of these complexes and the intensity of the free PKG protein it appeared that the number of bound peptide was low (i.e. no complete saturation was observed, where it was expected, considering the peptide concentrations used). However, the most important finding of these studies is the result

obtained from the nanoflow ESI experiments with PKG and DT2. The observation that activation of PKG by cGMP is a prerequisite for DT2 binding could imply that the N-terminal autoinhibition domain also competes with DT2 for binding to the active site of PKG. Furthermore, the strange stoichiometry could imply that DT2 binds to both catalytic sites of dimeric PKG, suggesting these are in the proximity of each other. To discern these last two speculations, derivatives of DT-2 with a (Tmd)-Phe positioned at the N-terminal residue (Ac-YGRKKRRQRRRPPLRKKKKKF*-NH_2) or at the C-terminal residue (Ac-F*GRKKRRQRRRPPLRKKKKKH-NH_2), as well as W45 with a C-terminal (Tmd)-Phe (Ac-LRKKKKKF*-NH_2), were synthesized. Several crosslink conditions were investigated, but unfortunately no cross-linking was observed with these peptides. A very critical point with this kind of experiments is the position of the photoaffinity label within the peptide. Obviously, with the peptides listed above, the wrong position for the photolabel was chosen. There are two scenarios possible when a photolabel is positioned on the wrong place: (*i*) The bulky side chain of the photolabel interferes with binding. (*ii*) The photolabel is on a place of the peptide that is not near the protein and covalent linkage cannot be formed. After evaluating the negative outcome of these crosslink attempts, two new photoaffinity labels were designed which might be more successful. The following W45 based peptides were synthesized and evaluated for crosslinking; LF^{bpa}RKKKKKY and LRKKKF^{bpa}KY. Initially the C-terminal residue was chosen as the position of the photoaffinity label, however since it showed not to crosslink with PKG, two other positions were evaluated. Re-evaluting of the SPOT-images of the library screen that identified W45 [4] learned that the N-terminal leucine is actually an important determinant for affinity of W45 towards PKG. Other amino-acids that are tolerated at this position are phenylalanine, tryptophan and isoleucine. To be able to find back cross-linked products, the photoaffinity label was put in between the N-terminal leucine (which was isotopically labeled for 50% with $6C^{13}$, $1N^{15}$ leucine) and the arginine. Instead of the C-terminal histidine, and tyrosine was chosen since the library screen data showed that this would be preferred with a phenylalanine (and presumably with the phenylalanine analog) at the N-terminal position. The other photoaffinity label contained a photoreactive amino acid, replacing the fourth lysine of the W45. Again the SPOT-image data revealed that also this lysine has an important role in the affinity of W45. Finally, in these peptides *para*-benzoyl-L-phenylalanine was used as photoaffinity label, instead of the originally used (Tmd)-Phe. This photoaffinity label has a lower reactivity for water compared to (Tmd)-Phe [5]. Both photoaffinity labels have estimated lengths of reaction of

approximately 3 angstrom, however the higher reactivity of Tmd-Phe towards water seriously reduces its effective reaction length. Since (Bpa)-Phe is practically inert towards reaction with H_2O it was assumed that cross-linking would be much more efficient and yields of cross-link product would be higher.

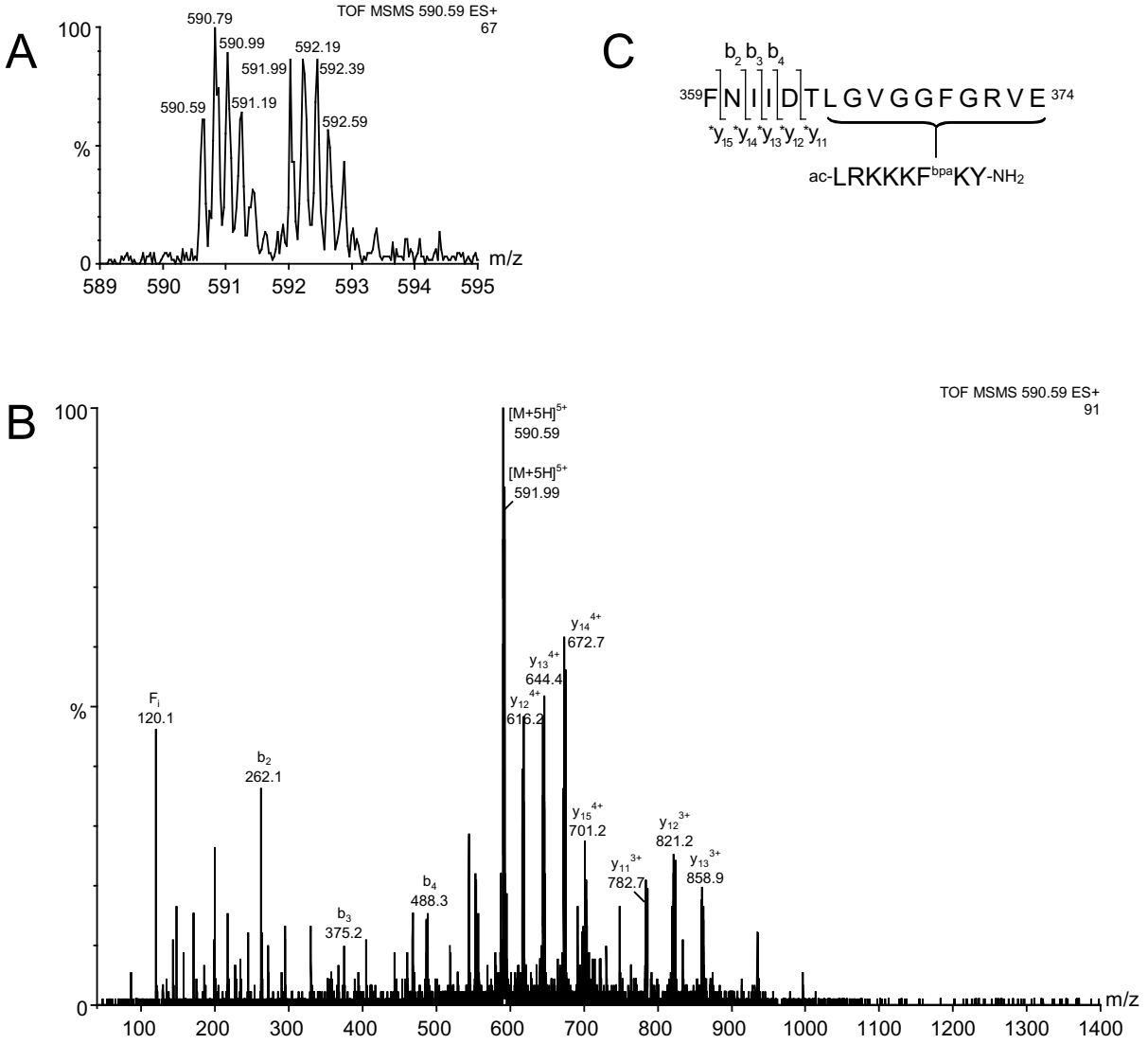

Figure 1: Tandem mass spectrometry analysis of a cross-linked product derived from a GluC-digest of PKG which was cross-linked with ac-LRKKKF^{bpa}KY-NH_2. **(A)** The $[M+5H]^{5+}$ precursor ion at *m/z* 590-593 that was selected by the quadrupole using a broad selection window (~5 *m/z* units). The characteristic peak pare is indicative for the presence of the isotopically labeled leucine from the photoaffinity label. **B)** MS/MS spectrum of the $[M+5H]^{5+}$ at *m/z* 590-593 **(C)** Primary sequence of the cross-linked product and identified fragment ions. The b and y" ions corresponding the primary sequence of PKG, without covalently attached inhibitor are annotated by b_n or $y_{n,}$ whereas b or y" ions of the primary sequence of PKG that carries the covalent attached photolabel are labeled $^{*}b_n$ or $^{*}y_n$.

The newly synthesized peptides were successfully cross-linked to PKG and analysis of the proteolytic digest of the cross-linked PKG showed that they were also cross-linked to the active site of PKG. Figure 1 shows the MS/MS spectrum of a peptide derived from a Glu-C digest of PKG labeled with ac-LRKKKF^{bpa}KY-NH_2. This peptide displayed the characteristic isotopic pear pare, which is due to the incorporation of 50% ^{6}C13, ^{1}N15-Leucine in the photoaffinity label. The mass for this cross-linked peptide is 2947.9 Da. The low energy CID spectrum shown in Figure 1B display several multiply charged fragment ions, each showing the characteristic peak pares. A partial sequence FNIID can be derived from this series of ions. This partial sequence tag appears to originate from the Glu-C fragment of PKG (D)^{359}–FNIIDTLGVGGFGRVE^{374}-(L). This proteolytic fragment has a theoretical mass of 1692.8 Da and together with the mass of the photoaffinity label (1254.7 Da) it matches the mass of the selected precursor ion (2947.9 Da). Unfortunately, the exact location of the covalent linkage could not be derived from this MS/MS spectrum, but it must reside somewhere on ^{364}TLGVGGFGRVE^{374}. This stretch of amino acids is the glycine rich loop of the catalytic domain of PKG. The substrate label which was photoaffinity-labeled to PKG in chapter 4 was also found to reside near this stretch of amino acids. Figure 2A shows the MS/MS spectrum of a peptide derived from a tryptic digest of PKG labeled with ac-LF^{bpa}RKKKKKY-NH_2. This peptide also displayed the characteristic isotopic peak pare, resulting from the incorporation of ^{6}C13, ^{1}N15-Leucine in the photoaffinity label. The mass for this peptide is 3170.1 Da. The low energy CID spectrum shown in Figure 2B displays several multiply charged fragment ions, each showing a characteristic peak pare. A partial sequence LSDFNIID could be identified from this series of ions. The partial sequence tag appears to originate from the tryptic fragment of PKG (K)^{356}LSDFNIIDTLGVGGFGRVELVQLK^{379}(S). This proteolytic fragment has a theoretical mass of 2589.4 Da and together with the mass of part of the photoaffinity label (ac-LF^{bpa}R , mass 580.3), it matches the mass of the selected precursor ion. Also from this fragmentation spectrum the exact location of the covalent linkage could not be derived but it must reside somewhere on ^{366}GVGGFGRVELVQLK^{379}. To summarize, these preliminary results clearly show that W45 based photoaffinity-label are targeted against the glycine rich loop of PKG. W45 was previously shown to be a competitive inhibitor of PKG [4], hence the finding that it binds to the glycine rich loop as well, thereby possibly preventing substrate binding is quite reasonable. On the other hand, W45 analogs in which each lysine was replaced by a serine showed to be very poor substrates of PKG (W. R. G. Dostmann, personal communication).

Finally, photoaffinity labeling of PKG with DT6 based photoaffinity labels are needed to complete the picture and to gain more insight into the real mechanism of DT2 inhibition.

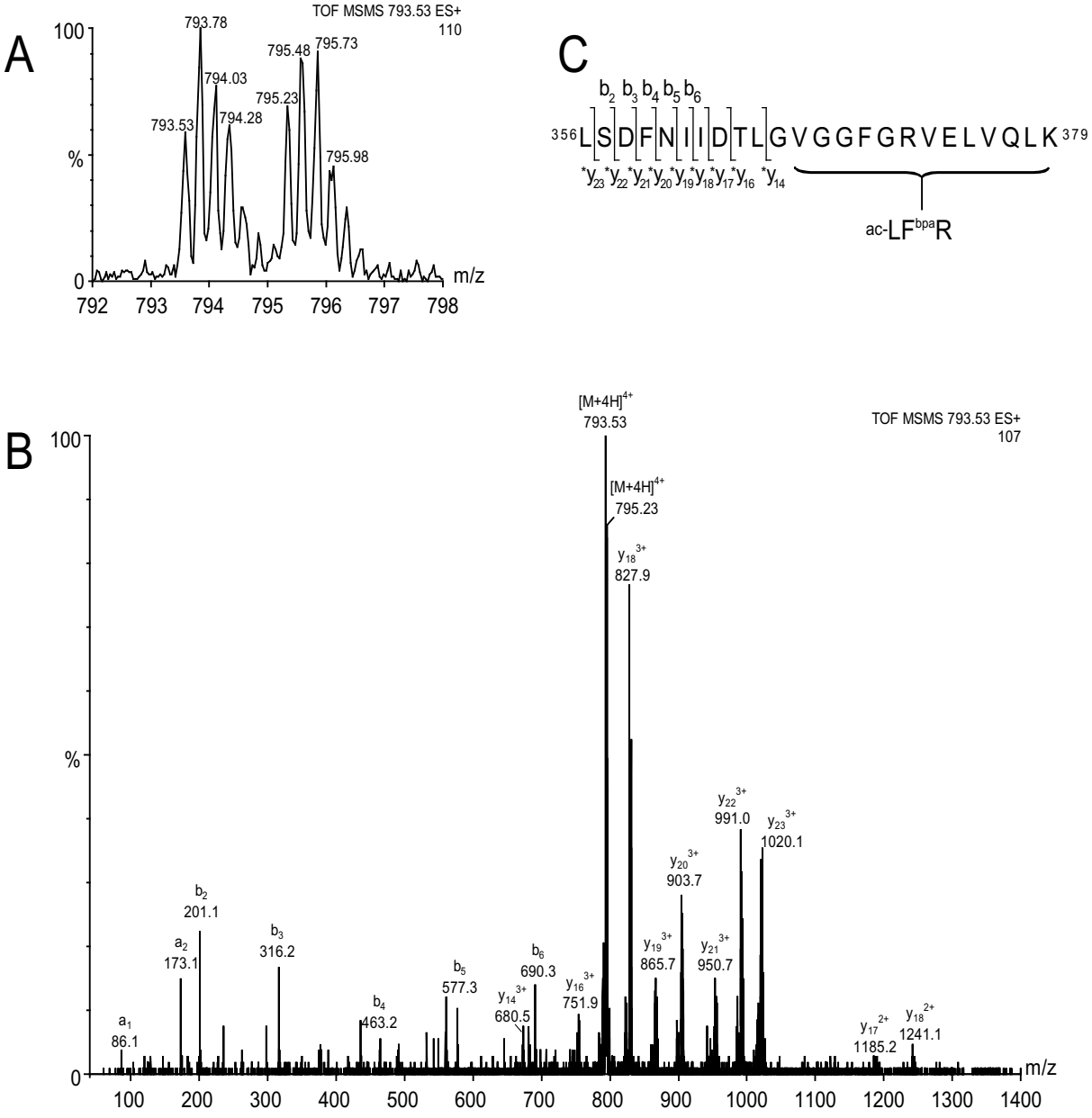

Figure 2: Tandem mass spectrometry analysis of a cross-linked product derived from a tryptic-digest of PKG which was cross-linked with ac-LF^{bpa}RKKKkKY-NH_2. **(A)** The $[M+4H]^{4+}$ precursor ion at *m/z* 793-797 that was selected by the quadrupole using a broad selection window (~5 *m/z* units). The characteristic peak pare is indicative for the presence of the isotopically labeled leucine from the photoaffinity label. **B)** MS/MS spectrum of the $[M+4H]^{4+}$ at *m/z* 793-797 **(C)** Primary sequence of the cross-linked product and identified fragment ions. The b and y" ions corresponding the primary sequence of PKG, without covalently attached substrate are annotated by b_n or $y_{n,}$ whereas b or y" ions of the primary sequence of PKG that carries the covalent attached photolabel are labeled $^{*}b_n$ or $^{*}y_n$.

References

1. Blom, N.; Kreegipuu, A.; Brunak, S. *PhosphoBase: a database of phosphorylation sites.* Nucleic Acids Res 1998, *26*, 382-386.
2. Hjerrild, M.; Stensballe, A.; Rasmussen, T.E.; Kofoed, C.B.; Blom, N.*, et al. Identification of phosphorylation sites in protein kinase A substrates using artificial neural networks and mass spectrometry.* J Proteome Res 2004, *3*, 426-433.
3. Kreegipuu, A.; Blom, N.; Brunak, S. *PhosphoBase, a database of phosphorylation sites: release 2.0.* Nucleic Acids Res 1999, *27*, 237-239.
4. Dostmann, W.R.; Taylor, M.S.; Nickl, C.K.; Brayden, J.E.; Frank, R.; Tegge, W.J. *Highly specific, membrane-permeant peptide blockers of cGMP-dependent protein kinase Ialpha inhibit NO-induced cerebral dilation.* Proc Natl Acad Sci U S A 2000, *97*, 14772-14777.
5. Weber, P.J.; Beck-Sickinger, A.G. *Comparison of the photochemical behavior of four different photoactivatable probes.* J Pept Res 1997, *49*, 375-383.

List of abbreviations

AMPPNP	β,γ-imidoadenosine 5'-triphosphate
amu	atomic mass unit
ATP	adenosine 5'-triphosphate
Bpa-Phe	*p*-benzoyl-L-phenylalanine
cAMP	adenosine 3'-, 5'-cyclic monophosphate
DT2	ac-YGRKKRRQRRRPP-LRKKKKKH-NH_2
DT6	ac-YGRKKRRQRRRPP-NH_2
CID	collision induced dissociation
cGMP	guanosine 3'-, 5'-cyclic monophosphate
ESI	electrospray ionization
HPLC	high-pressure liquid chromatography
IMAC	immobilized metal affinity chromatography
LC	liquid chromatography
m/z	mass-to-charge ratio
MS	mass spectrometry
MS/MS	tandem mass spectrometry
MALDI	matrix assisted laser desorption ionization
PKA	cyclic AMP dependent protein kinase
PKG	cyclic GMP dependent protein kinase
Tmd-Phe	4'-[(trifluoromethyl)diazirinyl-*L*-phenylalanine
ToF	time of flight
W45	ac-LRKKKKKH-NH_2
W64	ac-TQAKRKKSLAMFLR-NH_2

Nederlandse samenvatting

Signaal transductie is een belangrijk mechanisme, gebruikt in verschillende biologische processen, waarmee cellen kunnen reageren op signalen vanuit hun omgeving. Defecten in signaal transductie moleculen kunnen leiden tot het ontstaan van verschillende ziektes, zoals bijvoorbeeld kanker, en daarom worden signaal transductie paden veelvuldig bestudeerd. Ten grondslag aan cellulaire signaal transductie liggen eiwitten en eiwit-complexen, welke interacties met elkaar aangaan. Voor de overdracht van signalen op verschillende eiwitten wordt veelvuldig gebruik gemaakt van post-translationele modificaties. Dit omvat een modificatie van een eiwit nadat het gesynthetiseerd is en deze modificaties kunnen de werking van het eiwit sturen of reguleren. Een van de bekenste post-translationele modificaties is fosforylering. Hierbij wordt een fosfaat groep van ATP overgezet op de zijketen van één van de aminozuren van het eiwit, meestal een serine, threonine of tyrosine. Eiwit kinases vormen een speciale klasse van eiwitten welke verantwoordelijk zijn voor deze fosforylerings reacties en daarmee vervullen zij een zeer belangrijke rol in signaal transductie paden. Afwijking kinase activiteit kan leiden tot verstoringen in de fosforylerings balans, wat weer een ziekte of afwijking tot gevolg kan hebben. Mede hierdoor vormen eiwit kinases een belangrijk target bij het bestrijden van ziektes en het ontwikkelen van nieuwe drugs.

Het cGMP-afhankelijk eiwit kinase (PKG) is een eiwit kinase wat onder andere nauw betrokken is bij de regulatie van glad spierweefsel. Dit spierweefsel is onder andere te vinden in bloedvaten en aderen. Het spierweefsel trekt zich samen waardoor de bloedvaten op druk blijven en op die manier de juiste bloeddruk behouden. Wanneer PKG in de gladde spiercel wordt geactiveerd doordat de concentratie van cGMP omhoog gaat, ontspant de gladde spiercel, waardoor de bloeddruk verlaagt. Remming van PKG door middel van bijvoorbeeld de peptide remmer DT2, leidt uiteindelijk tot een samenspanning van de gladde spiercel, waardoor de bloeddruk stijgt. Hoewel veel duidelijk is over de fysiologische rol van PKG in onder andere glad spierweefsel is er grote onduidelijkheid over de exacte werking van PKG op moleculair niveau. Het PKG eiwit heeft een aantal functionele domeinen, en elk domein heeft zijn eigen specifieke rol. Het N-terminale domein is verantwoordelijk voor de dimerisatie van twee PKG-subunits. Daarnaast bevat het een sequentie met een remmende werking (het auto-inhibitie domein) en meerdere auto-fosforylatie residuen. Naast dit N-

terminale domein, liggen twee cGMP-bindings plaatsen welke een belangrijke rol spelen bij activiteits regulatie. In het C-terminal gedeelte van PKG is het catalytische domein gelegen, welke bestaat uit een ATP-bindings plaats en een substrate bindings plaats.
Men veronderstelt dat in afwezigheid van cGMP, het auto-inhibitie domein sterk bindt aan het catalytische domein, waardoor substraten niet meer kunnen binden. Als de cGMP concentratie omhoog gaat, zal cGMP binden aan de cGMP-bindingsplaatsen van PKG. Door deze binding verandert de structuur van PKG, waardoor het auto-inhibitie domein los laat van het catalytische domein en hiermee is PKG geactiveerd en instaat om zijn target eiwitte te fosforyleren alsmede zichzelf te fosforyleren.

In hoofdstuk 2 heb ik met behulp van nanoflow electrospray ionisatie massa spectrometrie gekeken naar de interacties tussen PKG, cGMP en een ATP-analoog. Het is namelijk mogelijk om intacte eiwitten direct in de gas-fase te krijgen en te ioniseren met behulp van electrospray ionisatie. Hierdoor is het mede mogelijk om de massa van een eiwit te bepalen door het ratio tussen massa en lading van het eiwit te meten met hebulp van massa spectrometrie Als het eiwit vanuit een neutral gebufferde oplossing wordt gesprayed blijft de structuur van het eiwit vaak behouden. Wanneer een eiwit bepaalde interacties aangaat in de oplossing met bijvoorbeeld liganden, remmers of substraten, kunnen deze worden waargenomen in het massa spectrum op voorwaarde dat deze interacties sterk genoeg zijn om het ionisatie proces te overleven. In hoofdstuk 2 toon ik aan dat met behulp van electrospray ionisatie massa spectrometry de interacties tussen PKG, cGMP en een ATP analoog kunnen worden waargenomen. Verder heb ik laten zien dat ATP, één van de substraten van PKG al kan binden aan het PKG wat nog niet geactiveerd is (d.w.z. in afwezigheid van cGMP). Dit zou betekenen dat de ATP bindingsplaats vrij toegankelijk is, zelfs wanneer de auto-inhibitie sequentie is gebonden aan het catalytische domein. Daarnaast is aangetoond dat met behulp van massa spectrometrie nauwkeurig de netto fosforylatie toestand van PKG na *in-vitro* auto-fosforylatie kan worden bepaald.

In hoofdstuk 3 is een nieuwe methode voor de verrijking en analyse van gefosforyleerde peptides ontwikkeld. De methode berust voornamelijk op de unieke capaciteit van titanium oxide om organo-fosfaat verbindingen te absorberen onder zure condities en de deabsorberen onder basische condities. Met behulp van een geautomatiseerde opstelling is aangetoond dat 125 femtomol van het gefosforyleerde peptide (RKIpSASEF) kan worden gescheiden van

zijn on-gefosforyleerde vorm (RKISASEF) met een opbrengst van meer dan 90%. Met deze ontwikkelde methode is de auto-fosforyleringsreactie van PKG bestudeerd. In totaal werden 8 fosforylerings plaatsen op PKG gekarakteriseerd, waaronder twee plekken die nog niet eerder waren gevonden. Een van deze plekken, Serine-26, wordt niet door PKG zelf gefosforyleerd, maar door een ander nog onbekend kinase. Van Serine-44 is aangetoond dat deze wel door PKG zelf wordt gefosforyleerd. Voor beide plekken geldt echter dat verder onderzoek nodig is om aan te tonen wat de consequenties zijn van deze fosforylerings reacties. De belangrijkste conclusie van dit hoofdstuk is dat titanium-oxide als kolom materiaal een zeer effectief middel is om gefosforyleerde peptiden te isoleren uit complexe mengsel van veelal niet gefosforyleerde peptides. De ontwikkelde methode is vrij eenvoudig te automatiseren en uit te voeren en lijkt op het eerste oog veel robuster dan de veelvuldig gebruikte IMAC-methode.

In hoofdstuk 4 heb ik met behulp van massa spectrometrie en foto-labeling getracht de bindings plaats van een substrate peptides op PKG te localiseren. Hiervoor is een substraat peptide gesynthetiseerd welke een amino-zuur derivaat bevat, welke na bestralen met ultra-violet licht een reactief intermediar vormt dat in staat is om een covalente binding te vormen tussen zichzelf en PKG. Vervolgens wordt het gekoppelde eiwit-substraat complex in stukjes geknipt met een protease en geanalyseerd met behulp van massa spectrometrie. Uiteindelijk kan een gekoppeld product gevonden worden waaruit duidelijk wordt waar het substraat zich precies bevond op het moment van belichting. De resultaten zoals verkregen in hoofdstuk 4 geven aan dat het gesynthetiseerde substraat peptide bind vlakbij de glycine rijke loep. Deze loep is het sterkst geconserveerde stukje sequentie in alle eiwit kinases en speelt een essentiele rol tijdens katalyse. Dit experiment werd uitgevoerd ter voorbereiding van fotolabelings experimenten met remmings-peptides, waarvan de bindingsplaats totaal onduidelijk is. Helaas vielen deze experimenten net buiten het tijdsbestek van dit proefschrift. Echter, de voornaamste conclusie van dit hoofdstuk is dat met behulp van fotolabeling en massa spectrometrie, bindings plaatsen van substraat peptiden eenvoudig kunnen worden achterhaald.

In hoofdstuk 5 heb ik met dezelfde massa spectrometrische methode welke gebruikt in hoofstuk 2, gekeken naar de interactie tussen PKG en een van de sterkste PKG remmers DT2. DT2 is een peptide van ca. 20 aminozuren welke is ontstaan door samenvoeging van een

W45, een octamerisch peptide welke sterkt bindt aan PKG en DT6, een membraan translocatie sequentie. Het is eerder aangetoond dat dit gecombineerde peptide een zeer sterk remmende werking heeft op PKG, echter het exacte mechanisme achter deze remming is voorlopig nog onduidelijk. De in hoofdstuk 5 verkregen resultaten tonen aan dat er slechts één DT2 molecuul bindt aan een dimeer van PKG. Verder is aangetoond dat deze interactie alleen wordt waargenomen wanneer PKG is geactiveerd met cGMP. Foto-labeling experimenten met de twee bestanddelen van DT2, het W45 en DT6 peptide zullen uiteindelijk moeten aantonen waar DT2 exact bindt. Initiële resultaten met twee foto-label derivaten van W45 hebben inmiddels aangetoond dat W45 direct bindt aan de glycine-rijke loep van PKG. Uiteindelijk zullen deze experimenten leiden tot een beter inzicht in de werking DT2 en de structuur van dimerisch PKG, alsmede een bijdrage kunnen leveren aan de verbetering van DT2-gerelateerd peptiden, welke nog efficiëntere werking hebben. Tenslotte heb ik alle verkregen resultaten nog eens samengevat en bediscussieerd in hoofdstuk 6.

Curriculum Vitae

Martijn Pinkse werd geboren op 12 augustus 1977 te Alkmaar. Na het behalen van het VWO diploma in 1995 aan het Jan van Scorel College te Alkmaar, werd begonnen aan een scheikunde studie aan de Universiteit van Amsterdam. Tijdens de studie werden onderzoekstages verricht bij de sectie Biocatalyze (onder begeleiding van dr. M. Merkx) en bij de sectie Massa Spectrometrie (onder begeleiding van dr. J.W. Back). In september 2000 werd het doctoraalexamen behaald. In diezelfde maand begon hij als assistent in opleiding bij de sectie Biomoleculaire Massa Spectrometrie aan de Universiteit van Utrecht. In deze functie werd het in dit proefschrift beschreven onderzoek verricht onder leiding van Prof. dr. Albert J. R. Heck. Onderzoeksresulstaten zijn onder meer gepresenteerd tijdens een lezing op de jaarlijkse bijeenkomst van de *British Society of Mass Spectrometry* in Southampton (2001) en in de vorm posters gepresenteerd op de jaarlijks bijeenkomsten van de *American Society for Mass Spectrometry* in Orlando (2002) en Montreal (2003). In september 2004 is hij begonnen als post-doc aan de Universiteit Utrecht in het Nederlands Proteomics Center.

List of publications

- Maarten Merkx, Martijn W. H. Pinkse, Bruce A. Averill. *Evidence for nonbridged coordination of p-nitrophenyl phosphate to the dinuclear Fe(III)-M(II) center in bovine spleen purple acid phosphatase during enzymatic turnover.* Biochemistry (1999), 38, 9914-9925.

- Martijn W. H. Pinkse, Maarten Merkx, Bruce A. Averill. *Fluoride inhibition of bovine spleen purple acid phosphatase: Characterization of a ternary enzyme-phosphate-fluoride complex as a model for the active enzyme-substrate-hydroxide complex.* Biochemistry (1999), 38, 9926-9936.

- Nora Tahallah, Martijn W. H. Pinkse, Claudia S. Maier, Albert J. R. Heck. *The effect of the source pressure on the abundance of ions of noncovalent protein assemblies in an electrospray ionization orthogonal time-of-flight instrument.* Rapid Communications in Mass Spectrometry (2001), 15, 596-601.

- Martijn W. H. Pinkse, Claudia S. Maier, Jung-In Kim. Byung-Ha Oh, Albert J. R. Heck. *Macromolecular assembly of Helicobacter pylori urease investigated by mass spectrometry.* Journal of Mass Spectrometry (2003), 38, 315-320.

- Martijn W. H. Pinkse, Pauliina M. Uitto, Martijn J. Hilhorst, Bert Ooms, Albert J. R. Heck. *Selective isolation at the femtomole level of phosphopeptides from proteolytic digests using 2D-nanoLC-ESI-MS/MS and titanium oxide precolumns*. Analytical Chemistry (2004), 76, 3935-3943.

- Martijn W. H. Pinkse, Albert J. R. Heck, Klaus Rumpel, Frank Pullen. *Probing noncovalent protein-ligand interactions of the cGMP-dependent protein kinase using electrospray ionization time of flight mass spectrometry.* Journal of the American Society for Mass Spectrometry (2004), 15, 1392-1399.

Dankwoord

Ik wil mijn promotor Albert Heck bedanken voor al zijn vertrouwen en de grote mate van vrijheid die ik heb gekregen in mijn onderzoek. Na het vetrek van Claudia werd je mijn directe begeleider, waarna je veelvuldig kwam vragen waar ik nu eigenlijk in godsnaam mee bezig was en of er al wat te publiceren was. Hoewel we in het begin vaak niet op dezelfde golflengte zaten, is het nu dan toch goed afgelopen en is het meeste werk toch afgerond. Jij was vaak enthousiaster dan ik met behaalde resultaten. Tevens drong je herhaaldelijk aan om het maar eens op te schrijven, wat er mede toe heeft geleidt dat mijn boekje wat voller is geworden. Ik wil je bedanken voor al je kennis, hulp met manuscripten en interesse in het onderzoek. Daarnaast ben ik je erg dankbaar voor het geven van de mogelijkheid om in 'jouw' Netherlands Proteomics Centre te mogen post-doccen op de FT.

Although I conducted all my work in Utrecht, throughout the years I was sponsored by Klaus Rumpel and Frank Pullen from Pfizer Global Research and Development. Klaus, I would like to thank you for all your enthusiasm and support throughout the years. Your caged-compound idea was very original and clever, it's a shame we never had the time to perform it. Frank, I would like to thank you for giving me the opportunity to do this work in Utrecht, as well as making it possible to stay in Sandwich for four weeks. It was certainly very interesting to have a look around in a big pharmaceutical company. Also our discussions regarding my work were very fruitful for me, since you often highlighted things from a different perspective. Wolfgang Dostmann, I would like to thank you for showing interest in our mass spectrometric approaches to study PKG, and for your hospitality during my short visit to your lab in Vermont. Your incredible knowledge on PKG and all our discussions about those strange inhibitor peptides in combination with the photolabeling experiments were certainly very useful to me.

Martijn Hilhorst en Bert Ooms wil ik bedanken voor het opzetten van de titanium oxide applicatie in Utrecht. In eerste instantie alleen bedoeld als een kort bij-beun project, maar uiteindelijk toch een belangrijk hoofdstuk uit mijn proefschrift geworden. Pauliina, thank you for your contributions to the initial titanium oxide work and for all your patience with the rather unusual and unconventional HPLC setup I devised for that. Dirk Rijkers, halverwege mijn onderzoek liep ik met het plan om foto-labeling te gaan gebruiken en per toeval kwam jij op dat moment met een fotolabel. Na een eerste succesje met het substraat, synthetiseerde jij een reeks DT2-gerelateerde peptides. Helaas bleek geen van deze te cross-linken met PKG

en dat lag echt niet aan jouw zuivere synthese werk. Terug aan de tekentafel kon ik jouw nog intereseren om drie labels te maken waarmee het hopelijk wel zou lukken. Inmiddels is het dan toch gelukt en hoewel de resultaten net buiten een hoofdstuk in dit proefschrift vielen komen ze hopelijk wel in een mooie publicatie. Ik wil je bedanken voor je altijd snelle en (zeer) zuivere synthese werk alsmede de uiterst nuttige discussies.
De bewoners van de 'terminale aio'-kamer; Edwin, ik kwam net op de kamer toen jij tijdens 'jouw' grote SILAC-experimenten aan het vechten was met de micro's en zorbax-kolommen. Gelukkig kon ik je snel overhalen om toch mijn eigen gemaakte kolommen te gebruiken, waarmee het al veel beter werkte. Tevens leerde ik dankzij jouw dat niet ieder waterglas het zelfde is en op mijn beurt kon ik jouw weer leren dat niet ieder fused silica het zelfde is. Ik wil je bedanken voor alle nuttige discussies over nanolc, dda en de qtof. Isabel, wij beiden stonden na het vertrek van Claudia alleen in ons eigen onderzoek. We zochten en vonden alletwee onze eigen weg en ik wil je bedanken voor al je interesse en enthousiasme dat je toonde in mijn onderzoek. Daarnaast was jij van de aio-groep de eerst UIPS-massa-aio en was erg behulpzaam bij geven van tips rond de ins en outs van het afronden. Bedankt voor al je hulp. Annemieke; *nanoLC'en en kolommetjes gieten, hoe moeilijk kon dat nou zijn*?. Na maanden test-peptides injecteren op een lc met b-klep stoornissen weten we inmiddels wel beter. Ook die ene keer, dat we na 8 uur te hebben doorgebracht tussen de nano separation goeroe's, diep teleurgesteld terugkeerde naar het Went met welgeteld één hele voorkolom, zal ik niet snel vergeten. Bedankt voor de goede samenwerking en (alvast) voor het paranimf willen zijn. Overige bewoners van de derde die ik wil bedanken. Op de eerst plaats; Cees, *welk apparaat hebben we nou niet een keertje moeten open schroeven?*. Bedankt voor alle technische ondersteuningen, je nimmer aflatende interesse en uiterst nuttige discussies, veelal buiten tijdens de koffie pauzes. Pauline, thank you for your fast introduction into the world of liquid chromatography. Although you were very busy finishing you own thesis, you still had some time to show me around, which was very much appreciated. Joost, die als student het niet erg vond om op vrijdag avond voor de zoveelste keer masslynx op de qtof te installeren. Bedankt voor al je hulp met de qtof-computer en veel succes met je eigen promotie-onderzoek (*waar blijven de vliegjes nou?!*). Arjen, halverwege mijn aio tijd begon jij bij Wolfgang aan een PKG project *(waar zat je verstand?)*. Ik wil jouw en Carla bedanken voor jullie gastvrijheid tijdens mijn korte verblijf in Vermont. Je was een uiterst bekwame gids op de route naar Montreal. Ondanks het mistige uitzicht boven op die berg, de goed verscholen overdekte houten bruggetjes en de lange wachtrij na afloop van de GP heb ik mij daar zeker

goed vermaakt. Bedankt voor de preps en veel succes met de pulldowns. Jeroen Krijgsveld; bedankt voor het beantwoorden van een spervuur aan vragen bij de titanium-oxide poster-presentatie in Nashville. Eef, wanneer gaan we nu eens die 'echte' fosfopeptiedjes van jouw over die titaan-kolommen van mij runnen? Hugo Meiring en Ad de Jong van het RIVM wil ik bedanken voor de hulp en technische tips omtrent 'the art of nano-lc'

Naast het door de weekse promotiewerk, heb ik veel tijd doorgebracht in de werkplaats van Theo van Baden, alwaar ik los van het promotie onderzoek bij kon komen met allerlei klusjes achter de draai- en/of freesbank. Theo, bedankt voor het geven van de mogelijkheid deze machines te gebruiken en het stukje rvs voor het maken van het 'bommetje'. Cheryno (*wanneer gaat die racer nou eens lopen?*), bedankt dat je altijd wel wat werk had liggen wanneer ik even niks te doen had. Lisette, vier jaar geleden gingen we nog dagelijks samen met de trein naar Utrecht. Uiteindelijk vond jij je heil weer terug in Alkmaar, en werden de momenten dat we elkaar 'live' zagen aanzienlijk minder. Toch ben ik dankbaar voor je interesse in mijn werk in de spaarzame momenten dat we elkaar zagen en ben ik blij dat jij nog een keertje naar Utrecht wilt komen als paranimf.
Bar en Ruup *(wanneer trekken we weer eens een blik open?)*, Wally, Alberto, Thijs en Nathalie voor de altijd gezellige concertjes van de kecks, beef, izj en de hardheid.
Pap en mam, regelmatig kon ik bij jullie mij ei kwijt over al de vergaarde frustraties in Utrecht. Mam, jij stond altijd klaar om te luisteren naar mijn verhaal en ik wil je bedanken voor al je hulp. Pap, telkens als ik dacht iets slims te hebben bedacht voor mijn metingen en dat even aan jouw wou meedelen stelde jij weer zo'n een kritische vraag over iets waar *ik* nog niet aan had gedacht. Bedankt voor het delen van al je technische kennis en interesse.
Lieve Astrid, het zit er dan eindelijk op. Vele keren was jij daar om mij weer op te vrolijken en te laten lachen als er weer eens iets niet goed was gelopen met de metingen. Bedankt voor al je begrip bij al die keren dat niet *ik* te laat was, maar de NS. Uiteindelijk is het boekje dan toch af. Zonder jouw had ik het zeker nooit volgehouden, maar nu dan, deze is voor jou...